Systematic diagnosis of factors to cyclic shear creep of airport asphalt surfaces

White, Gregory W

White, G. W. (2015). Systematic diagnosis of factors to cyclic shear creep of airport asphalt surfaces [University of the Sunshine Coast, Queensland]. https://doi.org/10.25907/00205
Document Type: Thesis

University of the Sunshine Coast

School of Science and Engineering

SYSTEMATIC DIAGNOSIS OF FACTORS LEADING TO CYCLIC SHEAR CREEP OF AIRPORT ASPHALT SURFACES

By Gregory William White

BE(Civil,Hons 1), MEng(UoN), ME(UNSW), ME(QUT), MTech(Pvmts), Grad Cert(App Stats), Cert IV(A&WT), RPEQ, CPEng, MIEAust.

A Dissertation submitted for the award of

Doctor of Philosophy

Submitted for Examination in August 2015

ABSTRACT

Two runways at the same Australian airport were resurfaced with 50-60 mm of asphalt between September 2010 and July 2011. The Marshall-designed 14 mm nominal sized asphalt was typical of airport-quality asphalt in Australia. A premium acid modified bitumen, locally known as multigrade or M1000, was used. Approximately six months after construction, horizontal shear creep deformations were observed. The failures were only observed in the braking zone associated with one landing direction. Only the second of the two resurfaced runways was affected. Around 60 isolated failures presented over two to three years, after which, new failures ceased to appear.

During construction, the fine aggregate (dust) source changed from one quarry to another. It followed that one runway received asphalt made with dust from one quarry and the other runway received asphalt made with dust from the other quarry. Both dust sources were olivine basalt with a track record of adequate performance in road asphalt production. Subsequent investigation identified that the second dust contained predominantly Hisingerite clay minerals. Hisingerite is a rarely encountered member of the Smectite-group of clays and possesses physical properties indicative of potentially adverse impacts on asphalt stability and shear stress resistance. The original dust contained Nontronite clay minerals, a more common and less concerning member of the Smectite-group.

Subsequent investigation determined that the M1000 feedstock (crude oil source blend) also changed at the same time as the quarry (dust source) change. It followed that one runway received asphalt made with M1000 from one feedstock and the other runway received asphalt made with M1000 from another feedstock. Retained bitumen samples from before and after the feedstock change indicated significantly different bitumen properties.

The two runways contained two substantially different mastics (bitumen feedstock and dust source) within an otherwise common coarse aggregate skeleton. The aim of this investigation was to determine the single, or combination, of asphalt constituents that led to the significant difference in runway surface response to high shear stress conditions. The mastic was concentrated on. However, significant effort was also made to exclude other potentially contributing and confounding factors.

As described below, the initial phases of the systematic investigation confirmed the change in mastic was responsible for the observed difference in surface performance. Firstly, aircraft-induced surface layer shear stresses were calculated for the three regularly used landing directions across the two runways. As a result, differential aircraft operation was discounted as a contributing factor.

Secondly, surface layer interface shear resistance was measured by direct shear and cyclic shear testing of cores recovered from the two runway surfaces. Poor bond between asphalt layers is a common cause of horizontal shear creep deformation. However, the direct shear testing discounted differential interface construction as a potentially contributing factor. The direct shear and cyclic shear test results were combined to demonstrate that the asphalt on the first runway had significantly higher resistance to deformation under cyclic shear stress than the asphalt on the second runway. This focused the investigation towards the two asphalt materials and their constituents.

Thirdly, a range of testing was performed on the various retained and representative constituent materials. The coarse aggregate and hydrated lime (added filler) were subsequently discounted as contributing factors. The confounded change in M1000 feedstock and dust source were identified as the remaining possible factors leading to the reduced shear stress resistance of the second runway surface.

Finally, performance-based repeated shear stress testing of mastic and binder samples was used to isolate the relative impact of the bitumen and dust changes on asphalt shear resistance. Mastic testing showed that the change in dust source, and associated incorporation of Hisingerite clay, did not adversely affect the asphalt on the second runway. Retained bitumen sample testing then measured the impact of the feedstock change on the M1000 resistance to repeated shear stress. The M1000 bitumen incorporated in the second runway asphalt showed lower resistance to deformation under repeated shear stress, as well as higher sensitivity to high stress levels.

It was concluded that the higher stress sensitivity and lower shear stress resistance associated with the bitumen used on the second runway resulted in an asphalt surface with reduced resistance to cyclic shear creep. Isolated zones of permanent horizontal deformation resulted under the high shear stresses associated with typical commercial aircraft braking. The observed self-correction of the surface was consistent with measured in-storage hardening of retained bitumen samples. The lack of resistance to shear creep of the second runway surface was determined to be an example of medium-term asphalt tenderness, due to the bitumen properties, resulting from the change in M1000 feedstock. However, all testing of bitumen at the time of construction indicated compliance with the Australian paving grade bitumen specification. This highlights the inability of the current Australian specification for bitumen to discriminant between more and less shear stress resistant bitumens of the same type and grade.

DECLARATION OF ORIGINALITY

The work contained in this Dissertation has not been previously submitted for a degree or diploma at any other higher education institution. To the best of my knowledge and belief, the Dissertation contains no material previously published or written by another person, except where due acknowledgement or reference is made.

Gregory William White
BE(Civil,Hons 1), MEng(UoN), ME (UNSW), ME(QUT) MTech(Pvmts),
Grad Cert(App Stats), CertIV(A&WT), RPEQ, CPEng, MIEAust.

8 November 2015

ACKNOWLEDGEMENTS

I would like to acknowledge and thank the following individuals and organisations for their assistance with this research. Such an undertaking cannot be achieved by an individual working alone and its timely completion is a reflection of the level of support that has been provided.

The preliminary investigation was jointly-directed by Fulton Hogan and Beca staff as the constructor and designer of the Melbourne Airport resurfacing work. Melbourne Airport staff also contributed as the owner of the airport and facilitated the taking of core samples and provision of aircraft frequency data.

Some of the preliminary investigation data was generated by materials testing performed by ARRB Transport Research, Professor in Physical Chemistry Hans Riesen University of New South Wales (ADFA Campus) and by Professor in Geology Philippa Black, of Auckland University.

Core samples were recovered from the two runways by a number of Fulton Hogan team members, under the direction of Beca and Melbourne Airport staff. Specific acknowledgement is made of Kevin Embleton, Mark Cachia and Dave Aubrey for their efforts, which were largely required at night.

Qantas Captain John Goodlet and Qantas Technical Pilot Alex Passerini provided aircraft technical and operational information such as landing speeds, brake settings and target turn-off taxiways. This information was essential to the calculation of typical aircraft-induced surface forces.

My employer, Fulton Hogan, allowed me to utilise the test data collected from the preliminary investigation and indulged my desire to extend the preliminary investigation into the academic research presented in this Dissertation. Specific acknowledgement is made of the Fulton Hogan laboratory staff members that managed and performed the bulk of the physical testing, including Kevin Embleton, Tom Gabrawy, John Lysenko, Khoa Vo, Glynn Holleran and Irina Holleran.

My supervisors and advisors from the University of the Sunshine Coast and beyond, who allowed me to benefit from their experiences. Specifically, I mention Steve Emery, John Yeaman, Mark Porter, Susan Tighe, Richard Burns and Bruce Rodway.

Finally, Claire, who tolerates my distractions and supports in ways that no one mentioned above could ever do.

Without your assistance and support, this Dissertation would not have come to fruition. Thank you all.

TABLE OF CONTENTS

Section *Page*

LIST OF TABLES

LIST OF FIGURES

LIST OF EQUATIONS

LIST OF PUBLICATIONS

A number of journal and conference papers have resulted from the research contained in this Dissertation. Some of these publications address related material that is ancillary, but inherently linked, to the research and/or the data generated. Where appropriate, some publications are referred to in the conclusions, under 9.4 Other Observations.

The following works have been published based on the research undertaken as part of this candidature.

White, G 2014, 'Asphalt surface slippages at Melbourne International Airport', *Proceedings 26th ARRB Conference*, Sydney, Australia, 19-22 October, ARRB Transport Research. Accepted following peer review but not presented at the request of Melbourne Airport.

White G 2014, 'Cyclic shear deformation of asphalt at an Australian Airport', *Proceedings 2014 Worldwide Airport Pavement Technology Transfer Conference*, Galloway, New Jersey, USA, 5-7 August, Federal Aviation Administration. Peer reviewed paper.

White, G 2014, 'Statistical analysis of in-service evolution of an airport asphalt surfacing', *Proceedings 2014 Worldwide Airport Pavement Technology Transfer Conference*, Galloway, New Jersey, USA, 5-7 August, Federal Aviation Administration. Peer reviewed paper.

White, G 2015, 'Effect of aircraft on the structure and response of asphalt', *Transportation Geotechnics*, vol. 2, pp. 56-64, Elsevier.

White, G 2015, 'Asphalt overlay bond strength', *Proceedings Airfield Pavements and Lighting Forum*, Sydney, Australia, 29 April-1 May, Australian Airports Association.

White, G 2015, 'Adequacy of Runway Asphalt Overlay Interface Construction', *AAPA International Flexible Pavements Conference*, Gold Coast, Queensland, Australia, 13-16 September, Australian Asphalt Pavement association. Peer reviewed paper.

White, G 2015, 'Asphalt Tenderness in an Australian Runway Overlay', *Transportation Geotechnics*', Article in Press, doi 10.1016/j.trgeo.2015.08.001.

White, G 2015, 'The Multiple Stress Creep Recovery test for Airport Asphalt Binders', *Road and Transport Research*, Article in Press, Article in press.

White, G 2015, 'Inter-batch and Inter-feedstock variability of an Acid Modified Bitumen', *Road Materials and Pavement Design*, Article in Press, doi 10.1080/14680629.2015.1108220.

White, G 2015, 'Shear Creep Response of an Airport Asphalt Mastic', *International Journal of Pavement Engineering*, Article in Press, doi 10.1080/10298436.2015.1095914.

In addition, the following publications are either submitted for peer review or are in pre-publication processing following peer review.

White, G 2015, 'State of the Art: Interface Shear Resistance of Asphalt Surface Layers', *International Journal of Pavement Engineering*, submitted but not yet published.

White, G 2015, 'Shear Stresses in an Asphalt Surface under Various Aircraft Braking Conditions', *International Joutnal of Pavemment Research and Asphalt Technology*, submitted but not yet published.

White, G, & Gabrawy, T 2015, 'Airport Asphalt Surface Interface Shear Resistance: Factors Affecting and Advanced Characterisation', *Pavement Engineering and Asphalt Technolody*, accepted but not yet published.

White, G 2015, 'Limitations and Potential Improvement of the Aircraft Pavement Strength Rating System to protect Airport Asphalt Surfaces', *International Journal of Pavement Engineering*, submitted but not yet published.

White, G 2015, 'Modification of the Airport Pavement Strength Rating System for Improved Protection of Asphalt Surfaces', *International Journal of Pavement Engineering*, submitted but not yet published.

White, G 2015, 'The Impact of Hisingerite on Asphalt Shear Resistance', *Road Materials and Pavement Design*, submitted but not yet published.

White, G, & Gabrawy, T 2016, 'Advanced Characterisation of the Interface Shear Resistance for Airport Asphalt Surfaces', 8th *RILEM International Conference on Mechanisms of Debonding and Cracking in Pavements*, Nantes, Frances, 7-9 June, asubmitted but not yet published.

White, G 2016, 'The Contribution of Asphalt Mastic to Shear Resistance', 6th Eurasphalt & Eurobitume Congress, Prague, Czech Republic, 1-2 June, submitted but not yet published.

LIST OF ABBREVIATIONS

ACN	Aircraft Classification Number.
ALF	Accelerated Loading Facility.
AMADEUS	Advanced Models for Analytical Design of European Pavement Structures.
ANCOVA	Analysis of Covariance.
ANOVA	Analysis of Variance.
APSDS	Airport Pavement Structural Design System.
AR	Average Recovery (from MSCR testing).
CBR	California Bearing Ratio.
CSC	Cyclic Shear Creep.
CV	Coefficient of Variability.
DS	Direct Shear.
DSR	Dynamic Shear Rheometer.
DV	Dependent Variable.
FAA	Federal Aviation Administration (of the USA).
FE	Finite Element.
FWD	Falling Weight Deflectometer.
GLM	General Linear Model.
GPR	Ground Penetrating Radar.
ICAO	International Civil Aviation Organisation.
IRIS	Inclined Repeated Interface Shear.
ISM	Interface Shear Modulus.
ISS	Interface Shear Strength.
ISW	Interface Shear Work.
IV	Independent Variable.
Jnr	Creep Compliance (from MSCR testing).
LE	Layered Elastic.

MANCOVA	Multiple Analysis of Covariance.
MANOVA	Multiple Analysis of Variance.
MEPDG	Mechanistic-Empirical Pavement Design Guide (of the USA).
MMLS3	Mobile Model Load Simulator Mark 3.
MSCR	Multiple Stress Creep Recovery.
MBV	Methylene Blue Value.
NDT	Non-Destructive Testing.
ONS	Octahedral Normal Stress.
OSS	Octahedral Shear Stress.
PCN	Pavement Classification Number.
PG	Performance Grade (of bitumen).
PMB	Polymer Modified Binder.
PPA	Poly-Phosphoric Acid.
QA	Quality Assurance.
RET	Rapid Exit Taxiway.
RTFO	Rolling Thin Film Oven.
RWY	Runway.
SARA	Saturates, Aromatics, Resins, Asphaltenes.
SD	Standard Deviation.
SHRP	Strategic Highway Research Program (of the USA).
TRB	Transportation Research Board (of the USA).
TSR	Tensile Strength Ratio.
UCL	Cantabro Losses Test (Italian).
USA	United States of America.
XCT	X-ray Computer Tomography.
XRD	X-Ray Diffraction.
XRF	X-Ray Fluorescence.

1. INTRODUCTION

With around 100 airports in Australia having asphalt surfaced runways, the current demand for airport quality asphalt surfacing is around 100,000 tonnes per annum (White 2013). In contrast to other countries, such as the USA, Australian airports have generally utilised thin (typically 50-60 mm) layers of asphalt as a surface over what is generally high quality fine crushed rock base course.

Airport asphalt has a life expectancy of around 15 years. Prior to resurfacing, Australian practice has been to texture the surface and remove any runway grooves. This is achieved by cold planing the top 5-10 mm from the surface. In some cases, the existing asphalt surface layer has been fully removed and replaced, but this is not the norm. As a result, some Australian airports, such as Melbourne and Sydney, now have 150 mm or more of asphalt over the original granular pavement base and sub-base.

1.1 ASPHALT FOR AUSTRALIAN AIRPORTS

The specification for Australian airport asphalt dates back to the Commonwealth Department of Works after the Second World War. The airports were Commonwealth owned and managed assets and resurfacing works were designed and specified by a team of Commonwealth employees. Following disbandment of what had by then become the Department of Housing and Construction in 1982, and the cessation of direct airport management by the Commonwealth in 1998 (Eames 1998) private corporations, mining companies and local Government bodies (Councils) became the primary operators of airports in Australia.

The responsibility for managing, maintaining and developing airport infrastructure then rested with these private airport owners and Councils, as remains the case today. One exception being the 28 airfields managed by the Department of Defence, on behalf of the Commonwealth. The other exception is a small number of remote offshore airports that fall under the control of the Department of Regional Australia as a service to isolated communities.

Since the privatisation of the majority of the airports in Australia, engineering consultants have become the primary specifiers and designers of asphalt for Australian airport pavements. The specification of these materials, however, remains based on the models developed by the various Commonwealth departments, with only minor changes to reflect challenges encountered and some new technologies.

Historically, conventional (unmodified by chemicals or polymers) asphalt binders have been used in the manufacture of airport asphalt in Australia. Prior to the introduction of viscosity based specifications in the 1980s, R90 penetration grade bitumen was common (Neaylon 2013). Under the viscosity-based specification, C320 was commonly used in airport asphalt (Emery 2005a). In response to a number of cases of asphalt stripping, Polymer Modified Binder (PMB) gained favour, particularly in the capital city and other major airports, with the elastomeric A10E grade being most commonly utilised. While A10E was effective at reducing stripping risk, it introduced other risks, particularly the risk of groove closure during hot weather (Emery 2005a). Since the start of the 21st century, Multigrade bitumen (M1000) has been utilised at many Australian airports for the production of asphalt. What Australia terms Multigrade bitumen is an acid modified bitumen without polymer modification. Multigrade bitumens are designed to exhibit reduced temperature susceptibility. Australian M1000 is intended to possess a viscosity similar to conventional C320 at low temperatures but more like that of what would be a conventional C1000 bitumen at higher temperatures (Shell 2013). The previous nomenclature for M1000 was M1000/320 to reflect the multi-grade nature of the product. There are currently two suppliers of M1000 in Australia with one supplier enjoying some 80% of the airport market.

There are a number of processes available to create the multi-grade response in bitumens. Australian manufacturers all utilise a similar acid modification. The specific chemical and dosage of acid is not disclosed by the suppliers. However, in 2007 three samples of M1000 from three different suppliers were determined to contain levels of phosphorous that were consistent with the addition of approximately 1.3% phosphoric acid (H_3PO_4) forming chemical to conventional bitumen (Austroads 2007). This was most likely in the form of

Phosphorous Pentoxide (P_4O_{10}) which forms molecules similar to Poly-Phosphoric Acid (PPA). PPA ($H_{n+2}P_nO_{3n+1}$) is well established as an additive for improving high temperature bitumen response to shear stress of bitumen without adversely affecting the cooler temperature response (Li et al. 2011; Domingos & Faxina 2015; Austroads 2007; Miknis & Schuster 2009). The advantage of PPA over other similar acids is the absence of free-water, which negates foaming when added to hot bitumen (TRB 2009).

Groove closure has not generally been an issue for asphalt manufactured with M1000 bitumen. Multigrade stability during heating and transportation has also provided some advantage over PMBs. There has been concern regarding potential segregation and degradation of some elastomeric PMBs during transportation, storage and heating (Austroads 2012; Austroads 2013; Austroads 2014).

Despite these changes in bitumen selection, the base specification for asphalt utilised on airport pavements in Australia has remained largely unchanged. The key requirements are summarised in Table 1 for the most common (14 mm and 10 mm) sized mixes. Mix design remains based on the Marshall method with 75 blows. In practice, the presence of material passing the 75 micron sieve in the manufactured sand sources necessitates the percentage passing 0.075 mm being set to around 6% while the hydrated lime content is commonly limited to 1%. All hydrated lime added to the mix passes the 75 μm sieve and directly adds to the overall percentage passing 0.075 mm.

Table 1 Australian airport asphalt specification (per Emery, 2005a).

Asphalt Property	Nominal mix Size	
	14 mm	**10 mm**
Percentage passing AS sieve (mm)	Target by volume (%)	
13.2	100	N/A
9.5	82	100
6.7	70	82
4.75	60	70
2.36	44	50
1.18	33	37
0.600	25	27
0.300	16	17
0.150	10	10
0.075	5-7	5-7
Filler Content (% by aggregate)	1.5 of hydrated lime	
Bitumen content (% by mix mass)	5.8	6.1
Minimum Marshall stability (kN)	12	8
Maximum Marshall Flow (mm)	3	4
Target Marshall air voids (%)	4	4
Target voids filled with bitumen (%)	75	80

1.2 ASPHALT SLIPPAGE AND DEFORMATION

When larger aircraft started applying more severe braking and shearing forces on airport pavement surfaces in the 1970s, a number of slippages did occur and these were mostly attributed to inadequate bonding of the surface layer to the underlying pavement. To address this, the following strategies were implemented, which now form part of the typical specification for asphalt overlay construction on Australian airports:

- Texturing of the full pavement surface by removal of the upper 5-10 mm of the existing layer with cold planing machines.

- Thorough cleaning of the textured surface by combination of skid-steer mounted mechanical brooms and vacuum or suction sweepers.
- Complete coverage of the cleaned surface with bitumen emulsion tack coat at a rate of 0.2 l/m^2 of residual bitumen which is required to have 'broken' over at least 80% of the surface prior to paving.

Asphalt slippage or horizontal deformation due to delamination of the surface layer from the underlying pavement structure has been rare since the introduction of these requirements.

1.3 STATEMENT OF PROBLEM

1.3.1 Runway surface construction

Between September 2010 and July 2011 the two runways at Melbourne Airport were resurfaced. The works were designed based on normal industry practice and included the various requirements intended to minimise the risks associated with horizontal deformation and slippage of the surface layer. The works were completed over ten months, primarily during night shifts, with the pavement returned to operation between each shift.

Due to an aggregate unavailability part-way through the job, each runway was resurfaced with asphalt manufactured using basaltic dusts from different quarries. The two asphalt mixes were otherwise not significantly different as summarised in Table 2 (key parameters) and Table 3 (particle size distribution). Both fine aggregate (dust) sources, and the coarse aggregate source, had a history of successful road and highway asphalt manufacture and performance. While basaltic rock was the norm for asphalt production at Melbourne Airport, the specific aggregate sources used were not known to have been utilised in asphalt mixes previously used at the airport.

Table 2 Comparison of key asphalt parameters

Parameter	Asphalt Mix and Area Used		Specification Limit
	RWY 09/27	RWY 16/34	
Fine aggregate (dust) source	Tylden Quarry (Tylden, Victoria)	Matthews Quarry (Traralgon, Victoria)	Basaltic
Methyl Blue Value for fines (mg/gram%)	4	8	< 10
Multigrade Bitumen Content (%)	5.8	5.8	> 5.6
Hydrated Lime Content (%)	1	1	0.5-1.5
Marshal Stability (kN)	15.3	17.5	> 12
Marshal Flow (mm)	3.3	3.1	< 3.5
Air Voids (%)	4.4	4.2	3-5
Resilient Modulus (MPa)	3,550	2,790	Report only
Indirect Diametrical Tensile Strength (kN)	903	960	Report only
Tensile Strength Ratio (%)	99	98	Report only
Wheel Tracking (mm)	3.7	3.4	Report only

Table 3 Comparison of asphalt particle size distributions

Australian Standard Sieve (mm)	Percentage Passing by Mass (%)		
	RWY 09/27	RWY 16/34	Specification Target
19.0	100	100	100
13.2	99	98	100
9.5	84	83	82
6.7	70	71	70
4.75	60	62	60
2.36	63	47	44
1.18	29	31	33
0.600	20	22	25
0.300	13	15	16
0.150	8.8	9.8	10
0.075	6.1	6.5	5-7

Both asphalts, including all constituents and the resulting mixes, were verified as being compliant with the design and specification. The construction processes were the same for both runways and were typical of airport asphalt overlay construction in Australia.

1.3.2 Runway Surface failure

Approximately six months after the completion of the works, a number of localised horizontal surface deformations were identified in one runway, concentrated in the heavy braking-turning zones. The deformation occurred only in one traffic direction (Runway 16/34 landing on the 16 direction). As shown in Figure 1 there was no rutting or vertical deformation identified in any of the failure areas, although some viscous groove closure was evident, primarily in the slower moving portions of the runway and associated Rapid Exit Taxiway (RET). Runway 09/27 was free of similar deformation.

Figure 1 Typical horizontal shear deformation at Melbourne Airport.

While not a unique mode of failure for asphalt on a major airport runway, the severity, extent and rapid appearance of these defects was unique to Melbourne Airport. In the most severe instances, the deformations resulted in tensile tearing of the surface at the trailing edge of the deformation zone. These severe failures presented an unacceptable operational risk to aircraft and patch repairs were performed. Patches were performed using the same asphalt mixture design except locally available A10E (elastomeric polymer modified) was utilised in place of M1000. The failures continued to become apparent and to grow in area and severity over time.

1.3.3 Research Questions

The deformations at Melbourne Airport raised a number of questions including:

- First, why were the failures primarily occurring in a very concentrated area, in a single landing direction, on only one runway?
- Second, was the failure mechanism the result of poor bond of the surface layer to the underlying asphalt or was it a failure of the surface layer itself?

- Third, was there some significant variability within the various batches and deliveries of the theoretically identical constituent materials or manufactured asphalt to explain the failures?
- Finally, given the only difference in the design of the two asphalt mixes was the source of the dust, was this the root-cause of the difference in performance, and if so, why had asphalts manufactured with the same dust for roads and highways not reported the same failures?

Melbourne Airport required a long-term solution to the failures. In order to design and affect a repair with confidence, the root cause of the failures needed to be determined and mitigated against.

1.4 AIM AND SCOPE

1.4.1 Aim

The aim of this research was to determine the mechanism and root-cause of the observed failures in the heavy braking zones of the runway at Melbourne Airport in order to affect sound repairs with confidence and prevent similar failures at Melbourne and other airports in the future. This aim is substantially achieved by addressing the questions raised above (1.3.3 Research Questions), testing the hypothesis developed later (3.7 Hypothesis) and addressing the gaps in existing knowledge identified below (Table 8).

1.4.2 Scope

This study focused on the failures that occurred at Melbourne Airport. The direct application of the investigation outcomes and conclusions are therefore limited to the asphalt materials and specific operational circumstance of Melbourne Airport. The processes and research methods utilised and the outcomes are, however, indirectly applicable to all airport asphalt surfaces, subject to the following limitations:

- Where the surface is an asphalt of similar mix design and is constructed to a similar specification. This is considered broadly to include all capital city and major regional airports in Australia and many airports around the world.

- Where the pavement is of similar construction, including nominal asphalt layer thicknesses of 50-60 mm over an existing asphalt surface. For outcomes that are specific to the level of bond to the underlying pavement, this must specifically exclude the first layer of asphalt placed over the crushed rock and asphalt placed over existing concrete pavement. This is considered broadly to include all existing, flexible pavements at capital city and major regional airports in Australia and many airports around the world.
- Where aircraft operations are similar. The aircraft traffic at Melbourne Airport is typical of capital city and major regional airports in Australia. Airport design and aircraft operations as governed by international bodies due to the nature of international travel starting in one country and finishing in another.

1.5 SIGNIFICANCE OF STUDY

The primary significance of this study is to allow the repair of the failures at Melbourne Airport to be affected with confidence. This includes the scope of the repair and the confidence in the remainder of the surface of the two runways as well as the performance of the repair, which included the replacement of a significant portion of the area in which the failures were concentrated.

Indirect significance includes the application of some or all of the outcomes of this research to the broader airport surfacing industry. These outcomes include:

- Understanding of aircraft-induced forces and stresses in asphalt surfaces for airports and the role of these stresses in asphalt surface shear failures.
- Determination of adequacy of bond strength achieved in the field under typical asphalt overlay construction methods.
- Determination of test protocols for the laboratory-based measurement of resistance to cyclic shear stresses and benchmarking to other airports.
- Understanding of typical resistance to cyclic shear stress achieved by asphalt overlays of airports.
- Understanding of constituent materials and characteristics that led to the lack of resistance to cyclic shear stress at Melbourne Airport.

More practical, Australian airport industry, changes that are expected to be considered as a result of this research include:

- Preventing proposed changes to the Australian airport asphalt specification that includes a screening test for Hisingerite clay minerals and prohibition of dust sources containing such minerals.
- Changes to the Australian airport asphalt specification to include either new bitumen types or additional testing to screen against otherwise compliant materials that are unlikely to perform well.
- Incorporation of the Multiple Stress Creep Recovery (MSCR) test used in the USA in high temperature bitumen performance assessment for airports and other high-demand applications.
- Improved diagnosis and more efficient forensic investigation of shear related distress in airport and other pavement asphalt surfacing.

1.6 OVERVIEW OF STUDY

This Dissertation consists of eight following Chapters across four main parts. Part I (Chapters 2 and 3) situates the study within the context of applicable existing knowledge and describes the initial investigations undertaken. Part II (Chapter 4) describes the research methods utilised.

Part III (Chapters 5 to 8) presents the results and analysis of the four Phases of the research. The process of broadly assessing the failure mechanism and then sequentially narrowing in on the actual root cause is reflected in the various Chapters comprising Part III. Part IV (Chapter 9) contains the conclusions and recommendations for industry as well as for further studies. A number of other (ancillary to the hypothesis) findings are also presented.

2. CONTEXT AND EXISTING KNOWLEDGE

The previous Chapter provided some background and introduced the real-life problem encountered at a real airport. This Chapter provides some context regarding changing aircraft wheel loads and tyre pressures as well as typical airport operations. It then presents germane existing knowledge and gaps in the knowledge that must be addressed to achieve the research aim.

The interface shear strength portion of this Chapter is currently undergoing peer reviewed for publication as a state of the art journal paper. The portion addressing the bitumen testing is also undergoing peer reviewed for publication as a journal paper. Copies are included in Appendix 1.

2.1 CONTEXT

Prior to presenting and reviewing the existing knowledge, some context is beneficial. This contextual information addresses aircraft and their operation, as well as asphalt surface design and construction.

2.1.1 Aircraft Pavement Strength Rating System

Aircraft pavements are designed to accommodate the aircraft forecast at the time of their construction. To protect aircraft pavements from inadvertent overload, a pavement strength rating system is internationally adopted by the International Civil Aviation Organisation (ICAO) Loizos & Charonitis (2004). The system has two elements, the primary and numerical element is designed to protect the pavement against subgrade rutting. The second element is categorical and is intended to protect less stress-resistant pavement surfaces from high tyre pressure effects.

Under the first element of the system, aircraft loads are expressed by an Aircraft Classification Number (ACN). ACN is a mathematically exact expression that allows no discretion. For a specific aircraft at given operating mass and tyre pressure, there is only one ACN per pavement subgrade category. Pavements are assigned a Pavement Classification Number (PCN). The PCN is assigned at the discretion of the airport owner, although most owners utilise the highest ACN of all the aircraft in the design traffic fleet (White

2007). Where the ACN-PCN ratio is less than or equal to 1.0, aircraft may operate without seeking special permission from the airport owner. Where the ACN-PCN ratio exceeds 1.0, a pavement concession is required and may incur a financial penalty at the option of the airport owner. Most airport owners will grant pavement concessions based on a balance of the ACN-PCN ratio, the condition of the pavement, previous overload history and the revenue to be generated by permitting the aircraft to operate.

The ACN is defined as twice the wheel load (in tonnes) which on a single wheel, inflated to 1.25 MPa, causes pavement damage equal to that caused by the actual multi-wheel gear at the actual gear load and the actual tyre pressure of the aircraft. The measure of pavement damage is the maximum vertical deflection calculated at the top of the subgrade.

The interaction between multiple wheels on a specific landing gear changes with pavement depth. This means that two aircraft with different landing gear configurations, but the same ACN, will cause relatively different damage depending on the pavement thickness. Pavement thickness is significantly affected by subgrade stiffness, usually expressed as the California Bearing Ratio (CBR). The application of ACN-PCN therefore changes with subgrade CBR. Rather than a continually varying ACN, across all possible subgrade CBR values, subgrades are categories and a representative CBR adopted (Table 4).

Table 4 ACN-PCN subgrade categories

Category	Representative CBR	CBR Range
A	15	Greater than 13
B	10	8-13
C	6	4-8
D	3	Less than 4

The second ACN-PCN system element is based on tyre pressure. The tyre pressure limits are categorical in nature and are inherently empirical. Aircraft manufacturers proposed an increase in the categorical tyre pressure limits in 2008 (Rodway 2009). There were approved in 2013 following full-scale testing efforts (Roginski 2013). However, the revised tyre pressure limits (Table 5) merely reflect aircraft that are already in common use, or are scheduled to be introduced imminently.

Table 5 Tyre pressure category limits

Category	Original Tyre Pressure Limits	Revised Tyre Pressure Limits
W	Unlimited	Unlimited
X	1.50 MPa	1.75 MPa
Y	1.10 MPa	1.25 MPa
Z	0.50 MPa	0.50 MPa

Aircraft with tyre pressures less than the assigned category limit are permitted to operate without specific approval. Aircraft with higher tyre pressures require a pavement concession. Some countries, such as Australia, have adopted airport-specific tyre pressure limits rather than tyre pressures categories and category limits.

2.1.2 Aircraft and Operations

2.1.2.1 Aircraft Growth

Aircraft have slowly increased in size since their invention. The aircraft technology developed during WWII formed the basis for accelerated growth in commercial aircraft since that time. The increase in overall size and weight was associated with increases in tyre pressures and wheel loads. One of the early significant steps in aircraft growth was the B727, first introduced in 1963. At that time, this aircraft was the most damaging commercial aircraft with 18 tonne wheel load on 1.14 kPa tyre pressure. On subgrade class C (CBR 4-8) the B727 had an ACN 49. It prompted the Australian airport authorities to develop a more intense roller to allow proving of new pavements for the unprecedented levels of stress in the upper granular pavement layers.

Since that time, tyre pressures and wheel loads have incrementally increased as new aircraft have been developed and entered service (Fabre et al. 2009; Roginski 2007). In 2001 Airbus introduced its extended body A340-600 commercial passenger jet. This modern and technologically advanced aircraft remains one of the most demanding aircraft on pavements. Tyre pressure of 1.61 MPa and wheel load of 30.8 tonnes (Airbus 2014) results in a subgrade C ACN of 83.

The A380-900 became known as the largest passenger aircraft in the world when it was introduced in 2005. Although heavier than other significant aircraft, its wheel load is less severe at 26.8 tonnes with a tyre pressure of 1.40 MPa (Airbus 2014) and an associated ACN of only 64 for subgrade C. The twenty wheel main landing gear allowed for the less critical pavement loading. The B787-800, introduced in 2009, was a smaller aircraft with 1.60 MPa tyre pressure and 27 tonne wheel loads (Boeing 2013). This provides a subgrade C ACN of 81. The most recent large aircraft advancement from Boeing was the B747-800F, introduced in 2010. With new gull-wing shaped wings, this aircraft joined the A380 as the only Code F (wingspan exceeding 65 m) commercial jets in the world. Based on a B747-400, the landing gear remained relatively modest at 1.55 MPa tyre pressure and 26.5 tonnes giving ACN 78 on subgrade C (Boeing 2013).

The newest Airbus aircraft, the A350, first flew in 2013. It is expected to enter service in 2015 (A350-900) and 2016 (A350-800). At 1.66 MPa and 31.8 tonnes the A350-900 will become the commercial aircraft with the highest tyre pressure and wheel load. The modest ACN 80 on subgrade C results from the wider wheel spacing. While this assists the pavement at depth, the tyre pressure and wheel load govern near the surface. The ACN system is designed to protect the subgrade and pavement thickness. This results in, for example, the B747-800F having a higher ACN that the A340-600 and the new A350-900. For a surface layer, the high tyre pressures of the A340-600 and A350-900 are significantly more damaging than those of the B747-800F.

The drive towards higher tyre pressures and wheel loads reflects a desire for fuel, emission and cost efficient airplanes. Every extra tyre on a new aircraft costs around $US1 M over the life of an aircraft and adds to aircraft mass, drag and rolling resistance (Fabre 2011). Both Airbus (Fabre et al. 2009) and Boeing (Roginski 2007) have invested in full scale high tyre pressure tests in support of increasing tyre pressure limits of airports (Table 5). Both reported no significant increase in damage caused by increased tyre pressures. However, it was assumed that asphalt mixture design and bitumen remain stable under these increased tyre pressures. Both testing efforts were performed at moderate asphalt temperatures, certainly lower than Australian in-service temperatures. Neither report considered shear stress related creep of asphalt surfaces in recognition that the larger aircraft brake harder to operate within existing airfield geometries. Both reports considered ACN to be the primary measure pavement distress.

2.1.2.2 Melbourne Airport

Melbourne Airport was opened at Tullamarine in 1970. It replaced Essendon Airport as the international gateway and the primary domestic airport for the state of Victoria. The airport services airlines flying to 33 domestic destinations across Australia and many cities across the globe. In 2012, the airport processed around 30,000,000 passengers on around 200,000 flights. This makes it the second busiest airport in Australia, behind Sydney, but in front of Brisbane, based on passenger numbers and passenger flights. Based on passenger numbers in 2012, Melbourne Airport was the 50th busiest airport in the world.

As detailed later (5.2 Aircraft Operations) Melbourne Airport is serviced by two runways. One approximately north-south (Runway 16/34) and the other east-west (Runway 09/27). Operating aircraft include the full range of commercial aircraft from the A380, A340 and B747 down to primarily domestic B737 and A300 aircraft as well as freighters, regional turbo props and general aviation aircraft. While Runway 16/34 is the main runway, significant aircraft also use Runway 09/27. All primary landing directions have parallel taxiways and RETs. The RETs all have a radius of around 500 m and the distance between the touch down aiming markers and the commencement of the RET is approximately 1,000 m in all cases.

This geometry is very typical of significant international airports around Australia and the region. There is nothing specific or unusual about the aircraft operations and airfield infrastructure at Melbourne Airport that would not be typical of other airports of similar size and capacity.

2.1.3 Asphalt Surface Design and Construction

2.1.3.1 Asphalt Specification and Design

Asphalt has been used as a structural element as well as a surface layer for airports for over 60 years. In a survey performed of European airports, two-thirds of major airports were found to have asphalt surfaced runways (EAPA 2003). Australia has utilised asphalt more exclusively as a runway surface than either Europe or North America, where concrete runways are also common. Some European countries have also used a porous friction course as a sacrificial surface layer in order to provide adequate skid resistance in wet weather. In contrast, the USA and Australia have generally utilised saw cut grooves in dense graded surfaces to promote friction (White & Rodway 2014).

As detailed previously (1.1 Asphalt for Australian Airports) the specification and design of asphalt mixtures for airport surfaces has not changed significantly for many years. However, asphalt binders have changed in recent years in response to a perceived decline in conventional bitumen performance and the availability of premium (acid or polymer modified) bitumens. Mix design remains based on a dense grading of high quality aggregate, added chemical filler and high bitumen content. Mix design follows Marshall's methods and properties, as does construction quality control testing. New technologies such as warm mix asphalt and inclusion of recycled asphalt millings have generally been avoided (White 2013).

2.1.3.2 Construction Processes and Variability

The construction processes associated with airport surfacing and resurfacing have changed little since the 1970s. Although, there have been some improvements made as a result of new construction equipment availability and to address specific issues that have arisen. New equipment includes vacuum sweepers, material transfer vehicles and cold planing machines. Asphalt production plants have also become more efficient and reliable and asphalt pavers have allowed more consistent surface finishes across greater paving widths.

Changes to airport overlay construction process have primarily related to the texturing and cleaning of the existing surface. This aims to minimise the risk of delamination or slippage failures as previously described (1.2 Asphalt Slippage and Deformation). The resurfacing at Melbourne Airport was similar to airport overlays performed around the same time at Sydney, Brisbane, Adelaide (two runways), Gold Coast, Townsville and Mount Isa airports. These are similar airports with comparable aircraft traffic. All of these projects were performed during overnight runway closures with the runways returned to serviceable condition each morning. All except Mount Isa Airport used M1000 bitumen.

2.1.4 Application

The design of the runway overlay at Melbourne Airport was similar to other projects performed at other airports in Australia. The operational circumstances, nominated binder type (M1000) and construction equipment and processes were also similar. The construction processes nominally identical for both runways. Issues relating to the design or construction process are unlikely to identify a possible root-cause of the failures observed.

Aircraft are becoming ever more demanding. While higher pressures do not impact significantly on the ACN of aircraft, the ACN system does not actively protect the asphalt surface from near-surface shear stresses. This issue should be addressed but is outside the scope of this Dissertation. What is clear is that as aircraft continue to grow, their wheel loads and tyre pressures will continue to increase. An improved understanding of how the resulting shear stresses under typical and extreme braking impact on the surface layer and its interface with the underlying pavement is critical.

2.2 CURRENT THEORY AND PRACTICE

The remainder of this Chapter is dedicated to a review of the existing applicable knowledge. Due to the sequential nature of this investigation, the applicable theory and practice is broad and diverse. The aim of this research was to determine the root-cause (constituent materials) of the known outcome (poor surface performance). The existing knowledge review therefore focused on research methods and their applicability to the phase of the investigation at hand. The methods and issues that became relevant during the sequential Phases of investigation were reviewed in more detail than those issues which were assessed early in the investigation and then dismissed as not being applicable to the root-cause or mechanism.

As a result, significantly disparate detail is presented on various topics. This is generally proportional to the importance of the topic being reviewed. The relevance of some elements of the presented existing knowledge will not become clear until the latter Phases of the investigation. Some commentary has been added in an attempt to provide context in such cases. The existing knowledge is presented in a similar structure to the remaining Chapters of this Dissertation:

- Aircraft forces and braking.
- Asphalt surface stresses and strains.
- Interface shear resistance.
- Asphalt deformation and creep.

2.3 AIRCRAFT FORCES AND BRAKING

The contact between aircraft tyres and pavement surfaces has traditionally been considered to be a circular area with uniform contact stress or pressure (Horak et al. 2009a). The contact area has been calculated as the ratio between the vertical force resulting from aircraft mass acting on the tyre and the tyre pressure. Non-vertical forces are rarely considered for practical design purposes (Yoo et al. 2006).

It is now universally acknowledged that the interaction between tyres and pavements is extremely complex (Horak et al. 2009a; Su et al. 2008; Yoo et al. 2006; Wang et al. 2012; Maina et al. 2012; Al-Qadi & Wang 2011; Hernandez & Al-Qadi 2014; Wang et al. 2014; De Beer et al. 2011). The inclusion of non-circular, non-uniform and non-vertical interactions between tyres and pavement is largely the realm of Finite Element (FE) model researchers, as such modelling is beyond the capability of more traditional layered elastic design tools.

In order to realise the potential benefit of finite element analysis tools, the shape, arrangement and magnitude of tyre-pavement interaction zones must be well understood. Both aircraft tyres and the forces applied by them must be defined. Despite significant efforts in this area, such understanding remains elusive and such interactions cannot yet efficiently be incorporated into routine pavement design (Al-Qadi & Wang 2011).

2.3.1 Aircraft Tyres

Aircraft tyres are complex structures. They are composite materials consisting of reinforcing steel and rubber compounds (Al-Qadi & Wang 2011). Typical tyres consist of treads, steel belts, sidewalls, plys, shoulders and beads. The properties of the rubber compound in each of these structural elements are different (Al-Qadi & Wang 2011). As the tyre rolls forwards, significant distortion of the tyre wall occurs and this should be accounted for in any tyre model development (Wang et al. 2012) The reluctance of the tyre industry to disclose details in relation to the structure and materials within their products creates a challenge for tyre-pavement interaction modellers (Al-Qadi & Wang 2011).

It is possible to measure the contact stresses imparted by stationary and very slow moving tyres. Su et al. (2008) measured vertical contact pressure over the tyre-contact area using pressure sensitive pins embedded in an asphalt slab. Other researchers have simply placed a loaded tyre with painted treads on a piece of paper to better understand the shape and size of the footprint (Yoo et al. 2006). Since 1996, arrays of five-axial pressure transducers were embedded in pavements to measure vertical, transverse and longitudinal stresses under slow moving tyres of various types, including an aircraft tyre, using a heavy vehicle simulator (De Beer et al. 1997) and later in full-scale pavements (De Beer et al. 2011).

The measurements made by various researchers and subsequent tyre modelling have led to a commonly accepted theory of tyre-pavement interaction. The model is illustrated in Figure 2 and is based on (Hernandez & Al-Qadi 2014):

- A series of rectangular ribs on which loads are applied with unloaded gaps between.
- Each gap has a mathematically calculated vertical stress distribution along its area.
- The transverse contact stress is 40% of the corresponding vertical contact stress.
- The longitudinal contact stress is calculated as two skewed parabolic distributions with a peak positive stress equal to 20% of the maximum vertical stress.
- A time-stepped loading and unloading process where the loaded area increases until the tyre is fully covering the analysis portion of pavement and then incremental unloading as the tyre passes on. The duration of each time-step is adjusted to reflect the simulated aircraft velocity.

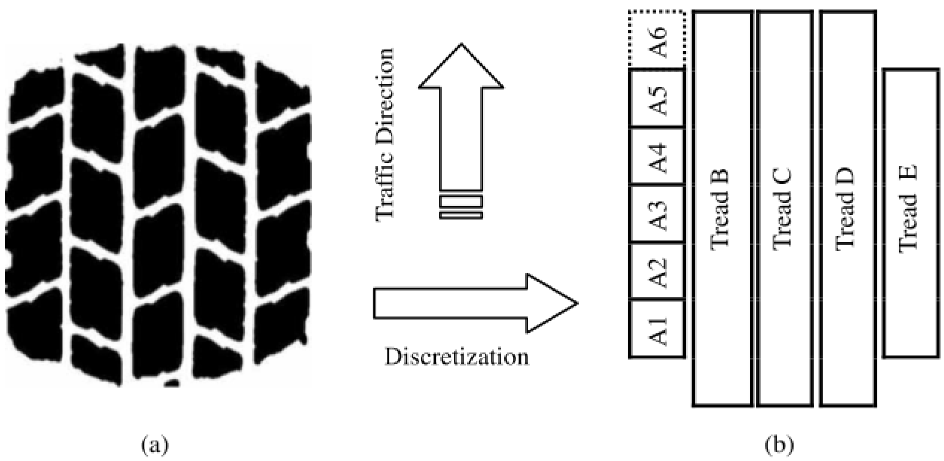

Figure 2 (a) Actual and (b) commonly adopted tyre-pavement contact model (Yoo et al. 2006)

2.3.2 Contact Stresses

Various tyre-pavement interaction studies have clearly shown the three dimensional nature of the stresses imposed on a pavement surface by a free rolling tyre. Longitudinal stresses were found to be compressive at the leading edge and tensile and the trailing edge while it was maximal at the centre of each rib and minimal at the edge of each rib (Yoo et al. 2006). The opposite trends were shown for transverse stresses which were maximum and at rib edges and minimal at the rib centres. De Beer et al. (2011) reported similar trends from their measured tyre pressure study.

In a comprehensive study Wang et al. (2012) calculated contact stresses during static, free-rolling and heavy braking conditions. In static mode, the maximum transverse and longitudinal stresses were around 25% and 12% of the maximum vertical stress, respectively. In free-rolling mode, the transverse stresses remained significant but the longitudinal stresses became small, due to the reduction in frictional resistance. However, during heavy braking, the transverse stresses were transferred to the longitudinal direction which then peaked at around 30% of the maximum vertical stress. In all cases distribution of these surface stresses was complex and generally following the shape and orientation of the tyre ribs as shown in Figure 3.

2.3.3 Vehicle Braking Condition

The distribution and relative magnitude of stresses in various directions changes significantly under braking conditions as demonstrated by Wang et al. (2012). Uzan et al. (1978) suggested that tyre pressure distribution would only ever be relatively uniform in heavy braking or skidding conditions. Horak et al. (2009a) and Mooren et al. (2014) both found that a braking aircraft induced longitudinal stresses to be critical to surface shear resistance. Certainly under braking conditions, the longitudinal stresses have been shown to be of the same order of magnitude as the vertical pressure (Horak et al. 2009a; Wang et al. 2012; Diakhate et al. 2006).

2.3.4 Application

Tyre-pavement surface interaction is highly complex and traditional design procedures make the significant simplification of a uniform contact pressure over a circular area. Traditional design also ignores non-vertical forces such as those associated with braking and turning vehicles. This reflects the fact that current design methodologies focus on the thickness of pavement and layers to protect the subgrade from vertical deformation and the bound layers (such as the asphalt surface) from flexural fatigue.

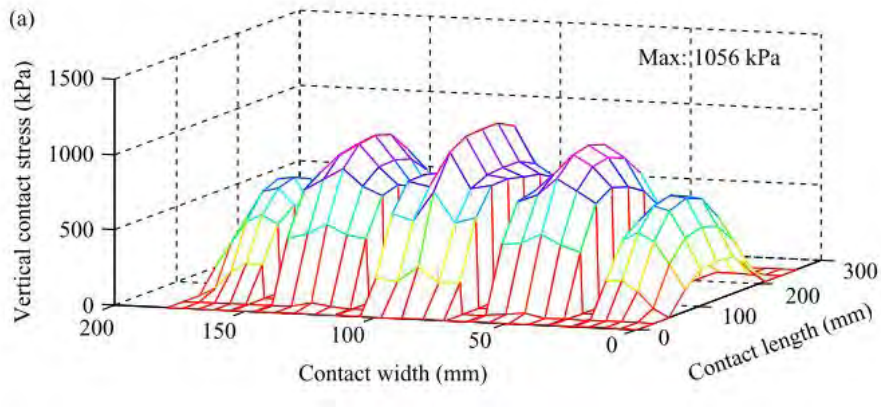

(a)

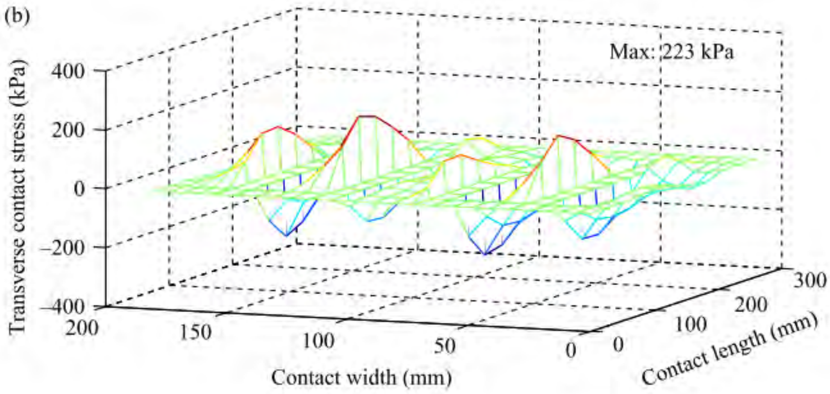

(b)

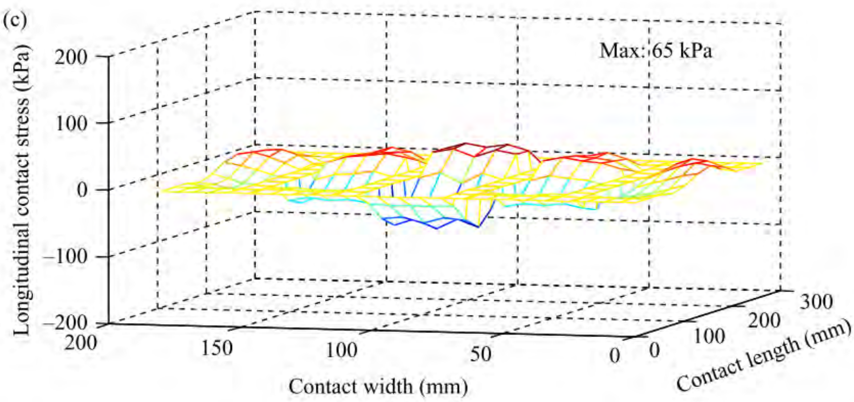

(c)

Figure 3 Calculated free rolling (a) vertical, (b) transverse and (c) longitudinal contact stresses (Wang et al. 2012)

Modelling of the tyre-pavement interaction has demonstrated that the stress imparted onto the pavement surface by rolling tyres acts in all three dimensions and not just vertically. During braking operations, the horizontal stress has been calculated to be as high as 30% of the vertical stress. When shear stress in the pavement surface is being investigated, understanding the non-vertical surface stress is critical. In this investigation, where the aircraft-induced shear stresses are considered, the braking condition must be modelled. This requires the non-vertical forces imparted by the tyre to be included. Comparison to the non-braking condition is also required in order to explain differential performance between braking and non-braking areas.

2.4 ASPHALT SURFACE STRESSES

Determining the interaction between the tyre and the pavement surface allows the distribution of the stresses and strains through the pavement to be considered. The study of non-vertical tyre-induced stresses is generally confined to the surface layer. At depth, the influence of the contact pressure and tyre-pavement interaction is swamped by the effects of wheel mass and multiple wheel interaction.

2.4.1 Modelling tools

Both Layered Elastic (LE) and FE methods have been used to calculate stresses and strains in pavements and their surfaces. Discrete element methods have been less commonly adopted. FE models are less accurate for calculating stresses at interfaces and discontinuities between elements, whereas LE tools lose accuracy at the load boundaries and at the pavement surface (Maina et al. 2012).

FE methods allow more precise modelling of tyre tread patterns, contact load shapes and interface conditions. Many studies have shown these factors can significantly influence the stress distribution and peak stress imparted on the pavement surface (De Beer et al. 2002; Yoo et al. 2006; De Beer et al. 2011; Al-Qadi & Wang 2011). However, Horak et al. (2009b) suggested that circular contact areas of uniform stress distribution were a reasonable simplification for many applications. Various computer based tools are available to perform the numerical calculations in LE or FE techniques. The most commonly reported tools include ANSYS, ABAQUS, BISAR and mePADS/GAMES.

The Circly-based Airport Pavement Structural Design System (APSDS) is a common tool for flexible pavement design in Australia (Wardle & Rodway 2010). APSDS is a LE tool that relies on calibration to empirical data at the critical points in the pavement. This implies that at other points in the pavement, such as near the surface, the predicted materials responses are not necessarily accurate (Rodway et al. 1999). As a result, Circly/APSDS has not been adopted by researchers for near-surface stress calculations. The Federal Aviation Administration (FAA) of the USA investigated and developed a FE model for rigid aircraft pavement design (FAA 1998). The improved calculation of stresses and strains around discontinuities (slab joints) was clearly demonstrated. The material characterisation, however, remained linear elastic. Linear elastic material characterisation does not take full advantage of the increased computation power of the FE tool. The value of the FAA approach is questioned.

The FE tool ANSYS was used to model 3D tyre and pavement surface interactions by Su et al. (2008). Hu & Walubita (2011) also used ANSYS in a 3D surface stress model. Pasindu et al. (2011) utilised ADINA in similar work while De Beer et al. (2002) adopted NASTRAN. Tran et al. (2011) utilised the 3D model BISAR to evaluate the effect of interface condition on pavement response and distress. Hachiya & Sato (1997) used BISAR to estimate the magnitude of stresses at the interface between the surface layer and underlying asphalt layer.

ABAQUS has been more widely used in these applications. Buonsanti & Leonardi (2012) performed surface layer stress analysis of aircraft during landing and braking with a 3D model in ABAQUS. ABAQUS was also used by Ali Shafabakhsh & Akbari (2013) for modelling of aircraft loads on concrete pavements. Wang et al. (2012) and Al-Qadi & Wang (2011) both used ABAQUS in related studies of tyre-pavement interaction. Hernandez & Al-Qadi (2014) furthered this work by comparing the response of airport pavements under various landing gear configurations. Wang & Al-Qadi (2010) calculated near-surface multiaxial stresses and compared them to asphalt shear strengths using a FE model in ABAQUS. Yoo et al. (2006) utilised ABAQUS to investigate the effect of different loading regimes on surface and interface response. It was found that an elastic stick model of the interface shear response provided better correlation to field measurements than a simple friction model.

Use of discrete element models in pavement analysis remains limited although Dai & You (2007) compared discrete and finite element models for mastic creep with reasonable agreement. Mohammad et al. (2011) used a 2D discrete element model in ABAQUS to assess tack coat properties on interface performance.

Of the LE tools, the GAMES routine within the mePADS software developed by Maina & Matsui (2004) has been used in a number of applications. LE tools are less commonly used in surface layer modelling due to inaccuracies at the surface and at the edge of the loaded area (Maina et al. 2012). However, the GAMES routine was specifically developed to provide more accurate modelling of stresses and strains near the surface. Comparison with results published in the Advanced Models for Analytical Design of European Pavement Structures (AMADEUS) report (EU 2000) returned good correlation and confidence in the GAMES-calculated pavement responses (Maina et al. 2008).

Maina et al. (2012) used GAMES to compare square and rectangular loads while Horak et al. (2009a) modelled the risk of shear slippage deeper in the pavement. Horak et al. (2009b) used GAMES to assess surface layer delamination. VEROAD, a LE based tool, was used to investigate cracking of asphalt surfaces at Amsterdam’s Schipol Airport (Mooren et al. 2014). Walubita & van de Ven (2000) successfully used LE methods to calculate three dimensional stress states in order to better predict asphalt cracking and rutting.

2.4.2 Stress and Strains

The calculation of stresses and strains in pavement structures is not a recent development. The use of computer-based software merely allows the processing of large numbers of complex calculations to be performed far quicker than any manual method. This has allowed more complex mathematics, such as those embedded within LE and FE methods, to be incorporated into research and design tools.

Current design methods for airport pavements generally only consider the vertical force applied to the pavement surface assumed to apply uniformly over a circular contact area. It has been shown that this simplification is not realistic

(Su et al. 2008; Yoo et al. 2006; Wang et al. 2012; Wang & Al-Qadi 2010). De Beer et al. (2002) found some stresses to be up to six times higher when modelling an actual tyre in comparison to a circular and constant contact pressure model free of non-vertical forces. Al-Qadi & Wang (2011) determined that the surface shear stress varied from 103% to 147% of those induced by an equivalent uniform contact pressure model when tyres are accurately modelled in three dimensions. Longitudinal and transverse horizontal stresses were found to be 12% and 48% respectively, of the vertical stress under a rolling tyre (Yoo et al. 2006).

The shear stress during a severe braking event can be up to 68% of the vertical stress (Horak et al. 2009b). These shear stresses are significant and can cause surface deformation. The impact of turning aircraft induced shear stresses at Amsterdam's Schipol Airport was investigated by Mooren et al. (2014). It was found that high centrifugal forces and rigidity of multi-axle main gears in tight curves could result in surface cracking at elevated surface temperatures. High-speed/high-radius turns were similarly capable of causing damage at high temperatures. It was concluded that asphalt cohesion (from a Mohr-Coulomb model) was a key factor in resisting surface cracking under tyre-induced shear forces.

2.4.3 Stress Indicators

When 3D stress states are taken into account, the coordinate system becomes highly complex. The coordinate system is rendered arbitrary as the combination of longitudinal and transverse stresses change the orientation of the critical shear stress. For a generally cross-anisotropic material such as asphalt, the orientation of the shear stress with maximum magnitude will be the orientation of critical asphalt performance. The ability to consider and compare complex combinations of three dimensional stresses is simplified by the use of the Octahedral Shear Stress (OSS).

OSS is a scalar parameter that combines the effect of nine stresses at a given point. It represents the effective stress state better than any other single parameter (Ameri-Gaznon & Little 1990). It provides a sound indicator of pavement response to shear and is very well suited to 3D analysis tools (De

Beer et al. 2002; Kim et al. 2009). OSS can be calculated as Equation 1. Where considering the plane where the shearing stresses are zero, the OSS will be greatest and Equation 1 reduces to Equation 2. The associated Octahedral Normal Stress (ONS) is calculated as Equation 3 which reduces to Equation 4 on the principal stress plane (Perdomo & Button 1991).

$$\tau_{OCT} = \frac{1}{3}\left[\left(\sigma_x - \sigma_y\right)^2 + \left(\sigma_y - \sigma_z\right)^2 + (\sigma_z - \sigma_x)^2 + \left({\delta_{xy}}^2 + {\delta_{yz}}^2 + {\delta_{zx}}^2\right)\right]^{1/2} \text{ .... } \textit{Equation 1}$$

$$\tau_{OCT} = \frac{1}{3}[(\sigma_1 - \sigma_2)^2 + (\sigma_2 - \sigma_3)^2 + (\sigma_3 - \sigma_1)^2]^{1/2} \text{ .... } \textit{Equation 2}$$

$$\varphi_{OCT} = \frac{1}{3}\left[\sigma_x + \sigma_y + \sigma_z\right] \text{ .... } \textit{Equation 3}$$

$$\varphi_{OCT} = \frac{1}{3}[\sigma_1 + \sigma_2 + \sigma_3] \text{ .... } \textit{Equation 4}$$

Where: τ_{OCT} = octahedral shear stress

φ_{OCT} = octahedral normal stress

$\sigma_x\ \sigma_y\ \sigma_z$ = normal stresses

$\delta_{xy}\ \delta_{xy}\ \delta_{xy}$ = shear stresses

$\sigma_1\ \sigma_2\ \sigma_3$ = major, intermediate and minor principal stresses

Cyclic shear testing of an asphalt mixture provides the cohesion (c) and internal angle of friction (ϕ) based on Mohr-Coulomb theory. These parameters can be combined with the ONS to determine the octahedral shear strength (Equation 5). This represents the OSS value at which the mixture is expected to fail in shear during a single load event.

$$\tau_{OCT\ STR} = \frac{2\sqrt{2}}{3 - sin\phi}[\varphi_{OCT} \times sin\phi \times cos\phi] \text{ .... } \textit{Equation 5}$$

Where: $\tau_{OCT\ STR}$ = octahedral shear strength of the asphalt mixture

The origins of OSS in pavement analysis lie in granular base course materials (Uzan 1999). Witczak & Uzan (1988) first introduced the calculated OSS as an input to stress-dependent modulus models for granular pavement layers (Kim et al. 2009). OSS has commonly been used in such models and for research purposes. Uzan (2004) used octahedral stresses to calculate permanent to elastic deformation ratios as a method for estimating base course rutting. Park & Lytton (2004) explained its advantage as being the ability to represent aggregate dilation effects under high principal stress ratios, such as those found directly below vehicle tyres. The Mechanistic-Empirical Pavement Design Guide (MEPDG) FE tool developed in the USA uses OSS in its generalised stress dependent model for granular materials modulus (Al-Qadi et al. 2010).

A number of researchers have also adapted OSS into asphalt material analysis. De Beer et al. (2002) used OSS at an indicator of critical stress state in thin asphalt surfaces. The evolution of OSS as the pavement progressed from an un-cracked to a cracked condition was modelled. Perdomo & Button (1991) used OSS to predict asphalt rutting. OSS has been recommended as an indicator of asphalt fatigue life based on it being unaffected by the geometry of loading and reference coordinate system (Kim et al. 2009).

2.4.4 Significance to Airport Pavements

Unlike vertical stresses, shear stresses do not peak at the surface. Uzan et al. (1978) stated that shear stress peaks at around the mid-depth of the surface layer. Su et al. (2008) used FE methods to show the shear stress peaking at around 60 mm below the surface while Wang et al. (2014) modelled aircraft tyre-pavement interaction with FE methods. Shear stress was found to peak around 20 mm below the surface. The depth of peak shear stress depends on the horizontal location being considered. This accounts for differences reported by various researchers. The depth of peak shear stress has been shown to be independent of the tyre pressure and wheel load (Wang et al. 2014; Su et al. 2008). OSS has been shown to peak, relatively uniformly, through a range of depths based on the wheel configuration. A single tyre had a peak zone of 40-65 mm while a dual tyre had a peak OSS zone at 50-70 mm (Perdomo & Button 1991).

Typical asphalt surface layers are placed at between 40 mm and 60 mm in thickness. The interface is often located in a zone of near-peak shear stress. Not surprisingly, a number of airports have experienced interface bond failures. There have been reports of delamination failures at Japanese airports, predominantly occurring during summer and usually in the heavy aircraft braking zones Hachiya & Sato (1997). Tsobakawa et al. (2007) reported surface delamination failures at Nagoya Airport in 2000 and Naha Airport in 2005. Although both failures were reported to occur in the summer and were assessed as being de-bonding failures, the root-cause was not reported. Significant delamination of the surface on an international airport in southern Africa was investigated by Horak et al. (2009a). It was concluded that wet weather and poor drainage during construction inhibited the adhesion between the surface and underlying layer. San Francisco airport experienced surface layer delamination and associated cracking under B747-400 turning during hot weather (Monismith et al. 2000b).

A number of instances of horizontal deformation of asphalt have also occurred in the high shear areas of airports (Bognacki et al. 2007; Monismith et al. 2000b; Vallerga et al. 2000). These failures were related to shear creep or instability of the upper layer of asphalt. The temperature dependent nature of bitumen increases the risk of such failures at elevated pavement temperatures, when the asphalt is less creep resistant. The highest pavement temperatures are experienced in the surface layer. It follows that the zone of lowest shear creep resistance coincides with the zone of peak shear stress.

Shear related asphalt failures have generally only occurred in the high shear force areas of the airfield. Some asphalt surfaces that have performed well in taxiways, aprons and non-braking areas of runway have failed catastrophically under aircraft braking. Aircraft tyre generated shear forces induced by heavy aircraft braking are significant enough to impact on the performance of asphalt surfaced pavements.

2.4.5 Application

A range of both LE and FE based tools are available for modelling stresses in pavements, including the near-surface stresses. FE methods offer more precise modelling of tyres, contact pressures and stress distributions. ABAQUS is a leading FE tool and has been used broadly in pavement analysis. LE methods have also been used and mePADS/GAMES has been frequently reported in similar applications. It has also been verified against results generated by the AMADEUS project. The decision to adopt a LE or FE approach to a given investigate is subjective. Where precision and complexity are important, FE methods are justified. LE tools are however simpler and computationally faster. They would be well suited to investigations where the relative stresses are more important than the absolute values.

When modelling stresses in three dimensions, there is no guarantee that the critical condition will occur on one of the principal directions or planes (eg. parallel to the direction of travel). OSS is the best known representation of the critical three dimensional stress condition. While initially incorporated into granular material models, OSS has also been used in asphalt evaluations. For critical stress calculations through the surface layer, OSS should be used as it negates the requirement to calculate the orientation of the critical stress state.

Tyre induced shear stresses impact on airport surface layers in Australia and around the world. Research has shown that these stresses peak somewhere between 20 mm and 60 mm below the surface. This zone includes asphalt that is susceptible to temperature variations due to thermal loading of the surface as well as the interface between the surface layer and the underlying pavement. Understanding these stresses and their impact on both the shear response of the surface mix and its interface is essential. As aircraft tyre pressures continue to increase with new aircraft developments, the risk of near-surface shear failures can only increase.

2.5 ASPHALT INTERFACE SHEAR RESISTANCE

A significant portion of asphalt surface slippages, like those observed at Melbourne Airport, have been attributed to a lack of bond between the surface layer and the underlying pavement, leading to surface layer delamination. Although some investigations have clearly demonstrated inadequate bond as the root-cause of such failures, it has also been common for bond to be the ‘assumed’ cause, despite a lack of appropriate testing or other evidence supporting such findings.

Interface shear resistance is a measure of the bond between two layers under shear loading. In the context of asphalt surface layers, it is a measure of the durability and adequacy of the interface between the surface layer and the underlying pavement. Bond is a non-specific term that more broadly considers adhesion between the layers as well as interlayer friction and mechanical interlocking of the two layers due to aggregate embedment. Interface shear resistance provides a holistic measure of the risk of loss of bond leading to delamination under certain shear loading conditions. Where the interface shear resistance is exceeded or fatigued by the imposed shear stresses, de-bonding can occur and delamination may result (Mohammad et al. 2009).

2.5.1 Importance to Pavements

Regardless of the terminology used, there is no doubt that adequate interface shear resistance and long term bonding of the surface to the underlying pavement are critical to a pavement structural performance. The current suite of LE and FE design tools generally assume complete bond is maintained through the pavement life. Although some packages allow interface bond to be set to any level, from complete bond to complete slip, this is rarely done for practical design purposes and the interface is not routinely modelled as a failure mechanism (Diakhate et al. 2011).

As recently as 2008, Muench & Moomaw (2008) stated that little investigation had been performed on the level of bond being commonly achieved in the field. There is also no clear definition of what constitutes an adequate level of bond in a given situation. Recognition of the importance of interlayer bond to pavement performance has generated much interest in interface condition in recent years (D’Andrea et al. 2013a). In an earlier landmark investigation of interface shear strength Uzan et al. (1978) noted the level of bond achieved in the field could be expected to range from complete bond to complete slip. This sentiment was later reinforced by Kruntcheva et al. (2005). While significant work has since been performed in this area, the understanding is far from complete and is clouded by some inconsistent results from different studies as well as the difficultly in replicating field conditions in the laboratory. It will be a useful advancement to pavement engineering when the state and response of the interface to shear loading can be taken into account in routine pavement design Diakhate et al. (2007).

The mechanisms that contribute to interface shear resistance are complex and interactive. Like many engineering phenomena interface shear resistance is difficult to measure or observe without impacting on the processes as they would occur in-service. It is also difficult to isolate the various components that contribute to overall shear resistance between asphalt layers. As a result there remain gaps in the knowledge and different opinions regarding the components that contribute to interface shear resistance, as well as the mechanisms associated with interface shear failure.

2.5.2 Components Contributing the Interface Strength

Uzan et al. (1978) described interface bond as being a combination of adhesion, friction and mechanical interlocking. It was also suggested that the friction component is likely to be represented through improved adhesion and interlocking, which results in a linear relationship between interface strength and applied normal stress. Canestrari & Santagata (2005) reduced the interface strength envelope into cohesion, dilatancy (or disengagement of macro texture) and friction (micro texture) components as shown diagrammatically in Figure 4. These two approaches are not necessarily inconsistent. What was referred to as 'cohesion' by Canestrari & Santagata was termed 'adhesion' by Uzan et al. (as well as most others).

Canestrari & Santagata (2005) stated that the friction element can be directly isolated by preparing samples that are compacted separately and held together without tack coat. Separate compaction would minimise the amount of aggregate interlock and its contribution to shear strength. The omission of tack coat would minimise the influence of adhesion. How the reduction in contact area resulting from separately compacting the two layers might impact on the interlayer friction was not considered. It is also expected to be difficult to test these samples which would rely purely on normal stress to keep the two layers in contact.

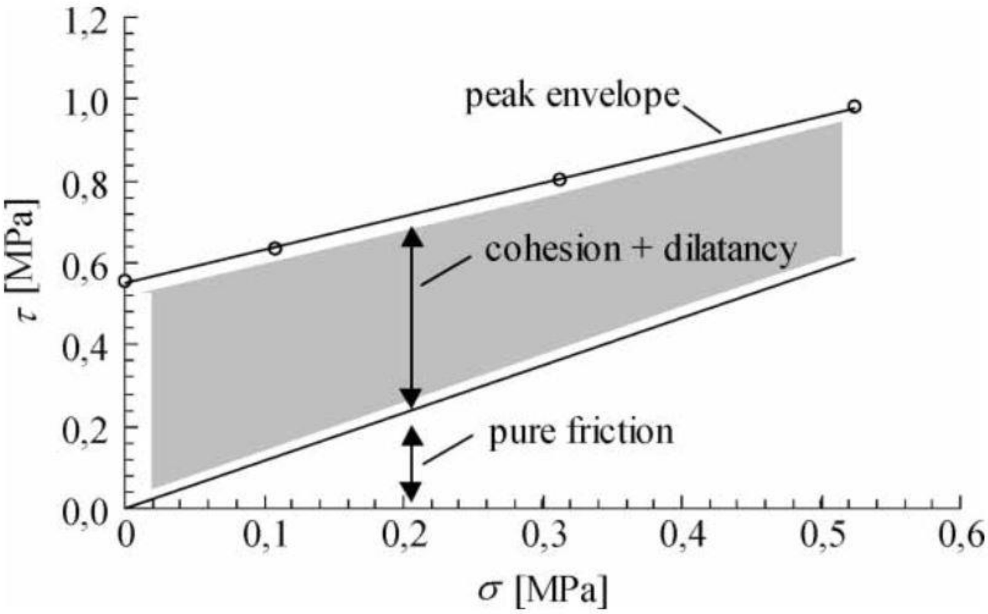

Figure 4 Shear strength (Ʋ) versus normal stress (σ) envelope (Canestrari & Santagata 2005)

The relationship between interface strength and applied normal stress has been commonly expressed as a linear function using the principles of the Mohr-Coulomb envelope. This adaptation of the Mohr-Coulomb model was first proposed by Uzan et al. (1978) and has been adopted and confirmed by many others (Santagata et al. 2009; Chen & Huang 2010; Mohammad et al. 2002b; Canestrari et al. 2005; Canestrari & Santagata; 2005; Santagata et al. 2008; Mohammad et al. 2009; TRB 2012; D'Andrea et al. 2013a). The general form of the linear Mohr envelope for interface strength is in Equation 6.

$\sigma = c + N \times \tan \phi$ .... *Equation 6*

Where: σ = interface strength

N = applied normal stress

ϕ = friction angle

2.5.3 Failure Mechanism

The interaction between vehicle tyres and the pavement surface is complex (Horak et al. 2009b). Despite significant research efforts in this area, there remains no routine method to account for tyre contact stress in pavement design (Al-Qadi & Wang, 2011). The general forces and mechanisms acting on a pavement from a passing tyre are, however, commonly accepted as including normal and shear forces. Shear forces are present under free-wheeling tyres but increase significantly during braking and turning operations (Yoo et al. 2006). Raab & Partl (2004) presented a simple diagrammatic description of the stresses induced in a surface layer by a moving tyre (Figure 5).

When the interface cannot resist the forces applied, it will fail and de-bonding will occur (Mohammad et al. 2009). Failure at the interface of layers could occur monotonically due to a single load event. However it is more likely to occur under fatigue due to cyclic loading Hakimzadeh et al. (2012).

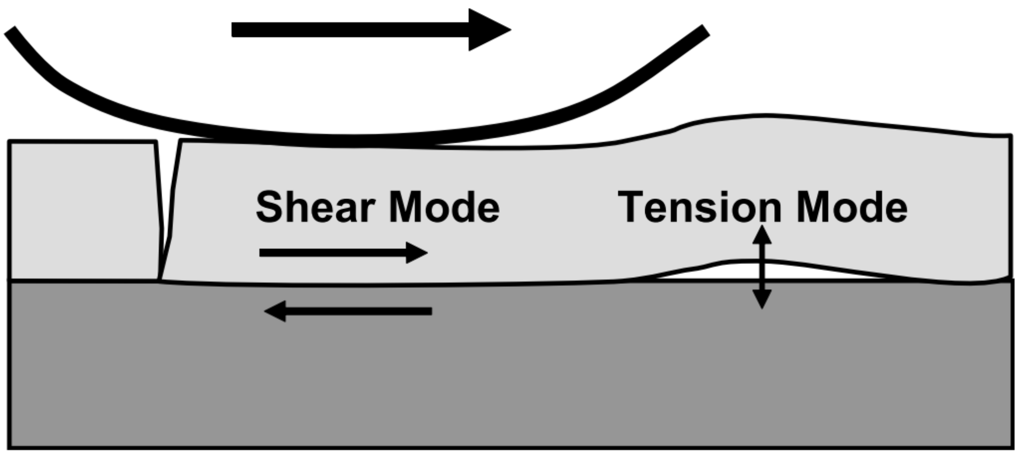

Figure 5 Stress under a moving tyre (Raab & Partl 2004)

2.5.4 Interface Fatigue

While significant research has been conducted on the strength of the interface, comparatively little effort has been made on the fatigue performance. However, interest in interface fatigue seems to have increased since around 2008, probably as a result of the significant efforts and progress being made on monotonic behaviour. Both Petit et al. (2012) and Diakhate et al. (2008) developed fatigue models for asphalt layer interfaces using a double shear test arrangement. It was concluded by Diakhate et al. (2008) that at load magnitudes of less than 50% of the monotonic interface strength, the interface will generally not fail in fatigue for a long time. This is consistent with asphalt and other material fatigue modelling. Researchers at the Sapienza University in Rome developed a linear (in the log-log scale) fatigue model using a repeated direct shear box test (Tozzo et al. 2014a) as well as a repeated inclined interface test (Tozzo et al. 2014b) with consistent trends. Significantly more effort is required before interface shear fatigue is well understood.

2.5.5 Field versus Laboratory Assessment

Interface shear strength testing can be performed in the field on full scale pavements, in the laboratory on cores recovered from the surface or in the laboratory using samples that were prepared in the laboratory. Like many areas of infrastructure research, comparing field and laboratory performance is not simple. Unlike samples prepared in the laboratory, field cores have actual interfaces achieved during construction. However, field testing and laboratory testing of field cores require full scale pavements to be constructed. Where an experimental full scale section can be constructed, more flexibility over some factors of interest is possible. Experimental full scale construction is, however, prohibitively expensive. While field testing best replicates the actual service conditions encountered, the laboratory offers more controllable and repeatable conditions. As an example Sholar et al. (2002) investigated the effectiveness of various tack coat conditions in the field and found inconsistent results between trials performed on two otherwise similar highways in the USA and did not report any logical explanation.

The decision to investigate interface shear strengths in the field or in the laboratory should therefore be made in light of the aim of the research. Where the research aims to assess field performance, field sampling and/or testing is appropriate. Where determination of the influence of specific factors on the interface strength is the aim, laboratory testing of laboratory prepared samples would be more applicable. Field testing or laboratory testing of field cores is an effective research tool only when all factors of interest can be accounted for. This requires that every factor that can influence the measure of interface strength is controlled, or at least measured.

2.5.5.1 Field Testing

Field testing of interface shear strength is less common than laboratory testing. The interface is not located at the surface of the pavement and therefore it is considered far more economical, controllable and practical to core the surface and test the interface in the laboratory. An extensive list of interface strength test methods is presented by TRB (2012) which is summarised below (Table 6). Of these, only the ATracker, UTEP pull off, torque bond and insitu shear stiffness tester are readily employable in the field. Only the insitu shear stiffness tester is truly intended for use in the field. As these tests apply forces to the surface of the pavement, they all rely on either tension or torsion modes. In the case of the UTEP pull off test, both tension and torsion can be applied by the same device. Laboratory testing of cores recovered from the field is likely to be more reliable and repeatable than field testing.

2.5.5.2 Non-Destructive Testing

While not a direct measure of the actual interface strength, a number of Non-Destructive Testing (NDT) methods have been employed to assess the location and extent of de-bonding in the field. Methods attempted have included Ground Penetrating Radar (GPR), impact echo testing, impulse response, Falling Weight Deflectometer (FWD) and infrared thermography (TRB 2013). Mejia et al. (2008) assessed a number of methods and concluded that GPR, impulse response, impact echo and thermography were the most viable methods. TRB (2013) recommended GPR and impact echo as the most viable project-level tools. Tsubokawa et al. (2007) reported successful results using infrared thermography to detect delaminated asphalt on Japanese airports. In a significant effort, Celaya & Nazarian (2014) evaluated various NDT methods for delamination detection at Boston-Logan and Portland International airports. It was found that sonic pulse, infrared thermography and FWD were the most promising, but that no method was conclusive.

One significant limitation of non-destructive methods is the inability to non-destructively confirm positive results or to determine the presence of false negatives. The actual strength of a sound bond cannot be measured by NDT methods. Another limitation is that the most viable technologies are too slow to be employed over large areas such as runways (Celaya & Nazarian 2014). Although an important capability, non-destructive testing for delamination is not considered further in this Dissertation.

2.5.5.3 Laboratory Testing

Laboratory testing of asphalt layer interfaces can be performed on cores recovered from the field or on cores manufactured in the laboratory. There are a large range of test methods and procedures for the measurement of interface bond and TRB (2012) provides a thorough collection of laboratory test methods which is adapted as Table 6, along with citations where the various methods have been used or detailing their development.

Table 6 Summary of laboratory interface bond test methods

Test Method	Load Regime	Remarks	Examples of Use/Reference
Tension tests			
Switzerland Pull-off Test	Stress controlled test		Hachiya & Sato (1997)
ATacker Test	Maximum force measure	Tack coat applied to two plates or a plate and a pavement surface	Buchanan & Woods (2004) Tran et al. (2011)
University of Texas El Paso (UTEP) Pull-off Test	Maximum force measure	Tack coat applied to two plates or a plate and a pavement surface	Tashman et al. (2008)
Louisiana Tack Coat Quality Test (LTCQT)	Controlled strain rate determined by the user at a constant temperature determined by the user	Based on the ATacker test	Mohammad et al. (2011)
Torque tests			
ATacker Test	Maximum force measure	Tack coat applied to two plates or a plate and a pavement surface	Buchanan & Woods (2004)
In situ Shear Stiffness Test	Stiffness measurement at in-service temperature	Trailer mounted field test device	Goodman (2000) Goodman et al. (2002) Bekheet et al. (2007) Abd El Halim (2007)
Un-specified of un-named Torque method			Diakhate et al. (2007) Tashman et al. (2008) Suntanto et al. (2007)
Direct Shear tests			
Leutner Shear Test	50 mm per minute strain controlled at 21°C	No normal load	Raab et al. (2010) Collop et al. (2003) Collop et al. (2009) Sangiorgi et al. (2002) Sutanto et al. (2007) Vismara et al. (2012)

Test Method	Load Regime	Remarks	Examples of Use/Reference
Superpave Shear Tester (SST)	222.5 N per minute load controlled		Mohammad et al. (2002a) Mohammad et al. (2002b) Medeiros et al (2012) Tayebali et al. (2004)
Louisiana Interface Shear Strength Test (LISST)	2.5 mm per minute strain controlled at 5, 25 and 60°C	Normal pressure of 207 kPa	TRB (2012) Mohammad et al. (2009) Mohammad et al. (2010) Mohammad et al. (2011) Bae et al. (2010)
Florida Shear Test	50 mm per minute strain controlled at 25°C	No normal load Similar to Leutner's test	Sholar et al. (2002) West et al. (2005) Tashman et al. (2008)
ASTRA Interface Shear Test	Strain controlled test at variable load rate and temperature	Fixed normal load of any value	Canestrari & Santagata (2005) Canestrari et al. (2005) Santagata et al. (2008) Santagata et al. (2009)
Layer-Parallel Direct Shear (LPDS) Test	Strain controlled test at variable load rate and temperature	Modified version of Leutner's test	Canestrari et al. (2005) Santagata et al. (2008) Santagata et al. (2009) Raab & Partl (2004)
NCAT Shear Test	51 mm per minute strain controlled at 25°C	Also called ALDOT 430 test	Medeiros et al. (2012) West et al. (2005)
Limoges Double Shear test	User set temperature and load controlled regime	Used in monotonic and cyclic load modes	Diakhate et al. (2007) Diakhate et al. (2008) Diakhate et al. (2011)
Sapienza Horizontal Shear Test (SHST) Machine	1.27 mm per minute strain controlled at 20°C	Normal load Used in monotonic and cyclic load modes	D'Andrea et al. (2013a) D'Andrea et al. (2013b) Tozzo et al. (2014a)

Test Method	Load Regime	Remarks	Examples of Use/Reference
Un-specified of un-named Direct Shear method			Romanoschi & Metcalf (2002) Chen & Huang (2010) Kruntcheva et al. (2006) Uzan et al. (1978) Lysenko (2006) Lysenko (2009)

The test methods and protocols detailed are generally grouped into three main load mechanisms; axial tension, torsional shear and direct shear. The general arrangements are shown diagrammatically in Figure 6. Limited use has also been made of a wedge-splitting arrangement (Hakimzadeh et al. 2012). This is considered to be more a measure of crack propagation or fracture and is not addressed further in this Dissertation.

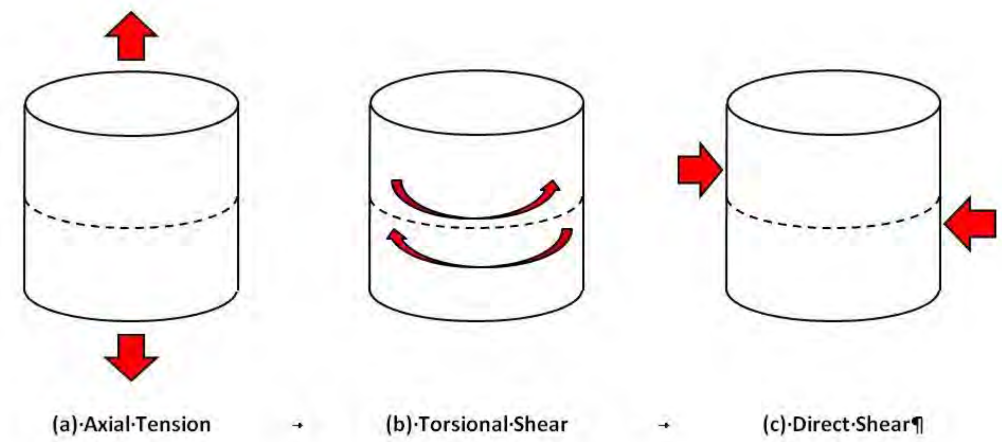

Figure 6 Three common test modes shown with cylindrical samples

Axial tension tests measure the degree of adhesion between the two layers. The resulting bond strength does not include any contribution from the aggregate interlock or frictional elements. Direct tension testing of interfaces is therefore suited to studies that are interested in comparison of the adhesion between layers. This is appropriate for research that is not primarily interested in replicating field conditions or the influence of interface friction and normal stress. Studies with such aims are more commonly focused on comparison of the effectiveness of various tack coat materials (Mohammad et al. 2002a;

Lysenko 2006; Hakimzadeh et al. 2012; Medeiros et al. 2012; West et al. 2005; TRB 2012), tack coat application rates (Mohammad et al. 2002a; Kruntcheva et al. 2006; Tashman et al. 2008; Bae et al. 2010; Hakimzedah et al. 2012; West et al. 2005; TRB 2012), test temperature (Mohammad et al. 2002a; Lysenko 2006; Mohammad et al. 2009; Bae et al. 2010; West et al. 2005; TRB 2012) and the presence of moisture and/or dust at the surface (Mohammad et al. 2010; Lysenko 2006; Sholar et al. 2002; TRB 2012; Collop et al. 2003) or a combination of all of the interface treatment conditions.

Torsional testing is less frequently reported. Although not reflective of the actual loading scenario in the field, torsion tests are capable of inducing pure radial and tangential shear forces across the interface (Goodman et al. 2002). The shear forces vary, however, from zero at the centre to maximum at the circumference of the sample (Diakhate et al. 2007). The torsional load is applied to the asphalt surface which is typically 50-60 mm from the interface. It is therefore more difficult to isolate deformation at the interface from that in the asphalt layer. The torsion test also relies heavily on the ability to efficiently transfer the torsional force from the test device to the upper surface layer. Despite these limitations, torsional test results correlate well with direct shear results (Tashman et al. 2008).

Direct shear tests offer a more comprehensive assessment of the full interface strength likely to be achieved in the field with adhesion, friction and interlock all contributing to the resulting interface shear strength. The load is also applied in a more representative manner and direction to that expected in the field. Field cores and laboratory prepared samples can both be readily tested and a number of test methods can accommodate both round and square samples (Santagata et al. 2009). While circular samples are easy to obtain by coring, square samples offer more reliable and uniform contact with the load platen. The most common arrangements for the direct shear test are the shear box test and the shear tube test. The shear box has been adapted from geotechnical applications and is shown diagrammatically in Figure 7 (a) as the ASTRA method. The shear tube test is based on the work by Leutner and is shown diagrammatically in Figure 7 (b). Due to the test arrangement, it is simpler to apply normal loads when using the shear box arrangement. Most researchers using the shear tube approach have not applied normal loads.

Direct shear testing is considered to be the most appropriate test method for field cores. However, a number of researchers have utilised this comprehensive test method for laboratory prepared samples at a constant or nil normal pressure and with un-textured interfaces (Lysenko 2006; Lysenko 2009; Medeiros et al. 2012, Bae et al 2010; West et al. 2005; Tayebali, et al. 2004). These studies were focused on the tack coat material and application rate. In these circumstances, a direct tension test may have been more appropriate as it would have omitted any unintended difference in the interlocking and friction contributions between samples.

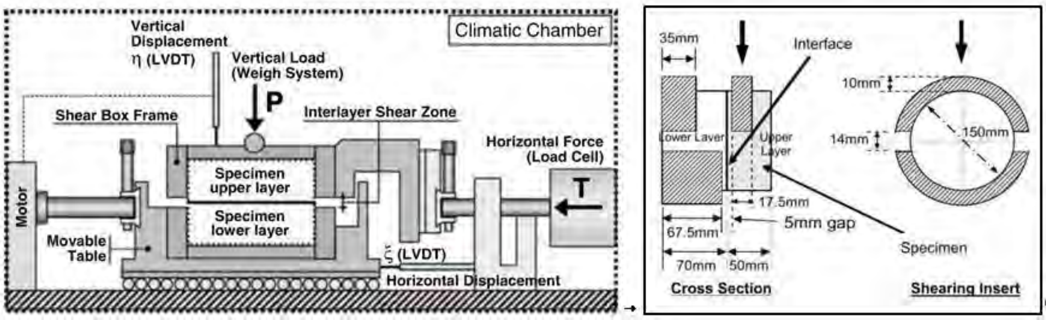

Figure 7 (a) Shear box (b) shear tube arrangements

Direct shear tests are unable to induce uniform shear stresses across the interface. To overcome this limitation Diakhate et al. (2007) used a double shear test which consisted of three interfaces between four layers of asphalt. The central interface was rigidly bonded while the other two interfaces were bonded with tack coat. The central 'double layer' was loaded to induce a uniform shear stress across both the tack coated interfaces. Petit et al. (2012) reported the successful use of this test arrangement for interface shear fatigue modelling.

A number of researchers have compared various test methods. Tashman et al. (2008) compared direct tension, torsion and shear modes in the laboratory and found that the torsion and shear tests returned similar results. The tension test results were significantly different. Tensile test results are dominated by tack coat condition as they omit the interlock and frictional contributions. Diakhate et al. (2008) compared a double shear test with a torsion test and reported that only some of the outcomes were consistent for both test methods. In a comprehensive study comparing the Leutner direct shear test at 50 mm/min shear rate and a torsional test at 600 Nm/min good correlation between the two methods was reported (Sutanto et al. 2007). A linear regression between the two sets of results was derived (R = 96%) across a moderate range of test temperatures and for different asphalt materials.

2.5.6 Measures of Interface Shear Resistance

Interface resistance to shear can be measured by its strength, modulus/stiffness or work/energy. The three concepts are illustrated using a typical shear load-displacement plot from a direct shear test (Figure 8). Monotonic strength is the simplest measure to calculate and is the most intuitively interpretable as the stress at failure. As a result, many researchers have compared interface shear resistance based on Interface Shear Strength (ISS) which can be calculated from Equation 7. The only protocol to be determined for this calculation is whether the area used should be the original area or the area at the time of failure. The difference would represent the amount of deformation parallel to the interface at the time of the peak load. This would typically result in an increase of around 5% in the reported ISS. Some researchers have presented ISS results without detailing whether the original or ultimate areas were used in the calculations (Mohammad et al. 2002a; Mohammad et al. 2009; West et al. 2005; TRB 2012).

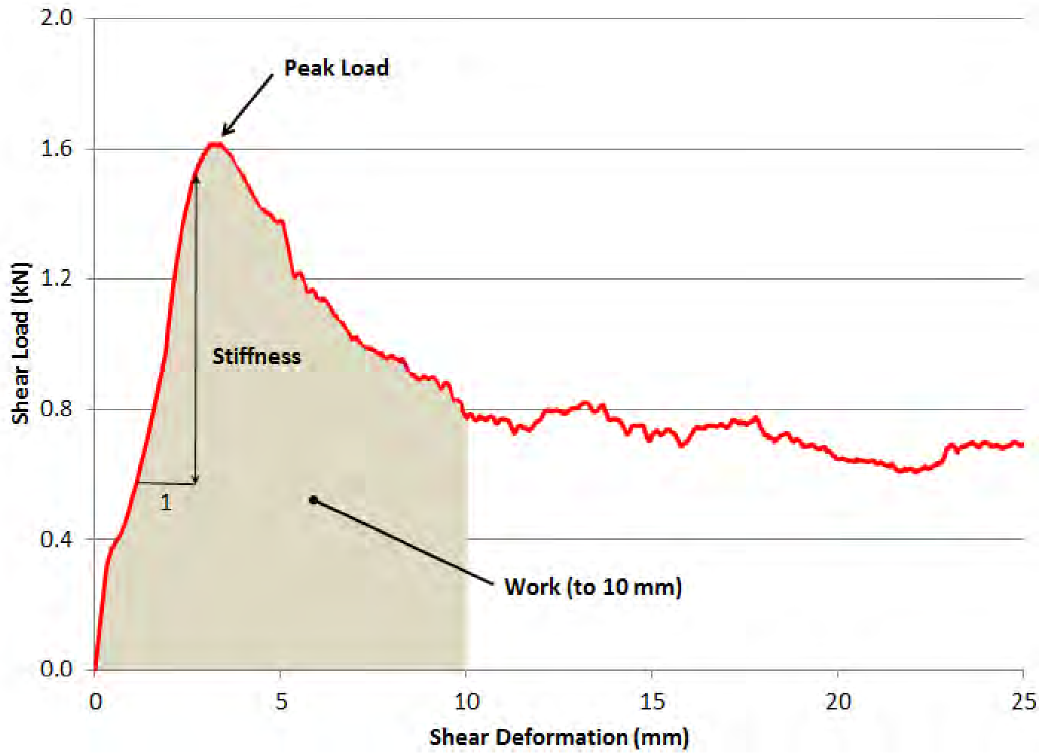

Figure 8 **Example load versus displacement plot and key measurement parameters**

Interface Shear Modulus (ISM) is the non-scalar equivalent of interface shear stiffness. Various researchers have used Goodman's Constitutive Law as expressed in Equation 8 (Canestrari et al. 2005; Mohammad et al. 2011; Kruntcheva et al. 2005; Romanoschi & Metcalf 2002). Equation 8 effectively represents the gradient of the stress/strain plot. Where stiffness is used in place of modulus, this becomes the load/displacement plot as per the example in Figure 8 and Goodman's Law becomes Hooke's Law. ISM is expressed using scalar equivalents for consistency with Figure 8.

Some researchers (Mohammad et al. 2011; Bae et al. 2010; TRB 2012) have used the peak stress and the strain at which the peak stress occurred to calculate the modulus. This secant approach assumes a straight line from the commencement of loading to the peak stress, which is not the norm. D'Andrea et al. (2013a) used the straight line portion of the stress/strain plot but assumed that stress started to increase linearly as soon as displacement commenced. Raab et al. 2010 isolated the straight line portion of the load-displacement plot by extending the tangent of the straight portion down to the x-axis and then shifting the plot to commence from the origin. Typically the straight line portion of the load-displacement plot from a direct shear test would occur between 25% and 75% of the peak load. Collop et al. (2003) developed an algorithm to determine the maximum tangential gradient of the stress-strain plot to calculate the ISM.

Interface Shear Work (ISW) is the area under the load-displacement plot until a given amount of shear deformation occurs, as expressed in Equation 9 and shown in Figure 8 as the shaded portion under the graph. The non-scalar equivalent is the interface shear energy. The amount of deformation over which to calculate the work/energy depends on the research aim. Santagata et al. (2009) used the energy to the peak stress to calculate an equivalent shear strain. The ISW is a useful measure to compare differences in interface shear resistance after the peak load has occurred for samples with otherwise similar ISS and ISM values. Santagata et al. (2009) and Romanoschi & Metcalf (2002) both stated that the retained strength after the peak load is dominated by the frictional properties of the interface.

$ISS = L_P / A$ .... *Equation 7*

$ISM = \Delta L / \Delta d$ .... *Equation 8*

$ISW = \sum(L \times \Delta d)$ .... *Equation 9*

Where L = load applied to the interface

L_P = peak load

A = area of the sheared interface (original or ultimate area)

d = displacement across the interface.

Canestrari et al. (2005) proposed the peak shear stress as the primary fundamental parameter for characterising interface shear resistance. However, significant differences in the slopes of the load-displacement graph and the post peak behaviour have been observed for interfaces with comparable shear strengths. ISM and ISW are also important considerations for monotonic interface shear resistance characterisation.

2.5.7 Factors Affecting Interface Shear Resistance

It is well established that interface characteristics are influenced by surface condition and preparation, temperature, tack coat material, tack coat curing time and tack coat application rate (Tashman et al. 2008). To this list Mejia et al. (2008) added the rate of loading while Kruntcheva et al. (2006) included traffic loading to their list of important factors. These findings are not inconsistent with those reported by Uzan et al. (1978). Numerous investigations have considered the influence of one or more parameters on the various measures of interface shear resistance using various test modes. Some parameters have been found to be more important than others. Some findings appear to be inconsistent but some of the apparent inconsistencies are explained when all the influencing factors are taken into account.

2.5.7.1 Measurement Parameter and Test Method

As outlined above (Figure 8) interface shear resistance can be assessed by measurement of strength (ISS), modulus (ISM) or work (ISW). Each of these parameters can be measured using a number of test methods, mainly classed as direct shear, tensile shear and torsional shear. For a given test method, a range of protocol details must be set such as rate of loading, normal stress and temperature. Not all these details are applicable to all test methods. For example, a normal stress cannot logically be applied during a tension test. These details are not always consistent and are sometimes not reported in literature. They can, however, have a significant impact on the reported measure of shear resistance.

Given this range of test modes, methods, parameters and protocols, most of which are not detailed in national or international standards, it is not surprising that significant variability and some apparently inconsistent findings exist within the literature. The influence of many parameters and test conditions on interface shear resistance is also interactive.

2.5.7.2 Tack Coat

Tack coat is generally recognised as critical to achieving good interlayer bond in the field (TRB 2012). Tack coat provides adhesion between the layers (West et al. 2005; TRB 2012) and neutralises the potentially adverse impact of dust, thereby significantly contributing to ISS (Mohammad et al. 2002a). Tack coats for asphalt layers can include neat bitumen, cutback bitumen or bitumen emulsion. Bitumen emulsion can be manufactured from conventional or polymer modified bitumen and is the most commonly used tack coat material

(TRB 2012). Environmental concern has seen cutback bitumen usage reduce significantly (Tran et al. 2011). In recent times there has been an increase in popularity of bitumen emulsion manufactured from polymer modified bitumen. These products are commonly referred to as 'trackless tack' due to their reduced tendency to be picked up by construction traffic tyres.

Tack Coat Type

Many researchers have compared the interface strength achieved by various tack coats, with specific emphasis on the benefits of trackless tack coats. There is general agreement that polymer modified emulsions result in higher measured interface strengths. A number of studies also reported the viscosity of various tack coat bitumens and this appears to be ordinally correlated to interface strength.

Tayebali et al. (2004) compared conventional penetration grade bitumen and rapid setting bitumen emulsion tack coats in both shear and tension. Across various temperatures and load application rates, the penetration grade bitumen consistently returned 20-50% higher strength in tension tests. When tested in shear, the difference was negligible. This was likely the result of aggregate interlock and friction being dominant factors in the direct shear strength test. Interlock and friction would not contribute at all to the tensile strength. The penetration grade bitumen had a significantly higher viscosity than the bitumen in the emulsion, but the results are contaminated by comparison of equal gross application rates. Bitumen and bitumen emulsion tack coats at the same gross application rate would result in significantly different residual application rates after curing (ie. after the 30-40% water content evaporated from the emulsion). This would subsequently affect the measured strength.

Mohammad et al. (2011) compared emulsion and polymer modified emulsion tack coats at 20°C using direct shear. The polymer modified tack coat provided ISS and ISM values around double that of the conventional emulsion tack coat. Interfaces with no tack coat, conventional bitumen emulsion and polymer modified bitumen emulsion were compared by Canestrari et al. (2005) with similar results at 20°C. However, at 40°C the modified and unmodified emulsion tack coat returned very different ISS values.

Mohammad et al. (2002a) compared six tack coats (four emulsions and two conventional bitumens) at applications rates from nil to 0.9 l/m^2 at 25°C and 55°C. It was concluded that the tack coat with the highest viscosity at 135°C also provided the strongest bond. It was also concluded that at low temperatures, increased tack coat rate reduced the measured ISS. At higher temperatures, the ISS was insensitive to tack coat rate. TRB (2012) reported that in all cases, polymer modified bitumen emulsion tack coat returned higher tensile strength and ISS values than standard bitumen emulsion in laboratory testing and tensile strength was ordinally correlated to the residual bitumen viscosity at 25°C.

Bae et al. (2010) compared conventional bitumen emulsion and polymer modified emulsion tack coats at various temperatures (-10°C to 60°C) and application rates (0.14 l/m^2 to 0.70 l/m^2). The results showed that at low temperatures, there was little difference between the two tack coats in terms of ISS. At temperatures between 10°C and 40°C the difference between ISS results increased until the polymer modified emulsion returned ISS values in the order of 10 times that of the conventional emulsion. At higher temperatures still, the ratio between ISS results for conventional polymer modified emulsion tack coats started to reduce. Similarly, Chen & Huang (2010) found that modified emulsion returned higher ISS and ISM values than conventional emulsion. The viscosity of the modified bitumen was around double that of the conventional emulsion.

In summary, there is consistent agreement that at lower test temperatures, polymer modified and conventional emulsion are similarly effective as tack coat materials. At medium temperatures, typically 25-55°C, polymer modified emulsion perform better than conventional emulsions. This improved performance is then reduced at higher test temperatures. It is likely that these results reflect the impact of polymer modification on the softening point of the bitumen rather than any significant improvement in the adhesive or cohesive properties of the tack coat material.

Tack Coat Rate

The optimum application rate of tack coat has been widely investigated with inconsistent results. Some have suggested that too much tack coat could create a slip plane at the interface, while too little tack coat could leave free-dust at the interface which may inhibit adhesion (Tran et al. 2011; Bae et al. 2010). It is expected that in the field, significant over application of tack coat would be required to create such a slip plane and that interface surface texture would mitigate against slip.

Mohammad et al. (2009) reported that ISS increased approximately linearly with increasing tack coat across the range 0.1 to 0.7 l/m^2. In subsequent work, Mohammad et al. (2010) found decreasing ISS results for increasing tack coat application rates. Then in further work Mohammad et al. (2011) specifically reported on the comparison of two emulsions, one polymer modified emulsion and one conventional bitumen at application rates of 0.14, 0.28 and 0.70 l/m^2 on the ISS and ISM. In all cases, increasing tack coat application rate had a beneficial effect on the ISS results. Increased tack coat application rate was, however, either detrimental or had no impact on the ISM values. Similarly, Romanoschi & Metcalf (2002) tested cores from field trials and measured ISS and ISM of interfaces with and without tack coat. Interfaces with tack coat were treated at a relatively low rate of 0.1 l/m^2. The data reported shows an average 210 kPa reduction in ISS and an average 40 MPa/mm reduction in modulus when tack coat was omitted.

In contrast, Lysenko (2006) reported increased ISS for laboratory samples when no tack coat was used. Similarly Canestrari et al. (2005) reported that at both 20°C and 40°C, the unmodified tack coat resulted in ISS values that were less than when the tack coat was omitted. Tashman et al. (2008) found no significant difference in ISS whether tack coat was used on not.

In the field, Tashman et al. (2008) compared milled and un-milled surfaces as well as the effect of various tack coat application rates (0.08 to 0.32 l/m^2) using the direct shear test and the pull-off test. It was found that the rate of tack coat was significant for direct shear strength of the non-milled sections but not for those sections with milled interfaces. For both milled and non-milled sections, the tensile strength (from the pull off test) decreased with increasing tack coat rate. Mrawira & Damude (1999) similarly concluded that for field cores with non-milled interfaces, the presence any tack coat created a slip plane and reduced the measured ISS.

In summary, it is logical that the rate of tack coat required to maximise ISS would depend on the texture of the interface. For interfaces with very low surface textures, for example for gyratory compacted layers in the laboratory, even modest tack coat rates would likely fill the texture and potentially lubricate the interface or create a slip plane. For field conditions, where the surface is likely to be more textured by ageing or by milling operations, higher tack coat rates would still allow good embedment of aggregate between the layers to create a high contribution to ISS from aggregate interlocking. Regardless of the laboratory and research findings, there is overwhelming evidence to support the continued use of tack coat between asphalt layers in the field, at rates that vary with surface texture and age (TRB 2012).

2.5.7.3 Test Temperature

Research has consistently found a decrease in interface shear resistance with increasing test temperature. The significance of the decrease is less consistent across studies. Bae et al. (2010) noted a ‘significant’ decrease in ISS with increasing temperature. Diakhate et al. (2006) found that shear strength decreased in a non-linear manner with increasing temperature. Chen & Huang (2010) suggested that at higher temperatures, where tack coat viscosity is low, texture becomes more important to achieving good ISS. This is consistent with the conclusions of Muench & Moomaw (2008).

Canestrari et al. (2005) measured ISS and ISW at 20°C and 40°C across a number of normal stress levels. The results consistently showed around 200 kPa reduction in ISS at the higher temperature. ISM values also reduced at the higher test temperature but to a significantly lesser degree. Although the magnitude of the ISS change was consistent across all normal stress levels, the ISW changed more significantly (as a proportion) when the normal stress was lowest.

Sholar et al. (2002) reported an average reduction in ISS of 92% from 25°C to 60°C for various mixes and interface conditions. West et al. (2005) similarly reported 90-95% reduction in ISS from 10°C to 60°C and concluded that the temperature was the most critical single factor affecting bond strength. Tayebali et al. (2004) only measured ISS in the range of 40°C to 60°C but still found an approximate 80% reduction at the higher temperature and concluded that the interface and mix had equal shear strength at 40°C. Hachiya & Sato (1997) reported ISS values at test temperatures at 0°C, 20°C and 40°C with a consistent drop in excess of 90% across this range.

Sutanto et al. (2007) measured ISS at 15°C, 20°C and 30°C. In comparison to the 20°C results, the 5°C reduction in temperature resulted in an average increase in ISS of 25% while the 10°C increase in temperature resulted in an average reduction in ISS of 33%. Romanoschi & Metcalf (2002) measured ISS and ISM of interfaces with and without tack coats. They concluded that both ISS and ISM reduced as the temperature increased with the data showing an average 60 kPa reduction in ISS and 25 MPa reduction in ISM per additional degree of test temperature. TRB (2012) reported a peak in tack coat tensile strength as a function of temperature. As expected polymer modified bitumen emulsion tack coats showed less sensitivity to temperature changes than standard bitumen emulsions, with up to 75% drops from the peak (at 45°C) to 65°C.

In summary, as bituminous tack coat temperature increases, the bitumen viscosity reduces. It is logical that this would result in a decrease in adhesion between the layers and reduced interface shear resistance. This view was supported by Mohammad et al. (2002a) who found the presence of tack coat was only significant at low temperatures. Shear strength contribution from friction and aggregate interlock would be largely unaffected by temperature. The influence of temperature on interface strength would be greatest when adhesion is the dominant contributor to the measured strength. That would include use of the tensile tests mode or interfaces that lack texture or are tested without normal stress. The greatest change in shear strength would occur as the test temperature transitions across the softening point of the tack coat material.

2.5.7.4 Normal Stress

Uzan et al. (1978) demonstrated the linear dependence of ISS on normal stress in direct shear mode. Mohammad et al. (2009) found that normal stress was a significant factor on ISS for dusty samples (whether wet or dry) but not for clean, dry samples. West et al. (2005) found that normal stress was not significant at 10°C test temperature but was linearly related to ISS at 60°C. At 60°C the adhesion would have been minimal so that frictional component created by the normal stress would have contributed the majority of the measured ISS.

Romanoschi & Metcalf (2002) tested interfaces with and without tack coat in direct shear, with normal stresses ranging from 138 kPa to 522 kPa. ISS and ISM increased with increasing normal stress at a rate that is equivalent to a friction angle of approximately 45°. Chen and Huang (2010) reported an approximate tripling (200 kPa to 600 kPa) of ISS from a normal stress of 138 kPa to 522 kPa. This represents a friction angle of 46°. ISM was less dependent upon the normal stress applied. D'Andrea et al. (2013a) presented shear strength as a function of normal stress with the shear stress increasing from 600 kPa to 1,500 kPa as the normal stress was varied from nil to 600 kPa. This is a friction angle of around 56°.

In summary, it has been demonstrated that as the normal stress applied to an interface increases, the friction between the two layers increases proportionally. This directly increases the measured ISS. The normal stress must be overcome prior to disengagement of interface texture and layer separation. The significance of the increase in measured ISS varies depending on the relative contributions of adhesion and friction to ISS for the specific test conditions. At higher temperatures, the contribution of adhesion is negligible due to the low viscosity of the tack coat. The effect of normal stress increase is greatest in such circumstances.

2.5.7.5 Loading Rate

For a given test configuration, the rate of load application has an influence on the interface behaviour and the measured shear strength. Uzan et al. (1978) found that as the rate of load application was slower, the ISS values reduced.

Sutanto et al. (2007) measured ISS values at load rates of 10, 50 and 100 mm of deformation per minute. The corresponding ISS values varied by approximately 33%, in proportion to the rate of loading. Sholar et al. (2002) reported an average increase in measured ISS of approximately 55% at 50 mm/minute rate of load application when compared to a 19 mm load rate. Tayebali et al. (2004) measured ISS without normal load, at 1.0 and 2.5 mm/minute rate of loading, and found a two to four fold increase in the results at the faster load rate when tested in axial tension. When a direct shear test was utilised, the difference in strength for 1.0 and 2.5 mm load rates was negligible.

In summary, the research indicates that for a given test configuration, the rate of load application has an influence on the interface behaviour and the measured shear strength. Tack coats are time dependent materials due to the visco-elastic nature of bitumen (Denneman 2007). Creep or relaxation is expected during slow loading or a fixed state of stress. The interface shear resistance increases with an increase in the rate of loading or deformation, when creep is minimised and the asphalt and tack coat show a more elastic response.

2.5.7.6 Interface Texture

There is a logical relationship between interface shear resistance and the texture of the interface. D'Andrea et al. (2013b) supported this view by stating that the texture between the layers assisted in overcoming the shear forces imposed by traffic. Interface texture contribution to bond is consistent for direct shear testing of interfaces but is less clear for other test modes. Tashman et al. (2008) compared the textured and non-textured ISS results from a field trial using direct shear, torsional shear and tensile tests. The direct shear results for textured interfaces were approximately three times the non-textured results. For the torque test, the milled and non-milled strengths were comparable except where the tack coat was omitted. The non-milled torque strength was negligible when tack coat was omitted. The tensile test results were around double for non-milled surfaces when compared to the milled surfaces.

Mohammad et al. (2010) concluded that textured surfaces result in higher ISS values than un-textured surfaces. Santagata et al. (2008) made a similar observation. Sholar et al. (2002) measured ISS on a number of cores recovered from full scale trials on a highway in the USA. A comparison of results from the milled and un-milled sections revealed a moderate 10-25% increase in ISS associated with milled interfaces. TRB (2012) reported a direct correlation between lower layer surface texture and ISS values with milled surfaces consistently providing higher values than un-milled surfaces. In a rare study of interface shear modulus, Bae et al. (2010) postulated that the ISM would be dominated by surface roughness or texture.

Texturing or milling of aged asphalt surfaces has long been an established practice for airport pavement resurfacing. The removal of the oxidised and contaminated asphalt surface is an established approach to reducing de-bonding risk in high shear stress situations (DoC 1978). The creation of a more textured interface also increases the resistance to de-bonding due to an increase in the contribution of aggregate interlock to interface strength.

In summary, greater interface texture results in increased interface shear strength with milled interfaces returning higher shear strengths than un-milled interfaces. Milling of existing surfaces has become normal practice in high stress applications such as airports. The reported (Tashman et al. 2008) reduction in tensile strength for milled interfaces contradicts this. This reduction in tensile strength for milled interfaces may be due to the direction of loading being parallel to the interface texture during a tensile strength test.

2.5.7.7 Asphalt Materials

Some researchers (Sholar et al. 2002; West et al, 2005) have found that otherwise similar interfaces have different ISS values as a result of the asphalt materials in the upper and or lower layers. Collop et al. (2009) reported that the gradation of the upper and lower mixes made a significant difference to the ISS values measured. Tran et al. (2011) reported that use of water-sensitive aggregates and/or the use of rounded particles can increase the risk of poor interface bond. Mejia et al. (2008) similarly found that polished or rounded particles would lead to increased de-bonding risk.

Upper layer compaction and density is also considered critical to interlayer bonding (Chen & Huang 2010). Canestrari et al. (2005) stated that good upper layer density would promote interlayer adhesion and bond. Santagata et al. (2008) went further to state that the method of compaction used in the preparation of laboratory samples had a significant influence on the resulting ISS for otherwise similar materials.

Santagata et al. (2008) also investigated the distribution of air voids in two layered asphalt systems. It was found that the upper and lower surfaces had the highest concentration of air voids within an asphalt layer. It was also concluded that optimum interface bond was achieved between 4% and 8% air voids. At lower air voids, a lack of interlocking resulted in low shear strength, while at higher air voids, adhesion was inadequate to promote good interlayer bond.

Collop et al. (2003) reported significantly different ISS values for similarly prepared interfaces between different combinations of asphalt materials. This work included 20 mm dense graded surface mix, 10 mm stone mastic asphalt and 20 mm and 28 mm dense graded macadams.

In summary, layer density, aggregate grading, aggregate shape and the presence of air voids all impact the surface texture and degree of aggregate interlock at the interface. It is expected that these studies have consistently, but indirectly, reported the importance of interface texture and the resulting interlocking across the interface. These studies did not report measured texture at the interface so the influence of the interface texture cannot be separated from the density, grading, compaction method and other factors. The only exception is aggregate micro texture, which could adversely impact on the micro friction between the aggregate particles in contact at the interface. Micro texture would be controlled by the shape and angularity of the aggregate particles rather than characteristics of the overall asphalt mix.

2.5.7.8 Interface Condition

Construction practice places significant importance on achieving a dry and clean surface prior to asphalt overlay. Wet or dusty interfaces are expected to have reduced interface shear resistance. However, based on laboratory prepared samples Lysenko (2006) concluded that ISS increased with the presence of dust at the interface. It was suggested that the dust stiffened the bitumen, similar to added filler in asphalt mastic. This increase in tack coat stiffness would have increased the adhesion potential of the tack coat material and improved interface adhesion. TRB (2012) also reported that the presence of dust increased the measured ISS values. It is noted that the 'dust' was a clean and angular sand which is unlikely to replicate mineral contamination created by milling processes in the field. In practice, fine slurry is formed in the presence of water used to cool the milling teeth.

Sholar et al. (2002) measured the ISS of cores from full scale trials on two highways in the USA. The construction of the field trials included purposely wetting the tack coat after breaking. For one field trial, the wet interface returned a 50-60% reduction in the ISS compared with dry interfaces. For the second field trial, the reduction for wetting averaged around 33%. This is in contrast to field work reported by TRB (2012) where wet and dry surfaces returned comparable ISS values, especially where emulsion-based tack coats were used. However, the rate of water application used by TRB was comparatively low.

Collop et al. (2003) found contradictory results when comparing tack coated interfaces with contaminated (by slurry) interfaces without tack coat, as well as heavily contaminated interfaces with heavier than normal tack coat. In some cases the normal tack returned the highest ISS, as expected, but in other cases the two contaminated surfaces returned very similar or even higher ISS values than the normally tack coated samples. It was concluded that for a given combination of layer materials, the ISM did not change for different interface tack/contamination conditions.

In summary a dry and clean interface is optimal for achieving the highest possible interface shear resistance. The impact of dust at the interface depends on the nature of the dust material as well as the texture of the interface and the rate of tack coat applied. For very smooth interfaces, dust may assist in preventing excess tack coat forming a slip plane between the layers. Similarly, the amount of moisture and the asphalt texture influences the significance of having a wet interface. Regardless of some research findings, there is overwhelming evidence that clean and dry conditions should be targeted during construction (TRB 2012).

2.5.7.9 Trafficking

The effect of post construction traffic on the internal aggregate skeleton of an asphalt surface has been demonstrated by various researchers (Kondo et al. 2003; Holleran et al. 2008; Chen et al. 2005a). It is also beneficial in toughening of a tender asphalt mix (Tarrer & Wagh 1994). Collop et al. (2009) found that a year of trafficking increased the internal shear strength of asphalt by an average of 30%. Mohammad et al. (2010) reported that increased asphalt density resulted in increased interface shear strength, but whether the increase in density was due to compactive effort during construction or trafficking was not detailed. Similarly, Oeser et al. (2008) showed that densification of asphalt led to increased inter-particle contact and a resultant ‘hardening’ of the asphalt mix. Sangiorgi et al. (2002) suggested that a 280 kN (33%) increase in ISS should be expected after one year of highway traffic based on comparison of trafficked and untrafficked cores from a full scale pavement.

In summary, trafficking is expected to increase the density of asphalt. This would also increase the aggregate interlock across any near-surface interface. Some improvement in the interfaces shear resistance would be result, as well as increased surface layer modulus.

2.5.7.10 Interaction among factors

A number of studies have reported contradictory and conflicting conclusions with regard to the importance of various factors and conditions on the different measures of interface shear resistance (TRB 2012). Other studies have made conclusions that are counterintuitive and inconsistent with established field practices. Examples of such inconsistencies are:

- Tack coat bitumen type was a significant factor for bond strength when tested in tension but not in shear (Tayebali et al. 2002).

- Higher bond strength achieved when tack coat was omitted (Tashman et al. 2008; Lysenko 2006).
- Normal stress was not significant for shear strength (West et al. 2005).
- The presence of dust at the interface was beneficial and the presence of moisture was not detrimental (TRB 2012).
- The presence of contamination with or without tack coat, was either detrimental, beneficial or not significant, depending only on the nature of the two asphalt layers (Collop et al. 2003).

It is noted that some of the above examples are only part-conclusions or are presented out of context. Such inconsistent findings all likely stem from the complicated interaction between the various interface conditions and testing protocols. Many studies have necessarily focused on one or few factors (eg. tack coat type and rate) that impact one measure (eg. torsional shear) of a single parameter representing interface shear resistance (eg. modulus). In such studies, the full interaction of other parameters cannot be captured. One of the more comprehensive studies of factors affecting ISS was performed by West at al. (2005). It was found that the interactive parameter consisting of tack coat type, test temperature and normal pressure was statistically significant for ISS across various asphalt mixes. Some general and intuitively expected trends were also found to reverse under particular conditions. Tran et al. (2011) also reported that tack coat material, tack coat rate surface condition and tack coat curing time were all statistically significant for ISS. The specific interaction between interface texture and optimal application rate was further reinforced by TRB (2012). It was recommended that different application rates be adopted for different surface conditions, such as new asphalt, aged asphalt and milled asphalt surfaces.

2.5.8 Application

Interface shear resistance between all layers is critical to pavement performance. Where slippages have occurred, interface failure or delamination has often been demonstrated or simply assumed to be the cause. Interface shear resistance can be measured in a number of ways with a direct shear test under constant strain rate being most common. While strength (ISS) is most commonly reported, modulus/stiffness (ISM) and deformation work/energy

(ISW) can also be calculated from direct shear test results. ISM and ISW can indicate differences in interface shear resistance other than the monotonic stress at which the interface fails.

Many factors affect the level of interface shear resistance achieved in the field or laboratory. For an investigation associated with relative shear resistance between pavements of similar construction, these factors become less important than the reliability and variability of the sampling and testing.

Fatigue testing of interfaces is less common but a number of attempts to develop interface fatigue models have been made and this is a likely area of focus for the future. For a failed two layered (with interface) system a layer-interface-layer shear fatigue test would identify the weakest layer in the system. Where this is shown not to be the interface, the failures would be deemed to have occurred within the asphalt layer. Such failures are likely associated with asphalt sheer deformation or creep rather than surface layer slippage.

2.6 ASPHALT DEFORMATION AND CREEP

In some cases, lack of interface shear resistance has been shown not to be the root-cause of slippages in asphalt surfaces. Where the asphalt has remained well bonded to the underlying surface and the interface has not failed, the asphalt must have deformed horizontally. If the bond remains sound, there is no other explanation for the symptoms observed at Melbourne airport or the crescent-shaped surface cracks reported by others (Sholar et al. 2002; Horak et al. 2009a).

Most studies into permanent deformation in asphalt have focused on vertical deformation characterised by near surface rutting. Where near surface shear forces are high and asphalt binder stiffness is reduced by high surface temperatures, horizontal deformation can become a significant issue, as discussed above (2.4.4 Significance to Airport Pavements).

2.6.1 Asphalt and Response to Load

Asphalt is a complex heterogeneous material consisting of aggregates, air voids and binder (Zelelew & Papagiannakis 2012). Asphalt is used around the world in many applications including the surfacing of airport pavements (Elnasri et al. 2013).

The time and temperature dependence of bituminous binder properties has a significant impact on the response of asphalt to loading (Scarpas et al. 1997). At the extremes, asphalt is purely elastic at low temperature/fast loading and purely plastic at high temperature/slow loading (Al-Qadi et al. 2009). The definition of 'high' and 'low' temperature as well as 'fast' and 'slow' loading changes significantly with bitumen type and grade. The temperature dependent nature of asphalt stems from the inherent nature of the bituminous binder used. The temperature and time dependence of bitumen is discussed in more detail below (2.6.6.4 Bituminous Binder). Under typical service conditions (0-75°C), asphalt behaves in an elasto-plastic manner. These important factors must be considered in any pavement response analysis.

2.6.2 Asphalt Deformation

Deformation is a general term that indicates strain under loading. Many materials exhibit cumulative strain or deformation under sustained, cyclic or repeated loading. Such materials are responding in a non-elastic manner. Deformation of asphalt is generally considered to comprise (Huang 1993):

- **Total deformation**. The total maximum deformation during the loaded duration and equal to the three components detailed below.
- **Elastic deformation**. Also referred to as instant deformation, it occurs and is recovered in an elastic manner.
- **Viscous deformation**. Also referred to as delayed deformation, it represents the delay between load application and response of bituminous materials. For elastomeric modified bitumen this component of deformation may take days to recover.

- **Permanent deformation**. The unrecovered deformation after complete loading and relaxation. This deformation is cumulative over subsequent loading cycles.

Permanent deformation in asphalt surfaces is often referred to as surface layer rutting. Asphalt rutting is correctly defined as the cumulate permanent deformation of the asphalt layer(s) through incremental densification under loading (Sousa et al. 1994). True vertical deformation is often confused with shear failures that are characterised by heaving or slip circle type deformation. True rutting is free of heaving at the extremities.

The bituminous element of an asphalt mixture affects the rutting potential of the material (Stastna et al. 2007). Rutting was traditionally thought to be the result of viscous flow of the bitumen. Recent research has shown that asphalt rutting is actually the result of shear creep rather than viscous flow (D'Angelo et al. 2007).

2.6.3 Asphalt Creep

Creep is the tendency of solid materials to permanently deform slowly under sustained stress. Creep can also accumulate during repeated application of short load durations. In an asphalt mixture subject to repeated loading, creep can include recoverable and unrecoverable strains (Oeser et al. 2008). The recoverable strain component of creep is the delayed deformation that does not recover prior to the next load event. It would have been recovered if the rest period was increased. Unrecoverable strain would not recover regardless the time until the next load application.

Creep can be measured under static or repeated loading. Creep under cyclic loading, becomes incremental, cumulative or cyclic creep. To be informative, asphalt creep should always be measured under cyclic loading regimes, especially where elastomeric bitumen is being assessed (Monismith et al. 2000a). Sousa et al. (1994) stated that sustained or non-cyclic creep testing allows lock-up of the aggregate matrix and excludes dilation effects. Dilation is an important aspect of shear response in the field.

Creep is modelled in three phases (Taherkhani et al. 2007; Al-Qadi et al. 2009; Oeser et al. 2008; Ziari & Divandari 2013; Chen et al. 2005b) as shown in Figure 9:

- **Primary**. A reducing rate of strain due to toughening or repacking of the aggregate skeleton in the mixture.
- **Secondary**. A constant rate of strain during which creep progresses slowly.
- **Tertiary**. An increasing rate of strain due to instability usually associated with reduction of air voids to near-zero and aggregate dilation.

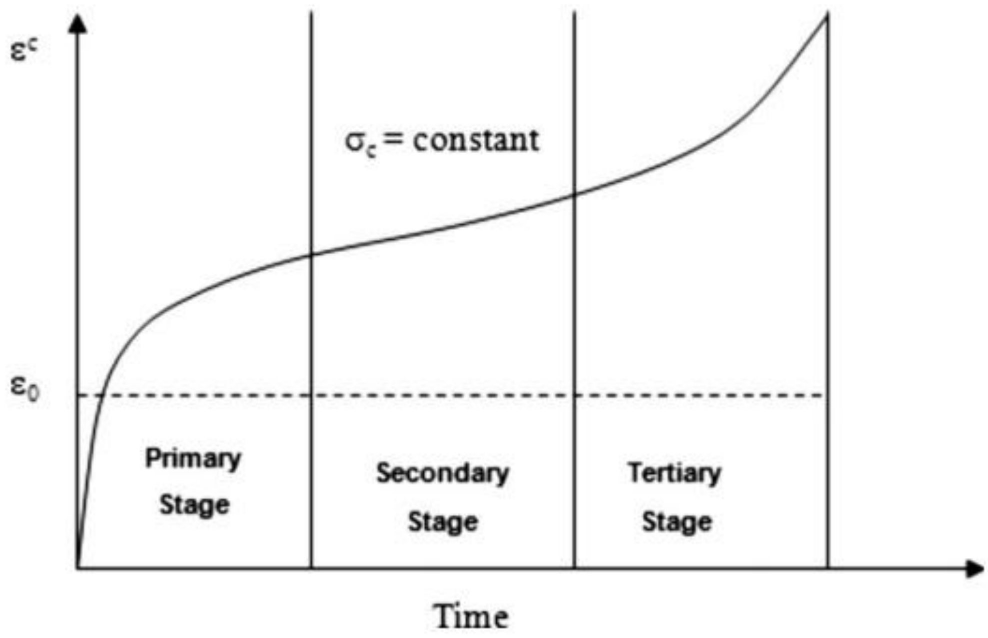

Figure 9 Phases of asphalt creep (Al-Qadi et al. 2009)

2.6.4 Asphalt Instability and Tender Mixes

Asphalt instability may occur for a number of reasons and can be short or long-term in nature (Tarrer & Wagh, 1994). Short term instability is often referred to as 'tenderness' and usually lasts only a few weeks or months, by which time bitumen/mastic stiffening hardens the mix.

Asphalt tenderness is generally associated with asphalt that is difficult to compact at the time of construction or asphalt that is slow setting (Crawford 1986). Slow setting asphalt is generally associated with slow stiffening of the bitumen but may only be evident in certain aggregate gradations (Crawford 1986). Where aggregate gradation and/or bitumen stiffness causes tender asphalt, there would be little remedy available except to wait for the bitumen to stiffen with age or to remove and replace the surface.

Long-term asphalt instability is generally attributed to aggregate grading or other characteristic that does not improve over time, but may be overcome by natural stiffening of the bitumen/mastic. Aggregate-related asphalt instability is commonly characterised by rutting and heaving of the surface (Sefidmazgi et al. 2012). The failures observed at Melbourne Airport did not include any rutting or heaving.

2.6.5 Mixture Testing

Creep and deformation testing are often performed on asphalt mixtures. This is most appropriate when the research focus is performance comparison of different asphalt mixes or characterisation of a specific mixture for further pavement analysis. Mixture testing for creep and deformation can be performed in a mechanical testing machine or under a controlled test wheel.

There are a number of scaled or controlled load wheel tests. Common machines include the Asphalt Pavement Analyzer, Hamburg Wheel Tracking Device and the French Rutting Tester (Pavement Interactive 2011; Williams & Prowell 1999). Australia commonly uses a version of what is known as Cooper's Wheel Tracker. This is similar to the Asphalt Pavement Analyzer (Emery & Mihaljevic 2008). These common scaled-load test devices are very useful for routine practical applications.

The University of Stellenbosch's Institute of Transport Technology in South Africa developed a mobile load simulator in the 1990s (Hugo et al. 2011). The current version, the Mobile Model Load Simulator Mark 3 (MMLS3) provides greater capability and flexibility for specialist of research applications and is described further below (2.6.5.2 Model Mobile Load Simulator).

Mechanical testing of asphalt mixtures may be static, monotonic, or cyclic in nature. The loading regime may be compressive, tensile or indirect tensile (Taherkhani et al. 2007). Due to simplicity and intuitive similarity to field conditions compression testing is most common with a number of simple performance tests developed and assessed.

2.6.5.1 Simple Performance Tests

The Transportation Research Board (TRB) of the USA selected and assessed a number of viable simple performance tests for asphalt (Kaloush 2001; Monismith at al. 2000b). The three most advantageous were the repeated load triaxial (returning a dynamic modulus), repeated uniaxial compression (returning a Flow Number) and static uniaxial compression (returning a Flow time) (TRB 2005).

Sousa et al. (1994) first investigated a repeated shear test for asphalt as an element of the Superpave mix design process. The Flow Number test is based around this work. The Flow Number is the number of compression cycles until the sample shows the initial signs of tertiary flow (Ziari & Divandari 2013). The Flow Time is the time until the same tertiary condition is reached, but in static compression mode. All three simple performance tests are conducted using friction breakers at the top and bottom of the asphalt samples. This is intended to ensure the samples are subject to shear rather than flexural rupture.

The Asphalt Material Performance Testing machine can readily perform the Flow Number test (FHA 2013). The coefficient of variability of Flow Number results for nominally identical samples should not exceed 20%, which is a reasonable level of repeatability (Anochie-Boetang & Maina 2012).

Uniaxial creep, similar to the Flow Time test, was used to assess steady-state deformation of two typical asphalt mixtures from the UK (Taherkhani & Javanmard 2011). This was later extended to include a monotonic triaxial assessment of the same mixtures (Taherkhani 2011). It was confirmed that at low temperatures/stresses, the asphalt behaved in a linear viscous manner. At higher temperatures/stresses, asphalt response became non-linear. Under triaxial testing at a given temperature, different mixes had a specific stress ratio that resulted in the mixture locking up and this prevented deformation from occurring (Taherkhani 2011). The reported locking up of the mixture is likely a function of the constant stress loading regime and would not be observed if a cyclic loading was applied. In earlier work it was demonstrated that simply measuring axial strain was adequate to characterise tertiary flow response of asphalt (Kaloush 2001). This allowed equipment and instrumentation to exclude the measurement of vertical strain without adversely impacting the reliability of tertiary flow characterisation.

Monismith at al. (2000b) reported to use of this simple shear test to successfully evaluate airport asphalt mixtures for San Francisco Airport where surface shearing failures had previously occurred. A cyclic 69 kPa shear stress with haversine loading of 0.1 second duration with 0.6 seconds between applications was applied. This loading was selected for consistence with other work conducted around that time (Monismith at al. 2000b). The results were well correlated with asphalt mixtures that were prone to surface shear failure under turning B747-400 loading.

2.6.5.2 Model Mobile Load Simulator

The MMLS3 is a one-third-scale, indoor accelerated loading facility and was first produced in 1997. In comprises four single wheels of tyre pressure up to 850 kPa and wheel load up to 2.7 kN. The four wheels cyclically traverse nine 100 mm diameter circular samples aligned in a track at between 1800 and 7200 load applications per hour. The test bed is temperature controlled (-5 to 60°C) and can be in a soaked or dry condition (Hugo et al. 2011).

The MMLS3 was evaluated by the Federal Highways Administration of the USA by comparing rut prediction against actual full scape rutting measured at the Westrack facility. The MMLS3 was assessed as being suitable as long as key environmental conditions were measured and the loading appropriately scaled (Epps et al. 2001).

Various researchers have used the MMLS3 in a broad range of applications. Emery & Mihaljevic (2008) used MMLS3 to predict rutting in a Dubai airport runway with excellent results where the Cooper's wheel tracker was unsuccessful. MMLS3 was used to compare bitumen performance for Sydney Airport (Horak et al. 2011). A major road in Namibia used the MMLS3 to assess the value of adding lime filler to asphalt as an anti-stripping treatment as well as to assess the effectiveness of compaction (Hugo et al. 2004). Molenaar et al. (2004) used MMLS3 to discriminate between asphalt mixture performance during the planning phase of a runway rehabilitation at Johannesburg Airport in South Africa. Kruger & Horak (2005) ranked various asphalt mixes in wet and dry test conditions at various temperatures and statistically compared MMLS3 rutting with mix parameters.

MMLS3 is considered by some as simply an ‘alternate’ wheel tracking machine. In reality, it is closer to a scaled-down accelerated load facility. Its key advantages over conventional wheel tracking devices lie in the ability to scale the load and tyre pressure and to test at a broad range of temperatures, in both soaked and dry conditions. Like other wheel trackers and many accelerated load facilities, the MMLS3 does not have the ability to impart braking forces.

2.6.6 Asphalt Mix Constituents

Asphalt is a complex heterogeneous material consisting of aggregates, air voids and bitumen as well as added (active) fillers (Zelelew & Papagiannakis 2012). Each of these constituents plays an important role in defining the overall mix characteristics and response to load. The combined fine aggregate, filler and bitumen is commonly referred to as the mastic (Pérez-Jiménez et al. 2008). The importance of the mastic characteristics in determining the mix performance is universally acknowledged (Delaporte et al. 2007; Tashman et al. 2005; Elnasri et al. 2013). The performance of the asphalt mastic provides a reliable indicator of asphalt mixture performance, when tested within a suitable common coarse aggregate skeleton.

Asphalt mixture constituents become more applicable when the research aim is to compare similar asphalt mixes with just one key component changed or where an explanation is sought for known poor mixture performance of nominally identical asphalts.

All the aggregates under investigation were basaltic in origin. Basalt is generally a hard, dark coloured and fine grained igneous rock. Basalt is a highly desirable and commonly used asphalt aggregate (Ibrahim et al. 2009). The use of Basalt aggregates is generally not problematic.

2.6.6.1 Coarse Aggregate

While the bituminous mastic dominates many mix properties, both the mastic and the aggregate skeleton are important to asphalt performance (Hassan et al. 2012). In fact, by mass, aggregate comprises some 95% of asphalt structure and can therefore have a significant impact on the mechanical properties of a surface layer (Chen et al. 2005a).

Aggregates are complex particles of minerals and ions (Labib et al. 2007). Aggregates are routinely characterised by a combination of the consensus properties (angularity, size and shape) as well as their source properties (abrasion resistance, strength, deleterious material content and chemical composition) (Bessa et al. 2012). Chemical composition, commonly estimated by petrography, is not well understood by engineers but can be of great importance to asphalt mixture performance and durability.

Petrography is the optical analysis of thin sections of rock by experienced technicians and interference of the material properties based on experience. It is necessarily limited to the sections that are inspected (Amaral et al. 2006). Chemical composition is analysed by X-Ray Diffraction (XRD) which is a semi-quantitative analysis of the chemical composition of powdered (30 μm and below) rock samples which, following calibration of equipment and analysis software, is very accurate and assessed the whole of the powdered sample (Amaral et al. 2006).

Consensus properties of shape and angularity of the aggregate particles as well as the overall combined skeleton are important for asphalt mixtures (Holleran et al. 2008; Shen & Yu 2011). The aggregate skeleton is determined by the coarse aggregates. The angularity of the fine particles has greater influence on asphalt performance than the angularity of the coarse aggregate particles. However, coarse aggregate fractured face counts do contribute significantly to deformation resistance, stability and stiffness of asphalt mixtures (Kandhal et al. 1991). Coarse aggregates shape is commonly characterised by the parameters; form, angularity and texture (Tashman et al. 2007; Masad & Button 2000). The scale of each parameter depends on the size of the particle being characterised (Bessa et al. 2012).

The skeleton of an asphalt mix is determined by the structure and gradation of the aggregates, primarily the coarse fractions. These properties can have a significant impact on the deformation resistance of the mixture (Motamed & Bahia 2011). The importance of air void distribution (Kutay et al. 2010; Masad et al. 1999a) and grading (Farcas 2012) have been established.

The aggregate skeleton within asphalt can be measured directly through microstructure assessment or via bulk material characteristics using macrostructure measurements (Chen et al. 2005b). For microstructure assessment two main approaches are commonly adopted:

- **X-Ray Computer Tomography (XCT)**. XCT provides an accurate 3D assessment of an aggregate structure. XCT is able to differentiate between a broad range of engineering materials with an accuracy of up to 5 μm (Tashman et al. 2007). Due to its non-destructive nature, XCT can be used to assess the same sample before, during and after wheel tracking or other performance test. It also offers the advantage of being able to measure air void distribution (Masad et al. 1999a).
- **Digital image analysis**. Digital image analysis is well established within the study of geomechanics of materials such as clays (Masad & Button 2000). Digital image processing includes three major steps; image acquisition, image processing and image analysis (Tashman et al. 2007). Common software can rapidly calculate the number of contact points, aggregate orientation distribution and aggregate segregation measures (Coenen et al. 2012). Requiring only a digital camera and software, digital image analysis offers an economical and rapid assessment of the aggregate skeleton, but only on a 2D basis.

Significant research has been conducted on the structure of asphalt skeletons using both techniques. Image analysis was used by Hamzah et al. (2013) to compare the aggregate skeletons produced by different compaction methods. Lv et al. (2011) analysed the voids, aggregate orientation and segregation of numerous asphalt mixes using similar techniques. In contrast, Masad et al. (1999a) used XCT to assess the air voids distribution and segregation of various asphalt mixtures prepared with various compaction methods. The effect of different compaction methods on asphalt structure was also investigated by Kutay et al. (2010) using XCT. Tashman et al. (2005) used XCT to characterise the aggregate structure as a means of verifying a viscoplastic model for asphalt deformation.

Research has shown asphalt performance to be affected by variation in the orientation and spatial distribution of coarse aggregate particles (Coenen et al. 2012). The number and length of contact points is known to influence asphalt shear strength (Masad et al. 1999b) as does the distribution of the air voids within the sample (Masad et al. 1998). Coarse and fine aggregate angularity provides an indication of aggregate internal friction and deformation resistance (Holleran et al. 2008). For asphalt samples of identical mix design and construction process, changes in the orientation of the particles within the aggregate skeleton can explain differences in performance (Chen et al. 2005b).

Aggregate orientation cannot be expressed as a single value or described by a single parameter (Hunter et al. 2004). Many researchers have used a combination of average angle of inclination ($\hat{\theta}$) and vector magnitude (Δ) (Masad et al. 1998; Hamzah et al. 2013; Tashman et al. 2007; Bessa et al. 2012; Chen et al. 2005b; Reyes & Zanzotto 2007; Lv et al. 2011). These concepts were advanced to their current form by Curray (1956) and are defined in Equations 10 and 11. Δ varies from 0 to 100 where 0 represents a completely random distribution of aggregate particle orientation and 100 represents all particles being in the same alignment. $\hat{\theta}$ varies from 0° to 90° while θ_k ranges from -90° to 90° (Masad et al. 1998).

$$\Delta(\%) = \frac{100}{n}\sqrt{\left(\sum sin\,2\theta_k\right)^2 + \left(\sum cos\,2\theta_k\right)^2} \quad \text{Equation 10}$$

$$\hat{\theta}(°) = \frac{\sum|\theta_k|}{n} \quad \text{Equation 11}$$

Where n = the number of aggregate particles in the sample section

θ_k = angle of inclination of the major axis of each aggregate particle

With the ready availability of digital cameras and computational software to analyse the images, much effort has recently been made assessing the orientation of aggregate particles resulting from different compaction methods. These efforts peaked in response to the introduction of the Superpave gyratory compactor in the USA (Coenen et al. 2012). Studies have assessed aggregate orientation with respect to the horizontal and vertical axis, as well as radially (for circularly compacted samples prepared in the lab).

Compaction effort has been shown to significantly change the aggregate orientation and structure (Hamzah et al. 2013). For example, with increasing gyrations of a gyratory compactor, the average angle of inclination reduced from 41 to 33 over 100 cycles and then increased again to around 38. At the same time the vector magnitude increased from 15 to 44 and then dropped to 22 (Masad et al. 1999a). The mode of compaction is also significant. Lv et al. (2011) reported average angles of inclination of 33 to 36 for gyratory compacted samples and 35 to 47 for vibratory compacted samples of various grading envelopes. In the same study, vector magnitudes of 25 to 30 for gyratory compacted samples, but only 15 to 25 for vibratory compaction, were reported. Vibratory compacted values of average angle and vector magnitude were concluded to be more sensitive to grading changes than results from gyratory compacted samples were.

2.6.6.2 Fine Aggregate

Fine aggregate is generally considered to be comprised of sand and dust sized particles. That is, all mineral material passing a 4.75 mm or 2.0 mm sized sieve, depending on the soil classification system being used (Holtz & Kovacs 1981). Fine aggregate generally excludes any added chemical or active fillers. The fine aggregate in an asphalt mixture is commonly sourced from natural or manufactured sources. Natural sources include river sands or sand pits. Manufactured sands are generally a by-product of crushing quarried materials to manufacture coarse aggregates and graded crushed rock. Manufactured sands are commonly referred to as ‘dust’ as they are the captured as airborne particles generated during quarry crushing operation.

The fine aggregate shape and packing properties impact on asphalt deformation resistance (Holleran et al. 2008). The fine aggregate shape contributes more to asphalt performance than the large aggregate shape does. The benefit of using angular fine aggregate has been demonstrated by many researchers (Kandhal et al. 1991). Shape and packing are routinely assessed by aggregate angularity and packing. ASTM D3398 provides a sound and common basis for this assessment (Holleran et al. 2008; Chen et al. 2005a).

ASTM 3398 is a time consuming test as the aggregate is fractionated and each fraction is tested prior to calculation of weighted average particle index. Kandhal et al. (1992) demonstrated that testing only the major fraction was a reliable indicator (R = 96% for a unity regression) of the overall fine aggregate particle index. This approach allows significant time saving. Other tests, such as the fine aggregate angularity, do not discriminate between fine aggregates of differing performance when incorporated into asphalt mixtures (Masad & Button 2000).

Although natural sands commonly have more rounded particles than manufactured sands, there is a significant overlap (Kandhal et al. 1991). Shape and texture of particles was found to be a more reliable differentiator of rounded and angular sands than generic categorisation as ‘manufactured’ or ‘natural’ (Kandhal et al. 1992). The detrimental nature of excessive natural (rounded) sand content has been well established (Masad & Button 2000).

2.6.6.3 Chemical Fillers

Fillers are added to asphalt mixtures to improve density and strength (Wang et al. 2011) through both physical and chemical interactions with the bitumen (Liao et al. 2013). Fillers stiffen bitumen by thickening it and reducing viscous flow (Bianchetto et al. 2007). They also reduce temperature susceptibility (Zoorob et al. 2012) and promote improved bitumen-aggregate adhesion (Lesueur et al. 2013). Fillers can be chemically active or inert minerals. Common fillers include limestone dust, hydrated lime, fly ash, general purpose or blended cement as well as sandstone and granite dusts (Liao et al. 2013). While a range of fillers are commonly incorporated into asphalt, their specific advantages and risks are not well understood (Pérez-Jiménez et al. 2008).

Different filler types and sources have very different chemical compositions as well as different shapes, densities and voids (Bryant 2005). The interaction between filler and bitumen as well as the resulting contribution to asphalt performance is prohibitively variable (Little & Petersen 2005).

The first documented investigation of filler and bitumen interaction was undertaken in 1905 (Faheem et al. 2010). Since that time significant research on filler properties, their interaction with bitumen and impact on asphalt performance has been undertaken. In 1947 Rigden's void factor was introduced and it was suggested that the voids content was the only filler property of importance, with chemical composition being irrelevant (Faheem et al. 2010). This would have been difficult to demonstrate as filler content and chemical composition of fillers are highly correlated and therefore confounded. Wang et al. (2011) measured the Rigden voids, fineness modulus, Methylene Blue Value (MBV) and Calcium Oxide (CaO) contents of various filler types and sources and found all four properties to be independent of each other. It was concluded that Rigden voids was the best predictor of filler effect on mastic creep performance and that the MBV value was not significant.

In some contrast, Faheem & Bahia (2010) found that Rigden voids, particle size distribution and CaO were all statistically significant predictors of bitumen stiffening effect of fillers. It was also found that the stiffening effect of fillers was not consistent across different bitumen types, including acid (PPA) modified bitumens.

Faheem et al. (2010) reviewed and tested 30 diverse fillers. The Rigden voids content ranged from 26-48. Hydrated lime was around 37. Bryant (2005) also tested a number of fillers and introduced the concept that filler may be absorbing bitumen in its voids, reducing the amount of 'effective' bitumen available to bind the aggregate together. It was determined that voids contents in compacted fillers exceeding 38% were problematic at typical asphalt binder contents.

The Cantabro losses test (UCL) was developed at the University of Catalonia in Italy to assess mastic effectiveness and durability by exposing the asphalt mixture to an abrasive condition and measuring the reduction in sample mass due to the breakdown or erosion (Bianchetto et al. 2007). The test was concluded to be an effective way of determining the filler content at which the mastic flexibility and durability started to degrade, resulting in accelerated loss of asphalt mass.

Of the various fillers, hydrated lime is most commonly specified in Australian airport asphalt. Lime became a common filler for asphalt in the 1970s. Lime was specified and included for all mixes used at Melbourne Airport considered in this investigation. Lime is a fine material with a particle density around 2.2 t/m^3 but an apparent density more typically around 0.3-0.8 t/m^3. This results in a surface area typically an order of magnitude greater than many other fillers (Lesueur et al. 2013). Lime is an effective asphalt filler as it promotes anti-stripping properties by reducing moisture sensitivity of asphalt mixes (Little & Epps 2001). Lime also reacts chemically to harden the bitumen while reducing the rate of post-production oxidation (Lesueur et al. 2013).

The assessment of the effect of lime filler on improved asphalt performance is generally based on performance testing before and after a short-term conditioning such as the tensile strength ratio (Little & Epps 2001). The conditioning commonly includes temperature changes and moisture exposure.

A number of investigations have clearly shown the benefits of using lime as filler. Ibrahim et al. (2009) found an increase in bond strength between bitumen and basaltic aggregates when lime was mixed into the bitumen. Lime dust significantly reduced creep deformation in various asphalt mixes (Abo-Qudais & Al-Shweily 2007a). Lesueur et al. (2013) demonstrated an increase in asphalt durability and life extension of two to ten years with the additional of 1.0-1.5% of lime filler. Bianchetto et al. (2007) reported significant reductions in bitumen ageing with even small percentages of added lime.

2.6.6.4 Bituminous Binder

Bitumen is a non-crystalline viscous material comprised of 80% carbon and 15% hydrogen in a complex mixture (Shell Bitumen 2015). It is soluble in organic solvents but not in water (BP Bitumen 2007). Of the 1,500 crudes oil sources in the world less than 100 are suitable for bitumen production and of those only very few are able to produce bitumens that meet Australian specification requirements (Neaylon 2013).

Conventional (unmodified) paving grade bitumen is the residue from the second distillation of crude oil. The first distillation is performed at atmospheric pressure at 350-380°C and the second distillation occurs under vacuum at 350-425°C (Shell Bitumen 2015). The unmodified bitumen is then either blown with hot air, modified with polymers, has oils added or is extended with propane precipitated asphalt and other products. Commonly a combination of these processes is used. Bitumen for industrial applications undergoes additional processing (BP Bitumen 2007). It could therefore be suggested that bitumen is the least improved version of the waste generated from the waste generated by the initial generation of petroleum gas, fuel, diesel and kerosene from crude oil.

The temperatures, pressures, blowing and other processes depend significantly on the crude oil source as well as the amount of gas, oil and other petroleum products extracted during the process (Shell Bitumen 2015). These variables subsequently impact on the properties of the resulting unmodified bitumen (Neaylon 2013). As does the crude oil source (Harnsberger et al. 2011).

It has long been acknowledged that bitumen properties can change and migrate over time and that multiple batches or shipments from the same source of crude will have variability (Abraham 1962). For example, bitumens manufactured from light crudes are believed to be more susceptible to high temperature asphalt shear creep than those from heavier crudes (Holleran et al. 2014). Crude source variability may require alternations and significant changes in the refining process. These processing changes could further alter some properties of the resulting paving grade bitumen in order to meet the applicable specification requirements.

Following the introduction of additional crude sources into New Zealand refineries, Holleran & Holleran (2012) identified that simply blending the various bitumens to the specified penetration was not sufficient to guarantee performance in hot climates, under heavy traffic. It was found that even small percentage changes in the crude blend could have significant impact on rheological structure and therefore performance (Harnsberger et al. 2011). Routine rheological analysis and performance testing of binders was introduced to New Zealand to address this risk (Holleran et al. 2014). In Australia, underlying (or zero shear) viscosity has been the recent focus of researchers addressing bitumen performance. Urquhart et al. (2010) investigated the relationships between bitumen consistence and underlying viscosity with asphalt rutting. No consistent relationships could be established across various bitumen types. This demonstrates the potential for variability of field performance within binders that are considered ‘similar’ based on a specific laboratory grading-type test.

In Australia, asphalt paving bitumens have been manufactured to a number of standards. Prior to 1997 Australian paving grade bitumens were produced to a penetration based specification. Since the introduction of AS 2008 in 1997 Australia adopted a viscosity (at 60°C) based specification. In 2010 a framework for the specification of polymer modified binders was introduced in Australia. This originally included the specification of Multigrade bitumen. In 2013 the Australian bitumen for asphalt paving specification (AS 2008) was revised. It now includes Multigrade bitumen while polymer modified binders remain under the framework document AP-T41/06 of 2006 (Neaylon 2013). The revision of AS 2008 considered alternate grading systems for bitumen, including potential adaptation of the USA’s Performance Grading (PG) system (Neaylon 2013). This proposal was rejected citing work by (Tredrea 2007). However, Tredrea (2007) assessed the original high temperature PG parameter. As detailed below (2.6.6.7 Multiple Stress Creep Recovery) the original PG parameter was replaced in 2007 for all the reasons identified by Tredrea (2007). The retention of a viscosity based grading system for Australian bitumen is based on the belief that viscous flow in hot temperatures is the key performance parameter. This is quite distinct, however, from shear creep, which has become the focus of bitumen grading in the USA. Controlling viscous flow potential does not guarantee shear creep performance (D’Angelo et al. 2007; Holleran et al. 2014). As recently as 2010 Australian road authorities investigated the relationship between various bitumen properties and permanent deformation in asphalt mixtures (Austroads 2010). Despite significant effort to link Dynamic Shear Rheometer (DSR)-derived $|G^*|/\sin \delta$ and zero shear viscosity parameters to rutting, the USA’s Multiple Stress Creep Recovery (MSCR) test was not explored or even acknowledged.

There is a widely held perception that bitumen properties have changed and performance has declined over the years (Button & Epps 1985; Emery 2005b;

Oliver 2009; Holleran & Holleran 2010; Holleran et al. 2014). There have certainly been changes in crude oil sources (Holleran & Holleran 2012; Emery 2005a) and associated rheological properties (Oliver 2009; Holleran et al. 2014). This is the result of refineries using new technologies to extract more high-margin product from crude oil sources of reducing quality and increasing variability. This has led to a lack of confidence in non-performance based specifications and increased the use of rheological bitumen testing (Baumgardner & D'Angelo 2012). The traditional binder testing regimes were largely empirical in nature and lack linkage to performance in the field (D'Angelo 2009a). In response to these concerns, the USA introduced PG grading of binders in the 1990s.

The contribution of the bitumen to asphalt performance is significant (Motamed & Bahia 2012). Otherwise identical asphalt mixes with different bitumen types, or even two sources of nominally identical bitumen, can respond differently due to differences in the complex chemical composition (Harnsberger et al. 2011). This suggests that compliance with specifications cannot be assumed to imply adequate performance in the field.

Bitumen response is inherently time and temperature dependent (Delgadillo et al. 2012). This time and temperature dependence is not consistent across all bitumen types. The type of bitumen is therefore significant in its characterisation. Australian airport asphalt has traditionally utilised C320 or a number of elastomeric polymer modified binders (Emery 2005a). Since the 1990s, acid (PPA) modified Multigrade (M1000) has become common for Australian airport asphalt.

PPA is added to bitumen as an economical improver of high temperature bitumen response without adversely impacting low temperature performance (Li et al. 2011). The primary concern for PPA bitumen is the lack of understanding regarding the mechanism of chemical modification process (Domingos & Faxina 2015). The ongoing chemical reaction and associated changes in response with time is also of concern. Baumgardner et al. (2005) presented a proposed mechanism of interaction between PPA and bitumen. It was concluded that the mechanism was different for different binders and sometimes affected the dispersed maltenes while in other bitumen sources it affected the matrix of asphaltenes. Such difference in chemical mechanisms could explain variable performance in PPA modified asphalts of the same nominal grade, but from different crude oil sources or refinery processes. A secondary concern is the potential for acid neutralisation by alkaline fillers such as hydrated lime. For a period of time this concern prompted airport asphalt specifiers in Australia to require non-acidic flyash to be used in place of hydrated lime in asphalt mixtures containing PPA modified bitumen. Miknis & Schuster (2009) investigated the addition of lime to PPA modified bitumen and concluded that in some circumstances, the chemical markers indicative of PPA modification could no longer be detected after mixing with hydrated lime. Despite this, Australian airport asphalt specifiers have continued to prefer hydrated lime as the active filler.

In 2009 a major workshop on the use and issues associated with PPA bitumen modification was held in the USA (TRB 2009). Key conclusions were the crude oil source dependence of the effects of PPA modification, the benefits of combining PPA with PMB and other modifiers and the unusual ability of PPA modification to increase temperature range of acceptable performance for a given binder. Each bitumen source has a particular useful temperature range based on its crude oil source. Under the USA's PG system, it is the difference between the high and low performance temperatures. Air blowing and polymer modification moves this performance window up and down but does not increase its width. By altering the high temperature response without significantly changing the low temperature response, PPA allows the magnitude of the useful temperature range to be increased (TRB 2009). This is highly advantageous in environments with high temperature changes between summer and winter.

A range of factors impact how bitumen will change with time after it is tested and released as a product that meets all specification requirements. The rheological composition, refinery processes and in-service ageing are two key factors. The rheology of bitumen is complex but is generally described in terms of Saturates, Aromatics, Resins and Asphaltenes (SARA) content (Holleran & Holleran 2010; Oliver 2009). SARA analysis by Iatroscan (a thin-layer chromatography-flame ionization detection system) has been found to be useful for discriminating between different crude oil sources utilised for the manufacturing of nominally identical bitumen samples (Holleran & Holleran 2012).

Binders harden due to chemical ageing, steric hardening, oxidation and loss of volatiles (Airey 2003; Wu et al. 2007; Bianchetto et al. 2007). Ageing is often measured via hardness. The hardening of bitumen during asphalt production may only be around 30% of the hardening expected over the life of the asphalt (Crawford 1986). Oliver 2009 found that ageing also significantly affected the rheological composition of bitumen.

There are a range of tests for the assessment of bitumen ageing in the laboratory. The Rolling Thin Film Oven (RTFO) is the most common accelerated ageing process (Airey 2003) and the Australian method is detailed AS 2341.109. The RTFO conditioning process is intended to simulate the ageing that would occur during asphalt manufacturing (Wu et al. 2007). Other ageing methods are used for simulation of in-service ageing (Airey 2003).

Within an asphalt mixture the interaction between the bitumen and mineral components becomes equally important as the behaviour of the bitumen itself. Interaction with coarse aggregate is characterised by the adhesion to aggregate particles that can be adversely impacted by moisture damage. Such damage is commonly referred to as bitumen stripping and is generally assessed by bitumen-aggregate compatibility testing. The study of interactions between the fine aggregate, filler and bitumen is generally simplified by characterisation of the mastic as a whole.

2.6.6.5 Bitumen-Aggregate Compatibility

The long-term stability of the adhesion between the bitumen and the aggregate particles is a key to asphalt durability (Bhasin & Little 2007). Poor adhesion between the bitumen and aggregate will make the asphalt susceptible to moisture damage, or stripping, in the presence of water (Abo-Qudais & Al-Schweily 2007). The presence of moisture within the mixture has been demonstrated to impact both the adhesion and cohesion properties of the aggregate-bitumen interface (Partl et al. 2008). This makes stripping an important distress for asphalt materials (Mehrara & Khodali 2013).

Mechanisms leading to moisture damage in asphalt mixtures include loss of cohesion within the bitumen film, loss of adhesion between the bitumen and the particles and breakdown of the particles leaving the bitumen free within the mixture (Moraes et al. 2011; Howson et al. 2012). True stripping is a failure by adhesion. Cohesion failures are not stripping but are the emulsification of bitumen in the presence of moisture (Sansefidi et al. 2014). Adhesion failures may stem from mechanical adhesion loss, chemical reaction at the interface or physio-chemical adhesion loss as a result of bitumen free energy (Bhasin & Little 2007). Adhesion failure can be modelled using mechanical, chemical, weak boundary and thermodynamics theories of adhesion (Moraes et al. 2011).

Moisture damage susceptibility is usually measured by a ‘whole of mix’ response (Canestrari et al. 2010). This approach fails to provide insight into the micro mechanisms and usually relies on the replication of long term moisture damage via accelerated laboratory conditioning. Other indicators of stripping include bitumen-aggregate interface testing (eg. pull-off tests) (Mehrara & Khodaii 2013).

The methylene blue (MBV) test is performed on the fines of a given aggregate source as an indicator of the presence of deleterious clays. MBV testing is not definitive and has led to the rejection of highly suitable fine aggregate sources (Lysenko 1991). Rickards & Gabrawy (2003) used beam bending and suggested it as a more reliable discriminatory assessment of stripping potential. Taking an adhesion approach, Canestrari et al. (2010) developed a controlled pull-off test to assess bitumen-aggregate compatibility.

The dominant routine test for moisture susceptibility in asphalt is the Tensile Strength Ratio (TSR), which is determined by the modified Lottman test. TSR measures the strength of the asphalt under indirect diametrical tension, before and after conditioning. The conditioning includes freeze and thaw as well as wet and dry cycles. An optional extended conditioning cycle is also allowed for more severe conditions.

In Australia, TSR is used by some jurisdictions for road pavements and is often tested for airport asphalt for information purposes. The process is documented in Austroads test method AG:PT/T232. This is based on the ASTM and AASHTO versions of the same general method. Testing is performed at 8% air voids and 25°C. Because of the destructive nature of the test, different samples of nominally identical mix are tested before and after conditioning. Inter-sample variability is indirectly considered with three replicates performed and the average value reported.

To overcome issues associated with the use of different samples for pre- and post-conditioning results to determine the TSR, Nosler & Beckedahl (2000) recommended a sub-maximal modulus ratio instead of a strength ratio. This would allow the same specimens to be tested before and after conditioning.

Australia also uses a plate stripping test for aggregate-bitumen compatibility. However, this is generally isolated to the compatibility of bitumen and aggregate for sprayed sealing (also called chip sealing and surface dressing) works (Lysenko 1991).

Aggregates have commonly found to have more influence on bitumen-aggregate adhesion than bitumen source (Labib et al. 2007; Hefer et al. 2007; Moraes et al. 2011). Aggregates are often hydrophilic making them more susceptible to stripping (Howson et al. 2012; Lysenko 1991). Rickards & Gabrawy (2003) suggested that at near saturation, even the most hydrophobic aggregate will likely suffer from stripping in the continuous presence of moisture during repeated loading.

Some form of anti-stripping agent, is recommended for hydrophilic aggregates (Abo-Qudais & Al-Schweily 2007b). Acid (PPA) modification of bitumen has been demonstrated to improve stripping resistance, especially for hydrophobic aggregate (Moraes et al. 2011). As described above (2.6.6.3 Chemical Fillers) lime is a highly effective and common anti-stripping agent in asphalt mixes. It has been shown to provide better anti-stripping properties than liquid anti-stripping agents (Little & Epps 2001; Abo-Qudais & Al-Schweily 2007b).

2.6.6.6 Asphalt Mastic

Asphalt mastic is commonly defined to be the combined bitumen, filler and fine aggregate particles (Pérez-Jiménez et al. 2008). There are varying definitions of the maximum particle size that constitutes the mineral component of the mastic. Delaporte et al. (2007) stated 100 microns while Little & Petersen (2005) proposed 74 microns. Liao et al. (2013) and Muraya et al. (2009) both nominated 63 microns. Australian practice uses 75 microns as the ‘fines’ and therefore the maximum size of the mineral component of mastic. These different definitions are based on the standard sieve sizes used in aggregate grading analysis in various jurisdictions.

What is in complete agreement is the importance of mastic to asphalt performance. Delaporte et al. (2007) and Qiu et al. (2013) both suggested mastic is the ‘real’ binder in asphalt. Tashman et al. (2005) supported this by stating that the micro-constituents governed behaviour of the overall mix. Testing mastic will provides greater insight into asphalt performance than testing bitumen (Elnasri et al. 2013). As Muraya et al. (2013) found, mastic has more impact on asphalt response of dense graded, high binder content mixes than it does in stone-to-stone mixes, such as stone mastic and porous asphalt. Airport asphalts are usually specified to be dense graded with high binder contents and rely heavily on mastic performance to resist stresses and deformation (Emery 2005a). It follows that mastic properties are critical for typical airport asphalt mixtures.

Despite this agreement regarding importance, less is known about mastic response than that of binders (Liao et al. 2013). Faheem & Bahia (2010) explained that mastics of seemingly similar constituents can behave significant differently. This can only be explained by physio-chemical interaction between the bitumen and mineral elements. Such interactions cannot be assessed by considering the bitumen and mineral components separately.

Mastic can be characterised in a number of ways. DSR temperature/frequency sweeps have been used to compare binders and the resulting mastics (Pérez-Jiménez et al. 2008; Faheem & Bahia 2010; Liao et al. 2013; Qiu et al. 2013). Delaporte et al. (2007) used a similar annular shear rheometer. In contrast, Pérez-Jiménez at al. (2008) adopted the Spanish UCL (Cantabro losses) of the asphalt mixture to assess mastic durability. Tashman et al. (2005) also assessed the impact of various mastics on the whole mixture but used triaxial testing of asphalts at various strain rates. Muraya et al. (2005) used confined and unconfined monotonic compression. When testing the whole of asphalt mixture with different mastics, the challenge is isolating the change in mastic properties. This requires overall grading and other factors to be maintained consistent for each bitumen-filler-aggregate combination.

Like bitumen, mastic exhibits plastic, elastic and viscous properties that are inherently temperature dependent (Drescher et al. 2010). Creep and recovery type testing is therefore well suited to mastics. Elnasri et al. (2013) used DSR based creep and recovery to assess various filler concentrations in mastics. Clopatel & Bahia (2012) also used creep and recovery to assess mastics using the new PG criterion (MSCR). The MSCR and its application to bitumen and mastic testing are detailed below (2.6.6.7 Multiple Stress Creep Recovery).

The ratio of filler to bitumen in mastic has been shown to be critical. As the filler portion increases, the mastic stiffens (Pérez-Jiménez et al. 2008; Qiu et al. 2013). Liao et al. (2013) found that the filler portion had a greater impact on mastic response than filler type did. Little & Petersen (2005) demonstrated that filler type and portion had different effects on different bitumen sources. Using a range of bitumen, mastic and mixture tests, it was found that a good relationship existed between filler:binder ratio and mixture creep performance (Ping et al. 2013).

Delaporte et al. (2007) found the maximum particle size of fillers to be of little importance for mastic behaviour. It was also found that the relative effect of filler was dependent on the temperature and frequency of loading. This would reflect the change in relative contributions of bitumen and mineral components to the stiffness of the mastic as the bitumen viscosity was reduced at higher temperatures.

Bitumen type was found to be important for mastic response, with PMB and non-PMB binders producing significantly different mastics (Bianchetto et al.

2007; Faheem et al. 2010). Ageing of the bitumen has been found to impact mastic dynamic modulus in a consistent manner regardless of filler type and portion (Faheem et al. 2010).

UCL testing (Cantabro losses) of mastics showed that below a critical concentration, the filler type was not significant. It was also found that fillers with higher critical concentrations are more thickly coated in bitumen and therefore are more resistant to the UCL test (Pérez-Jiménez et al. 2008). At higher filler portions, the mastic became fragile and Cantabro losses increased (Bianchetto et al. 2007). It is therefore important to keep filler contents below the critical concentration. In Australian airport asphalts, the bitumen:filler:aggregate ratio is generally around 6:1:6. It can be as high as 6:2:6 to maintain overall aggregate grading where the dust/sand sources are void of material passing 75 microns.

2.6.6.7 Multiple Stress Creep Recovery

Linear or Newtonian behavior is defined as a linear stress-strain response relationship while non-linear (or non-Newtonian) behavior is characterised by stress being strain-rate dependent (Zelelew & Papagiannakis 2012). At stress levels below 2 kPa, bitumen behaves in a linear manner. At higher temperatures and stress levels, non-linear behavior is commonly observed (Motamed & Bahia 2011). This stress dependence is now a commonly accepted property of bitumen. This adds complexity to characterisation and performance modelling (Zoorob et al. 2012).

The non-linear response of bitumen prevents linear viscoelastic models from accurately predicting permanent strain in bitumen (Masad et al. 2009). This explains a lack of correlation between linear models of bitumen response and field performance (D’Angelo et al. 2007). The accuracy of modern FE methods of pavement modelling relies on non-linear characterisation of materials that exhibit such behaviour. A method of non-linear characterisation of bitumen was therefore of high importance (D’Angelo 2009a).

The US Strategic Highway Research Program (SHRP) was initiated in 1987. Of the $US150 M budget, $US50 M was allocated to asphalt mixtures (Tredrea

2007). This project led to the introduction of the Superpave asphalt design method. Part of the Superpave system was the characterisation of binders by the PG system. The original parameter used for high temperature grading of bitumens was the DSR derived $|G^*|/\sin\delta$. The PG system also assesses fatigue cracking (intermediate temperature) and brittle fracture (low temperature). However, for most bitumen supplies, these requirements are easily exceeded (Holleran et al. 2014). The shear resistance at high temperature is the most common difference between various bitumens under the PG system of grading. Low temperature performance is of low importance for airport asphalt. Airport pavements are generally stiff and thick and traffic repetitions are low compared to road pavements. Fatigue cracking and brittle fracture of asphalt is not a common failure mode for airport asphalt.

The original USA Superpave system for asphalt included assumptions around linearity that did not reflect observed behaviour (TRB 2001; Masad et al. 2009). The original Superpave parameter, based on complex modulus and phase angle, $|G^*|/\sin\delta$, is measured at low strain during oscillatory loading in the DSR (Santagata et al. 2013). A number of studied consistently demonstrated the inadequacy of the $|G^*|/\sin\delta$ criteria for bitumen performance characterisation (Santagata et al. 2015). Tredrea (2007) provides a very good explanation and analysis of $|G^*|/\sin\delta$, its limitations and inappropriateness for polymer modified binders. Masad et al. (2009) clearly showed that binders with similar $|G^*|/\sin\delta$ PG grade could exhibit very different permanent strains under non-linear creep testing. As described in a detailed review of bitumen characterisation, this approach assumes that bitumen behavior is not impacted by film thickness or sample size/shape and the bitumen is assessed within the linear viscoelastic response range (TRB 2001).

In 2001, Gv, a parameter derived from a fixed stress repeated creep test, was proposed to replaced $|G^*|/\sin\delta$ as the Superpave high temperature PG criterion (TRB 2001). This was further developed to a multiple stress test which initially included 11 stress levels but was later reduced to two stress levels (0.1 and 3.2 kPa). This became known as the MSCR (D'Angelo et al. 2007).

The MSCR was developed to be performance-based and easily performed in the laboratory (FHA 2011). The MSCR is blind to modification and site in the non-linear response domain, which made it an attractive replacement for the |G*|/sin δ (D'Angelo et al. 2007). The MSCR test, as detailed in AASHTO TP 70-12, formed the basis of the high temperature PG grading detailed in AASHTO MP 19-10 (DuBois et al. 2014) which was replaced by AASHTO M332-14 in 2014. MSCR results were validated against Accelerated Loading Facility (ALF) and field performance monitoring as part of its acceptance into the Superpave regime (D'Angelo et al. 2007). During ALF trials, the MSCR results showed consistently better agreement with measured permanent deformation than |G*|/sin δ across a range of asphalt binders tested at 64°C. A similar level of correlation was also found between MSCR results and measured rutting from a field trial performed on an interstate highway in Mississippi (FHA 2011).

MSCR has been demonstrated to be easy to perform in the laboratory using modern DSR equipment (D'Angelo 2009a) and takes only around 15 minutes to complete (DuBois et al. 2014). The primary output from the MSCR test is termed the creep compliance (Jnr) which is related to an upper service temperature depending on the assigned level of traffic severity (D'Angelo 2009b).

The standard MSCR test includes 0.1 and 3.2 kPa stress levels with ten cycles of loading and unloading at each stress level. The two stress levels are intended to cover the linear and non-linear behaviors respectively (Wasage et al. 2011). The difference between the two provides an indication of stress sensitivity (Soenen et al. 2013). The load is applied for 1 second followed by a 9 second recovery phase between each load application. The same 9 second recovery phase occurs between stress levels (D'Angelo et al. 2007). The standard test has a 1 mm gap between two 35 mm parallel plates (D'Angelo 2009b). A schematic representation of the test outputs is shown in Figure 10.

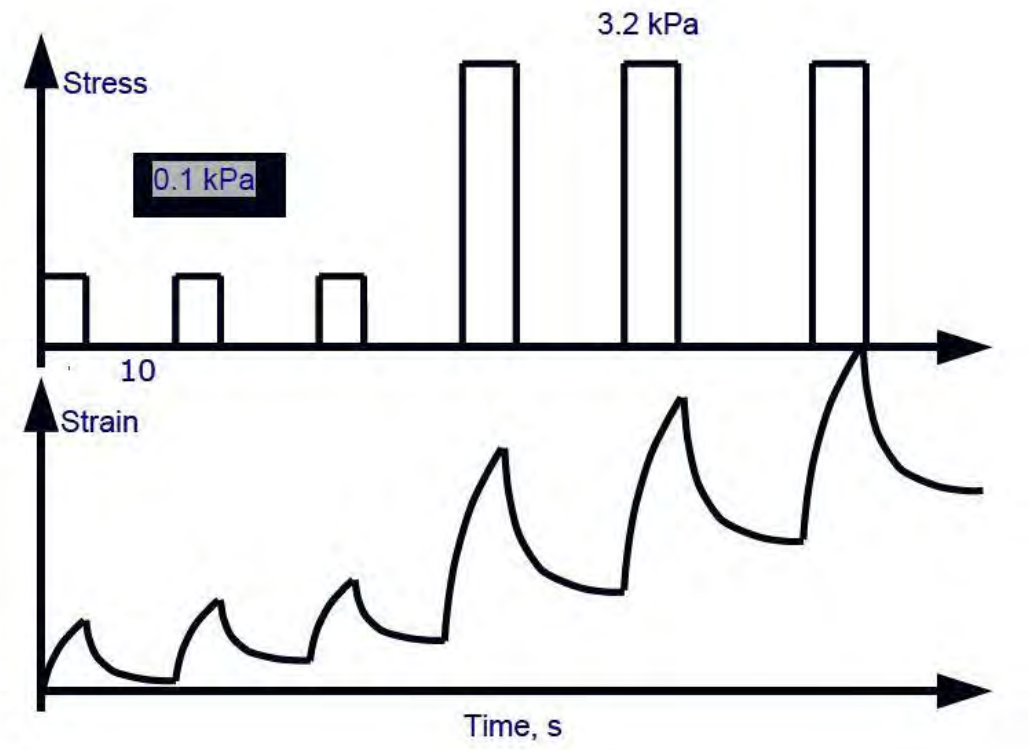

Figure 10 Schematic of MSCR output (D'Angelo 2009b)

The MSCR protocol returns a number of parameters indicative of various performance characteristics (Table 7). The primary PG system high temperature grading parameter is the non-recoverable creep compliance, Jnr(3.2). This is calculated from the cumulative permanent strain over the ten cycles at 3.2 kPa stress level.

Table 7 Summary of MSCR test parameters

Parameter	Symbol	Indication of Performance
Average Recovery at 0.1 kPa	AR(0.1)	Elastic recovery in linear response to stress range
Average Recovery at 3.2 kPa	AR(3.2)	Elastic recovery in nonlinear response to stress range Primary indicator of elastomeric polymer modification
Percentage Difference in Average Recovery	%AR	Sensitivity of polymer modification to stress increases
Non-recoverable creep compliance at 0.1 kPa	Jnr(0.1)	Permanent deformation in linear response to stress range
Non-recoverable creep compliance at 3.2 kPa	Jnr(3.2)	Permanent deformation in nonlinear response to stress range Primary indicator of rutting potential
Percentage Difference in Average Recovery	%Jnr	Sensitivity to shear stress increases

The reproducibility and repeatability of the MSCR protocol was investigated and found to be better for non-polymer modified binders. Most of the variability measured for PMB samples was explained by poor sample handing and preparation methods (Soenen et al. 2013) which can readily be avoided.

Since its introduction in 2007 MSCR has been used in a broad range of research and investigation applications. This is in addition to its use in the PG grading of binders. It is normal to age bitumen using the RTFO prior to MSCR testing in order to simulate hardening during asphalt production. Most researchers have adopted this protocol (Motamed & Bahia 2011; D'Angelo & Dongre 2009; Clopatel & Bahia 2012; Hafeez & Kamal 2014; Domingos & Faxina 2015; Riaz et al. 2013). However, Santagata et al. (2013) maintained that bitumen testing should always be performed on both unaged and aged samples. This is only applicable to fundamental research applications focused on the effect of ageing bitumen performance.

The original MSCR protocol included 11 stress levels (0.025, 0.05, 0.1, 0.2, 0.4, 0.8, 1.6, 3.2, 6.4, 12.8 and 25.6 kPa). This was reduced to just 0.1 and 3.2 kPa as this was believed adequate for the purposes of PG grading of binders (D'Angelo et al. 2007). The standard stress levels are arbitrary and do not necessarily represent stresses experienced in pavements (Delgadillo et al. 2013). Many researchers continue to use all 11 stress levels (Zoorob et al. 2012).

The primary concern regarding MSCR testing of binders relates to the adequacy of the recovery period for higher modified elastomeric binders. Some binders have been shown to take up to 100 seconds to fully recover (Motamed & Bahia 2011). Domingos & Faxina (2015) and Santagata et al. (2015) echoed these concerns for slow recovering bitumen characterisation. Santagata et al. (2013) demonstrated the inability to separate slow elastic recovery from viscous flow where full recovery exceeds the recovery phase period. Some elastomeric PMBs were shown to have full recovery times exceeding seconds.

A number of researchers have also raised concerns about the geometry of the standard 1 mm gap between two parallel plates. For crumb rubber modified binders, the gap is inadequate to accommodate the relatively large particles. A cup-and-bob geometry with 6 mm gap resulted in increased result reliability (Baumgardner & D'Angelo 2012). It was concluded that a 1 mm gap was insufficient for materials containing particles greater than 250 microns. It follows that the standard 1 mm gap between parallel plates is appropriate for mastic manufactured from aggregate and filler all passing the 75 μm sieve.

Santagata et al. (2013) used a 35 mm diameter cones with 4° angle and plate to improve results. Delgadillo et al. (2012) also preferred a cone-plate arrangement to provide a homogenous shear rate. This is important for non-linear bitumen testing. Motamed & Bahia (2011) preferred a cone-plate geometry to avoid tertiary flow from occurring around the plate ends. This study on variable cones angles showed little impact for angles of less than 4°.

To counter some of these limitations, a number of advanced analysis protocols have been developed. These focus on the recovery phase analysis and the adequacy of the nine second period for slow recovering binders. A method of separating the linear viscoelastic and non-linear viscoelastic strains was developed (Shirodkhar et al. 2012). Masad et al. (2009) presented a method for the isolation of the recoverable viscoelastic strain from the truly irrecoverable permanent strain. Santagata et al. (2015) characterised single load creep response of bitumen. This was used to determine the portion of recoverable strain was not recovered during the nine second recovery phase. The reported Jnr values were then adjusted to reflect the true unrecoverable strain, regardless the nature of the bitumen being assessed. There has been no suggestion that the nine second recovery period is not adequate for conventional, plastomeric modified or acid (PPA) modified bitumen, which all exhibit rapid recovery.

MSCR has been used to compare bitumen performance as well as to characterise binders for other applications, such as Prony series models of asphalt response in FE modelling. Others have simply evaluated the appropriateness of the test and standard protocols for various contexts.

Motamed & Bahia (2011) assessed the influence of loading time and stress level on MSCR results for various binders. Wasage et al. (2012) similarly assessed the influence of stress level on Jnr values and correlated this to wheel tracking results for four binders at temperatures ranging from 30 to 70°C.

Comparison of binders is a common use of the MSCR. Two conventional and one elastomeric PMB were compared and it was found that MSCR results and DSR temperature/frequency sweep test did not rank binders in the same order. It was also concluded that MSCR can only be used as a ranking tool (Zoorob et al. 2012). Shirodkar et al. (2012) assessed 13 binders under MSCR and found that for a common polymer, the polymer content was inversely correlated to Jnr. It was also found that different base bitumen sources, of the same grade, with the same polymer modification, returned significantly different Jnr values. Riaz et al. (2013) investigated aged (RTFO) and unaged samples of conventional and polymer modified binders. It was found that binders with identical $|G^*|/\sin\delta$ grading could have significantly different Jnr values. Similarly, $|G^*|/\sin\delta$ was not well correlated to stress sensitivity of different binders.

Hafeez et al. (2013) studied the impact of various polymers on binders using MSCR. This was later extended to include the assessment of five binders and correlation with wheel tracking performance of asphalts (Hafeez & Kamal 2014). The relationship between Jnr and wheel tracking performance was significantly different for polymer modified and conventional binders. Wasage et al. (2011) stated that higher than standard stress levels may be required to bring some bitumen types/grades well into the non-linear range in order to replicate a wheel tracking test. This ‘higher stress level’ would vary between conventional and modified binders.

MSCR was adopted to assess the impact of ageing on binders. Extracted (from asphalt), RTFO conditioned and unaged bitumen were all assessed. The hardening of bitumen during ageing was demonstrated. The RTFO conditioning generally had less ageing impact on binders than asphalt manufacturing did (Li et al. 2011). This included a range of bitumen types including acid (PPA) modified bitumen and elastomeric PMB, with results being well correlated against asphalt dynamic modulus.

DuBois et al. (2014) correlated MSCR Jnr values to the simple creep performance parameter Flow Time. Jnr was clearly better correlated to Flow Time than |G*|/sin δ and the MSCR derived elastic recovery. In an earlier study, MSCR Jnr values were correlated to uniaxial compressive results of asphalt mixtures, as well as laboratory wheel tracking results (Stastna et al. 2011). This work enabled the development of a simpler model for the linear to non-linear transition of asphalt response to higher stress levels.

The performance of acid (PPA) modified bitumen was investigated by MSCR as well as DSR temperature/frequency sweeps, wheel tracking and the shear strength of the asphalt mixture (Fee et al. 2010). It was found that hydrated lime filler was very compatible with PPA modified bitumen, even when dual-modified with plastomeric or elastomeric polymer, although consistence of PPA modification across multiple crude sources was not considered. Even bio-oil blends have been evaluated by MSCR in recent times (Yang & You 2015).

In developing a non-linear model for bitumen, MSCR was used as a verification tool (Delgadillo et al. 2012). Two binders with similar linear response were shown by the model to not necessarily have the same non-linear response. Under real tyre loads, bitumen transitions from linear to non-linear response and back again. Zoorob et al. (2012) found consistent results. It was shown that binders that performed similarly at 3.2 kPa performed very differently at 12.8 kPa level of stress. It was also found that binders that performed similar at 55-60°C showed very different response at 65-80°C.

Less research has been conducted specifically on mastics using the MSCR. Wang et al. (2011) tested binders, mastics and asphalt mixture modulus and flow. Four binders and two aggregates were considered along with a range of added fillers. Filler Rigden void content was found to have a significant influence on Jnr value. It was also concluded that fillers have different effect on bitumen of different origin and grade and their associated Jnr. Clopatel & Bahia (2012) also tested bitumen and mastic. Three fillers were considered along with elastomeric PMB, PPA and other modifiers for two base bitumens. Both mastics and bitumens were found to show good agreement between DSR elastic recovery and MSCR Average Recovery (AR).

A single base bitumen was used to produce four mastics with limestone, cement, flyash and hydrated lime fillers (Li et al. 2012). Testing included measurement of |G*|/sin δ and Jnr of bitumens and mastics using the DSR. It was concluded that mastic with hydrated lime showed significantly less temperature sensitivity than the other mastics. This was the result of the chemical interaction between lime and the rheological elements of the bitumen. It was also concluded that mastic and asphalt mixtures had different response to shear stress, but the relative response was consistent. While this was insightful, the research only included a single bitumen source so no assessment could be made of consistence across bitumen types or sources.

2.6.6.8 Clay and Hisingerite

Clay minerals are commonly present in quarried aggregate sources (Little & Epps 2001). Aggregates containing clay minerals that exhibit significant plasticity are known to be potentially deleterious and are either avoided or treated with active filler such as hydrated lime (Lesueur et al. 2013). The presence of even significant portions of non-plastic clay minerals in asphalt aggregates is of little concern to asphalt performance.

Clay minerals mostly belong to the silicates group and must be considered in terms of both the chemical composition and their physical structure. Clays are subdivided into sub-groups and individualised based on type of layer structure and elemental inclusions (Brindley 1952).

Clay minerals are hydrous phyllosilicates (sheet forming silicate minerals) that form 2D tetrahedral or octahedral sheets. Clays are characterised by the combinations and stacking of their sheets, the charge on their sheets and any anomalies or interlayer elements. The di-octahedral 1:1 clay minerals include the Kaolin Group which includes, among others, Halloysite and Hisingerite. Structural features of mixed-layer minerals are usually interpreted by comparing measured XRD patterns with computer generated patterns for pre-defined structures. The minerals within each group, despite their structural similarity, can have significantly different characteristics. Structural features of mixed-layer minerals are usually interpreted by comparing measured XRD patterns with computer generated patterns for pre-defined structures (Brigatti et al. 2013).

Smectite is a common mineral that belongs to the 2:1 clay group, characterised by an octahedral sheet between two opposing tetrahedral sheets. These minerals tend to hold moisture between the layers and this is readily driven off by heating to over 100°C.

Hisingerite is a rarely encountered and poorly studied clay mineral. First described in 1810, Hisingerite has been variously regarded as a non-crystalline Silicate, a ferric Allophane, a poorly crystallised Nontronite and an iron rich spherical Halloysite (Brigatti et al. 2013). Hisingerite is commonly identified by XRD via the presence of broad peaks at 4.4, 2.6 and 1.5 Å. The spherical structures generally range from 50-100 Å (Eggleton & Tilley 1998). Hisingerite was identified in a Basalt quarry in Fyansford west of Geelong and was identified by XRD analysis and comparison to other Hisingerites found near mine sites in Broken Hill, Cobar, Western Australia and overseas (Shayan 1984).

The Geelong Hisingerite was shown to have a common genesis to Saponite but a separate genesis to Nontronite seams in the same quarry. The different materials were probably formed by different levels of exposure to steam from the lava bed during the Basalt flow formation (Shayan et al. 1998).

Hisingerite is characterised by the presence of spherical bodies which are curved and largely in a random arrangement. These spherical bodies are very different from the flat sheets observed in Saponite, Nontronite and other clays. The pH of the Geelong Hisingerite suspension and very low measured cation exchange capacity (0.69 meq/g) suggested the presence of negatively charged surfaces which was confirmed by the absorption of 3.4 grams of methylene blue dye by 1 g of Hisingerite in a 4% aqueous suspension. The Geelong Hisingerite is highly hydrous, even more so than many other identified Hisingerite sources around the world (Shayan 1984).

No literature could be found on the physical effects of Hisingerite on the performance of civil construction materials such as asphalt concrete and crushed rock.

2.6.7 Application

Permanent deformation in asphalt is creep related and is generally governed by the time and temperature dependence of the bituminous binder. Deformation testing of asphalt can be performed in a mechanical laboratory testing device or using repeated wheel trackers. Of the wheel tracking devices, Australia has adopted a version of Cooper's wheel tracker. The MMLS3 developed in South Africa lies part-way between a wheel tracker and a scaled-down accelerated load facility. There is no MMLS3 available in Australia at this time. For mechanical mixture testing, there are a number of simple performance tests including Flow Number and Flow Time. To prevent aggregate lock-up and to allow realistic aggregate dilation, repeated loading is essential. Repeated loading is provided by the Flow Number test which has been performed on many asphalt mixtures around the world in routine mixture design, forensic investigation and research applications.

For comparison of asphalt mixtures that are similar, investigation of the asphalt constituents is as important as testing of the mixtures. For comparison of two mixtures that are nominally identical except for a single constituent, the changed constituent would be a natural focus. However, an unintended change in one or more of the other constituents must also be considered.

Coarse aggregate and the overall aggregate grading are important to asphalt shear response. Where materials are tightly specified and quarry processes and fractionation of the aggregates are transparent and actively managed, there is little risk of a significant unintended change to asphalt performance. Filler selection and source can affect asphalt mixtures through their contribution to mineral material grading as well as their chemical-physical interactions with bitumen. The filler is an active element of the asphalt mastic which is considered to be the real binder within as asphalt mixture. Unintended significant changes in the filler and coarse aggregate are unlikely to occur.

The fine aggregate at Melbourne Airport was known to change at about the transition from one runway to the other. The dust change coincided with the commencement of surface failures in the braking zones. The fine aggregate properties contributing to asphalt deformation resistance include deleterious clay content and shape. The fine aggregate provides the majority of the overall mineral grading passing the 75 micron sieve. This fine aggregate material is an important element of the asphalt mastic. A combination of mineral composition and shape testing will be shown to indicate a fundamental difference between the two dusts sources. Mastic testing should incorporate the dust in order to replicate the overall mastic response. A change in dust source that introduced rare and potentially deleterious clay minerals, such as Hisingerite, could impact on mastic and asphalt performance. Unusually hydrous Hisingerite has been identified in Basalt flows around Victoria. The impact of such hydrous clay minerals of spherical morphology on asphalt mixtures does not appear to have been reported in the literature and is not understood.

Bitumen is a complex material that is essentially the waste of crude oil refining to generate gas, fuel oil and diesel. It is then modified, blended and processed to meet empirical specification requirements in Australia. Bituminous binder is the least transparently produced materials in asphalt production. Apart from compliance with a given empirical specification, little information is available regarding crude oil source, refinery processing or subsequent modification or blending of a specific batch of paving-grade bitumen. Given its demonstrated importance to asphalt performance, this is concerning. Certainly it has been established that an unintended or unknown change in the crude oil source or refining process could impact the rheology and/or shear creep performance of the bitumen and the manufactured asphalt. Such changes would not necessarily render the product non-compliant with the current Australian specification.

Of the various tests available for bitumen characterisation, SARA analysis of rheology would seem to give the greatest insight into changes in bitumen properties. It would be an indicator that a part of the non-transparent processing may have changed. However, it too is only empirically related to field performance. Where field performance is the focus, the MSCR test represents best-practice. MSCR testing has an established record of discriminating between binders of identical nominal grading (even using the original PG system |G*|/sin δ criterion). Its major criticism is the rest time for slowly recovering binders. Acid (PPA) modified bitumen has been shown not to recover slowly between load applications. The MSCR test is readily performed on locally available modern DSR equipment and has already been used in forensic investigations of bitumen in Australia.

The mastic is the real binder in asphalt. Two seemingly similar asphalts can show very different performance based on mastic properties. It follows that mastic performance provides a reliable indicator of asphalt performance in nominally identical coarse aggregate mixtures. Mastic characterisation must include the fine aggregate, filler and bitumen. Because of the importance of bitumen:filler ratio, mastic characterisation must target the bitumen:filler:aggregate ratio present in the asphalt mixture. While the mastic constituents can also be characterised in isolation, this will not identify any physio-chemical interactions between the various components. A number of mixture tests have been used to investigate the impact of mastic on asphalt. The challenge is isolating the contribution of the mastic from the impact of any unintended changes in asphalt grading or bitumen content. Mastic investigation should therefore include testing of the mastic separately from the mixture.

The MSCR test has been used to investigate mastics as well as bitumen. Only slight modification to the DSR equipment is required to allow for larger (>100 μm) mineral particles. MSCR characterisation of mastics has shown good correlation to asphalt mixture shear response and field performance. It represents best-practice in assessment of mastic response to shear stress.

2.7 SUMMARY

This Chapter has presented some context around the problem being investigated as well as a summary of the existing knowledge applicable to the planning and execution of the research. A range of test methods and investigation techniques has been summarised and a number of important findings from previous germane investigations presented.

Major themes included aircraft tyres and contact stresses, stress modelling through surface layers, interface shear resistance and asphalt deformation and creep. This will assist in forming the basis for the research methods adopted. A number of gaps in the existing knowledge were identified (Table 8). These gaps generally relate the adaptation of knowledge to aircraft and airport pavements and must be addressed in order to achieve the research aim.

Table 8 Summary of existing knowledge gaps

Item	Gap	Requirement
1	Near-surface shear stress states induced by commercial aircraft during typical landing operations	To exclude differential aircraft operations and braking as an explanation for the differential surface performance of the two runways at Melbourne Airport
2	The impact of typical aircraft braking on near-surface shear stresses	To understand the difference in shear stress state in the braking and non-braking zones of airports
3	The interface shear resistance achieved by typical airport asphalt overlay construction practices	To make an assessment of the adequacy of current practice to provide interfaces capable of resisting aircraft-induced near-surface shear stresses
4	Standard test methods for the assessment of asphalt overlay interface shear resistance under monotonic and cyclic loading	To allow project-specific materials to be adequately assessed with the equipment available
5	Potential impact of Hisingerite clay minerals on the performance of asphalt mixtures	To determine the impact of the change in dust source to be considered as a factor leading to shear creep in asphalt surface layers
6	Magnitude of impact of changes in crude oil source on the properties of bitumen and the performance of asphalt mixtures	To determine the impact of the change in bitumen feedstock to be considered as a factor leading to shear creep in asphalt surface layers

The next Chapter will present the preliminary investigation that was conducted prior to the initiation of this academic investigation. This will provide direction for the subsequent (academic) investigation presented in this Dissertation. The preliminary investigation will review the broader potential causes of the failures observed and focus the investigation towards the cyclic shear creep resistance of the asphalt.

3. PRELIMINARY INVESTIGATION

The previous Chapter presented contextual information as well as a review of existing germane knowledge. The existing knowledge review focused on methods of investigation that would allow the root cause of the failures to be isolated in a sequential manner.

This Chapter will present the findings and conclusions from a preliminary investigation. The preliminary work focused on the adequacy of the materials and construction methods as well as determining whether the failures were likely initiated by interface bond failure (bottom-up) or shear creep within the asphalt layer (top-down). No evidence was found to suggest any construction related issue and the failures will be shown to be initiated by shear creep within the asphalt and not by delamination due to interface bond failure. Following this, the research methods proposed for the remaining (academic) portion of this research will be presented in the following Chapter.

This Chapter is a revised version of a peer reviewed conference paper. A copy is included in Appendix 1.

3.1 INTRODUCTION

Shortly following the identification of the failures at Melbourne Airport, it was realised that these were more severe and more prolific than could be considered normal. A preliminary investigation into their cause and implications was instigated. The initial investigation hoped to determine:

- Whether the design was fundamentally flawed in a way that would explain the surface failures.
- Whether the various constituent materials and the resulting asphalt mix were compliant with the specification or could somehow explain the surface failures.
- Whether the construction processes, including surface preparation, tack coating, paving and rolling were compliant with the specification or could somehow explain the surface failures.

- Whether the mix was deforming in a 'top-down' manner or whether the bond to the underlying asphalt layer was inadequate, allowing the surface to delaminate in a 'bottom-up' manner.

3.2 DESIGN AND CONSTRUCTION REVIEW

The quality of construction and its conformity with the design and specification are generally the first elements of a project to be assessed during any forensic investigation. With the design and specification representing best practice for this work, the Melbourne Airport slippages were no different.

3.2.1 Construction Quality Assurance

The works were constructed under a Quality Assurance (QA) system maintained by the contractor. The design consultant superintended the works and actively participated in the release of hold and witness points during all stages of the resurfacing.

Site diaries, QA records, non-conformance reports and photographic records were all reviewed. Site representatives for both the contractor and superintendent were interviewed to clarify any discrepancies or ambiguity in the construction records.

The QA documentation and associated construction records did not identify any specific issue that could explain the asphalt slippages. While minor non-conformances and variability in the construction processes were evident, there was no evidence that the construction was not within expected construction tolerance. The works were therefore considered to be in accordance with the design and specification, to the extent that could be assessed from the construction QA records available.

3.2.2 Compliance Testing

Despite the construction records indicating that the construction was in accordance with the design and specification, to confirm this view a regime of forensic compliance testing was performed. Cores recovered from the runway surface were tested along with retained samples of bitumen.

Compliance testing included:

- **Asphalt density**. All density results were consistent with those achieved during construction.
- **Asphalt volumetrics**. Some of the gradings were marginally finer than specified. It is accepted, however, that increased fineness occurs through the core cutting process. Binder contents were consistent with the approved mix design.
- **Resilient modulus**. Modulus values varied across the pavement surface as expected. The results were consistent with typical airport asphalt mixes used in Australia and consistent with laboratory manufactured sample results from the mix design process.
- **Wheel tracking**. Values were generally around 3 mm which is considered good for typical airport asphalts used in Australia.
- **Bitumen compliance**. Bitumen was extracted from a number of forensic cores and subject to DSR assessment as well as viscosity assessment. These results did not suggest that the bitumen was other than compliant and uncontaminated M1000 (Multigrade). Retained bitumen samples were also tested and were within or slightly above the post-RTFO viscosity requirement of the specification two years after manufacture.

The forensic testing did not find the asphalt cores to be significantly outside the requirements of the design and specification.

3.2.3 Outcome

The construction conformity assessment found no systemic or significant non-compliance to the design and specification for the works. This included the asphalt materials, the texturing, cleaning and tacking of the existing surface, as well as the construction of the asphalt layer. Based on the construction conformity information available, it was considered that the works were compliant with the design and specification and within the variability of normal construction tolerance.

No indication of inadequate surface performance was identified by assessing compliance of the materials and construction processes against the project specification. The project specification represented best practice for the scope of work performed. It follows that an unusual issue, not identifiable by compliance testing, had caused the observed difference in surface performance at Melbourne Airport. A regime of destructive and non-destructive testing was required in search of a specific cause for the failures, which were unprecedented at an Australian airport.

3.3 NON-DESTRUCTIVE TESTING

A regime of non-intrusive evaluation (NDT) was performed in parallel to the construction conformity review. The NDT regime aimed to assess whether the surface was adequately bonded to the underlying layer and, if not, whether the extent and location of any inadequate bond could be defined.

3.3.1 Ground Penetrating Radar

GPR was employed in areas of known slippage failures, as well as areas of observed good performance. The GPR was operated in a transverse direction at 1 m spacing. In one location, directly above a surface slippage, responses consistent with de-bonding were recorded at 60-80 mm below the surface level. In the opposite wheel path, at the same chainage, a similar (but less well defined) response was also detected, in an area of no surface deformation. A core later performed in that location confirmed that the surface layer was well bonded to the underlying layer. The GPR response was a false positive. No similar responses were detected in the other scanned areas of good surface performance.

3.3.2 Impact Hammer and Impulse Response

No significant difference could be detected between the areas of sound and slipped surface with either the Impulse Response or Impact Hammer devices. Similarly, no response consistent with what would be expected of de-bonded layers was found.

3.3.3 Thermal Imaging

Thermal imaging of the surface was performed in areas of known surface slippage as well as areas observed to be performing well. No differences in temperature, indicative of de-bonding, could be detected in any location. However, it was overcast and cool on the days of testing, meaning that the surface was not highly radiated during the day. It followed that the relative cooling of the surface during the night was less significant than it would have been during a period of hot sunny days. This may have affected the differential cooling of the surface on which thermal imagery analysis relies.

3.3.4 Outcomes

With the exception of GPR, no NDT results were obtained that were consistent or indicative of surface layer de-bonding. The GPR testing showed potential promise, although this was subsequently shown, by surface coring, to be a false positive.

3.4 DESTRUCTIVE TESTING

A series of destructive tests were performed on 33 cores recovered from various 'conditions' of the airfield (Table 9**)**. It was not possible to obtain untrafficked cores from patched areas as patches were only performed in heavily trafficked pavement. Similarly, only trafficked and patched cores could be obtained from failure zones as the failures only occur in heavy braking/turning areas.

Table 9 Destructive testing core condition

Core Condition			Assigned Condition Code
Failure Zone	**Trafficked**	**Underlying Patch**	
Yes (failure)	Yes (trafficked)	Yes (patched)	FTP
No (sound)	Yes	Yes	STP
No	No (untrafficked)	No (unpatched)	SZU
No	Yes	No	STU

3.4.1 Visual Assessment

Of the 33 cores, Table 10 summarises the location, surface condition and interface condition frequencies. All cores were recovered from Runway 16/34, the runway with deformation failures. Moderate (10-20 mm) and slight (5-10 mm) levels of deformation were measured at the surface. The interface was assessed as being either de-bonded or intact.

Table 10 Core condition frequency

Location	Surface	Interface	Frequency
Within slippage	Moderately Deformed	De-bonded	5
Within slippage	Moderately Deformed	Intact	6
Edge of slippage	Slightly Deformed	De-bonded	1
Edge of slippage	Slightly Deformed	Intact	3
Outside slippage	Not deformed	De-bonded	0
Outside slippage	Not deformed	Intact	18

Table 10 shows that of the moderately (10-20 mm) deformed areas, approximately half of the interfaces were intact. Of the slightly (5-10 mm) deformed cores, three out of four showed well bonded interfaces.

Of particular note is a core that was taken from the lateral edge of a surface slip. The surface showed moderate (10-20 mm) deformation in the grooves. The interface to the underlying layer showed de-bonding over about 70% of the core area. However, the interface directly under the extremity of the surface deformation showed a freshly fractured face, indicative of having been broken during the coring process. This area of coring-induced interlayer fracturing was located directly under a moderately (10-20 mm) slipped surface. This indicated that the asphalt deformation had likely occurred before the de-bonding commenced.

Visual inspection of the sides and interfaces of cores revealed that the bonded interfaces were of high quality and showed no sign of poor bond or imminent failure (Figure 11). All of the de-bonded interfaces showed signs of grinding of the two faces.

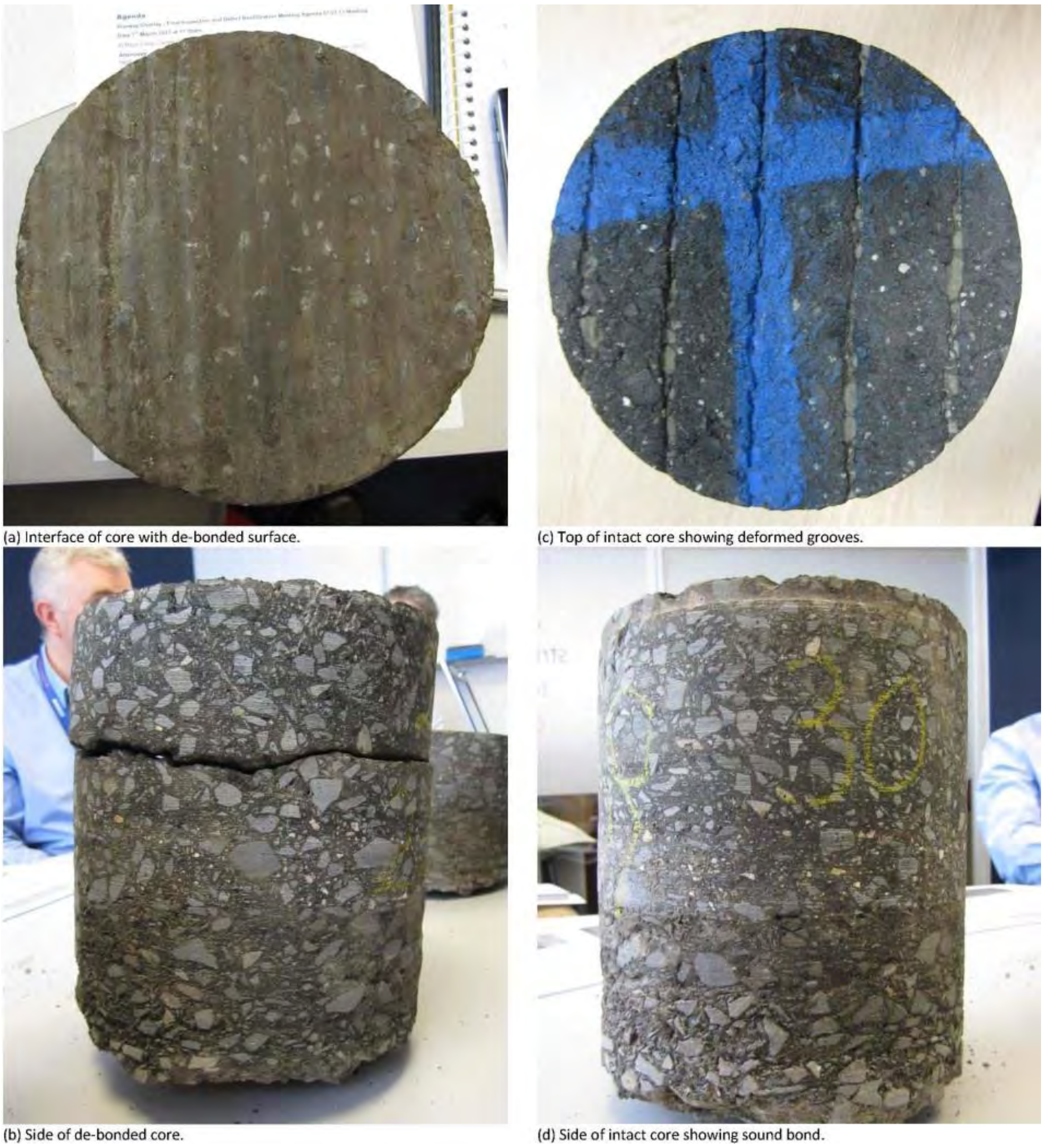

Figure 11 Typical intact and de-bonded cores from Melbourne Airport

3.4.2 X-Ray Fluorescence Testing

XRF analysis was performed on thin sections of one core from each of the conditions detailed in Table 9 in an attempt to detect any tack coat contamination through differential chemical composition across the interface. A typical output is shown in Figure 12. The testing could detect differences in the aggregate type between the new and old asphalt surfaces. It could also detect the relative absence of aggregate at the interface. It could not, however, detect any difference in the chemical composition across the interface between the various cores assessed.

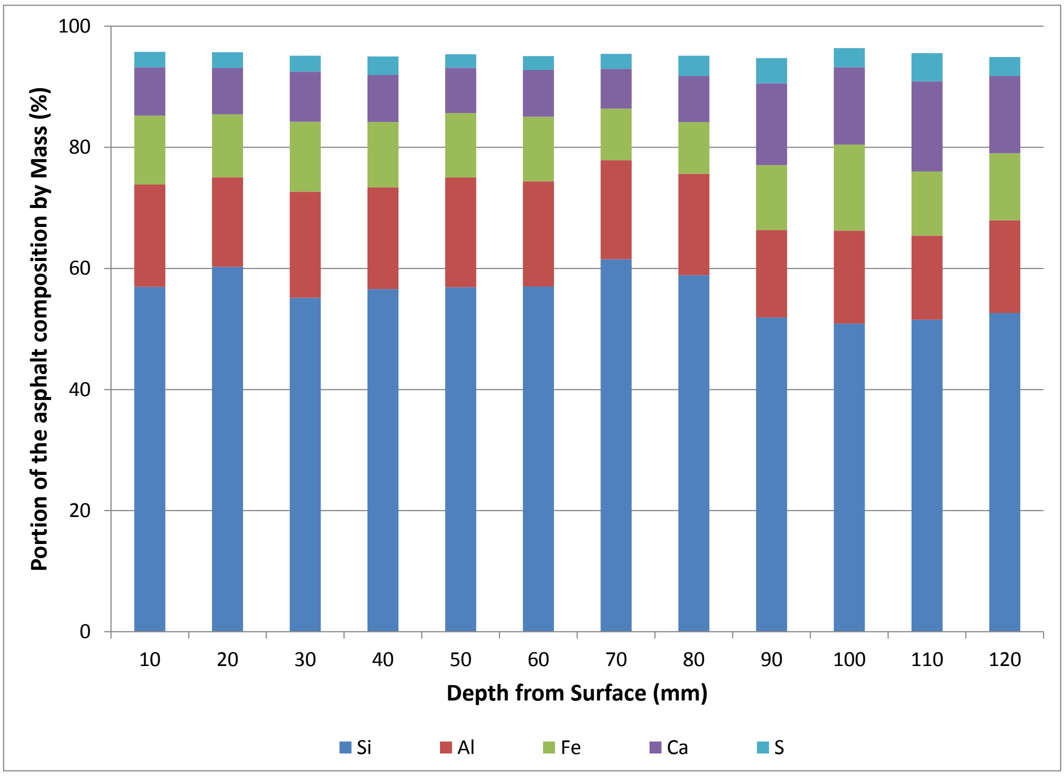

Figure 12 Typical XRF output for cores from Melbourne Airport

3.4.3 Direct Shear Testing

Direct shear testing was performed on a single core from each condition detailed in Table 9. Protocols for the Direct Shear (DS) test are detailed later (4.4.1 Direct Shear Test). The results are shown in Figure 13 along with best fit lines which were extrapolated to the y-axis.

Of the 25 tests performed, only one result was rejected as an outlier (shown as a hollow data point). Figure 13 indicates low variability (R = 95-99%) for the five results (at different normal stresses) from each core.

From the regression lines shown in Figure 13 it was concluded that all samples with underlying patches (FTP and STP) had similar friction angles (45-55°) which were typical for well compacted asphalt. The two samples that were not constructed on new patches (SZU and STU) had friction angles around 25°. This was a significant difference that was not expected.

It was noted that the lack of an underlying patch for the STU samples was the result of a lack of loading in that area of the runway, which is located near the runway end. What was reported as trafficked and unpatched may actually have been relatively untrafficked and unpatched. The confounded nature of the underlying patches with the level of traffic did not enable the relative importance of each to be determined. Further investigation is required to consider the difference in friction angle and the relative contribution of trafficking and/or underlying patches.

All cores showed consistent adhesion values of 250-470 kPa. This is high for asphalt tested at 55°C and is not dissimilar from values expected for monolithic asphalt.

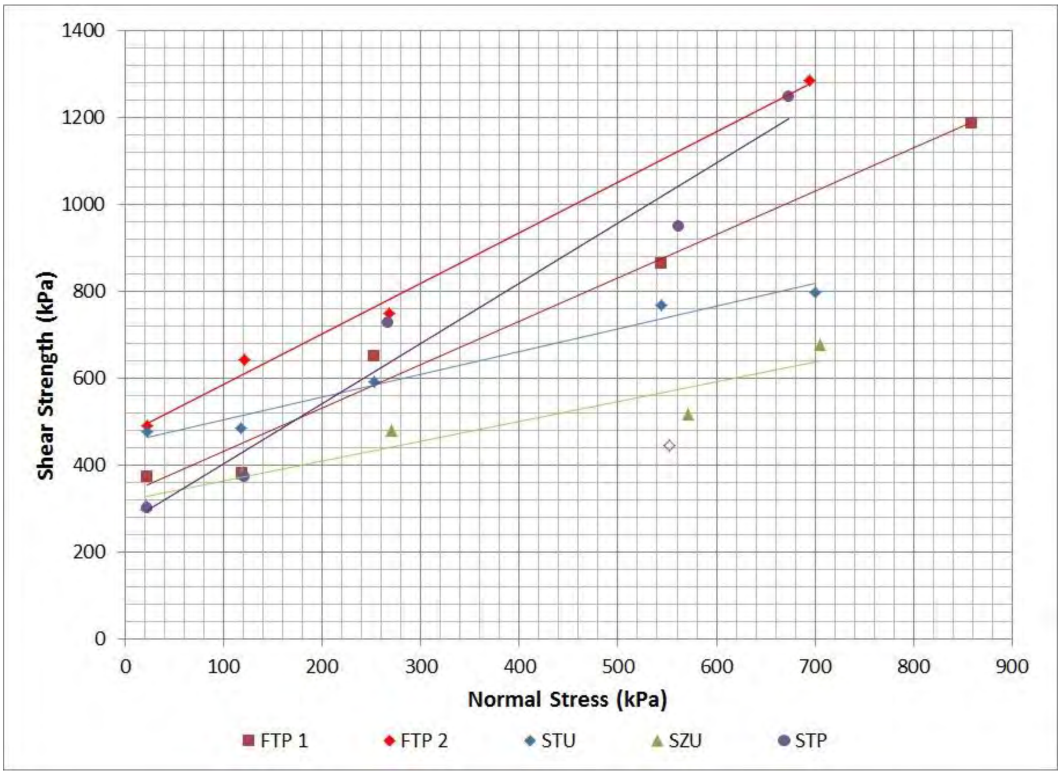

Figure 13 Direct shear strength results

3.4.4 Inclined Repeated Interface Shear Testing

A single core from each of the conditions detailed in Table 9 was subject to Inclined Repeated Interface Shear (IRIS) testing. Protocols for the IRIS test are detailed later (4.4.2 Inclined Repeated Interface Shear Test). Table 11 provides a summary of the results.

Table 11 Inclined repeated interfaces results

Core Code	Cycles to Tertiary Flow	με @ Flow	με @ 400 cycles	με @ 2000 cycles
FTP	4,620	75,000	32,720	58,960
STP	> 20,000	N/A	30,560	60,490
SZU	> 20,000	N/A	31,480	73,150
STU	13,363	86,000	17,740	40,680

More informative than the test results was the inspection of the cores after testing and dissection such as the examples shown in Figure 14. This showed that the Melbourne Airport (Runway 16/34) samples deformed up to 25 mm without any loss of the interface bond. The asphalt crept under repeated sub-maximal load, while the bond remained in good condition. The mode of failure contrasts with cores from unrelated asphalt of similar mix composition (from a port facility) used to assess the effectiveness of the test procedure. The 'port' core failed at the interface in around 100 load cycles. Runway 09/27 was not assessed by IRIS testing during the preliminary investigation.

(a) Control (Port Asphalt) Core after IRIS testing. (b) Melbourne Airport Core after IRIS testing.

Figure 14 Typical cores after IRIS testing and dissection

3.4.5 Outcomes

Based on visual assessment of the 33 cores, it was determined that surface deformation occurred prior to de-bonding of the interface. XRF assessment of cores could detect no significant difference between the various core conditions, including those from the failure zone, those from areas free of slippage and even those that were not trafficked.

Direct shear testing of the interface found that the surface was well adhered to the underlying asphalt and the strength of the adhesion was consistent for all core conditions. It also suggested that the interlayer friction was similar (and typical) in slipped and slip-free areas but may be different in untrafficked/unpatched pavement.

IRIS testing indicated some difference between the various core conditions but the significance of which is unknown due to the uniqueness of the test. It was clear, however, that the cores deformed significantly with no apparent disturbance of the interface. This was in contrast to other asphalt mixtures tested under the same conditions, which failed at the interface after around 100 load cycles. No benchmark for monolithic asphalt shear strength and/or creep performance under this specific loading regime is currently available to allow direct comparison of test results.

3.5 PAVEMENT PERFORMANCE

The performance of the two runway surfaces was monitored from the time the first failures were identified in early 2012. Inspections were performed on a periodic basis and new failures were logged from June 2012. The location, number and severity of the various failures were tracked. The number of newly identified failures is shown in Figure 15. By November 2012 the performance of Runway 16/34 asphalt significantly improved. At no stage were similar failures identified in the Runway 09/27 asphalt surface. No additional failures were identified in either runway after May 2013.

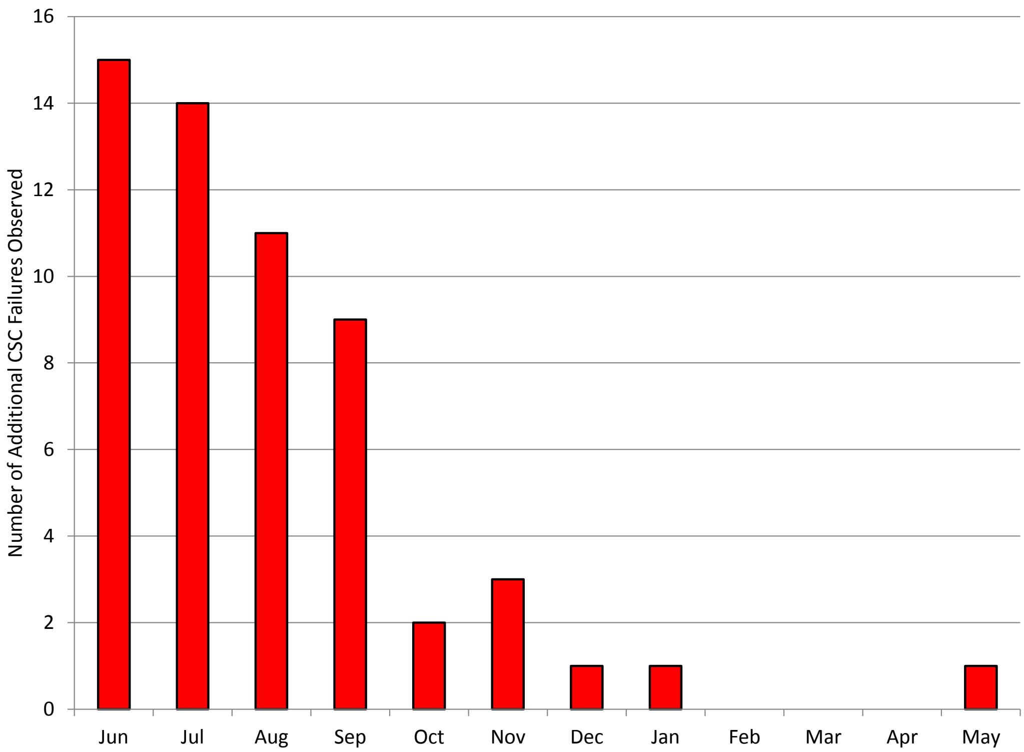

Figure 15 New deformations in Runway 09/27 June 2012 to May 2013

3.6 OUTCOMES AND LIMITATIONS

The surface slippage failures at Melbourne Airport occurred only in heavy braking/turning areas, which had been deep patched prior to the resurfacing. A review of the design and specification confirmed that best practice had been adopted in the design to address common slippage risks. Review of the construction records and significant forensic compliance testing confirmed that the works were constructed from compliant materials and in a manner that was conforming to the design and specification. Some minor variability was evident in the various construction processes but all was considered to be within normal construction tolerance.

NDT methods found no evidence of poor or inadequate bond of the surface to the underlying layer, which is accepted as the most common cause of asphalt surface slippage. XRF assessment detected no difference in the composition of the interface and tack coat between the failure zone and other areas of the runway. DS testing of the interface suggested that the adhesion of the surface to the underlying layer was similar in the failure zone and other areas of the runway, as well as being consistently in the upper range of published values. It was concluded that the interface between the surface and the underling layer was unlikely to be the primary cause of the slippage failures at Melbourne Airport.

The IRIS testing found that the asphalt deformed significantly under cyclic sub-maximal loading. The interface bond remained undetectable between the two layers. The deformations measured were greater than expected of typical asphalt mixes.

The slippages at Melbourne Airport were concluded to likely be the result of a peculiarity in the compliant asphalt mix that was not able to be detected during the mix design process under the current Australian airport asphalt specification. The slippage failures were concluded to be the result of a currently inexplicable lack of resistance to Cyclic Shear Creep (CSC). The improvement in the Runway 16/34 surface indicated that the lack of CSC resistance lasted less than three years and was therefore an example of medium-term asphalt ‘tenderness’.

Further investigation is required to determine the characteristic or constituent within the compliant asphalt mix responsible for the CSC failures. Additional investigation is also required to determine a method to discriminate against the responsible constituent material and/or the asphalt mix during the mix design process to prevent reoccurrence. Other explanations such as differential shear stress induced by varying aircraft operations must also be explored to be excluded as potential contributing causes. Additional DS and IRIS testing was also required to confirm the findings of the preliminary investigation which relied on small sample sizes and limited replication of specific sample conditions.

3.7 HYPOTHESIS

The failures in the asphalt surface at Melbourne Airport were concentrated in the heavy braking zone of only one runway landing direction. The design and construction of the asphalt overlay did not explain these failures.

Based on the preliminary investigation conducted, it was hypothesised that a single or combination of the constituent materials used for the Melbourne Airport asphalt, despite being compliant with the specification, resulted in a resistance to CSC that was unusually low for Australian airport asphalt. The focus of the original (academic) research presented in this Dissertation was to determine whether the single constituent could be isolated and other potential explanations excluded, as well as explaining the observed distribution and isolation of failures to the braking zone of just one runway landing direction.

3.8 SUMMARY

This Chapter summarised the execution and findings of a preliminary investigation. No evidence was found that suggested any fundamental issue associated with the design and specification or systemic construction practice that could lead to the observed failures. Through a range of forensic testing it was determined that the failures were likely being initiated by shear creep of the surface layer. The failures were shown to be unlikely the result of delamination due to inadequate bond between the surface layer and the underlying pavement. This allowed the following (academic) investigation to focus on the asphalt layer and mix.

The next Chapter will present the research methods used to determine the root cause of the CSC failures observed in Runway 16/34 at Melbourne Airport. This will establish the analysis, testing and statistical methods to be utilised during the sequential Phases of investigation and presented in the subsequent Chapters.

4. METHOD STATEMENT

The previous Chapter presented the preliminary investigation. It showed that the design and construction of the resurfacing at Melbourne Airport did not explain the slippage failures observed in the surface of Runway 16/34, only in the landing Runway 16 braking zone. It determined that the failures were likely related to a lack of resistance to shear stress induced creep (CSC) most likely the result of one or more constituents within the mixture.

This Chapter details the research methods adopted during the remaining Phases of investigation. This investigation was necessarily sequential. The broad failure mechanism was initially investigated prior to honing in on the asphalt mixture and then the mastic. The contribution of the mastic constituents (bitumen and dust) was finally isolated.

Following this Chapter, the investigation is presented in its four sequential Phases as illustrated by Figure 16. Climate was immediately discarded as the two runways are located at the same airport and are adjacent one another at their intersection. Therefore this investigation starts by demonstrating that the stresses and strains induced by braking aircraft do not explain the distribution of failures across the airfield. Second, the interface shear strength measurements are presented, followed by the shear creep resistance of the asphalt-interface system. This will show that the two asphalt mixtures exhibited significantly different performance. Third, the two mixes are broken into their constituents and the coincidental changes in the bitumen and dust source are focused on. The final stage of the investigation isolates the contribution of each to the lack of cyclic shear creep resistance.

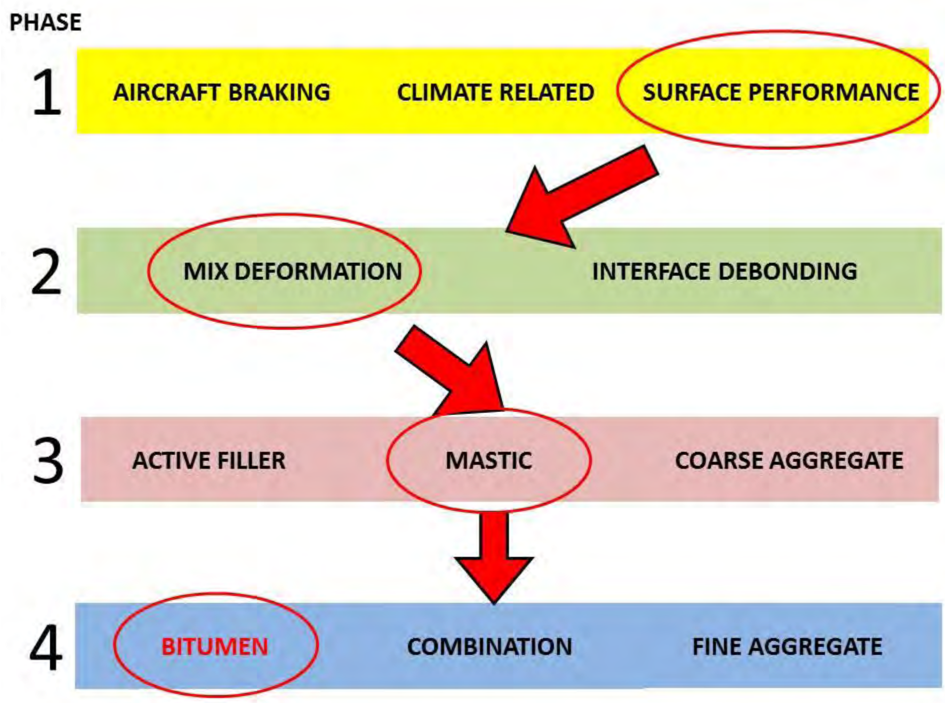

Figure 16 Sequential investigation framework

4.1 AVAILABLE AND ADOPTED METHODS

The research methods adopted to assist in answering the research questions posed are detailed following the structure of the remaining Dissertation Chapters. Decisions regarding adopted methods were based on a balanced compromise between the:

- Suite of tools and options available.
- Resources required by each option.
- Importance of that element of the study to the overall research aim.
- Recommendations and previous use within the literature.
- Continued utilisation of methods successfully used during the preliminary investigation.

Due to the sequential nature of the investigation, some of the methods described do not become clear until the outcomes of the previous Phases of investigation are understood. Some commentary has been added to clarify such issues.

4.1.1 Aircraft Induced Stresses

During the preliminary investigation, it was identified that CSC failures were occurring primarily in the braking zone associated with landings on Runway 16. No failures were identified in the braking zone of Runway 34 or Runway 09/27. This raised a question about why the failures were occurring in a specific area within only one landing direction. And did the differential performance reflect differences in loading or surface response? This prompted a number of subsequent and more specific questions:

- Why was the same asphalt mixture failing in the Runway 16 braking zone but not the Runway 34 braking zone?
- Does the absence of failures in Runway 09/27 reflect a difference in the aircraft traffic and/or operations or does it reflect a difference in the CSC resistance between the two asphalts used on the two runways?
- What are the forces imparted on, and through, the surface layer by braking aircraft and are these consistent across all runway landing and braking zones?

To address these issues, the frequency and distribution of aircraft across the four landing directions was assessed. The single-event aircraft-induced shear stresses were then calculated at various locations and under various braking conditions across the airport. This Phase of investigation was designed to understand the magnitude and frequency of aircraft traffic induced shear stresses as a potentially confounding variable.

The calculation of stresses required the typical aircraft landing operations and settings to be understood. The various three dimensional surface forces were then calculated. The distribution of these surface forces as stresses through the asphalt layers and interface with the underlying pavement were calculated. Various depths and locations under the aircraft tyre were considered. Various braking conditions were also considered, including benchmarking against a heavily braking truck.

The geometry and aircraft frequency/distribution at Melbourne Airport were obtained from airport staff. The surface forces induced by operating aircraft are highly variable and subject to the specific aircraft, airport, operation and pilot. Most aircraft have automatic braking systems fitted, with the various levels of braking selected by the pilot depending on airline policies, wind, and runway length, slope and surface conditions. The system targets a pre-selected deceleration rate (m/s^2). These can be over-ridden by the pilot at any time. The frequency of operations and typical surface forces were determined from actual information gathered from experienced pilots and the airport.

The stresses through the asphalt layer were calculated using computer-based modelling tools. As detailed above (2.4.1 Modelling tools) there was a need to decide between LE and FE methods for these calculations. Of the LE tools, mePADS/GAMES was considered to be the most viable in terms of near-surface stress modelling. It has been verified against results published by the AMADEUS project and used by a number of researchers in similar applications. If a more complex FE method was selected then the readily available and widely used ABAQUS would have been the preferred tool. While more mathematically powerful and precise, FE tools are far more demanding in terms of inputs and parameters.

To realise the benefits of FE methods, a typical FE tool would require a bituminous material response model such as a Prony series (Park & Kim 2001; Bandyopadhyaya et al. 2008; Wang & Al-Qadi 2010). This requires fitting a model to actual asphalt relaxation test results. A rolling tyre sub-model would also be required. Tyre-pavement interaction modelling is complicated by the difficultly and time required to measure contact stresses and the reluctance of tyre manufacturers to share tyre composition information (Al-Qadi & Wang 2011).

The LE-based mePADS/GAMES was selected over ABAQUS for this research. It was decided that there was little benefit in using a FE method if similarly simple inputs were assumed. Further, the research was comparative in nature. The relative shear stresses were compared under different braking conditions. The absolute accuracy of the calculated stresses was of less interest. The increased accuracy offered by FE methods was not warranted in light of the increased computational and material property effort required.

The calculated stresses in the surface layer were compared for various braking conditions. Octahedral shear (OSS) was used as the primary basis for the comparisons. Calculated OSS values were compared at depths of 5, 25 and 45 mm below the surface to represent the near-surface, mid-layer and near-interface stresses within the nominal 50 mm surface layer. Critical locations were selected under the centre of the tyre, just prior to the leading edge of the tyre and just in front of the tyre. In additional to the calculated OSS values, the horizontal shear was also assessed and mePADS/GAMES generated contour graphs of various calculated stresses were examined. Inspection of these graphs assisted in determining the critical locations and stress distributions. Finally the normal stress (ONS) was used to calculate the asphalts shear strength and associated stress-strength ratios at various locations to determine the critical shear state.

4.1.2 Interface Shear Resistance

The shear stress calculation Phase of the investigation determined that differential shear stresses were an unlikely explanation for the differential performance of the asphalt in the various braking zones. Calculated shear stress was not well correlated to observed performance. It focused the investigation on the surface layer and its interface to the underlying pavement.

As described above (3.4 Destructive Testing) the interface shear resistance testing performed during the preliminary investigation was enlightening. It was, however, constrained to testing only five direct (DS) and four inclined (IRIS) core samples. Further testing was considered essential to improve the understanding of the two layered (and interface) system response to monotonic and cyclic shear stress.

4.1.2.1 Direct Shear Response

The aim of the DS testing was to confirm the preliminary findings in relation to the adequacy and level of the interface or bond strength. This Phase of investigation was primarily focused on confirming the exclusion of the interface strength as a potentially confounding variable leading to the observed failures. The specific questions to be addressed included:

- Was there a systemic difference in the interface direct shear response between the two runways or inside and outside the zone where slippages were observed?
- Were any of the variables across the airfield, including traffic exposure, presence of underlying asphalt patches, bitumen type or the dust source, significant factors affecting the interface response to direct shearing?
- Could a consistent direct shear response across the airfield be utilised as a benchmark for the cyclic shear response of the various asphalt layers?

A total of nine cores (45 sub-samples) were obtained from various areas across the runway to represent the various conditions. A single core (five sub-samples) was obtained from a concurrent project at Brisbane Airport. The Brisbane Airport asphalt was designed to the same specification requirements and construction methods and the surface had shown only good performance. This provided an independent benchmark.

Limited discretion was available in planning the location and condition of the various cores. Access to the various areas of the airfield was not always available and the airport was desirous of minimising both forensic coring of their surface as well as disruption to airfield operations. Even well backfilled core holes represent a maintenance liability for the remainder of an asphalt surface life. Analysis of the results was required to accept that the sampling could not be completely randomised and was partly opportunistic.

The samples were prepared, tested and results analysed as detailed below (4.4 Description of Non-Standard Tests). Analysis included the calculation of interface shear resistance parameters of strength (ISS), modulus (ISM) and work (ISW) over the first 10 mm of deformation. Each parameter was assessed using Mohr-Coulomb type failure envelopes as is accepted practice for these parameters (Uzan et al. 1978). This provided a more thorough understanding of the variability, factors affecting and overall adequacy of the direct shear response of the surface interface with the underlying pavement.

4.1.2.2 Cyclic Shear Response

The aim of IRIS testing was to mimic the cyclic nature of the aircraft induced shear stresses across the interface. The IRIS testing was designed to consider the same questions as the DS testing was, but in relation to cyclic shear response. It was suspected, however, that rather than exclude a potential confounding variable, the IRIS testing would confirm significantly different response between the two runways.

A total of 20 cores were recovered from the surface for IRIS testing. These cores were obtained from similar locations as the DS cores. Two additional cores were obtained from the concurrent project at Brisbane Airport. In some cases, two sub-cores were obtained from a single large core. In other cases, a single large core was used to manufacture a single IRIS core and multiple DS samples. As detailed below (4.4 Description of Non-Standard Tests) the IRIS results were analysed to calculate the number of cycles to tertiary flow initiation, as well as deformation after 400, and 2,000 load cycles.

It was originally expected that the IRIS testing would evaluate the difference in response to cyclic shear loading of the interfaces. As will be explored in detail later (6.4 Outcomes and Limitations) the IRIS test actually identified the weakest link in the two layered system. This could be the surface layer, the interface or the underlying asphalt layer. The numerical results became less important than the failure mode, which identified the weakest element in each sample. In combination with the consistent (across the airfield) direct shear strength of the interfaces, IRIS results enabled the relative cyclic shear resistance of the two surface asphalt mixtures to be assessed.

The IRIS test assisted in confirming the failures were occurring within the asphalt mixture (and not at the interface). A more conventional 'mixture-only' asphalt shear response test was preferred for future Phases. The alternate shear response test is discussed below (4.1.4 Asphalt Mastic).

4.1.3 Constituent Asphalt Materials

The interface shear resistance Phase of the investigation focused the remainder of the project on the asphalt mix. The interface was excluded as being a likely contributor to the failures, along with differential aircraft induced shear stresses. The constituent materials Phase of the investigation aimed at determining any fundamental difference between the asphalt mixtures constructed on the two runway surfaces.

It was known and acknowledged that the dust source changed at the transition between two runways. The properties of the two dusts were therefore focused on. Bituminous binder was also focused on as a significant factor affecting asphalt shear response. The specific questions to be answered by this Phase of the investigation included:

- Was there a fundamental difference between the two dust sources, undetected at the time construction, that might explained differential asphalt performance under cyclic shear stress?
- Given the importance of bitumen and the lack of transparency around its origins and processing, was there an unintended change that might adversely affect asphalt shear response?
- Could any evidence be found of any other constituent material unknowingly changing in a significant way during the project?

The change in dust source became the ‘obvious’ explanation once the Hisingerite clay mineral was identified and its properties understood. The assessment of all the other constituents was initially considered to be a process of eliminating potential confounding variables. However, it was found through this process of elimination, that there was some evidence of a previously unidentified change in the bitumen, also around the transition from one runway to the other as detailed later (7.3 Confounded Changes).

A philosophy of screening the various constituents using the most appropriate locally available test was adopted. The screening avoided repeating specified compliance testing as the QA records were reviewed during the preliminary investigation and no evidence of systemic deficiency was found. Any issues identified by screening were highlighted for more detailed assessment during subsequent Phases. The methods adopted to assess the consistence of each of the constituent materials are summarised in Table 12 and detailed in the following sections.

Table 12 Constituent material test plan

Constituent	Test(s)	Basis
Coarse aggregate	QA records	No known change during the project and lowest risk of contribution to failures that would not have been identified from QA records
Fine Aggregate	Angularity and Packing	The significant contribution of fine aggregate shape and friction to contribute to asphalt stiffness and resistance to deformation
Fine Aggregate	Petrography and chemical composition	The potential for a geological difference in the two dusts given the dust was the only constituent of different sources in the two mixes
Active Filler	Voids in Compacted Filler	The potential for bitumen to become ‘fixed’ within porous fillers and not available to contribute to the asphalt’s stability.
Bitumen	SARA by Iatroscan	Assessment of the relative wax, asphaltene and other fractions
Bitumen	Post-RTFO Viscosity	Difference in response to ageing and consistence across the airfield
Bitumen	Pre- and post-RTFO Dynamic Shear Rheometer temperature sweeps	Difference in response to ageing and consistence across the airfield
Mastic	Dynamic Shear Rheometer temperature sweeps	The potential for some interaction between the fine aggregate, filler and bitumen

4.1.3.1 Coarse Aggregates

The coarse aggregate source quarry was visited and the quarry manager interviewed. Any variation in the source rock due to changes in the working face was discussed as well as the crushing processes and stockpile management. The fractionated aggregate and asphalt mixture QA records were also reviewed to screen for systemic variation in overall grading of the aggregate skeleton.

4.1.3.2 Fine Aggregate

Representative areas of the two quarries were sampled for fine aggregate (dust). The quarry managers were involved to provide the best chance of obtaining samples representative of the dust supplied at the time of construction. Unlike bitumen, there were no retained reference samples of dust.

The two dust sources were assessed for un-compacted voids. Methods A, B and C of the ASTM 1252-06 were utilised. Each dust sample was split into four sub-samples to provide some replication for each measurement method. For two basaltic dust sources from similar geographical locations, the shape or mineralogy of the fine aggregates were considered the only possible significant differences. The un-compacted void content was adopted as a recognised indicator of relative shape and angularity.

A detailed analysis of the chemical features of the two dust sources was also undertaken. The analysis included the chemical composition of the material interpreted from XRD testing. Following the initial XRD analysis, further geological testing was performed on the components of interest to allow identification of the specific minerals. XRD analysis was selected as this would provide a more detailed assessment of the chemical composition and clay minerals within the dust sources than the original petrographic analysis did.

4.1.3.3 Active Filler

A representative sample of the hydrated lime was obtained from the original supply. The supplier was questioned about the chemical composition and source of the filler to determine if it remained representative of the materials used during asphalt production. There was no reason to believe that the properties or source of the hydrated lime would have changed during the project.

The filler sample was assessed for Rigden's voids using AS 1141.17 as well as apparent density. Rigden's void content was measured as an indicator of the potential for unusual fixing of binder. Hydrated lime filler was also incorporated into mastic testing.

4.1.3.4 Bituminous Binder

A total of 14 retained bitumen samples were recovered from storage. Based on the recorded sampling dates, six retained samples were from Runway 09/27 (free of failures) while eight were from Runway 16/34 (with failures). An unrelated sample of the same nominal M1000 bitumen was also obtained from a project underway in 2013 (Brisbane Airport) as a benchmark.

All 14 retained bitumen samples were tested in the laboratory for viscosity at 60°C (to AS 2341.2) after ageing by RTFO (to AS 2341.109). This is the primary compliance parameter for Multigrade bitumen in Australia and is the primary control during M1000 production. This was performed as a screen for any originally undetected change in the bitumen during the works.

One of the Melbourne Airport samples from each runway was sub-sampled for rheological composition (SARA) analysis by Iatroscan, as described by Holleran & Holleran (2010). A sample from an unrelated project (Brisbane Airport) using the same grade of Multigrade bitumen of sound performance was also tested. These samples were also tested (unaged) for:

- Penetration at 25°C.
- Penetration at 40°C.
- Viscosity at 60°C.

Bitumen was also tested as mastic as detailed below.

4.1.3.5 Mastic

Mastic was manufactured in the laboratory using the procured dust samples selected to be representative of the two dusts utilised during the project and a single sample of M1000 bitumen obtained from another (Brisbane Airport) project occurring at the time of this Phase of the investigation (2013).

Mastic samples were prepared in a 1:1 (bitumen:aggregate) ratio. To obtain the fine aggregate, the dust samples were sieved to remove particles larger than 75 microns. The bitumen:aggregate ratio was fixed for all samples despite some variation between the two mixes during the project. A fixed mastic ratio was selected to remove any effects associated with differential mastic composition. A common sample of M1000 bitumen was selected in order to remove any effects associated with inter-batch variation. A sample of dust was also procured from another airport project underway at the time of the research (Brisbane Airport) and was used to make an otherwise identical mastic sample as a benchmark.

The bitumen sample was aged in the RTFO. This mastic testing was focussed on assessing the impact of the different dust sources. At that time, there was no reason to believe that the bitumen properties had changed part-way through the project.

The mastic samples were assessed by temperature/frequency sweeps in the DSR and master curves of complex modulus were generated. The relative response to shear of the mastic was considered alongside the response of the bitumen samples under the same test conditions.

4.1.4 Asphalt Mastic

During the asphalt constituent material Phase of the investigation, it was determined that there had been an unintended change in the bitumen properties. Although all bitumen was fully and consistently compliant with AS 2008, the retained samples pre-April 2011 and post-April 2011 responded significantly differently to ageing when re-tested in 2013. The bitumen supplier subsequently confirmed that the feedstock crude oil blend had changed in April 2011. By coincidence this unintended change in bitumen feedstock was confounded with the known change in dust source. The final Phase of the investigation therefore aimed at isolating the relative contribution of the unintended change in bitumen and the intended change in the dust source on the asphalt performance.

The bitumen and the dust make up the majority of the mastic. Testing of mastic was therefore used as the basis for determining the relative contribution of each to the differential asphalt performance. The 14 retained samples of bitumen from the project were used. The previously described representative samples of dust from each of the two sources provided the fine aggregate material. The common source of retained hydrated lime filler was also used.

Assessment of the mastic included three approaches:

- **Bitumen testing**. Advanced (MSCR protocol with the DSR) shear creep testing was used due to the commonly used (in Australia) DSR protocols failing to identify any significant difference.
- **Mastic testing**. Using both dust sources and retained bitumen samples from before and after the identified crude oil blend change, a fully factorial suite of mastic samples were manufactured and tested using the MSCR protocols.
- **Mixture testing**. It was expected that a difference in mastic response would be identified. To verify the mastic contribution to the asphalt mixture shear response, mixture shear testing was planned. The Flow Number test was selected as an established and simple performance test for asphalt mixture shear response. As detailed below, this testing was subsequently cancelled (4.1.4.3 Mixture Testing).

4.1.4.1 Bitumen Testing

The 14 retained bitumen samples were again tested for viscosity at 60°C following RTFO ageing (AS 2341.109 and AS 2341.2). Three recently retained samples of M1000 from other projects were also tested as a benchmark. All samples were then assessed using the MSCR (AASHTO TP 70-12) protocol for the DSR. The testing was performed at 64°, 70°C and 76°C. An assessment of the suitability of the bitumen samples for different traffic severity was also made using the PG system (AASHTO M332-14).

4.1.4.2 Mastic Testing

Six retained bitumen samples were used to manufacture mastic samples in the laboratory. The bitumen samples were selected to be three from before the crude oil blend change and three from after the blend change. While the samples were selected by convenience, they were not selected with bias. Each bitumen sample was used to manufacture two mastics, one with each of the two dust sources. The common hydrated lime filler was included in all mastic samples. The bitumen:filler:aggregate ratio was kept at 6:1:6 to be representative of the original mix designs. Testing was performed to the MSCR protocols at 64°C, 70°C and 76°C to replicate the bitumen testing.

4.1.4.3 Mixture Testing

It was originally intended to manufacture asphalt mixtures in the laboratory for simple shear testing. The samples were to be manufactured using the four mastics (both dust sources with both binder feedstocks). The common hydrated lime filler and coarse aggregate were to be used to replicate, as closely as possible, the overall grading of the asphalt mixtures used on the two runways.

However, this plan was subsequently discontinued. As will be demonstrated, the in-storage hardening of the retained bitumen samples prevented the MSCR identifying explanatory differences between the bitumen samples before and after the crude oil blend change. Identification of explanatory differences in the shear response of laboratory manufactured mixtures was rendered unlikely and testing was not performed.

If performed, each asphalt sample was to be compacted in the shear box compactor as developed and described by Gabrawy (2000) and previously used to compact mixtures in the laboratory Rickards & Gabrawy (2003). Compaction was to be continued to a target air voids content of 4% to replicate the mixture design and compaction requirements of the project. Each slab of asphalt would have then been cored to create three cylinders. Each cylinder was to be assessed for shear response using the Flow Number test (AASHTO TP 79-13). Testing would have been performed at 64°C and with a deviator stress of 115 kPa.

4.1.4.4 Addressing Potentially Confounding Factors

As the ultimate Phase of the investigation, significant attention was paid to potentially confounding variables. Much of the preliminary investigation, as well as this academic research, were dedicated to excluding factors such as aircraft induced stresses, construction variability and other constituent material changes. Potentially confounding variables that could have impacted this final Phase of investigation included:

- **Bitumen re-heating**. Some of the retained bitumen samples had been re-heated in the laboratory five times by the completion of this investigation. That is in addition to the supply, transportation and asphalt production heating cycles. To confirm the limited impact of cyclic reheating on bitumen samples, a re-heating assessment was performed, as detailed below (4.1.4.5 Bitumen re-heating Assessment).
- **Representative dust**. Regardless the effort made with the quarry managers, there was no guarantee that the dust samples were truly representative of the material used during the project. The two asphalt mixtures were recreated using the procured materials and tested under the specified mixture design requirements. This gave the highest possible confidence in the representativeness of the materials available to the investigation but some residual risk remained.
- **Filler changes**. An unintended and undetected change in the filler may have contributed to the difference in the field performance of the two asphalts. This is considered unlikely based on the continuous supply used during the project as well as the reviewed literature. If the filler was responsible, then this would likely result in no significant difference in performance for the two dust sources and two crude oil blend bitumens being considered. The low risk of an inconclusive result was significantly higher than the negligible risk of an erroneous one.
- **Bitumen ageing**. The previous Phases of investigation had demonstrated that the retained bitumen samples changed in storage. This was the result of ageing as well as the ongoing chemical reaction between the acid (PPA) modifier and the bitumen. This was considered to be the greatest risk to the outcome of this project. However, there was no way to obtain fresh samples

of bitumen that adequately reflect the unintended difference in properties and response.

All reasonably viable controls were put in place to avoid the introduction of potentially confounding variables. Where avoidance was not possible, these factors were evaluated or maintained consistent across the factors of interest. To reinforce confidence in the conclusions a triangulated approach (bitumen testing, mastic testing and mixture testing) was intended for the isolation of the bitumen effect from that of the dust source. The risk of not identifying a significant difference (Type I error) was significantly higher than erroneously reporting a significant difference that did not exist (Type II error). As explained below (4.2 Statistical Analysis) this balance of risks is statistically robust.

4.1.4.5 Bitumen re-heating Assessment

During this research some samples were re-heated and sub-sampled up to six times. The impact of this cyclic reheating was evaluated by a controlled reheating assessment. This comprised sub-sampling and testing after one, two and three heating cycles. Testing included viscosity at 60°C in accordance with AS 2341.2 before and after accelerated ageing by RTFO as detailed by AS 2341.109. The cyclic re-heating included placing the sample in an oven (165°C) until the temperature stabilised and then allowing it to completely cool at ambient conditions for 24 hours. As detailed later (8.2 Bitumen Sample Re-heating Assessment) the short-term cyclic re-heating associated with periodic sub-sampling did not significantly impact subsequent test results.

4.2 STATISTICAL ANALYSIS

For any engineering improvement there must be change. Investigative data and conclusions are required to support and justify the proposed change. This aims to prevent process modifications being made based on judgment alone. This raises the related questions of what data is required to justify a change and how should that data be analysed and interpreted? Statistics provides the answer to these questions (Lawson & Erjavec 2001).

The statistical methods and tools used to analyse the data collected as part of any research investigation must be selected based on the research question being posed as well as the structure of the data (Tabachnick & Fidell 2001). Good data structures allow for good statistical analysis so any experimental investigation should, where possible, consider the proposed analysis methods and the preferred data structure, prior to data collection rather than after.

4.2.1 Research Aim

As detailed in the previous Chapter, the aim of this research was focused on determining and demonstrating the specific cause of poor repeated shear (CSC) performance of the asphalt on Runway 16/34 at Melbourne Airport. This was heavily reliant on comparison of mixture and constituent material test results for the poorly and adequately performing asphalts. Comparison with similar asphalt mixtures from other airports was also considered. The statistical comparison of the quantitative test results and the relative significance of qualitative and quantitative factors was therefore a key element of this research.

4.2.2 Form of Data

The structure and type of data collected as part of this investigation varied. Some data was simple in nature, being multiple measurement of batches or lots of theoretically identical material. This was generally assessed using comparison of means and variance as well as other descriptive statistics.

Other data was more complex, including unbalanced factors, covariates, multivariates with both continuous and categorical elements. This required more complex analysis methods. Table 13 summarises the structure and nature of the data collected, including the Independent Variables (IVs) and Dependent Variables (DVs).

Table 13 Summary of structure and nature of data to be collected

Test Type	DVs	Nature of DV	IVs	Nature of IVs
Single material properties	Various	Singular Continuous	Nil	N/A
Single material properties	Various	Singular Continuous	Singular Group	Categorical
Density	Density	Singular Continuous	Bitumen Dust Aggregate Trafficked Patched	Categorical, primarily Dichotomous
Modulus	Modulus	Singular Continuous	Bitumen Dust Aggregate Trafficked Patched	Categorical, primarily Dichotomous
Direct Shear	Interface Strength Interface Modulus Interface Work	Multiple Continuous Covariates	Normal Stress Bitumen Dust Aggregate Trafficked Patched	Continuous Covariate Categorical, primarily Dichotomous
Inclined Shear	Failure Mode Cycles to deformation	Multiple Mix of Categorical and Continuous	Bitumen Dust Aggregate Trafficked Patched	Categorical, primarily Dichotomous
MSCR	Creep compliance and other parameters	Multiple Continuous Covariates	Bitumen Dust	Categorical and Dichotomous

Data is considered to be balanced when an equal number of measurements from each treatment or group are being compared (Lawson & Erjavec 2001). This investigation, particularly in the early stages, focused on variability or systemic differences within the theoretically homogenous asphalt within the area that was performing poorly in the field. Further, the ability to obtain samples from the field represented a significant cost to the investigation and a significant operational impost to Melbourne Airport.

It follows that the data collected was unavoidably unbalanced. The poorly performing area of asphalt was sampled and tested significantly more frequently than the theoretically identical asphalt that was performing well. Testing of the alternate asphalt mixture used at Melbourne Airport was also limited. Sampling of similar asphalt from other airports, for benchmarking, was similarly expensive and disruptive and was limited. The selection of statistical techniques had to take the unbalanced nature of the data into account.

4.2.3 Statistical Techniques

There are generally multiple techniques that could validly be used to analyse the same set of data to address the same research aim (Lawson & Erjavec 2001). It is desirable that the simplest and more efficient techniques be employed to analyse the data collected. Broadly speaking, there are two schools of analysis techniques that are generally suited to the two types of primary research question (Tabachnick & Fidell 2001):

- Degree of relationships among variables.
- Significance of difference groups or treatments.

This project is firmly focused on the significance of differences between groups, where groups were determined by the value/level of the various IVs described in Table 13. The following statistical analysis methods were therefore selected for the various sets of data to be collected.

4.2.3.1 Summary Statistics

The comparison of simple data is often best performed by comparison of summary statistics. Commonly adopted summary statistics include:

- **Mean**. The average of all the samples in the population or sub-population. An expression of the expected value for a sample selected at random.

- **Standard Deviation**. A mathematical indicator of the spread of the data. A higher Standard Deviation (SD) implies more spread or variance in the sample population of sub-population.
- **Coefficient of Variability**. The ratio between the SD and the mean. Coefficient of Variability (CV) is a normalised expression of the SD (as a percentage of the mean) allowing comparison of sample population and sub-population across measurements that have different means.

Mean, SD and CV are commonly reported in this Dissertation, sometimes in isolation and sometimes in combination with other statistical parameters.

4.2.3.2 Analysis of Means

For simple data of a continuous nature comparing various measurements of a single parameter, simple statistical comparison of the values, the mean value and the standard deviation were performed. An assessment of outliers was also undertaken.

Where the continuous DV was being compared for two groups, the difference between the two groups was compared based on the mean and variance for each. The significant of the difference between the groups was assessed using the Student's t-test. Depending on whether or not the assessment was considered to be one or two sided and whether or not the sample sizes were equal and the variances were considered to be equal, one of the following was adopted:

- Single/two sided t-test for comparison of means with known variance. Where both the sample size and variances were considered to be equal.
- Single/two sided t-test for comparison of means with unknown variance. In all other cases.

4.2.3.3 Analysis of Variance

For data that contained multiple categorical IVs representing multiple and inter-related groupings, Analysis of Variance (ANOVA) is appropriate and was utilised. Where there were multiple DVs, Multiple ANOVA (MANOVA) applies. This technique measures the variance of the results within all the groups based on:

- The within group estimate of variance, which is insensitive to differences in the group means.
- The between group estimate of variance, which is the most sensitive to differences in the group means.

By comparing the measured overall variance from these two methods, inference can be made regarding the likelihood that the groups come from a single population of common mean value (Wheeler 1988). ANOVA makes a number of assumptions including, the important and somewhat limiting, equality of sample sizes within each group and equal variance with each group. Where these assumptions are not satisfied, the reliability of the ANOVA outputs becomes questionable (Pallant 2005) and a more robust approach should be considered.

4.2.3.4 Analysis of Covariance

Analysis of Covariance (ANCOVA), and by extension Multiple ANCOVA (MANCOVA) and more generalised versions of ANOVA and MANOVA that allow for (Tabachnick & Fidell 2001):

- Unbalanced data where the number of samples is not equal for all groups.
- Unequal variances within the various groups.
- The influence of covariates on the DVs to be taken into account prior to the effect of the groups being analysed.

ANCOVA and MANCOVA utilise sets of contrasts to separate the effects of the various IVs. To completely separate the effects of the various IVs, the sets of contrasts must be orthogonal. Orthogonality is complete non-association between variables. It allows the effect on the DV attributable to each of the IVs to perfectly sum to the total change in the DV. Orthogonality of contrasts is equivalent to mutual exclusivity of events (Tabachnick & Fidell 2001). Where interpretable, orthogonal contrasts can not be developed, either the interpretability or the reliability of the results must be compromised (Wheeler 1988).

4.2.3.5 Linear Regression

Regression analysis is the development of a simple model that uses the IVs to predict the average value of the DV (Ramsey & Shafer 2002). Multiple linear regression allows for multiple IVs while multivariate regression allows for multiple IVs and DVs. Non-linear relationships and interactions can be catered for by mathematical operations within the linear regression model.

In observational studies, causation can be not assumed, with ‘association’ being a more appropriate term. Causation can only be implied from the result of randomised experiments (Ramsey & Shafer 2002). Inferences from regressions require the various input parameters to have equal variances and each treatment to have the same number of observations. Where these requirements are not met, alternate methods, such as General Linear Models (GLMs) are more appropriate (Lawson & Erjavec 2001). However, where these is a clear theoretical basis for believing that a specific causal relationship exists between IVs and the DV, linear regression can be very useful where prediction of the DV is of interest (Tabachnick & Fidell 2001). Where (other) appropriate methods have identified a causal relationship between the IVs and the DV and prediction of the DV is desirable, linear models can be generated to estimate the DV based on the statistically significant IVs.

4.2.4 Computer Software

There are a number of readily available commercial software packages for the performance of statistical analysis. Common packages include SPSS (Pallant 2005) and Minitab (Minitab 2010). Microsoft Excel is also useful for simple summary statistics, univariate analyses and graphical displays but not for multivariate and more complex techniques. Due to availability and familiarity, Minitab Version 16 was utilised for all analysis that exceeded the limitations of Excel in the research presented in this Dissertation.

Minitab 16 allows for all of the proposed analysis techniques detailed above. Where the ANOVA/MANOVA assumptions were not satisfied, more general analysis was performed under the GLM routine in Minitab.

The GLM is the most generalised form of a regression-based statistical tool and does not depend on many of the assumptions adopted by ANOVA/MANOVA or linear regression (Tabachnick & Fidell 2001). As a result, the risk of making a Type II error (not rejecting a false null hypothesis) is increased but this must be accepted where the assumptions required to justify a more specific analysis technique are not met. Type II errors are considered to be more desirable than Type I (rejecting a correct null hypothesis) errors.

The GLM routine in Minitab incorporates both ANCOVA and MANCOVA. The specific calculations are determined by the GLM routine based on the structure of the data and any user-defined covariates. This approach is specifically applicable to:

- Analysis of data that is unbalanced and/or or unknown or unequal variance.
- Comparing the means of groups (defined by categorical and/or dichotomous IVs) after taking the effect of one or more covariates.
- Analysing multiple DVs that are measured on the same scale.

4.2.5 Significance Level

As is common practice in statistics, science and engineering in Australia and other countries, the significance level was set to 5%. That is, the probability of making a Type I error was 5% or 1:20. This is reported as a p-value. For example, a p-value of 5% indicates a 5% change of a Type I error being made.

Where the analysis supported the rejection of a null hypothesis, it was concluded that the analysis has indicated a ‘statistically significant’ difference. As is also common in engineering and scientific research, results that would have been considered statistically significant at a significance level of 10%, were noted as being ‘marginal’ but were not referred to as ‘significant’. These terms, statistically ‘significant’ and ‘marginal’ are utilised throughout the presentation of the data analysis.

4.2.6 Normality, Variance Equality and Outliers

Some of the statistical analysis techniques to be used rely on assumptions regarding:

- The samples being drawn from populations that are normally distributed.
- The equality of variances within the various groups.

For all statistical analysis, normality of the populations from which the samples were drawn was checked by the Anderson-Darling assessment as well as visual inspection of the residual plots. Where techniques that assume variance equality were utilised, this was assessed by Lavene's test (Minitab 2010).

Data points that were highly influential and/or likely to be considered outliers are automatically highlighted by the various Minitab (2010) routines. Where outliers were removed from the data set prior to finalisation of the analysis, this is highlighted throughout the presentation of the test results and data analysis.

4.3 SOURCES OF DATA

Each Phase of this research relied on the analysis of data using the statistical techniques detailed above (4.2 Statistical Analysis). Some data was used as an input to calculations and other data was measurements of properties of various materials that were then statistically compared. The sources of data required were diverse. Table 14 summarises the primary sources of data utilised as part of this investigation as presented in this Dissertation.

Table 14 Data sources

Data	Use	Source
Airport aircraft traffic statistics	Determine frequency of braking induced shear stress by runway	Provided by Melbourne Airport operations staff as part of the preliminary investigation
Aircraft landing operational parameters	Calculation of surface stresses applied by aircraft during typical landing operation	Obtained from senior Qantas pilots with years of experience operating critical aircraft to/from Melbourne Airport

Data	Use	Source
Airfield geometry	Calculation of surface stresses applied by aircraft during typical landing operation	Provided by Melbourne Airport operations staff as part of the preliminary investigation
Representative pavement structure of the two runways	Calculation of near-surface shear stresses during typical landing operation by runway	Provided by Melbourne Airport operations staff as part of the preliminary investigation
Monotonic interface shear resistance	Comparison of interface shear resistance across the two runways	Measured by laboratory testing of cores recovered from Melbourne Airport
Cyclic layer-interface system shear resistance	Comparison of system resistance to cyclic shear across the two runways	Measured by laboratory testing of cores recovered from Melbourne Airport
Constituent material production/quality properties	Assessment of material consistence across the two runways	Provided by Fulton Hogan and Beca as part of the preliminary investigation
Constituent material screening properties	Assessment of material consistence across the two runways	Measured by laboratory testing of samples obtained from the various material suppliers or retained as part of the project quality processes and provided by Fulton Hogan
Fine aggregate geological composition	Comparison of geological impacts of change in fine aggregate source	Measured by laboratory testing of representative samples of fine aggregate by Auckland University
Retained bitumen properties	Assessment of magnitude of change in properties from change in crude of source	Measured by laboratory testing of samples retained as part of the project quality processes and provided by Fulton Hogan
Retained bitumen resistance to shear stress	Comparison of bitumen performance impact of change in crude oil source	Measured by laboratory testing of samples retained as part of the project quality processes and provided by Fulton Hogan
Asphalt mastic resistance to shear stress	Comparison of asphalt performance impact of changes in fine aggregate and crude oil sources	Measured by laboratory testing of samples manufactured from representative constituent material samples obtained from the various material suppliers or retained as part of the project quality processes and provided by Fulton Hogan

4.4 DESCRIPTION OF NON-STANDARD TESTS

Where available, Australian Standard and other national and international test methods were adopted for all Phases of this investigation. The primary exception was the interface shear resistance. As detailed above (2.5 Asphalt

Interface Shear Resistance) there are no internationally recognised or published standard test methods for characterisation of interfaces under shear loading. Various researchers have developed test methods appropriate to their needs based on their locally available equipment. A method for direct monotonic (DS) and repeated inclined (IRIS) testing of interfaces was modified based on a method previously utilised by Fulton Hogan's national research laboratory in Sydney. The test methods are included in Appendix 2 and are described below.

4.4.1 Direct Shear Test

Direct (DS) testing was designed to measure the monotonic characteristics of the interface between the surface and the underlying layer. Mohr-Coulomb type envelopes were used to characterise and compare the calculated characteristics.

4.4.1.1 Test Method

A shear box style test was selected over a shear tube test. This selection was based on the available test equipment configuration, the desire to apply a normal stress during the shearing and the preferred sample shape. Up to six prismatic samples were cut from each single 240 mm core and tested at various normal stresses. Square samples are not commonly used for direct shear strength testing but were selected to avoid any point-loading associated with imperfectly matching circular sections. The samples had nominal 50 mm by 50 mm interface dimensions and were nominally 100 mm thick (two 50 mm layers). The interface was identified prior to cutting to ensure it was located at the centre of the prismatic sample thickness.

The available test equipment had been developed for testing laboratory prepared samples with relatively smooth interfaces. The use of samples cut from field cores with a milled interface was of concern. Variation in the interface texture could result in high variability in results for the samples cut from the same core and tested at difference normal stresses. The applied normal stress ranged from approximately 20 kPa to 700 kPa, in order to generate Mohr-Coulomb type envelopes. These normal stresses were selected as being indicative of the range of stresses experienced by an interface as an aircraft passes.

DS testing was performed on samples conditioned to 55°C to represent the mean summer pavement temperature approximately 50 mm below the asphalt surface. The samples were sheared at a constant rate of 50 mm per minute. This rate was selected as being consistent with the rate used by most other researchers.

4.4.1.2 Analysis Protocols

During DS testing, temperature, deformation, normal force and shear force were all measured and recorded. These parameters were logged every 0.1 seconds throughout the deformation. From these parameters, the normal stress and shear stress were calculated along with the peak shear stress and the deformation at which the peak shear stress occurred.

For each sample the interface strength (ISS), modulus (ISM) and work (ISW) were calculated. The ISS was calculated based on Equation 7 using the remaining interface contact area at the time of the peak shear load. The ISM was calculated using Equation 8. The ISW was calculated as the area under the load-displacement graph (Equation 9) during the first 10 mm of deformation.

A linear regression was subsequently performed on the ISS, ISM and ISW results for each core. For the ISS, the linear regression y-intercept represented the interface cohesion which is provided by the adhesion between the layers provided by the tack coat. The slope of the regression provided the friction angle of the interface strength. Similar representations (intercept and gradient angle) were calculated for ISM and ISW.

4.4.2 Inclined Repeated Interface Shear Test

The inclined interface (IRIS) test was designed to imitate the cyclic shear stresses expected to occur in an asphalt surface layer in the field during aircraft braking. The test was designed to assess interface resistance to cyclic shear loading. As will be demonstrated later (6.3.2 Outcomes and Limitations) it was found to be an effective tool for the determination of the weakest element in the layer-interface-layer system.

4.4.2.1 Test Method

The IRIS testing was performed in a cyclic compression manner. To induce a shear stress across the interface, the interface was orientated at 45° to the vertical and at the vertical centre of the sample. To achieve this, 75 mm diameter cores were cut on a 45° angle to the vertical from a 240 mm diameter core. After the depth of the interface from the surface was determined, the required location of the core was calculated to provide the central location of the interface within the 75 mm tall cores.

In many cases, the sample was not sufficiently tall to allow the tops to be trimmed to the required sample height. An epoxy of approximately matching stiffness was provided to the tops of the cores after coring and before final trimming. Prior to testing, the samples were measured and pre-conditioned to the test temperature of 55°C.

The test temperature was selected to be consistent with the DS testing and to be representative of the mean summer temperature at the interface. The samples were subjected to cyclic compression loading as:

- Load rate/frequency. 0.1 second haversine loading.
- Rest time. 0.9 seconds.
- Confining stress. 138 kPa.
- Cyclic axial (deviatory) stress. 828 kPa.

Each sample was tested under a sub-maximal cyclic load until 20,000 cycles or failure occurred as either asphalt deformation or interface deformation exceeded 100,000 µƐ. The sample deformation was measured and recorded against load cycles. Following completion of the test, the cores were inspected to determine the failure mode. Failure mode could include surface layer asphalt deformation, interface de-bonding or underlying asphalt layer deformation.

4.4.2.2 Analysis Protocols

Test temperature, confining pressure, vertical load and axial strain were logged every 0.1 seconds during the cyclic loading. From these parameters the vertical stress and axial strain were calculated. The strains after 450 and 2,000 cycles were reported as well as the number of cycles at which tertiary asphalt creep commenced. The deformation after 20,000 cycles was also recorded. Where 100,000 µɛ of deformation occurred before 20,000 load cycles, the number of cycles until reaching 100,000 µɛ was recorded. The failures mode was reported based on visual inspection of dissected samples after IRIS testing.

The test results were used to calculate the cumulative strain and strain rate after each cyclic load application. The strain rate at cycle n was calculated as the difference between the cumulative strains measured after cycle n and cycle n-1. To reduce the 20,000 data points (one per cycle) to a manageable number, 19 characteristic cycles were selected ranging from n=5 to n=20,000. As the number of cycles increased, the gap between values of n also increased. This reflected the reduction in change in strain rate as the test progressed up to the point of tertiary creep initiation.

4.5 SUMMARY

This Chapter presented the various research methods to be utilised during the various Phases of the project. In broad terms this included stress calculation tools, interface shear resistance measurement, repeated shear response testing and screening for consistence of the various asphalt mixture constituents. Finally, the methods for assessing the mastic (specifically the bitumen and dust source) were presented. In all cases, the selected methods were a compromise between the state of the art, the equipment and resources available to the project as well as the significance to the overall research.

The following Chapter details the calculation of differential shear stresses under braking and non-braking aircraft during landing on the various runway directions. The differences in calculated shear stress are considered as a potentially confounded contributing factor to the CSC failures.

5. AIRCRAFT INDUCED STRESSES

The previous Chapter detailed the available and selected test methods adopted as part of this research. In broad terms, the methods included stress calculation tools, interface shear resistance measurement, repeated shear response testing and screening for consistence of the various asphalt mixture constituents.

This Chapter details the calculation of the near-surface stresses induced by aircraft in braking and non-braking conditions. The stresses calculated in each of the landing directions at Melbourne Airport are compared. This is the primary element of Phase 1 of this investigation as shown in Figure 17.

This Chapter is a revised version of a journal paper currently under peer review. A copy is included in Appendix 1.

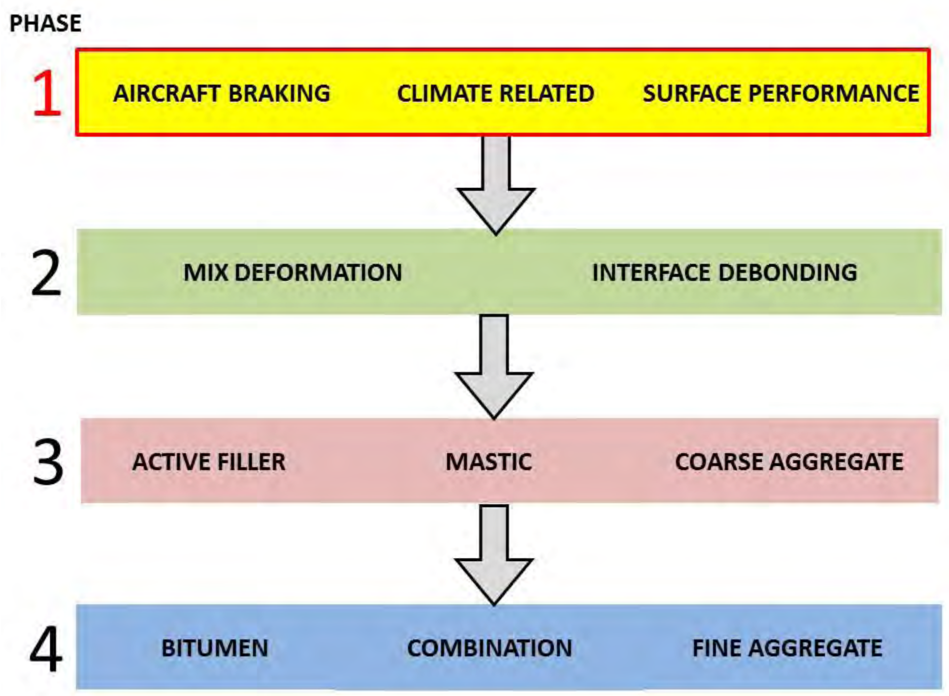

Figure 17 Phase 1 of sequential investigation framework

This analysis demonstrates that neither frequency nor magnitude of shear stress explains the difference in surface performance. The impact of aircraft braking on surface layer stress state is also demonstrated. This allowed the investigation to focus on the asphalt surface layers and the subsequent Chapter considers the interface shear resistance.

5.1 AIM OF RESEARCH PHASE

The aim of this Phase of the investigation was to confirm the preliminary investigation findings by excluding differential shear stresses induced by braking aircraft as an explanation for the differential shear performance between the two runways. The specific questions to be answered by this Phase of the investigation included:

- Why was the same asphalt mixture failing in the Runway 16 braking zone but not the Runway 34 braking zone?
- Does the absence of failures in the Runway 27 reflect a difference in the aircraft traffic and/or operations?
- What are the forces imparted on, and through, the surface layer by braking aircraft and are these consistent across all runway landing braking zones?

As detailed above (4.1.1 Aircraft Induced Stresses) the LE tool mePADS/GAMES was used to calculate various stresses in the asphalt surface layer. Various braking conditions were considered and a heavy braking truck was compared as a benchmark.

5.2 AIRCRAFT OPERATIONS

5.2.1 Airfield Geometry and Aircraft Usage

Melbourne Airport has two runways (Figure 18). The main Runway 16/34 is 3,600 m in length and caters for the majority of the heavy aircraft. The secondary, or cross, Runway 09/27 is capable of aircraft operations up to B767 in size. Both runways have generally uniform longitudinal gradients.

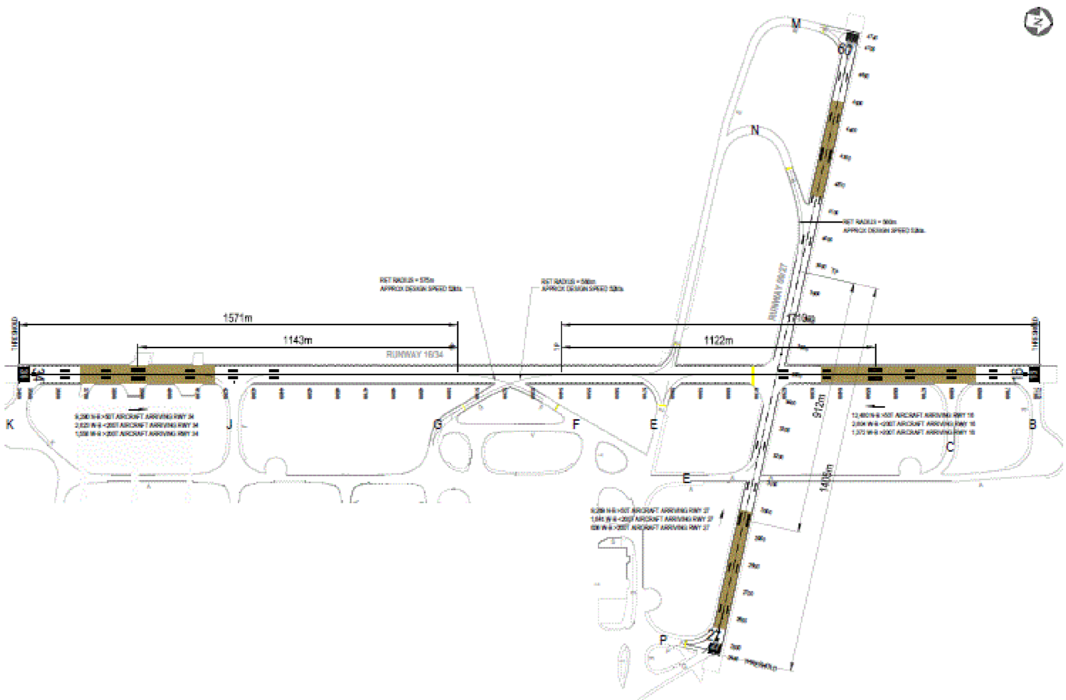

Figure 18 Melbourne Airport airfield layout

Runway 16/34 is provided with two Rapid Exit Taxiways (RETs). These are termed RET G (used when landing on Runway 16) and RET F (used when landing on Runway 34). Runway 09/27 has a similar taxiway termed RET N (for landing on Runway 27). Landings on Runway 09 are uncommon for commercial aircraft so no RET is provided.

The distances from each touch down zone to the entry of the associated RET and the average runway gradients are shown in Table 15. These distances are comparable for the three landing directions with RETs. The distribution of aircraft landing on the various runway directions is provided in Table 16 for various aircraft sizes. The distribution of B737 to B767 sized aircraft is similar for Runway 16, Runway 34 and Runway 27 landings.

Table 15 Distance from touch down to RET and gradient of runways

Landing Direction	Touch Down to RET	Average Runway Gradient
RWY 16	1,120 m	-1.0%
RWY 34	1,140 m	+1.0%
RWY 27	912 m	-0.5%
RWY 09	N/A (no RET)	+0.5%

Table 16 Traffic distribution by aircraft maximum mass

Landing Direction	Narrow Body	Wide Body	
	> 50 tonnes	< 200 tonnes	> 200 tonnes
RWY 16	40%	40%	39%
RWY 34	30%	37%	44%
RWY 27	30%	23%	18%
RWY 09	~0%	~0%	~0%

Over 50% of the Narrow Body (>50 tonnes) and light Wide Body (<200 tonnes) aircraft exit at the respective runway RETs. This included the B737 and B767 aircraft and Airbus aircraft of equivalent size. In contrast, only around 20% of the heavy Wide Body (>200 tonnes) aircraft make RETs G and N (Runway 16 and Runway 27 landings) while over 50% make RET F (Runway 34 landings). Heavy Wide Body (>200 tonnes) aircraft include A340, A380, B777 and B747. It follows that light Wide Body (<200 tonnes) aircraft braking triggered the failures as these aircraft land on Runway 16, braking in the area where failures were concentrated prior to turning into RET G. Larger aircraft did not brake heavily in the failure zone as they continued further down the runway prior to turning off.

The traffic loads and frequency were similar for the braking zones associated with the landing and exiting on the RET for all three regularly used landing runway directions. The frequency of aircraft type was therefore excluded as a potentially confounding variable associated with the differential runway surface performance.

5.2.2 Typical Operations

The Chief Pilot of the Qantas' Melbourne Airport Base was interviewed along with a Qantas Technical Pilot based in Sydney. The interview focused on the aircraft characteristics and operation during typical B737 and B767 aircraft landings at Melbourne Airport on Runway 16, Runway 34 and Runway 27.

The salient outcomes of the interview were:

- Aircraft land at 250 km/h regardless of runway direction or aircraft mass and are limited to 90 km/hr at the commencement of the turn into the RET and 20 km/hr to make a 90° turn into a perpendicular taxiway.
- Aircraft generally land long of the target touch down point rather than short. For runways with a downward grade, the tendency to land long will be exacerbated by the runway falling away from the aircraft.
- All domestic B737 and B767 pilots would aim and be expected to exit at the respective RET.
- Generally when the wind is coming from the north, the wind is strong while winds from the south are often lighter.
- All significant aircraft have autobrake systems as well as airbrakes. Airbrakes become ineffective below around 150 km/hr. Even at landing speeds, the air brakes contribute only around 10-15% of the total braking effort.
- Autobrake settings target the following aircraft decelerations:

    - Autobrake setting 1. 0.9 m/s^2.
    - Autobrake setting 2. 1.2 m/s^2.
    - Autobrake setting 3. 2.1 m/s^2.
    - Autobrake setting 4. 3.0 m/s^2.
    - Autobrake setting Max. 4.3 m/s^2.

- At around 150 km/hr and above, the portion of the aircraft landing mass supported by the wings becomes negligible.
- Autobrake setting are pre-selected prior to landing and brakes automatically engage 1.5 seconds after touch down. Typical autobrake settings at Melbourne Airport are:

    - Runway 16. Autobrake setting 3 (2.1 m/s^2).
    - Runway 34. Autobrake setting 1 (0.9 m/s^2).
    - Runway 27. Autobrake setting 3 (2.1 m/s^2).

- Runway 09 is rarely used for landings by commercial aircraft.
- The significant difference between the brake setting for Runway 16 and Runway 34 landings reflects the direction of the runway slope as well as the

typical strength of the prevailing winds from each direction, as well as the tendency to land longer on the down sloping runway.

- When landing on Runway 34, aircraft speed would be typically around 20 km/hr less when entering the RET than it would for a Runway 16 landing, despite the reduced autobrake setting.
- Aircraft autobrake to around 110-130 km/hr at which time the autobrakes are manually disengaged and a gentler, largely natural or manual, deceleration maintained until turning off onto the RET at around 90 km/hr.

5.3 SURFACE FORCES

Based on the typical operating parameters derived from discussions with experienced pilots, the peak surface forces in three dimensions were calculated. Two critical locations were considered. The first was just prior to the disengagement of the autobrakes, where the deceleration was maximal and the air brakes ineffective. The second was at the commencement of the turn into the RET. At this location the aircraft is travelling at 50 km/hr and experiencing a centripetal force determined by the radius of the RET entrance curve.

The vertical force on a single wheel, the braking force (Equation 12) and the centripetal force (Equation 13) were calculated. Trigonometry was used to resolve the horizontal and vertical forces into their parallel and normal (to the surface) components. The contribution of air brakes was ignored on the basis that they are ineffective at the critical braking points. Air/wind resistance was also ignored as it was reflected by the differential autobrake settings. Table 17 summarises the calculated forces at the critical points for landing of a B767 on each runway direction considered.

$$Braking\ Force\ (kN) = mass \times deceleration\ /\ 1000 \qquad \text{Equation 12}$$

$$Centripetal\ Force\ (kN) = (mass \times velocity^2)\ /\ (radius \times 1000) \qquad \text{Equation 13}$$

Where:

Where:	mass (kg)	= the aircraft mass on a single aircraft wheel
	deceleration (m/s^2)	= the rate of aircraft deceleration
	velocity (m/s)	= the aircraft velocity parallel to the direction of travel
	radius (m)	= the turning radius

In calculating the various forces, the following approximations were adopted for all landing directions:

- Mass equal to the Maximum Landing Mass for the aircraft.
- Radius of turn for entrance onto the RET equal to 500 m.
- No braking during the turn into the RET.
- No effective lift on the wings at the critical points.
- No effective air-brake contribution at the critical points.

Equivalent calculations for other aircraft showed the B737-800, which is around half the mass but with half the number of main gear wheels, imparted very similar forces to the B767 on the surface (Table 18). These were the two primary aircraft using the RETs associated with each of the runways. Runway 09 is rarely used for landings by commercial aircraft.

Table 17 Critical B767 peak aircraft forces

Landing Direction	Location	Vertical Force	Braking Force	Centrifugal Force
RWY 16	Just prior autobrake disengagement	160 kN	35 kN	0 kN
	Commencement of turn into RET	160 kN	0 kN	20 kN
RWY 34	Just prior autobrake disengagement	160 kN	14 kN	0 kN
	Commencement of turn into RET	160 kN	0 kN	20 kN
RWY 27	Just prior autobrake disengagement	160 kN	34 kN	0 kN
	Commencement of turn into RET	160 kN	0 kN	20 kN

The vertical force did not change across the various critical locations for each runway direction. The centrifugal force and the braking forces were of the same order of magnitude but did not occur simultaneously due to braking being complete prior to commencing the turn off the runway. The conditions associated with centrifugal forces were therefore omitted from analysis as they were less severe than the corresponding braking force.

Table 18 Critical B737 peak aircraft forces

Landing Direction	Location	Vertical Force	Braking Force	Centrifugal Force
RWY 16	Just prior autobrake disengagement	150 kN	33 kN	0 kN
	Commencement of turn into RET	150 kN	0 kN	19 kN
RWY 34	Just prior autobrake disengagement	150 kN	13 kN	0 kN
	Commencement of turn into RET	150 kN	0 kN	19 kN
RWY 27	Just prior autobrake disengagement	150 kN	32 kN	0 kN
	Commencement of turn into RET	150 kN	0 kN	19 kN

Further, the forces associated with landings on Runway 27 were very similar to those associated with landings on Runway 16. Within the limits of accuracy of the assumptions, these two conditions were considered to be identical. Runway 27 landings were therefore excluded from detailed analysis. Runway 16 shear stress analysis provided a proxy for Runway 27 shear stress states.

As a benchmark, a free-rolling aircraft without braking was also considered, as was an extreme (brake setting 4) scenario. To tie this work to more commonly reported road applications, a truck braking heavily on a highway was modelled based on the following typical conditions (Vadnais & Grimes 2005; Bayan et al. 2010):

- 5 tonne per single wheel axle.
- 850 kPa tyre pressure.
- Deceleration rate of 4 m/s^2.
- No turning at the time of heavy braking.

The resulting surface force conditions are presented in Table 19. Modelled tyre pressures were 1,350 kPa and 850 kPa for aircraft and truck loads, respectively.

Table 19 Modelled surface forces

Scenario	Vehicle	Vertical Force	Shear Force
Extreme Braking Aircraft	B767	160 kN	52 kN
RWY 16 landing	B767	160 kN	35 kN
RWY 34 landing	B767	160 kN	14 kN
Non Braking Aircraft	B767	160 kN	0 kN
Heavy Braking Truck	Truck	30 kN	12 kN

5.4 STRESS MODELLING

5.4.1 Pavement Structure

In addition to the vehicle configuration and associated surface forces, the mePADS/GAMES model also required the pavement structure to be nominated. The pavement structure adopted for the two runways was:

- Asphalt surface. 50 mm thick with a modulus of elasticity (E) of 3,500 MPa.
- Additional asphalt. 100 mm, E = 2,500 MPa representing 2 x 50 mm layers.
- Fine crushed rock base. 250 mm, E = 300 MPa.
- Fine crushed rock sub-base. 1150 mm, E = 150 MPa.
- Subgrade. CBR 3%, E = 30 MPa.

The pavement layer types and thicknesses were determined from existing pavement construction records provided by Melbourne Airport. The moduli assigned to the various layers and materials were estimated from values expected of typical aircraft pavements in Australia.

5.4.2 General Stress Distribution

The stress distribution was examined from contour graphs generated by mePADS/GAMES under the various braking conditions. In mePADS/GAMES, X is the longitudinal direction, Y is the transverse and Z is vertical. The horizontal force was applied by the tyre in the X direction to represent braking.

For Non Braking Aircraft the shear stress distribution was symmetrical in both the X and Y directions. The shear stresses peaked around the perimeter of the tyre/pavement contact area over a depth range of 30 to 90 mm. This peak depth is consistent with the findings of others (Perdomo & Button 1991; Wang et al. 2014; Su et al. 2008). The peak shear stress was 733 kPa, which is 54% of the vertical contact stress. This is similar to the values reported by Wang et al. (2014).

When horizontal (braking) forces were applied at the surface, the shear forces at depth increased and the distribution around the tyre shifted towards the leading edge of the tyre. The peak shear stress calculated at the leading and trailing edges of the tyre are presented in Table 20 for the various braking conditions. For Extreme Braking Aircraft the peak shear stress was 879 kPa which is 65% of the vertical contact stress.

Table 20 Calculated peak shear stresses

Scenario	Peak Shear Stress	
	Leading Edge of Tyre	Trailing Edge of Tyre
Extreme Braking Aircraft	879 kPa	615 kPa
RWY 16 landing	828 kPa	651 kPa
RWY 34 landing	771 kPa	691 kPa
Non Braking Aircraft	733 kPa	733 kPa
Heavy Braking Truck	397 kPa	201 kPa

For Non Braking Aircraft there was a significant zone of negligible shear stress under the central portion of the tyre. Figure 19 demonstrates how this zone reduced and became a zone of near-constant shear stress near the surface as the braking force increased. By comparing Figure 20 and Figure 21, the stress distribution for Extreme Braking Aircraft is shown to approach that for the Non Braking Aircraft within 45 mm below the surface.

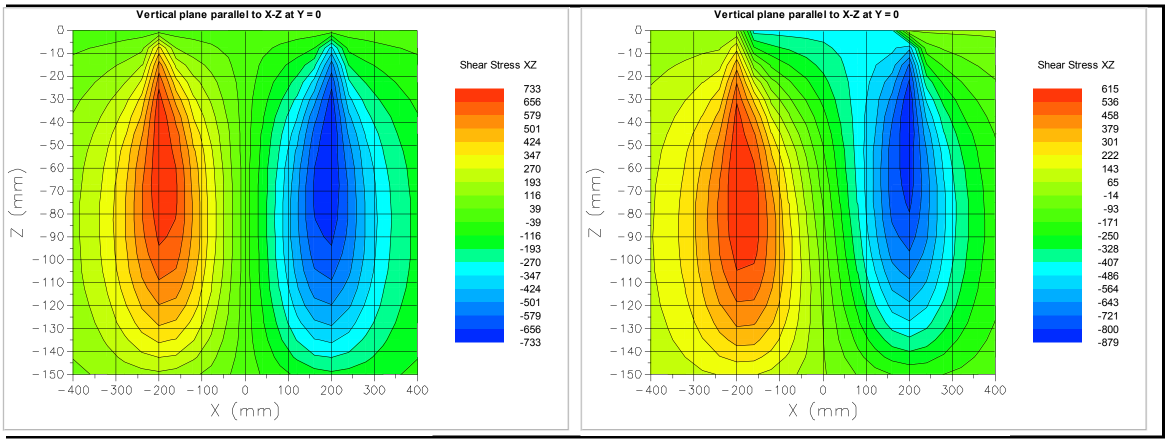

(a) (b)

Figure 19 Shear stress with depth for (a) non braking aircraft and (b) extreme braking aircraft

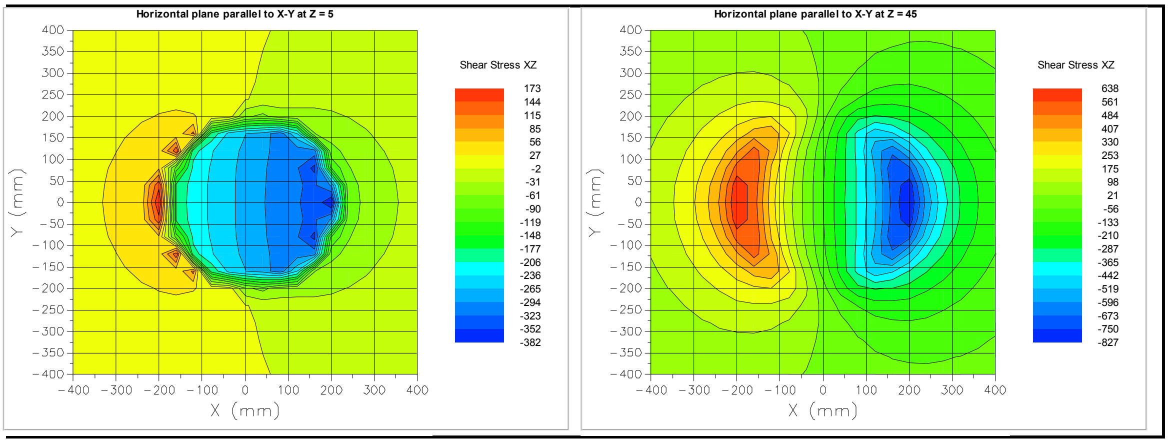

(a) (b)

Figure 20 Shear stress distribution under extreme braking aircraft at (a) 5 mm and (b) 45 mm depth

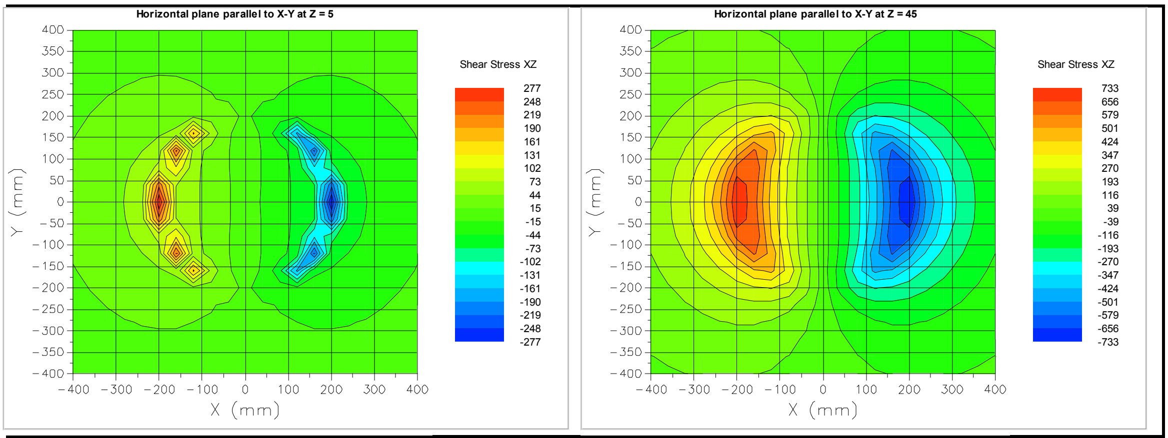

(a) (b)

Figure 21 Shear stress distribution under non braking aircraft at (a) 5 mm and (b) 45 mm depth

5.4.3 Shear Stresses

The shear and normal stresses calculated at the various critical locations and depths are presented in Appendix 3. Interestingly, the peak shear stress under the leading edge of the tyre did not increase significantly with increased braking effort. The peak shear stress for Runway 34 landing was only 5% higher than for Non Braking Aircraft. Even for Extreme Braking Aircraft, the peak shear stress was only 20% higher than for Non Braking Aircraft. Greater increases were expected given the significant horizontal force applied during braking conditions. The calculated increases were, however, consistent with the findings of Wang et al. (2014) who reported a 10% increase in asphalt response during braking.

The OSS and ONS were calculated at each location using Equations 2 and 4 and the mePADS/GAMES calculated principal stresses. These are also presented in Appendix 3. The OSS distribution was generally similar to that for the shear stress. In comparison to Non Braking Aircraft, the maximum calculated OSS values were only 2% and 4% greater during Extreme Braking Aircraft and Runway 16 landing respectively. The maximum calculated OSS for Runway 34 landing was less than 1% greater than for Non Braking Aircraft.

5.5 ANALYSIS OF RESULTS

The maximum calculated OSS induced by a heavy braking truck was only 53% of that for the moderate braking effort for Runway 34 landing. This indicated that asphalt mixtures manufactured from the same materials would likely perform well in road pavements, but not on Runway 16/34. The comparison of aircraft induced OSS focused on Runway 16 landing and Runway 34 landing conditions. It was expected that the approximate doubling of the horizontal force at the surface would translate to an approximate doubling of the OSS at depth. This was found not to be the case. The maximum OSS occurred at the centre of the tyre in all cases. This was due to the high calculated normal (vertical) stress directly under the tyre. In all cases the OSS was less than the ONS, which indicated a high level of confinement. The ONS/OSS ratio was lowest at the leading edge of the tyre where the shear stresses peaked, indicating a low level of confinement.

At the leading edge of the tyre the maximum OSS for Runway 16 landing was 1,047 kPa (Appendix 3). This was 18% higher than the corresponding value of 888 kPa for Runway 34 landing. An 18% increase in OSS at the critical location did not explain the difference in performance of nominally identical asphalt in the two landing directions of the same runway. Maximum OSS values indicate that the asphalt mixes were not being stressed significantly differently.

The distribution of the shear stresses was considered further. The most significant difference in the stresses calculated at the various locations was the shear stresses directly under the centre of the tyre. For Runway 16 landing (275 kPa) these are more than double those for Runway 34 landing (110 kPa). For Non Braking Aircraft these shear stresses were insignificant (<1 kPa). As detailed above, increasing braking force resulted in a decreasing of the zone of near-zero shear stress under the tyre. This transformed the stress state from two short periods of shear (with a relaxation period in between) to a single (extended) period of constant shearing under a passing tyre. Shear stress with depth graphs are shown in Figure 22 for Runway 16 landing and Runway 34 landing. The zone of moderate shear (greater than 280 kPa) between the leading and trailing edges of the tyre is evident for the Runway 16 landing.

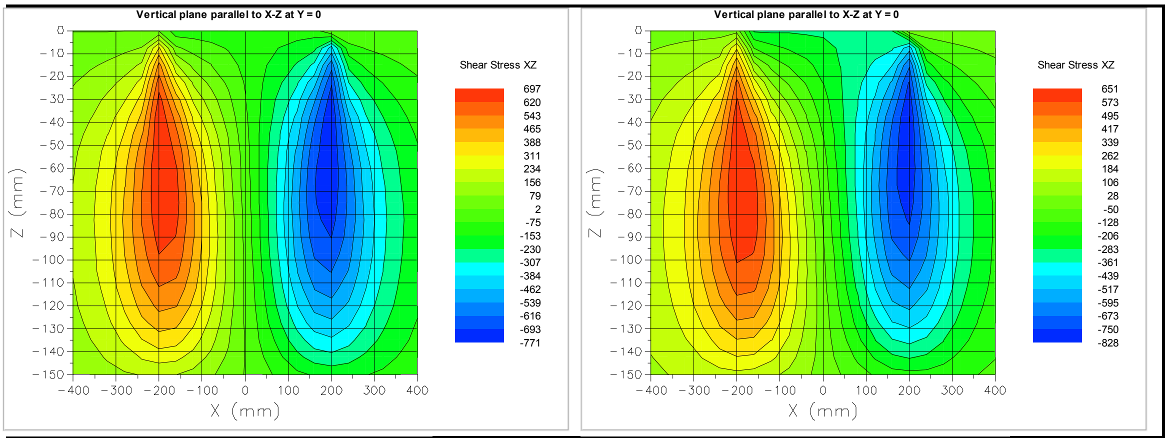

(a) (b)

Figure 22 Shear stress with depth for (a) Runway 34 landing and (b) Runway 16 landing

The asphalt octahedral shear strength was calculated from Equation 5 using the calculated normal stress (ONS) at each critical location for Runway 34 landing and Runway 16 landing. Asphalt mixture parameters c (400 kPa) and ϕ (40°) were assumed (Wang & Al-Qadi 2010). The octahedral shear stress-to-strength ratios were then calculated as presented in Appendix 3. The results were all below 100%. The critical stress condition, indicated by the highest stress-to-strength ratio, was consistently at the leading edge of the tyre (Table 21). This is the most likely location for the initiation of shear-related failures.

Table 21 Runway 16/34 Landing OSS Stress and Stress Ratios

Location	Depth (mm)	Octahedral Shear Stress/Strength (%)	
		Landing on RWY 16	Landing on RWY 34
Centre of Tyre	5	45	44
	25	33	32
	45	16	14
Inside Leading Edge	5	54	50
	25	57	55
	45	65	63
In front of Leading Edge	5	70	67
	25	66	64
	45	70	68

The observed surface failures were concentrated in the braking area associated with landings on Runway 16. Failures were not associated with landings on Runway 27. The calculated surface forces were similar for Runway 27 and Runway 16 landings. Runway 16/34 and Runway 09/27 were surfaced with different asphalt mixtures. Similarity of braking-induced horizontal forces on the surface indicated that the difference in observed shear creep performance between Runway 16/34 and the Runway 09/27 was not explained by aircraft induced shear stress. A difference in the response of the two asphalt mixtures to shear stress was a more likely explanation for the difference in observed field performance.

Further, the calculated peak shear stresses were very similar for landings on Runway 16 and Runway 34. However, failures were only observed in the braking zone associated with landings on Runway 16. The increased braking forces associated with landings on Runway 16 created a zone of near-constant shear under the tyre. This zone did not exist for landings on Runway 34 or for free-rolling braking aircraft. This zone of near-constant shear explained the presence of failures only in the braking zone associated with landings on Runway 16, while the braking zone associated with Runway 34 free of failures.

5.6 OUTCOMES AND LIMITATIONS

The calculated surface forces were consistent with the difference in field performance observed in the braking areas of aircraft landing on Runway 16 and those landing on Runway 34. It was expected that the approximate doubling of forces applied at the surface would translate to a similar doubling of the shear peak stresses in the surface layer. This was found not to be the case. Regardless of the braking condition, the maximum shear stress and OSS values were not significantly different.

However, analysis of the shear stress distributions identified a significant change with increasing braking effort. As the horizontal surface force increased, the zone of negligible shear between the leading and trailing edge of the tyres reduced and become a zone of near-constant shear stress. The similarity in peak OSS and shear stress for all braking conditions indicated that the asphalt would not fail in slip circle shear.

The shear stresses were found to peak under the leading edge of a braking tyre. A zone of near-uniform peak shear was consistently found between 30 and 90 mm below the surface. Peak shear stress values were in the order of 800 kPa, which is around 60% of the vertical stress at the surface and around double the vertical stress 45 mm below the surface. In all locations, the critical shear condition existed under the leading edge of the tyre based on calculated stress-strength ratios.

The difference in field performance of the nominally identical asphalt in the two braking zones of Runway 16/34 was not explained by the peak OSS values calculated. The failures were, however, found to have been caused by the duration of the calculated near-constant shear stress associated with a passing tyre during aircraft braking. This is consistent with the observed nature of the failures, which were creep related and not conventional slip circle shear failures.

The calculated shear stresses during braking conditions approached a magnitude and distribution similar to that for non-braking aircraft 45 mm below the surface. This indicated that there was no significant difference in shear stress, at the asphalt interface, whether the aircraft was braking or free-rolling. Delamination resulting from interface bond failure would therefore be expected to occur equally in braking and non-braking areas of runways. As a corollary, observation of horizontal deformations located only in the braking zone of runways would be indicative of internal asphalt mixture deformation close to the surface. Only near the surface is there a significant difference between the shear stresses associated with braking and non-braking aircraft. Such failures would be the result of an inadequate shear creep resistance in the asphalt. They would not be the result of delamination, which would more likely occur over the full trafficked area of the runway.

It must be acknowledged that Australian experience is that historical surface deformation has occurred mainly in the braking areas of runways. These historical failures were generally associated with delamination and therefore assumed to have been initiated by inadequate bond strength. It is possible that surface deformation previously diagnosed as bond-related could in fact have similarly been the result of inadequate shear creep resistance within the asphalt mixture.

5.7 SUMMARY

This Chapter has demonstrated that aircraft operations did not explain the difference in observed field performance of the asphalt surfaces of the two runways at Melbourne Airport. Aircraft operations were therefore excluded as a potentially confounding explanation for the slippage failures observed in the Runway 16/34 asphalt surface.

The next Chapter will detail the measurement and analysis of interface shear resistance of the two runways. Both monotonic and repeated load shear testing is considered for interfaces recovered by coring the runway surfaces.

6. INTERFACE SHEAR RESISTANCE

The previous Chapter presented the analysis of aircraft-induced near-surface shear stresses. Differential aircraft operation was excluded as a potentially confounded contributing factor to the CSC failures in the braking zone of Runway 16/34. The asphalt surface systems, including their interface conditions, became the focus.

This Chapter details the measurement and analysis of interface shear resistance of the two runways. Direct monotonic (DS) and inclined cyclic (IRIS) testing of interfaces from cores recovered from the two runway surfaces is presented. As explained above (4.1.2.2 Cyclic Shear Response) the IRIS testing was intended to assess the interface response to cyclic shear. As will be explained, the IRIS test failed to do this. However, the IRIS test proved to be an effective tool for identifying the weakest link in the multi-layer (asphalt-interface-asphalt) system. This forms Phase 2 of this investigation as shown in Figure 23.

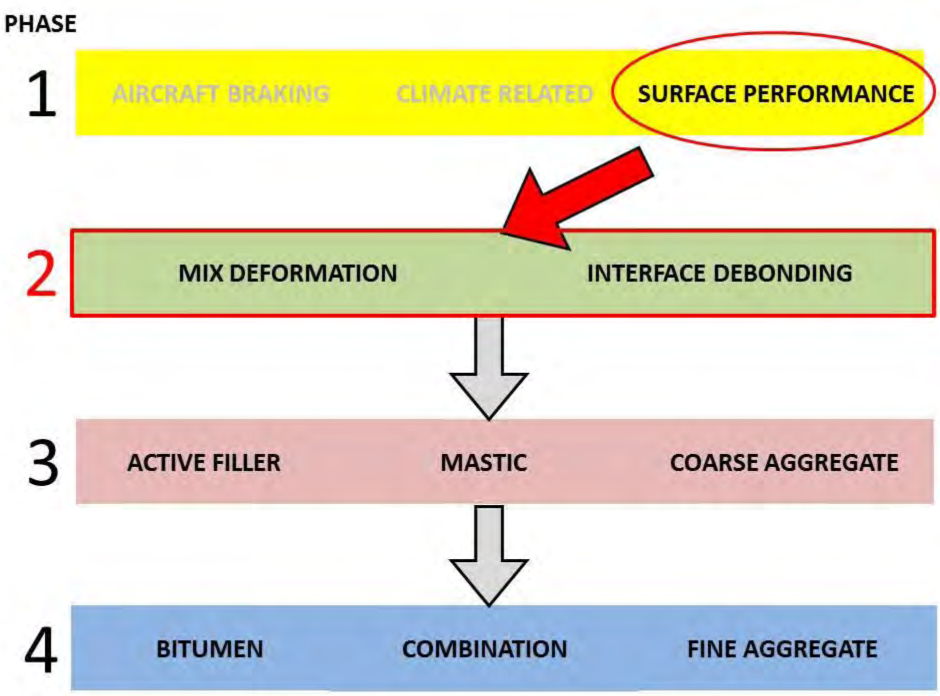

Figure 23 Phase 2 of sequential investigation framework

The interface shear resistance analysis demonstrates that there was no significant difference in the interface shear resistance between the two runways. Differential monotonic interface shear resistance was excluded as a potentially confounded contributing factor to the CSC failures observed in Runway 16/34. However, cyclic response of the asphalt-interface-interface system was found to be significantly different for the two asphalt runway surfaces. This finding allowed the next Phase of investigation to focus on fundamental differences between the two asphalt materials.

6.1 AIM OF RESEARCH PHASE

This Phase of the investigation aimed to assess and compare the asphalt surfaces of the two runways. First, the interface between the surface layer and the underlying pavement was assessed by DS testing. Second, the layer-interface-layer system was assessed using the IRIS test. The specific questions to be answered in this Phase were:

- What was the typically achieved interface shear resistance to monotonic loading?
- Were the interface strength (ISS), modulus (ISM) and resistance to displacement (ISW) different for the two runways?
- Was the layer-interface-layer system response to cyclic shear (IRIS) loading different for the two runways?

As detailed above (4.1.2 Interface Shear Resistance) cores were recovered from the two runway surfaces for DS and IRIS testing. From the DS test results, ISS, ISM and ISW were compared. From IRIS results the cumulative strain and strain rates were compared as well as the observed failure modes. Cores were also recovered from Brisbane Airport for DS and IRIS testing as a benchmark.

6.2 CORE LOCATIONS AND CONDITIONS

A total of 26 cores were recovered from the surface for DS and IRIS testing. These cores provided a total of 45 DS prisms from nine cores and 20 IRIS sample cores. The cores were obtained from both Runway 16/34 and Runway 09/27. The cores were obtained from areas with and without underlying deep asphalt patches and both inside and outside the regularly trafficked portion of the pavements.

Two cores were also obtained from a recent project at Brisbane Airport. The Brisbane Airport asphalt was manufactured with M1000 bitumen to an identical mix specification. Table 22 defines the condition and coding of the various cores. The number of cores recovered for DS and IRIS testing from each condition is summarised in Table 23. The assigned codes are used to describe the condition of the various cores in the rest of this Chapter. The numbering for multiple cores of the same condition was separate for DS and IRIS testing. That it, core MPH_1 for DS testing was not the same core as sample numbered MPH_1 for IRIS testing.

Table 22 DS and IRIS core condition codes

Dust	Patched	Traffic	Code
Matthews (M)	Yes (P)	Heavy (H)	MPH
Matthews (M)	No (U)	Medium (M)	MUM
Matthews (M)	No (U)	Light (L)	MUL
Tylden (T)	No (U)	Light (L)	TUL
Tylden (T)	No (U)	Heavy (H)	TUH
Tylden (T)	Yes (P)	Heavy (H)	TPH
Brisbane (B)	No (U)	Light (L)	BUL

'Heavy' traffic indicates samples from within the normal aircraft wheel paths. 'Light' traffic was outside the normal aircraft wheel paths. 'Medium' traffic was marginal and indicated samples that were close to taxiway and runway intersections where some turning aircraft would pass. A number of replicates were obtained for the conditions of most interest, including MPH and TPH. This allowed some assessment of intra-condition variability.

6.3 ANALYSIS OF RESULTS

6.3.1 Direct Shear

A total of 50 samples were prepared from ten cores for DS testing, including 5 samples from one of the Brisbane Airport benchmark cores. The test results and core conditions are presented in Appendix 2. The Mohr-Coulomb envelopes calculated for each are summarised in Table 24 (for ISS), Table 25 (for ISM) and Table 26 (for ISW). Coefficients of linear regression (R) are also provided. The terms c and ϕ are reserved for ISS analysis. Therefore, the generic and less meaningful terms ‘intercept’ and ‘angle’ are used for ISM and ISW.

Table 23 Number of cores for DS and IRIS testing

Condition Code	DS testing	IRIS testing
MPH	4	7
MPL	-	2
MUM	1	1
MUL	1	1
TUL	1	1
TUH	1	1
TPH	1	5
TPL	-	2
BUL	1	2

Table 24 Calculated Mohr-Coulomb envelope parameters for ISS

Core Number	C (kPa)	ϕ (°)	R (%)
MPH_1	316	46	0.99
MPH_2	309	46	0.97
MPH_3	435	30	0.85
MPH_4	493	36	0.85
MUM_1	445	26	0.95
MUL_1	309	23	0.96
TUL_1	295	18	0.78
TUH_1	291	39	0.94
TPH_1	489	29	0.98
BUL_1	173	43	0.99

Table 25 Calculated Mohr-Coulomb envelope parameters for ISM

Core Number	Intercept (kPa)	Angle (°)	R (%)
MPH_1	85	6.1	0.71
MPH_2	94	6.1	0.95
MPH_3	146	1.3	0.53
MPH_4	143	5.1	0.82
MUM_1	161	-3.3	-0.54
MUL_1	109	4.7	0.77
TUL_1	99	0.8	0.09
TUH_1	96	8.8	0.96
TPH_1	99	6.0	0.91
BUL_1	84	8.0	0.84

Table 26 Calculated Mohr-Coulomb envelope parameters for ISW

Core Number	Intercept (kN.m)	Angle (°)	R (%)
MPH_1	5.2	1.15	0.99
MPH_2	4.3	1.36	0.98
MPH_3	5.9	0.98	0.80
MPH_4	8.6	1.01	0.87
MUM_1	5.0	0.96	0.97
MUL_1	3.9	0.72	0.95
TUL_1	4.4	0.57	0.88
TUH_1	5.5	0.99	0.99
TPH_1	8.8	0.78	0.99
BUL_1	5.1	0.89	0.99

6.3.1.1 Interface Shear Strength

The correlation coefficients for ISS ranged from 0.78 to 0.99. This provided confidence in the repeatability of the test and reliability of the results. ISS cohesion values (c) ranged from 291-493 kPa with the exception of the core from Brisbane at 173 kPa. The Brisbane core was recovered within 48 hours of the overlay being constructed and the low cohesion likely reflected the ongoing curing and maturing of the emulsion tack coat. The Melbourne Airport c values are high for testing at 55°C and this reflects the high level of surface interlock that results from texturing of the underlying surface as well as the high quality of interface construction specified for airport resurfacing works.

ISS friction angles (ϕ) ranged from 18-46°. This was initially considered to be a wide range but was explained by the effect of aircraft traffic as detailed below. The average value of ϕ (34°) is consistent with values reported in the literature as detailed above (2.5.7.4 Normal Stress).

The ISS results were statistically assessed by ANCOVA, performed as a GLM routine. After the initial ANCOVA, two outliers were removed (core MPH_3 tested at 553 kPa normal stress and core TUL_1 tested at 120 kPa normal stress). These outliers showed a standardised residual exceeding 2.0. The subsequent ANCOVA output is presented in Table 27.

Table 27 ANCOVA output for ISS after outlier removal

Variable	Levels	p-value
Normal Stress	Continuous	<0.01
Patched	Yes, No	0.15
Dust	Matthews, Tylden, Brisbane	0.18
Traffic	Heavy, Medium, Light	<0.01

The normal stress applied was statistically significant (p-value < 0.01) as expected based on the literature and Mohr-Coulomb model for ISS. The impact of two years of exposure to traffic was also statistically significant (p-value < 0.01).

The presence (or otherwise) of asphalt patches in the underlying surface and the source of the dust were not significant for ISS. The regression coefficient associated with the ANCOVA for ISS was 0.92. This implied that the variables included in the ANCOVA accounted for 92% of the variance in the ISS results.

6.3.1.2 Interface Shear Modulus

The ISM results were more variable with correlation coefficients ranging from 0.09 to 0.96, with a single negative correlation value resulting from one substantial outlier. The intercepts for the regressions equations ranged from 84-161 kPa. The regression slope angles ranged from -3.3-8.8°. With little literature against which to compare, limited inference could be made of these values.

ISM ANCOVA outputs, after removal of the one outlier (core TUL_1 at 120 kPa normal stress) are in Table 28. Similar to ISS ANCOVA, normal stress and traffic exposure were statistically significant. The presence of underlying patches was not and the dust source was marginal.

Table 28 ANCOVA output for ISM after outlier removal

Variable	Levels	p-value
Normal Stress	Continuous	<0.01
Patched	Yes, No	0.13
Dust	Matthews, Tylden, Brisbane	0.09
Traffic	Heavy, Medium, Light	<0.03

6.3.1.3 Interface Shear Work

The ISW results were more consistent that ISM results with correlation coefficients ranging from 0.80 to 0.99. The intercepts for the regressions equations ranged from 39-88 kN.m. The regression slope angles were consistent but low. With little literature against which to compare, limited inference could be made from these results.

ISW ANCOVA outputs, after removal of three outliers (core MPH_3 tested at 553 kPa normal stress, core MPH_4 tested at 715 kPa normal stress and core TUL_1 tested at 120 kPa normal stress) are presented in Table 29. Similar to ISS and ISW ANCOVA, normal stress and traffic exposure were statistically significant. The presence of underlying patches was not. One difference was the significance of the dust source for ISW (p-value 0.02).

Table 29 ANCOVA output for ISW after outlier removal

Variable	Levels	p-value
Normal Stress	Continuous	<0.01
Patched	Yes, No	0.15
Dust	Matthews, Tylden, Brisbane	0.02
Traffic	Heavy. Medium, Light	<0.03

The samples containing Tylden dust generally showed a higher resistance to deformation after the peak load (Figure 24). This indicated that the Matthews dust asphalt had less frictional contribution to ISS than the Tylden dust asphalt. At lower normal stresses, the cohesive contribution to ISS was less and the difference in the post-elastic-peak behaviour was greatest. Further research is required to better understand the difference in the post-elastic peak response of the two surfaces to direct shearing.

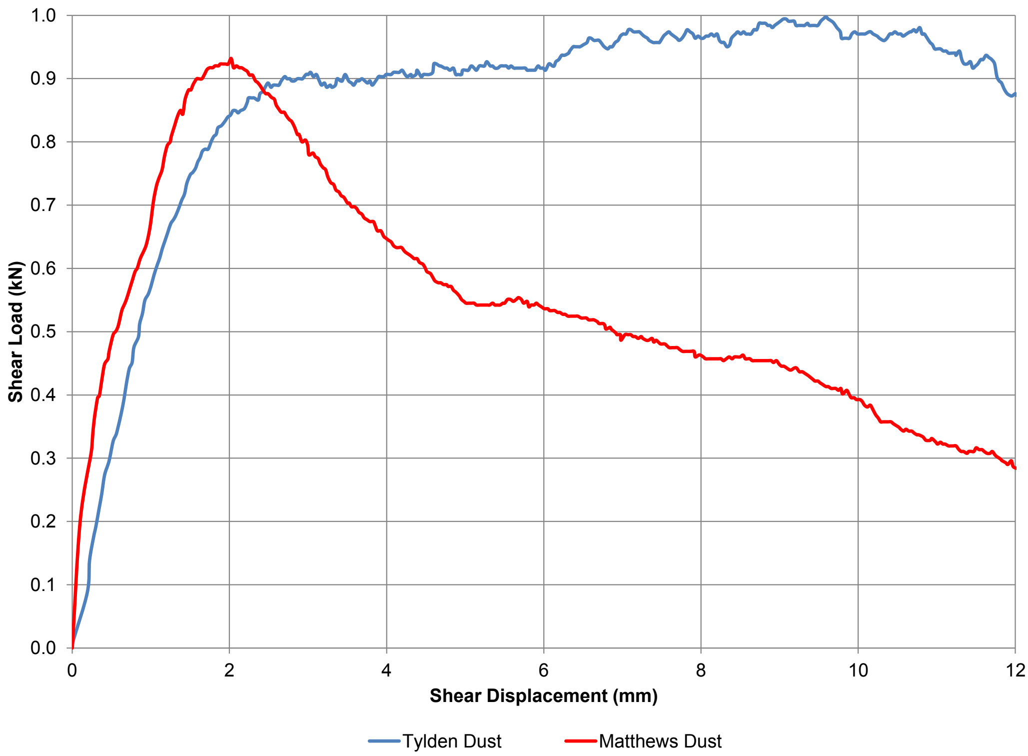

Figure 24 Comparison of Tylden and Matthews dust asphalt ISW

The difference in ISW was not significant to the observed difference in CSC resistance between the two runways. The failures were demonstrated to be initiated within the asphalt mixture and not at the interface. It follows that the measured difference in ISW had no impact on the CSC resistance of the two surfaces. However it did indicate that the Runway 16/34 (Matthews dust) surface would debond after moderate CSC deformation. The CSC deformation required to debond the Runway 09/27 (Tylden dust) surface would be greater, as indicated by the higher resistance to displacement of the interface post the elastic-peak.

Analysis of DS strength (ISS) and modulus (ISM) results indicated no statistically significant difference between the responses to direct monotonic shear of the interfaces on the two runways at Melbourne Airport. The only significant difference between the two runways was the ISW behaviour after the peak shear load was exceeded. This would not have affected the risk of delamination, which would occur concurrently with the peak shear stress.

The benchmark core from Brisbane Airport showed comparable ISS, ISM and ISW results with the exception of the ISS intercept (cohesion). This reflected the short (less than 48 hours) period between overlay construction and core recovery or may have been an anomaly of the single Brisbane Airport core tested.

Two years of exposure to regular aircraft traffic significantly improved the measured ISS, ISM and ISW across both runways. This is consistent with observations reported by other researchers (2.5.7.9 Trafficking). This unexpected observation is discussed later (9.4.2 Effect of traffic on interface shear resistance).

6.3.2 Inclined Repeated Interface Shear

A total of 22 samples were subject to IRIS testing including two from Brisbane Airport (as a benchmark). The test results and core conditions are presented in Appendix 2 and a summary is provided in Table 30.

Only eight samples commenced tertiary flow while two samples were tested to 20,000 cycles without exceeding 100,000 $\mu\varepsilon$ deformation. Ten samples exceeded 100,000 $\mu\varepsilon$ prior to 2,000 cycles being complete.

Table 30 Summary of IRIS results

Core Sample	Cycles to Tertiary Flow	Microstrain at 400 cycles	Microstrain at 2,000 cycles	Failure Mode
MPH_1	-	31,480	73,150	Surface
MPH_2	-	17,740	40,680	Surface
MPH_3	-	22,530	45,370	Surface
MPH_4	20,000+	20,380	35,230	Surface
MPH_5	-	19,750	38,270	Interface
MPH_6	-	80,630	-	Surface
MPH_7	-	69,150	-	Surface
MUM_1	4,620	32,720	58,960	Surface
MUL_1	-	30,560	60,490	Interface
MPL_1	312	40,000	-	Interface
MPL_2	-	39,820	82,720	Interface
TPH_1	-	77,800	-	Interface
TPH_2	-	67,300	-	Interface
TPH_3	147	-	-	Second
TPH_4	156	54,290	-	Interface
TPH_5	20,000+	32,000	52,500	Second
TPL_1	-	35,490	-	Interface
TPL_2	140	100,000	-	Interface
TUL_1	75	91,110	-	Interface
TUH_1	-	41,050	81,490	Second
BUL_1	65	-	-	Interface
BUL_2	100	-	-	Interface

The IRIS testing was initially intended to rank and assess with interface under cyclic loading. However, some samples did not fail at the interface. Instead, failure occurred within the asphalt surface mixture (similar to Figure 14) or within the underlying layer. Figure 25 illustrates the IRIS accumulated strain by cycles and Figure 26 illustrates the association rate of strain.

A failure mode of 'surface' indicates deformation within the surface layer, 'Interface' indicates delamination and shearing across the interface between the layers while 'Second' indicates deformation within the underlying (older) asphalt layer.

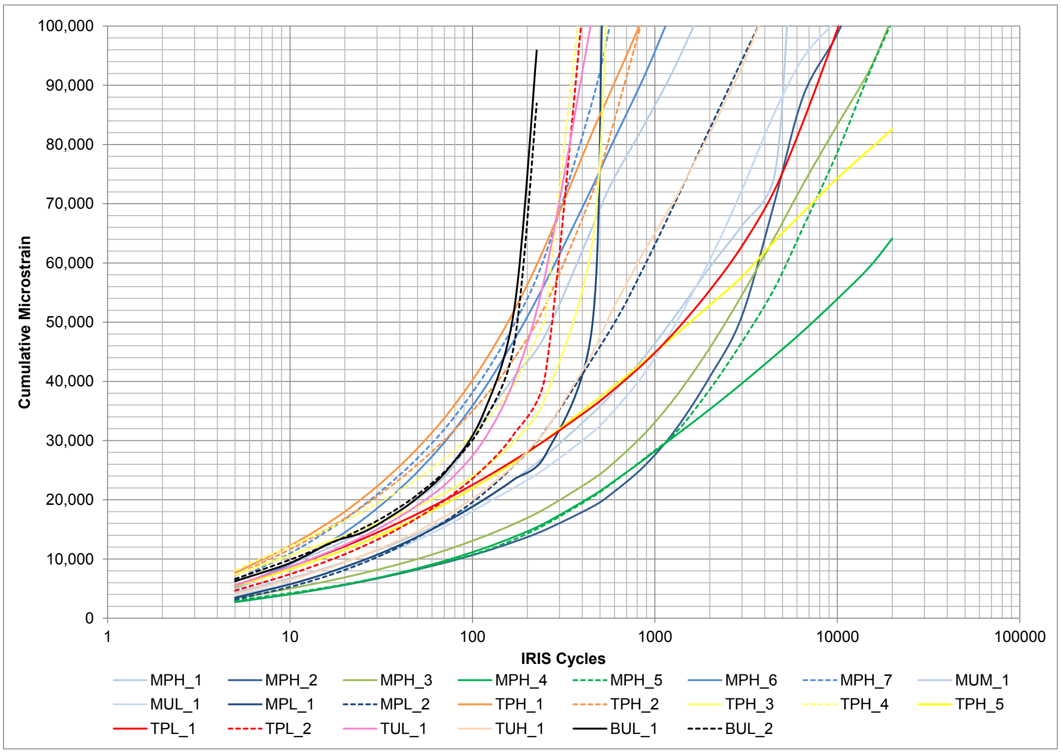

Figure 25 **IRIS accumulated strain versus load cycles**

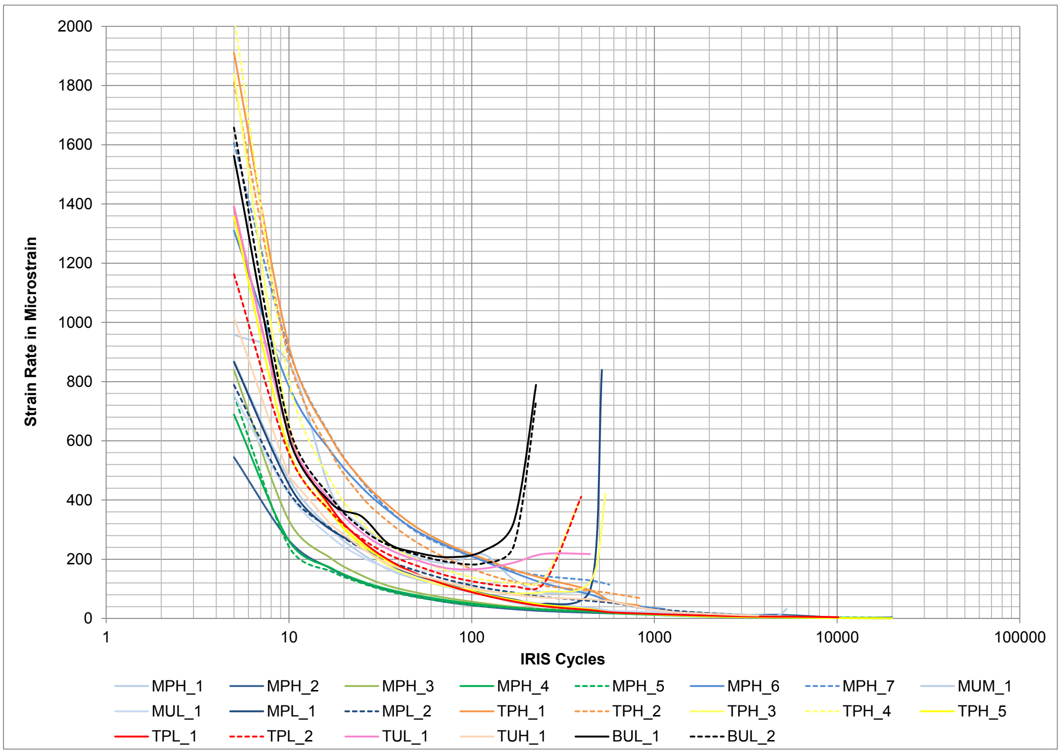

Figure 26 IRIS strain rate versus load cycles

The IRIS results generally fell into one of two categories. Firstly, some samples failed rapidly (within 1,000 cycles) often with an increasing strain rate per cycle (tertiary creep). Secondly, the other samples tended to reach 100,000 µƐ after 10,000 cycles and usually with continually decreasing or steady strain rate per cycle (secondary creep).

Numerical IRIS results were difficult to interpret as three different failures modes were observed. The measured strain at 400 and 2,000 cycles and the number of cycles to tertiary flow initiation could not separate the mode of failure. Two samples could have deformed by the same about after 400 and 2000 load cycles, but one may have deformed in the surface layer while the other displaced across a de-bonded interface. More informative was the frequency of the failure mode by dust source (Table 31**)**.

Table 31 IRIS failure mode frequency by dust source

Dust Source	Interface	Surface Layer	Second Layer
Tylden Quarry	6	0	3
Matthews Quarry	4	7	0
Brisbane	2	0	0

Only Matthews Dust samples failed by deformation of the surface layer. This indicated that in the Matthews Dust samples, the surface layer was the weakest link in the multi-layer system. In contrast both of the Brisbane Airport samples failed at the interface. The interface was the weakest element in the Brisbane Airport multi-layer system. Similarly, the majority of the Tylden dust samples failed at the interface, indicating the interface was the weakest element.

6.3.3 Multi-layer System Analysis

IRIS testing was intended to assess the comparative response of the interfaces to cyclic shear stress. However the unexpected difference in failure mode prevented such an assessment from being possible. Rather, the IRIS test became an effective means of determining the weakest link in each of the multi-layer (layer-interface-layer) systems. The consistent interface strength (ISS) across all samples provided a benchmark for comparison of the two asphalt mixtures.

For the Tylden Dust asphalt, six samples failed at the interface and three samples failed in the underlying asphalt. The three samples that failed in the underlying asphalt were all heavily trafficked. The heavy traffic had increased the ISS, ISM and ISW significantly and the underlying layer become and weakest link in the system. No Tylden Dust samples indicated the surface layer as the weakest link in the system. This was consistent with the two samples tested from Brisbane Airport.

For the Matthews Dust samples four samples failed at the interface but seven failed in the surface layer. For 63% of Matthews Dust samples, the surface layer was the weakest link in the system. Three of the four samples that failed at the interface were exposed to only light traffic. The interfaces would have received no benefit from being trafficked. If follows that the interfaces remained nearer their ‘as-constructed’ condition.

The Tylden Dust asphalt was more resistant to shear stresses than the average Runway 09/27 interface. The average Runway 09/27 interface was not, however, significantly different to the average Runway 16/34 interface. In turn the average Runway 16/34 interface was more resistance to shear stress than the Matthews Dust asphalt. This indicated that the Tylden Dust asphalt must have been more resistant to shear stress than the Matthews Dust asphalt. This was consistent with the observed field performance of the two runways at Melbourne Airport. It followed that the cause of the deformations in the braking zone of Runway 16 (Matthews Dust) reflected a significantly lower resistance to repeated shear (CSC) resistance within the Matthews Dust asphalt mixture compared to the Tylden Dust asphalt. The interface construction was excluded as a potentially contributing factor leading to the CSC failures in Runway 16/34 at Melbourne Airport.

6.4 OUTCOMES AND LIMITATIONS

The DS testing indicated that the ISS was consistent across both Runway 16/34 and Runway 09/27. Melbourne Airport measured ISS values were also consistent with the interface constructed at Brisbane Airport. Differential interface construction was excluded as a potentially confounded factor impacting the performance of the two runway surfaces.

The measured ISW was significantly different for the two runways at Melbourne Airport. Visual inspection of the load-deformation plots indicated this reflected a difference in the post-elastic-peak response of the interface. The post-elastic-peak behavior is governed by the frictional properties of the interface (Santagata et al. 2009; Romanoschi & Metcalf 2002). Further work is required to understand the significance of this difference. The difference in measured ISW did not explain the difference in runway surface performance.

The other observation made from DS testing was the consistently significant impact of two years traffic on the interface response to direct shearing. This was not expected, but reflected the improvement in interface condition resulting from frequent exposure to heavy tyre pressures and wheel loads. This is discussed later (9.4.2 Effect of traffic on interface shear resistance).

Combining the DS and IRIS testing results and analysis allowed the weakest element of the multi-layer system to be determined. This indicated that the asphalt containing Matthews Dust (Runway 16/34) was significantly less resistance to CSC than the asphalt containing Tylden Dust (Runway 09/27). It followed that differential interface construction was excluded as a factor leading to the observed CSC failures in the braking zone associated with Runway 16 landings.

6.5 SUMMARY

This Chapter presented interface shear resistance using both monotonic and repeated shear stress loading. The not significantly different ISS results were used as a benchmark to compare the significantly different failures modes from the IRIS testing. This allowed the construction of the interface to be excluded as a potential cause of the deformation failures observed in the braking zone associated with landings on Runway 16 (Matthews Dust). Rather, the failures were determined to be a lack of CSC resistance within the asphalt mixture on Runway 16/34, which was manufactured with the Matthews Dust.

The next Chapter will compare the constituent materials within the two asphalt mixtures in order to identify one or more elements responsible for the difference in the CSC resistance of the two asphalt surfaces. The coarse aggregate, fine aggregate, active filler and bituminous binder are all considered.

7. CONSTITUENT ASPHALT MATERIALS

The previous Chapter presented the analysis of the direct monotonic (DS) and inclined cyclic (IRIS) interface shear resistance of the two surfaces. Based on the IRIS and DS results, interface construction was excluded as a confounded contributing factor leading to the CSC failures observed in the Runway 16 braking zone. This indicated that the poor performance of the Runway 16/34 asphalt was the result of some fundamental difference in properties within the asphalt materials. However, the two asphalt mixtures were designed to be nominally identical except for the dust source. It followed that the dust and other constituent materials were focused on rather than the overall mixtures.

This Chapter details the initial screening of the various asphalt constituents. Constituents considered included the coarse aggregate, fine aggregate, active filler (hydrated lime) and bituminous binder. This forms the primary element of Phase 3 of this investigation (Figure 27).

This Chapter is a revised version of a journal paper that has been peer reviewed but not yet published. A copy is included in Appendix 1.

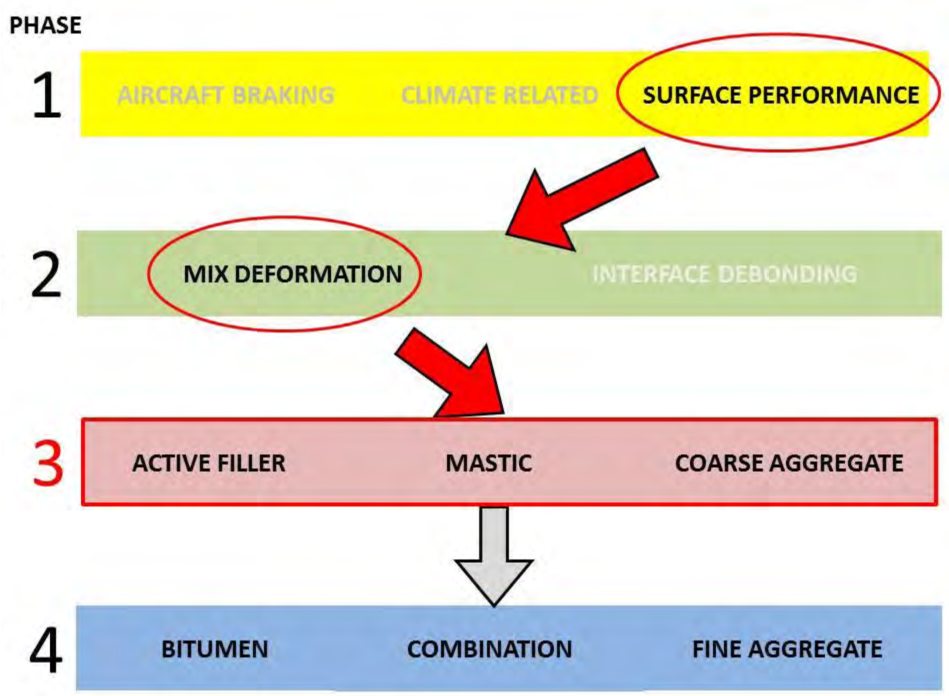

Figure 27 Phase 3 of sequential investigation framework

This analysis demonstrates that there was no significant difference in the various constituent material properties with the exception of post-storage bitumen properties and the clay minerals in the fine aggregate. The active filler (hydrated lime) and coarse aggregate are excluded as likely causes of the CSC failures observed in Runway 16/34. This allowed the investigation to focus on the properties and constituents of the asphalt mastic in the subsequent Chapter.

7.1 AIM OF RESEARCH PHASE

This Phase of the investigation aimed to screen for differences between the constituent materials within the two asphalt mixtures. The change in dust source was known at this time. The confounded change in bitumen feedstock (crude oil source) was not. No change in other constituent material was expected.

As detailed above (4.1.3 Constituent Asphalt Materials) constituent material testing was performed on material extracted from asphalt cores recovered from the two surfaces. It was also performed on retained bitumen and representative aggregate samples. Testing focused on non-specification properties as the specification compliance testing had not identified any significant changes during the works.

7.2 CONSTITUENT MATERIALS TESTING

Constituent material testing found significant differences in the post-RTFO properties of the retained bitumen samples as well as clay mineralogy of the fine aggregate. Other constituent materials were not found to be significantly different between the two runway asphalts (Table 32). Details of the screening test results are provided in the following sections.

Table 32 Constituent material screening summary

Constituent	Test(s)	Result
Coarse aggregate	QA records	No significant difference identified
Fine Aggregate	Angularity and Packing	No significant difference identified
Fine Aggregate	Petrography and chemical composition	Hisingerite clay identified in Matthews Dust source
Active Filler	QA records Voids content	No significant difference identified
Bitumen	SARA by Iatroscan	No significant difference identified
Bitumen	Post-RTFO Viscosity	Significantly different results at time of manufacture (2011) and during screening tests (2013)
Bitumen	Pre- and post-RTFO Dynamic Shear Rheometer temperature sweeps	Significant difference in the post-RTFO viscosity of retained bitumen samples reflective of a change in crude oil source
Mastic	Dynamic Shear Rheometer temperature sweeps	No significant difference identified between mastics with different dust source but a common bitumen

7.2.1 Coarse Aggregate

The coarse aggregate source did not change during the project. During the preliminary investigation (3.2 Design and Construction Review) the production compliance records were reviewed and no evidence of any change or abnormal variability in the coarse aggregate was identified. Volumetric testing (aggregate grading and voids content) of the asphalt was also reviewed (3.4 Destructive Testing) and similarly found no evidence to indicate the coarse aggregate properties had changed. The single coarse aggregate source quarry was inspected and no change in the quality of rock in the working face was observed.

7.2.2 Fine Aggregate

The fine aggregate (dust) source was known to have changed from Tylden Quarry to Matthews Quarry at around the transition from Runway 09/27 to Runway 16/34. This change correlated with the CSC failures in the Runway 16/34 surface as detailed previously (1.3 Statement of Problem). Representative samples of fine aggregate from each of the two quarries were assessed for petrology (at the time of construction and again during the constituent screening) as well as chemical composition analysis (only during the constituent screening in 2013) by XRD. Petrology included visual examination of fine rock and fine aggregate samples by an experienced professional petrographic analyst. Samples were also tested for fine aggregate angularity.

7.2.2.1 Fine Aggregate Angularity

Voids in dry compacted and uncompacted samples of the fine aggregate were measured as indicators of the internal friction. Table 33 summarises the results, including the three difference methods (as-received grading, standard grading and select sample fractions) for measuring the uncompacted voids. Matthews dust returned a slightly lower uncompacted voids and slightly higher dry compacted voids. All results were in the typical range for these materials.

Table 33 Fine aggregate angularity and compacted voids

Test Method	Tylden Dust	Matthews Dust
Un-compacted voids (Method A)	52%	49%
Un-compacted voids (Method B)	57%	54%
Un-compacted voids (Method C)	44%	43%
Dry compacted voids	44%	46%

7.2.2.2 Petrography

Petrographic analysis of the two dusts found both to be olivine Basalt of hard, grey, robust particles of slight to moderate weathering. Matthews Dust was slightly more weathered than the Tylden Dust as indicated by the higher smectite (clay) and accessory mineral contents (Table 34). Both dusts were found to contain secondary minerals in and around cracks in the olivine structure. Secondary minerals in both dusts were identified as most likely being Nontronite, a Smectite-group clay mineral.

Table 34 Summary of fine aggregate petrographic composition

Item / Mineral Content	Tylden Dust	Matthews Dust
Rock type	Olivine Basalt	Olivine Basalt
Apparent density (t/m^3)	2.89	2.79
Absorptivity (%)	2.0%	2.5%
Methyl Blue Value (%)	4	8
Plagioclase	71%	59%
Magnetite	12%	4%
Olivine	4%	5%
Augite	4%	13%
Smectite-group (clays)	8%	13%
Glass and Accessory minerals	1%	6%

7.2.2.3 Chemical Composition

Initial chemical composition analysis, by XRD, determined that both dust sources contained a comparable amount of clay mineral within otherwise typical olivine Basalt. Further analysis of observed brown chips within the Matthews Dust determined that what the initial petrographic assessment reported as Nontronite clay was, in fact the rare clay mineral Hisingerite. Negligible Hisingerite existed in the Tylden Dust (Table 35). This erroneous petrographic identification reflected the rareness of Hisingerite, which has previously been inappropriately classified as poorly crystallised Nontronite (Brigatti et al. 2013).

Table 35 Fine aggregate source Hisingerite content

Dust Source	Tylden Dust	Matthews Dust
Percentage of Clay minerals in Dust	8%	13%
Hisingerite Percentage of Clay	<1%	82%
Percentage of Hisingerite in Dust	Negligible	10.7%

A description and classification of Hisingerite was provided above (2.6.6.8 Clay and Hisingerite). No literature addressing the physical effects of Hisingerite on the performance of civil construction materials such as asphalt, concrete or crushed rock was located.

Specialist geotechnical interpretation of the unique properties of Hisingerite minerals indicated potential interaction with acid modified bitumen (such as M1000) and lime (used in both mixtures) in the production and performance of asphalt. It was advised that the highly hydrous nature of Hisingerite could trap excess moisture in the asphalt mastic. These potential interactions indicated an ability to adversely affect mastic stability and cause tenderness in an asphalt surface.

7.2.3 Active Filler

The active filler (hydrated lime) source did not change during the project. The manufacturer/supplier was questioned and no changes were identified or suggested in the raw material source, properties or processing.

The Rigden voids content was measured for a sample of hydrated lime from the same source. The result of 36% was consistent with hydrated lime voids reported in literature. No retained samples were available to allow comparison between the two runway surfaces. The supply of hydrated lime from a single source was stable and the risk of a change in fundamental property or performance was low.

7.2.4 Bituminous Binder

Retained samples of M1000 bitumen were recovered from storage and tested for rheological composition, post-RTFO viscosity and temperature/frequency sweeps in the DSR. Significant differences were identified in the post-RTFO viscosity of the retained bitumen samples when re-tested in 2013 (two years after manufacture).

7.2.4.1 Rheological composition

Rheological composition (SARA) analysis of four samples, two from each runway surface, is summarised in Table 36. The results do not indicate a significant rheological difference between the bitumen used for the two runway surfaces. A sample was also obtained from a M1000 batch manufactured in 2013 and was tested as a benchmark.

Some variability was observed but this was not correlated with the asphalt surface performance or with manufacture and sampling date. The results were consistent with expectations for these materials and did not fall into the ranges indicative of poor performance suggested in the literature.

Table 36 Rheological Composition of retained M1000 samples

Sample Date	Asphalt Dust Source	Saturates	Asphaltenes	Resins	Aromatics
27 Jan 2011	Tylden	8.8%	28.9%	7.0%	55.3%
07 Mar 2011	Tylden	8.1%	36.7%	7.0%	49.1%
25 May 2011	Matthews	7.2%	37.7%	5.5%	48.7%
01 Jun 2011	Matthews	8.6%	28.0%	6.2%	57.2%
2013	N/A	7.1%	27.4%	9.4%	56.1%

7.2.4.2 Temperature/Frequency Sweeps

Temperature/frequency sweeps were performed on the four M1000 samples that were also tested for rheological composition (Table 36). The complex modulus was calculated for each (Table 37). No substantial difference was identified and the associated master curves were very similar for each.

7.2.4.3 Post-RTFO Viscosity

The post-RTFO viscosity was measured at 60°C for the fourteen retained bitumen samples. Six samples represented M1000 batches used to manufacture Tylden Dust asphalt. Eight samples were from M1000 batches used to manufacture Matthews Dust asphalt. Table 38 contains the bitumen testing results from the time of manufacture (2011) as well as during the screening testing (2013). Table 39 provides summary statistics and the p-values from t-tests for equality of means for the samples representing the asphalt manufactured with the two dust sources.

Table 37 Complex modulus of retained M1000 samples

Sample Date	Asphalt Dust Source	Complex Modulus at 60°C and 1 rad/s (Pa.s)
27 Jan 2011	Tylden	1,607
07 Mar 2011	Tylden	1,310
25 May 2011	Matthews	1,697
01 Jun 2011	Matthews	1,512
2013	N/A	1,197

Table 38 Retained bitumen sample viscosity screening results

Sample Date	Asphalt Dust Source	Post RTFO Viscosity at 60°C (Pa.s)	
		Manufacture (2011)	Screening (2013)
28 Jan 2011	Tylden	4,740	5,338
02 Feb 2011	Tylden	5,860	6,199
10 Mar 2011	Tylden	4,077	4,664
12 Mar 2011	Tylden	4,673	4,472
17 Mar 2011	Tylden	4,076	5,204
19 Mar 2011	Tylden	5,228	5,608
15 May 2011	Matthews	5,673	6,428
17 May 2011	Matthews	4,875	6,284
17 May 2011	Matthews	6,311	6,653
19 May 2011	Matthews	5,182	7,786
24 May 2011	Matthews	4,328	5,738
26 May 2011	Matthews	6,221	6,327
21 Jun 2011	Matthews	6,274	7,903
23 Jun 2011	Matthews	6,388	6,465

Table 39 Retained bitumen sample Viscosity at 60°C (Pa.s) statistics

Bitumen	Manufacture (2011)		Screening (2013)	
	Mean	SD	Mean	SD
Tylden Dust Asphalt	4,776	688	5,248	630
Matthews Dust Asphalt	5,657	781	6,698	756
T-test on means p-values	0.046		0.002	

Based on the screening testing, the probability of the two sub-populations of bitumen coming from the same overall population was calculated to be 0.2%. At the time of manufacture this probability was 4.6%.

The post-RTFO viscosity testing indicated a significant difference in the bitumen used in the manufacture of Tylden Dust and Matthews Dust asphalts. The difference was magnified by retained sample storage time. The bitumen used in Matthews Dust asphalt production had a higher viscosity that the Tylden Dust asphalt bitumen. Higher viscosity would generally be associated with improved resistance to shear and deformation. However, various researchers have shown that bitumen viscosity is not a reliable indicator or bitumen shear creep resistance (D'Angelo et al. 2007). The increase in post-RTFO viscosity was an indicator of a significant difference between the batches of bitumen used in the manufacture of the two asphalts. It was not, however, a specific explanation for the observed asphalt tenderness.

The bitumen supplier was advised of the observed CSC failures and the bitumen test results (Table 39). The supplier subsequently advised that the specific crude oil blend used in the manufacture of M1000 feedstock (conventional C170 to AS 2008) had changed in April 2011. April 2011 was around the transition of work from Runway 09/27 to Runway 16/34. The feedstock change appeared to be minor (Table 40) and coincidentally occurred at the same time as the change in dust source. The change in the crude oil blend may have also indicated an important change in oil refining processes and/or M1000 production. Any associated change in the refining process or M1000 production remains unknown.

Table 40 Pre- and post-April 2011 crude oil blends

Period	Crude Oil Source as a Percentage of Feedstock	
	Arab Light	Basrah Light
Pre April 2011 (Feedstock 1)	92%	8%
Post April 2011 (Feedstock 2)	97%	3%

A significant change was measured in retained bitumen sample properties, resulting from a change in M1000 feedstock. This change was not known at the time of construction. The feedstock and bitumen property changes may have been indicative of a change in bitumen performance that resulted in a reduction in CSC resistance in the Runway 16/34 asphalt.

7.2.5 Asphalt Mastic

Asphalt mastic (without hydrated lime) samples were prepared and tested using a common (manufactured in 2013) bitumen sample. The mastic testing was intended to assess the impact of dust source on mastic response to dynamic shear. Mastic was also manufactured with a sample of dust retained from the Brisbane Airport runway overlay.

At this stage, mastic testing was not intended to compare the bitumen samples from the two surfaces. Mastic samples were prepared without hydrated lime filler and adopted a 1:1 (bitumen:aggregate) ratio to replicate the asphalt mastics in the field. Hydrated lime filler was excluded to isolate the impact of the dust source.

Samples were tested before and after RTFO conditioning. Mastic and (neat) bitumen master curves were generated for complex modulus (Figure 28). As expected, the mastic had a higher complex modulus than the bitumen. Mastic complex increased with RTFO conditioning. However, the source of the dust (Matthews, Tylden or Brisbane Airport) had no substantial impact on the mastic response.

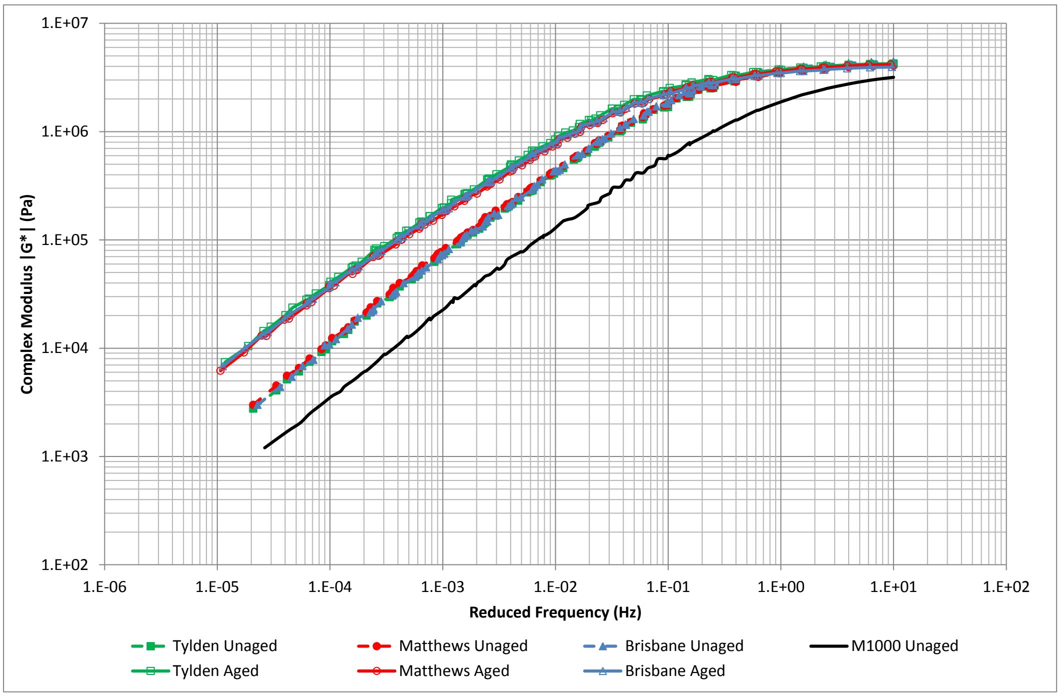

Figure 28 Master curves for mastic complex modulus with a common bitumen

7.3 CONFOUNDED CHANGES

At the time of construction there was an intended change in the fine aggregate (dust source) at the transition from one runway to the other. The bitumen testing and subsequent review of feedstock composition identified a previously unknown change in the crude oil blend used to manufacture the bitumen. This change occurred at around the same time as the change in dust source. Although the change in feedstock appeared minor, the impact on post-RTFO viscosity after two years of retained sample storage was significant.

The two asphalts were found to contain bitumen of significantly different properties, resulting from the change in crude oil blend. The two asphalts also contained fine aggregates from two different dust sources and one contained potentially detrimental Hisingerite clay. The combined change in bitumen feedstock and dust source represented a complete change in the asphalt mastic.

The changes in bitumen and dust were concurrent and correlated with the observed CSC performance of the two runway surfaces (Figure 29). The dust change and the bitumen feedstock change were confounded and their relative impact on the field performance of the asphalt surface could not be separated.

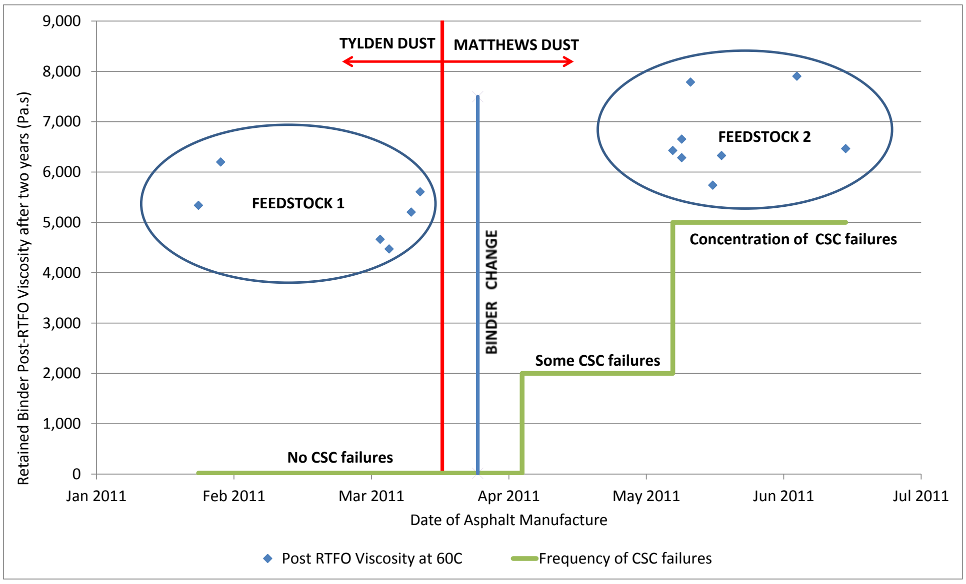

Figure 29 Time series of dust and bitumen changes

7.4 OUTCOMES AND LIMITATIONS

Non-specification testing of each of the asphalt constituents was performed to screen for changes over the project duration that correlated with the difference in CSC resistance observed between the two runways. Coarse aggregate and hydrated lime filler sources did not change and screening did not identify any evidence of a significant change in the production properties of these materials during the project. The risk of either the coarse aggregate or hydrated lime filler being a significant factor affecting the surface CSC resistance was low.

In contrast the fine aggregate (dust) source was known to have changed. The Matthews Dust (Runway 16/34) was found to contain a rare clay mineral with potentially detrimental (to asphalt performance) properties. A change in retained bitumen sample properties associated with a change in bitumen feedstock (crude oil source blend) was also identified (at the transition between runways). These two changes were confounded and correlated with the CSC performance of the two runway surfaces.

The retained bitumen samples had been stored for two years at the time of testing. Testing identified that the samples had changes significantly since their production. There was no way of testing unchanged bitumen samples manufactured for this project two years after its completion. Representative aggregate and hydrated lime filler samples were either not retained or could not be located. Therefore testing of these materials was not possible. These limitations were unavoidable. However, the risk of an additional significant change remaining unidentified was low.

7.5 SUMMARY

This Chapter screened the various asphalt constituents used to manufacture the surface of the two runways. The known change in dust source and the identified change in bitumen feedstock were confounded and both had the potential to impact on asphalt surface CSC performance. The bitumen and the dust form 92% of the asphalt mastic and mastic performance is a substantial indicator of asphalt performance.

Having excluded other asphalt constituents, surface layer interface bond and aircraft-induced stresses as potential causes of the CSC failures, the changes in mastic became the focus of this research. The change in mastic materials (bitumen and fine aggregate) was determined to have affected the asphalt resistance to CSC. This change resulted in the observed failures in the Runway 16/34 surface associated with Runway 16 landings.

The next Chapter will present a performance-based assessment of mastic and bitumen samples comprising both dust sources with retained samples of bitumen manufactured from both feedstocks. This isolates the relative impact of the two changes in the asphalt mastic on the CSC performance of the two runway surfaces.

8. ASPHALT MASTIC

The previous Chapter presented the screening of the various asphalt constituent materials. Significant differences were found between the M1000 bitumen feedstock and aggregate clay minerals. These changes were confounded and correlated to the shear (CSC) performance of the two runway surfaces (Figure 29). This indicated that the poor performance of the Runway 16/34 asphalt was the result of a fundamental difference in the mastic properties.

This Chapter details the performance-based testing of mastic and retained bitumen samples, as well as re-testing of the retained bitumen samples for specification parameters. To isolate the relative impact of change in bitumen feedstock and change in dust source, mastics were manufactured with both dusts in combination with retained bitumen samples manufactured from both feedstocks. This forms the final Phase 4 of this research (Figure 30).

This Chapter is based on a combination of two journal papers. One focused on bitumen testing (currently under peer review) and the other addressing mastic testing (awaiting publication following peer review). A copy of each is included in Appendix 1.

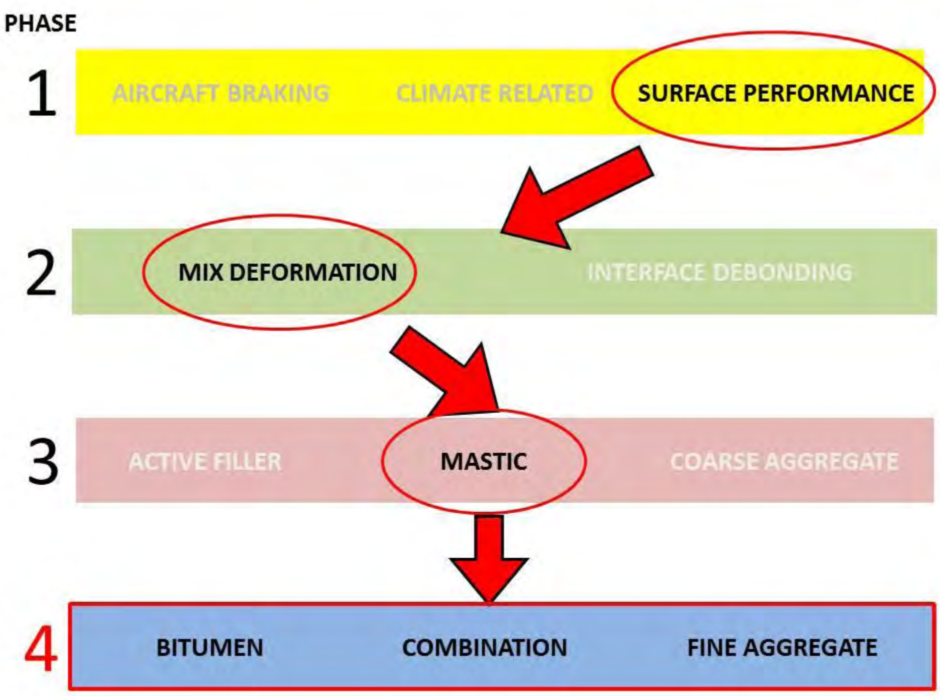

Figure 30 Phase 4 of sequential investigation framework

This analysis demonstrates the change in the crude oil source used to manufacture the bitumen had a significant impact on the shear stress resistance of the bitumen and the subsequent asphalt. The fine aggregate source had no significant impact on mastic performance, despite the presence of Hisingerite clay minerals.

8.1 AIM OF RESEARCH PHASE

The aim of this final Phase of investigation was to isolate the impact of the change in bitumen feedstock (crude oil source blend) and change in fine aggregate (dust source) on mastic performance. Mastic performance was assessed as an indicator of asphalt surface CSC performance. Retained bitumen samples were also subject to performance and other testing. Any interactive impact of bitumen and fine aggregate was also assessed.

The Matthews Dust clay fraction predominantly contained the rare and potentially detrimental Hisingerite clay mineral. The Tylden Dust contained the more common and benign Smectite clay mineral. Apart from the dominant clay mineral, the two dusts were otherwise similar. By measuring the impact of the two dust sources on mastic performance, the impact of Hisingerite on asphalt performance was indirectly assessed.

8.2 BITUMEN SAMPLE RE-HEATING ASSESSMENT

Changes in bitumen properties accelerate at elevated temperature. During this research some samples were re-heated and sub-sampled up to six times. The impact of this cyclic reheating was evaluated by a controlled re-heating assessment as detailed above (4.1.4.5 Bitumen re-heating Assessment).

The results of the re-heating assessment are presented in Appendix 5 and illustrated in Figure 31. Table 41 summarises the calculated means and standard deviations from the re-heating assessment. The p-values for t-tests on means were determined for each pair of one, two and three re-heating cycles.

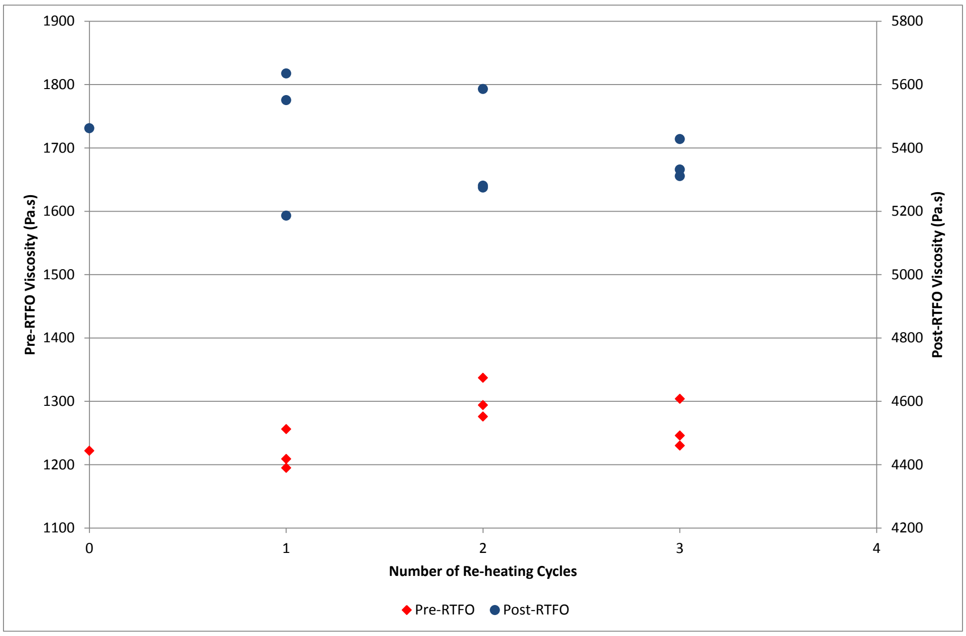

Figure 31 Re-heating assessment results

Table 41 Sample re-heating results and statistics for a single sample

Re-heating Cycles	Pre-RTFO Viscosity (Pa.s)		Post-RTFO Viscosity (Pa.s)	
	Mean	SD	Mean	SD
0	1,222	N/A	5,462	N/A
1	1,220	32	5,457	239
2	1,302	31	5,381	178
3	1,260	39	5,357	62
p-value 1 versus 2	0.03		0.68	
p-value 2 versus 3	0.22		0.84	
p-value 3 versus 1	0.24		0.52	

Re-heating cycles had no significant effect on the measured pre- and post-RTFO viscosity. The only p-value of significance (pre-RTFO change between one and two re-heating cycles) was likely the result of the small sample sizes.

This assessment confirmed that the short-term cyclic re-heating associated with periodic sub-sampling did not significantly impact subsequent test results.

8.3 BITUMEN COMPLIANCE REVIEW

Compliance (at the time of release in 2011) test results for all fourteen retained bitumen samples are presented in Appendix 5. The crude oil source blend designation, Feedstock 1 or Feedstock 2 (from Table 40) is also annotated.

Summary statistics for the various compliance test results for each feedstock are in Table 42. The p-values associated with comparison of means are also presented. Although all samples complied with the M1000 specification, the pre-RTFO viscosity at 60°C and penetration at 25°C were significantly different for the two feedstocks. This reflects different processing requirements of what were two feedstocks of different bitumen origin.

Table 42 Statistics for bitumen point of release compliance testing

Property	Feedstock 1			Feedstock 2			p-value
	Mean	SD	CV	Mean	SD	CV	
Viscosity at 135°C (Pa.s)	1.10	0.06	6%	1.17	0.05	4%	0.06
Viscosity at 60°C (Pa.s)	1,085	73	7%	1,219	45	4%	<0.01
Penetration at 25°C (pu)	45	2	5%	48	2	4%	0.01
Viscosity at 60°C post RTFO (Pa.s)	4,931	778	16%	5,784	843	15%	0.10
Penetration at 25°C post RTFO (pu)	33	3	11%	35	2	6%	0.19

8.4 MASTIC MSCR PROTOCOL

The bitumen samples for mastic manufacture were aged by RTFO. The hydrated lime was then added followed by the required amount of dust sample passing the 75 µm sieve. The mastic samples were tested for cyclic shear stress response (MSCR protocol). MSCR testing was performed at 64°C, 70°C and 76°C to be consistent with the bitumen testing detailed below (8.5 Bitumen

Testing). Results from the MSCR testing of the laboratory manufactured mastics are contained in Appendix 5.

For convenience, the samples were assigned a two character alpha-numeric code. The number indicated the retained bitumen sample and the letter represented the dust source (Table 43).

Table 43 Mastic sample codes

Sample Number	Bitumen Sample	Feedstock	Dust Source
1T	28 Jan	1	Tylden
1M	28 Jan	1	Matthews
2T	02 Feb	1	Tylden
2M	02 Feb	1	Matthews
3T	10 Mar	1	Tylden
3M	10 Mar	1	Matthews
4T	26 May	2	Tylden
4M	26 May	2	Matthews
5T	21 Jun	2	Tylden
5M	21 Jun	2	Matthews
6T	23 Jun	2	Tylden
6M	23 Jun	2	Matthews

8.4.1 Mastic Response

The shear strains measured during the MSCR testing of neat bitumen and each mastic sample are illustrated in Figure 32 for 70°C test temperature. Figure 33 shows the same data with the neat bitumen samples removed and the scale modified to focus on the 3.2 kPa stress level cycles for mastic samples only. Trends were consistent at 64°C and 76°C with the magnitude of the strains increasing with higher temperature. Sample recovery (AR) decreased and creep compliance (Jnr(3.2)) increased with increasing temperature

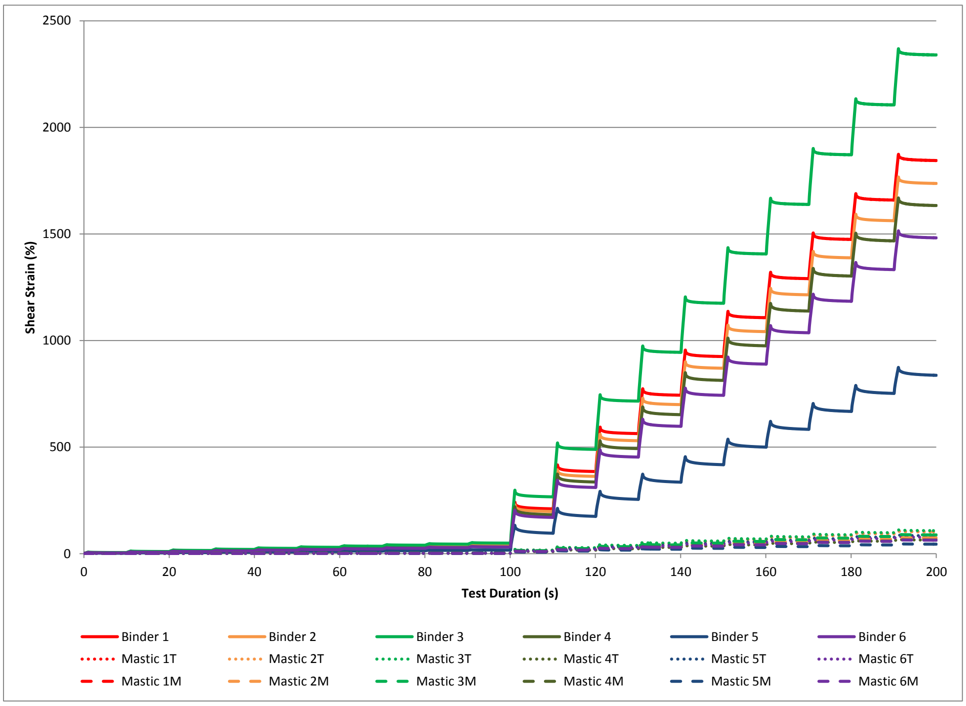

Figure 32 Bitumen and mastic MSCR strains at 70°C

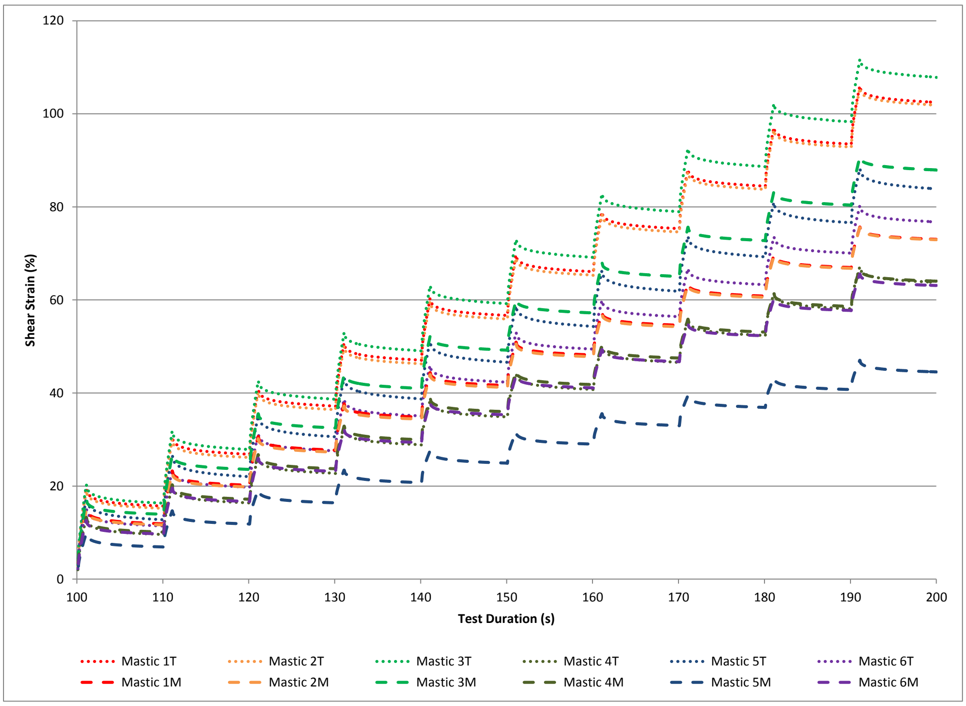

Figure 33 Mastic MSCR strains at 70°C

The contribution of added fine aggregate to resisting cumulative unrecovered strain during cyclic shear stress was significant (Figure 32). The accumulated strain was consistently a full order of magnitude lower for the mastic samples than the bitumen samples. The significant impact of stress level was also evident.

The stress impact on the bitumen and the mastic were evidenced by the ranges of cumulative unrecovered strains for mastic and bitumen samples after the 0.1 kPa and 3.2 kPa stress cycles (Table 44). Ratios between mastic and bitumen, as well as between stress levels, were calculated. The stress sensitivity of mastic samples was less than for bitumen samples, as indicated by the lower values of Ratio(3.2/0.1) for mastic and the higher values of Ratio(B/M) at 3.2 kPa stress level.

Table 44 Cumulative unrecovered strain during MSCR protocol

Stress Level	Mastic Samples	Bitumen Samples	Ratio(B/M)
0.1 kPa	1.14-2.99	16.5-49.3	15-17
3.2 kPa	44.5-107.8	836-2,340	19-22
Ratio (3.2/0.1)	36-39	47-51	-

Ratio(3.2/0.1) is the ratio between the cumulative strain after the ten 3.2 kPa stress cycles and the cumulative strain after the 0.1 kPa stress cycles. Ratio(B/M) is the ratio of the cumulate strain for bitumen samples divided by the equivalent cumulative strain for the mastic samples.

8.4.2 Effect of Temperature on Mastic

Mastic and bitumen response to shear stress was consistent across the range of test temperatures (Figure 34) which were representative of pavement surface temperatures in Australia. All bitumen and mastic samples showed a similar increase in creep compliance (Jnr(3.2)) as the test temperature increased. The difference in Jnr(3.2) between samples increased at higher test temperature. At 70°C and 76°C the order of Jnr(3.2) for mastic samples mirrored the order of the bitumen sample Jnr(3.2). However, at 64°C, some mastic sample Jnr(3.2) values were ordinally different to the bitumen samples. This is illustrated by the crossing of lines between 64°C and 70°C for some mastic samples (Figure 34). Mastic Jnr(3.2) values were two orders of magnitude smaller than typical bitumen Jnr(3.2) values. This likely reflected the small strains experienced by mastic at lower temperatures in comparison to the accuracy of the measuring equipment. Expected errors in measurement became significant when the total strains were relatively small.

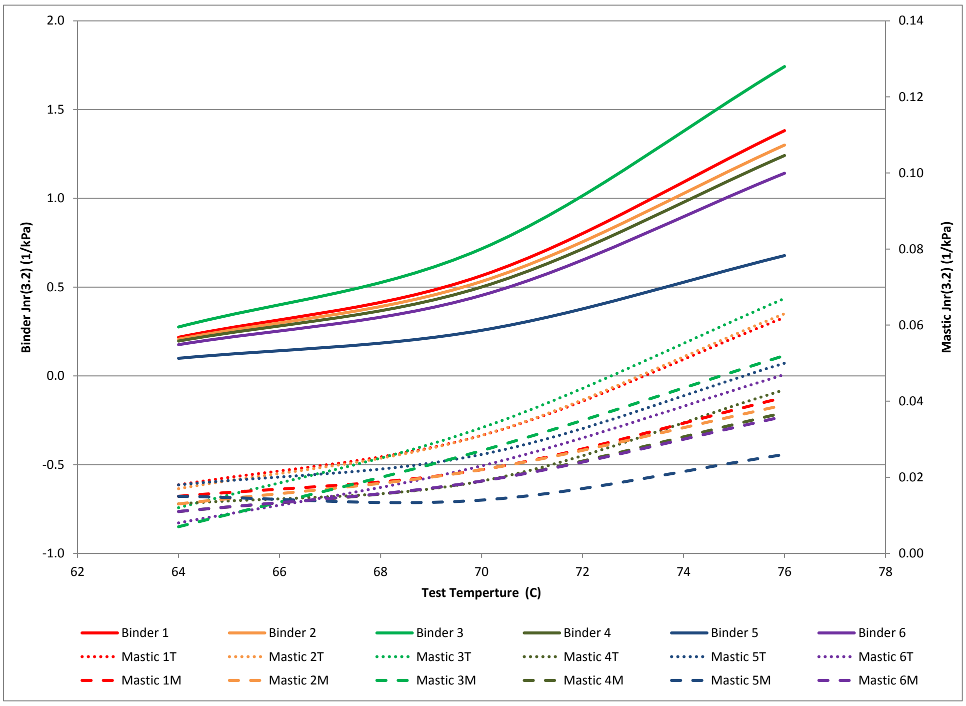

Figure 34 Bitumen and mastic MSCR Jnr(3.2)

8.4.3 Effects of Feedstock and Dust Source

The p-values associated with the t-tests for comparison of means between dust source and between bitumen feedstock are summarised in Table 45 and Table 46, respectively. Recovery (AR) and cumulative deformation (Jnr) are reported for both the 0.1 kPa and 3.2 kPa stress levels. The results in Table 46 considered all mastic samples manufactured with a particular feedstock to be a single sub-population. That is, mastic samples with Tylden Dust and Matthews Dust were combined for the comparison of feedstocks. When the Tylden Dust and Matthews Dust mastics were considered separately, the relative impact of the change in bitumen feedstock was similar.

Table 45 Mastic MSCR summary statistics for means of Dust

Statistic	AR(0.1) (%)		AR(3.2) (%)		Jnr(0.1) (1/kPa)		Jnr(3.2) (1/kPa)	
	T	M	T	M	T	M	T	M
Tested at 64°C								
Mean	67	68	41	39	40	41	0.010	0.009
SD	3	4	6	6	7	5	0.002	0.003
CV	5%	5%	15%	14%	17%	13%	20%	32%
p-value	0.44		0.63		0.58		0.66	
Tested at 70°C								
Mean	61	61	31	31	50	50	0.024	0.019
SD	3	4	4	4	5	5	0.005	0.005
CV	5%	7%	14%	13%	10%	10%	21%	26%
p-value	0.58		0.48		> 0.90		> 0.90	
Tested at 76°C								
Mean	57	57	22	22	61	60	0.042	0.033
SD	3	4	4	3	5	4	0.007	0.008
CV	5%	7%	16%	14%	7%	6%	16%	25%
p-value	0.59		0.44		> 0.90		> 0.90	

T is Tylden Dust. M is Matthews Dust.

No mastic shear creep (MSCR protocol) parameter suggested that either Matthews Dust or Feedstock 2 adversely affected mastic shear response at 64°C, 70°C or 76°C. On the contrary, the linear regression on results (Equation 14) indicated, on average, a slight reduction in Jnr(3.2) for both the change in dust source (from Tylden Dust to Matthews Dust) and bitumen (Feedstock 1 to Feedstock 2). Similar trends were observed in the regression analysis for Jnr(0.1) (Equation 15), AR(0.1) (Equation 16) and AR(3.2) (Equation 17). Although, the change in average AR value was opposite to that of the Jnr value at each stress level. Opposite trends are expected for these two inversely proportional properties. That is, as recovery increases, cumulative deformation is expected to decrease.

Table 46 Mastic MSCR summary statistics for means of Feedstock

Statistic	AR(0.1) (%)		AR(3.2) (%)		Jnr(0.1) (1/kPa)		Jnr(3.2) (1/kPa)	
	FS 1	FS 2	FS 1	FS 2	FS 1	FS 2	FS 1	FS 2
Tested at 64°C								
Mean	65	70	40	40	40	41	0.010	0.009
SD	3	2	7	5	7	5	0.002	0.002
CV	4%	3%	18%	12%	18%	12%	24%	27%
p-value	> 0.90		0.47		0.73		0.66	
Tested at 70°C								
Mean	60	62	28	34	54	46	0.025	0.018
SD	3	4	1	3	1	2	0.004	0.004
CV	4%	6%	4%	8%	2%	4%	18%	20%
p-value	0.89		> 0.90		> 0.90		> 0.90	
Tested at 76°C								
Mean	56	58	20	25	64	57	0.043	0.032
SD	3	3	1	2	1	2	0.008	0.006
CV	6%	6%	5%	10%	2%	3%	19%	18%
p-value	0.85		> 0.90		> 0.90		> 0.90	

FS is the Feedstock.

$$Jnr(3.2) = -0.162 + 0.0028 \times T - 0.0082 \times D_M - 0.0064 \times F_2 \ (R = 91\%) \quad \text{Equation 14}$$

$$Jnr(0.1) = -0.136 + 0.0023 \times T - 0.0049 \times D_M - 0.0054 \times F_2 \ (R = 93\%) \quad \text{Equation 15}$$

$$AR(0.1) = 120 - 0.854 \times T - 0.33 \times D_M + 3.0 \times F_2 \ (R = 84\%) \quad \text{Equation 16}$$

$$AR(3.2) = 133 - 1.47 \times T - 0.28 \times D_M + 2.1 \times F_2 \ (R = 87\%) \quad \text{Equation 17}$$

Where T = test temperature (°C)

D_M = 0 for Tylden Dust and 1 for Matthews Dust (dummy variable for Dust)

F_2 = is 0 for Feedstock 1 and 1 for Feedstock 2 (dummy variable for Feedstock)

The results implied that Runway 16/34 had better shear resistance than Runway 09/27 had. That is, that the change to Matthews Dust and Feedstock 2 improved the asphalt mixture resistance to shear (CSC). It is more likely, in fact, that the lower mastic deformation in Matthews Dust samples reflected the lower apparent density and higher absorption of Matthews Dust (Table 34) and the significant in-storage hardening of Feedstock 2 retained bitumen samples over the four years since manufacture.

The lower apparent density required a larger volume of Matthews Dust in order to maintain the target 6:1:6 (bitumen:filler:aggregate) mass ratio. Although the bitumen:filler:aggregate ratio was the same for all mastic samples by mass, when expressed by volume, the Matthews Dust mastic samples had a higher portion of aggregate than Tylden Dust mastics. The greater aggregate volume in Matthews Dust mastic samples stiffened the mastic to a greater extent than Tylden Dust did. The higher absorption of Matthews Dust exacerbated this by reducing the 'effective' bitumen available within the Matthews Dust mastic samples.

As described in detail below (8.5 Bitumen Testing) all retained bitumen samples showed significant in-storage hardening had occurred by the time MSCR testing was performed in 2015. Feedstock 2 samples will be shown to have hardened significantly more than Feedstock 1 samples. This will be demonstrated by comparison of post-RTFO viscosity at 60°C. The significant reduction in Feedstock 2 mastic Jnr(3.2) reflected the significantly greater increase in bitumen viscosity.

Considering the difference in hardening of retained bitumen samples and differences in volumetric mastic composition, it is more appropriate to conclude that Runway 16/34 (and the associated Hisingerite clay in the Matthews Dust) did not adversely affect the mastic or asphalt response to shear stress at any test temperature. The same conclusion can not be made for the change in bitumen (M1000 feedstock). To verify this conclusion, mastic samples must be prepared at the same effective bitumen volume, taking account of any difference in apparently density of the fine aggregate particles as well as their potential to absorb bitumen. Whether the active filler (hydrated lime) dosage should be maintained by volume or mass must also be considered. This additional testing was not possible due to the retained bitumen samples being exhausted.

8.5 BITUMEN TESTING

Appendix 5 contains the retained bitumen sample test results. This includes:

- Bitumen point of release (specification) results from 2011, as described above.
- Specification parameter re-testing in 2014 for three samples representing each feedstock.
- Post-RTFO viscosity at 60°C re-testing in 2013 and 2015 for all fourteen retained bitumen samples.
- MSCR testing at 64°C, 70°C and 76°C in 2015 for all fourteen retained bitumen samples.
- Independent M1000 post-RTFO viscosity at 60°C and MSCR for unrelated (benchmark) samples.

The point of release testing results (2011) were assessed above (8.3 Bitumen Compliance Review). The other retained bitumen sample test results are analysed as follows.

8.5.1 Bitumen Specification Re-testing

When re-tested in 2014 (three years after manufacture) the specification parameters were more variable than at the time of manufacture as indicated by the means, standard deviations and CV (Table 47). The average values measured in 2014 were significantly different from those measured at the time of release. The pre-RTFO viscosity of Feedstock 1 samples had become more variable, as had the post-RTFO viscosity of Feedstock 2 samples. Comparing the results in Table 47 with those in Table 42, samples manufactured from both feedstocks had ‘hardened’ in storage over three years. This was evidenced by increased viscosity and reduced penetration.

Table 47 Statistics for bitumen specification testing in 2014

Property	Feedstock 1			Feedstock 2		
	Mean	SD	CV	Mean	SD	CV
Viscosity at 135°C (Pa.s)	1.21	0.16	13%	1.57	0.09	5%
Viscosity at 60°C (Pa.s)	1,252	309	25%	2,036	140	7%
Penetration at 25°C (pu)	43	7	16%	42	4	4%
Viscosity at 60°C post RTFO (Pa.s)	7,573	654	9%	12,242	1,661	14%
Penetration at 25°C post RTFO (pu)	25	1	5%	27	1	2%

The p-values associated with t-tests for means are presented in Table 48, as are the results of paired t-tests for changes in parameters between the time of release (2011) and three years later (2014). In 2014, samples from the two feedstocks had significant differences in all the measured parameters, with the exception of the pre-RTFO penetration. The Feedstock 1 pre-RTFO properties had not changed significantly during storage. The Feedstock 2 pre-RTFO properties had. All post-RTFO properties had changed significantly for samples from both feedstocks. The measured change in storage likely reflects an ongoing chemical interaction between the acid (PPA) and bitumen molecules. Conventional (unmodified) bitumen would not undergo such significant changes during controlled storage (Oliver 2009).

Table 48 Bitumen specification testing p-values in 2014

Property	Comparison of Feedstocks (in 2015)	Change in Feedstock 1 (2011 to 2015)	Change in Feedstock 2 (2011 to 2015)
Viscosity at 135°C (Pa.s)	0.04	0.41	0.01
Viscosity at 60°C (Pa.s)	0.03	0.41	0.01
Penetration at 25°C (pu)	0.82	0.44	0.02
Viscosity at 60°C post RTFO (Pa.s)	0.03	0.01	0.02
Penetration at 25°C post RTFO (pu)	0.03	0.01	0.01

8.5.2 Post-RTFO Viscosity

Significant in-storage changes were observed in the post-RTFO viscosity results measured two (2013) and four (2015) years after manufacture. Summary statistics and p-values associated with t-tests for means are presented in Table 49. Each individual bitumen sample was sub-sampled and tested in 2013 and then again in 2015. The impact of age and the difference between the two feedstocks can be seen in Figure 35. Six samples show a data point in 2014 reflecting the results of specification parameter re-testing in 2014.

Table 49 Bitumen post-RTFO viscosity (Pa.s) with storage time

Statistic	Feedstock 1			Feedstock 2		
	2011	**2013**	**2015**	**2011**	**2013**	**2015**
Mean	4,931	5,248	8,685	5,784	6,698	15,831
SD	778	630	1,520	843	756	1,496
CV	16%	12%	18%	15%	11%	9%
p-value (Feedstocks)	N/A	< 0.01	< 0.01	As per Feedstock 1		
p-value (change from release)	N/A	0.01	< 0.01	N/A	0.03	< 0.01

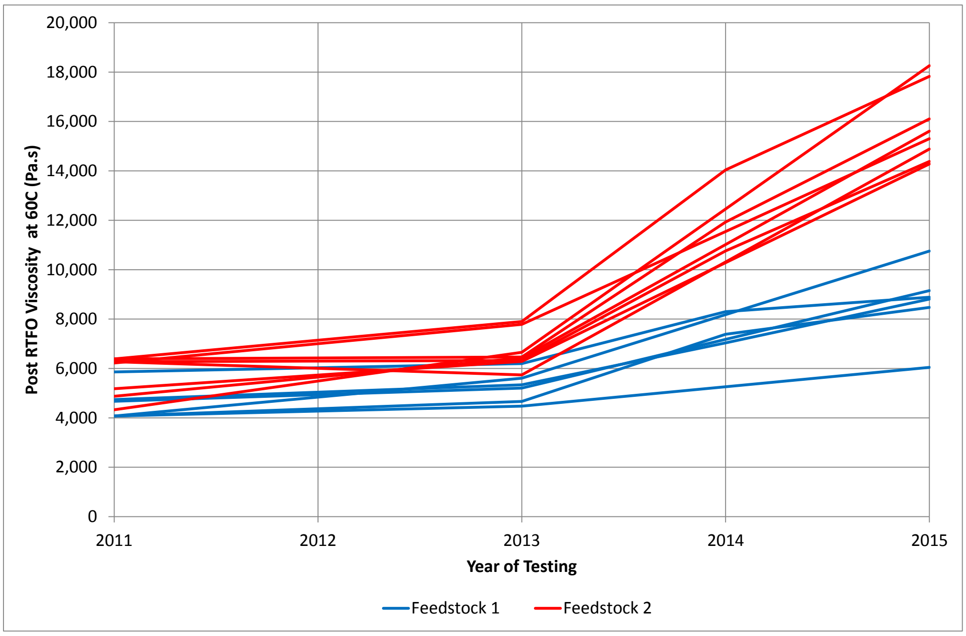

Figure 35 Post-RTFO viscosity increase with sample storage time

The Feedstock 1 samples showed an increase in post-RTFO viscosity over time. However, the increase was relatively small in comparison to that measured for samples from Feedstock 2.

The majority of the Feedstock 2 post-RTFO viscosity increase occurred between 2013 and 2015 (Figure 35). This timing of the significant in-storage hardening of Feedstock 2 M1000 samples was consistent with the self-correction of the Runway 16/34 surface as indicated by the cessation of new CSC failures observations (Figure 15).

8.5.3 Bitumen MSCR Protocol

Summary statistics for cyclic shear testing (MSCR protocol) of retained bitumen samples outputs are presented in Table 50.

Table 50 Statistics for bitumen MSCR results

Statistic	AR(0.1) (%)		AR(3.2) (%)		Jnr(0.1) (1/kPa)		Jnr(3.2) (1/kPa)	
	FS 1	FS 2	FS 1	FS 2	FS 1	FS 2	FS 1	FS 2
Tested at 64°C								
Mean	45.5	54.7	28.1	36.5	0.17	0.13	0.23	0.17
SD	2.2	3.5	2.3	5.2	0.02	0.03	0.03	0.04
CV	5%	6%	8%	14%	12%	21%	13%	23%
Tested at 70°C								
Mean	39.3	49.2	14.6	21.3	0.40	0.28	0.58	0.44
SD	2.5	3.9	1.9	5.0	0.06	0.06	0.08	0.10
CV	6%	8%	13%	24%	14%	21%	13%	23%
Tested at 76°C								
Mean	32.3	42.6	5.6	9.2	0.90	0.61	1.43	1.10
SD	2.6	4.1	0.9	3.0	0.13	0.12	0.18	0.22
CV	8%	10%	16%	32%	15%	20%	12%	20%

FS is the Feedstock.

The p-values associated with comparison of means of feedstocks are summarised in Table 51. Recovery (AR) decreased and cumulative deformation (Jnr) increased, with increasing temperature. The variability of results increased with temperature and stress level.

The p-values associated with comparison of means of feedstocks are summarised in Table 51. The average PG traffic rating, based on 2015 MSCR results, are summarised in Table 52 by feedstock. All MSCR parameters indicated a significant difference between the samples manufactured from the two feedstocks. As the temperature increased and stress level increased, the difference in MSCR results was greater.

Table 51 Bitumen MSCR testing p-values for means of Feedstock

Temperature	AR(0.1) (%)	AR(3.2) (%)	Jnr(0.1) (1/kPa)	Jnr(3.2) (1/kPa)
64°C	< 0.01	< 0.01	< 0.01	0.01
70°C	< 0.01	0.01	< 0.01	0.01
76°C	< 0.01	0.01	< 0.01	0.01

Table 52 Average PG for bitumen samples by Feedstock

Feedstock	64°C	70°C	76°C
Feedstock 1	PG 64 E	PG 70 V	PG 76 H
Feedstock 2	PG 64 E	PG 70 E	PG 76 H*

* indicates samples that would not have been assigned a PG due to stress sensitivity (%Jnr) exceeding 75% (Table 53).

Table 53 Statistics for MSCR %Jnr for Feedstocks

Statistic	64°C		70°C		76°C	
	FS 1	FS 2	FS 1	FS 2	FS 1	FS 2
Mean	30%	35%	47%	59%	59%	81%
SD	1.1%	5.5%	1.7%	7.4%	3.7%	10.2%
CV	4%	16%	4%	12%	6%	13%
p-value	0.03		< 0.01		< 0.01	

FS is the Feedstock.

The shear stress sensitivity (%Jnr) of bitumen is assessed by the relative difference between Jnr(0.1) and Jnr(3.2) (Riaz et al. 2013). Table 53 presents the summary statistics for %Jnr for all three test temperatures. At all test temperatures, the %Jnr of Feedstock 2 samples were significantly higher than for samples from Feedstock 1. AASHTO M332-14 limits %Jnr to 75% for all bitumens at all traffic levels. Six out of eight Feedstock 2 samples exceeded this limit at 76°C. In contrast, Feedstock 1 samples averaged less than 60% at the same temperature and all were below the 75% limit. Bitumen samples manufactured from Feedstock 2 were consistently more sensitive to high shear stress conditions than Feedstock 1. This higher shear stress sensitivity increased with increasing temperature. The significantly higher stress sensitivity of Feedstock 2 was measured despite the significantly greater 'hardening' (during four years of controlled storage) measured in Feedstock 2 samples, compared to samples manufactured from Feedstock 1.

8.5.4 Estimated 2011 Bitumen Response to MSCR

Mastic MSCR testing indicated that neither the dust source nor the bitumen feedstock had a significant impact on the mastic response to shear stress that explained the observed CSC failures. However, between the bitumen samples being taken on site (2011) and mastic testing (2015) Feedstock 2 post-RTFO viscosity increased by up to 322%. In contrast, Feedstock 1 samples increased their post-RTFO viscosity by an average 76% over the same period. The different increase in post-RTFO viscosity between the two feedstocks also decreased the Jnr(3.2) values differently. As a result the measured 2015 mastic Jnr(3.2) values were similar for both feedstocks. As detailed above (8.4.1 Mastic Response) differential in-storage bitumen hardening contributed to preventing explanatory differences between the mastic samples being identified by MSCR testing in 2015.

8.5.4.1 Estimation of 2011 MSCR Parameters

The ability to estimate the time of release Jnr and AR values from the available test data was examined. Firstly, relationships between post-RTFO viscosity and Jnr/AR measured in 2015 were developed using simple linear regression (Equation 18 and Equation 19 for 70°C, Equation 20 and Equation 21 for 76°C).

The 70°C data and relationships are shown in Figure 36 and those for 76°C are in Figure 37.

$AR(3.2@70°C) = -4.318 + 0.002287 \times V\ (R = 91\%)$ .... Equation 18

$Jnr(3.2@70°C) = 0.98 - 0.0000481 \times V\ (R = 89\%)$ .... Equation 19

$AR(3.2@76°C) = -4.968 + 0.001285 \times V\ (R = 89\%)$ .... Equation 20

$Jnr(3.2@76°C) = 2.33 - 0.0001098 \times V\ (R = 88\%)$ .... Equation 21

Where V = post-RTFO viscosity at 60°C (Pa.s)

The '@70' and '@76' indicate the applicable test temperature as 70°C or 76°C, respectively. Equivalent relationships were not developed at 64°C due to the comparatively small differences between feedstocks at that temperature.

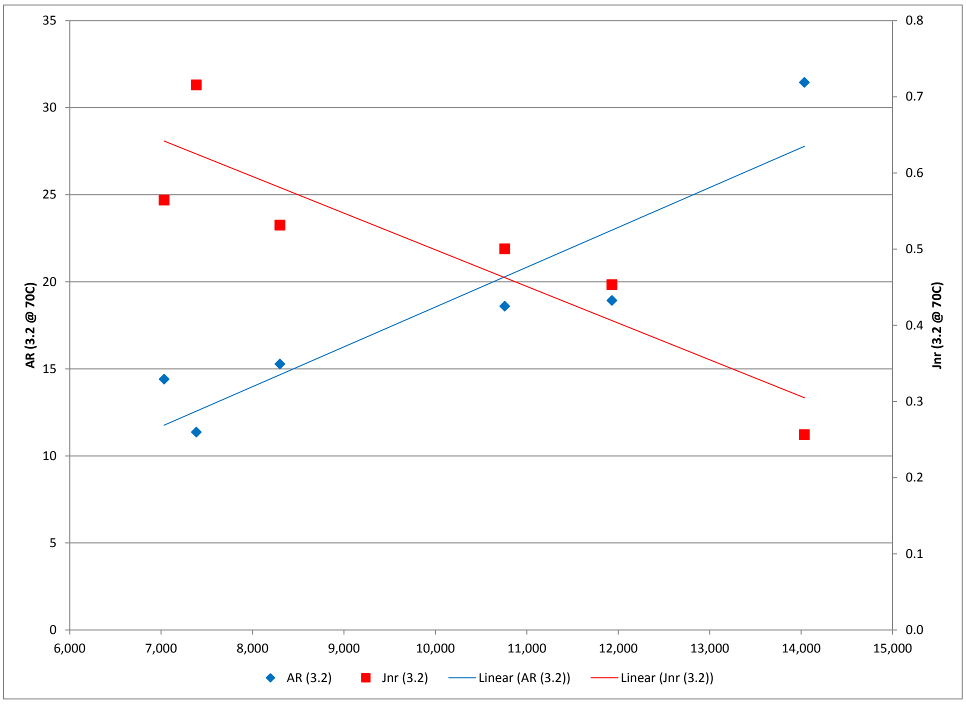

Figure 36 Correlations between Jnr/AR (70°C) and viscosity in 2015

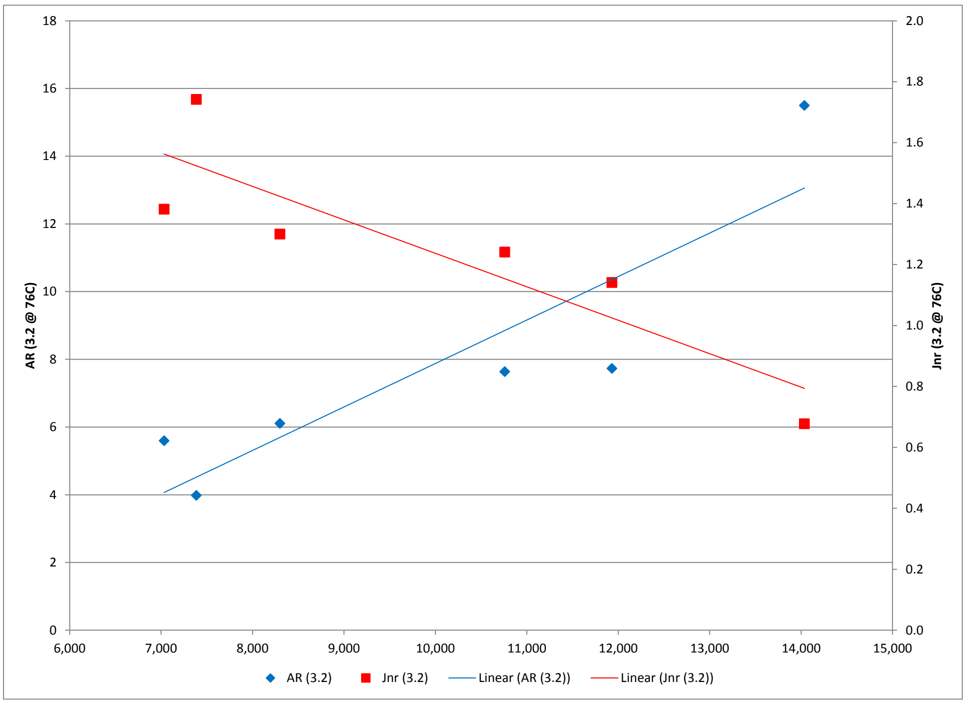

Figure 37 Correlations between Jnr/AR (76°C) and viscosity in 2015

The correlation coefficients were approximately 90% and the data showed a consistent and linear relationship. However, these relationships must be regarded as being specific to the particular bitumen grade and supply being investigated. There is no basis for their application to other bitumen supplies or types.

The change in measured post-RTFO viscosity between release (2011) and in 2015, as well as measured Jnr values in 2015, were used to estimate the AR and Jnr values (at 70°C) in 2011 (Equation 22 and Equation 23, respectively). Equivalent estimation models were developed for 76°C as Equation 24 and Equation 25, for AR and Jnr, respectively.

$AR_{2011@70} = AR_{2015@70} - 0.002287 \times (V_{2015}-V_{2011})$ .... *Equation 22*

$Jnr_{2011@70} = Jnr_{2015@70} + 0.0000481 \times (V_{2015}-V_{2011})$ .... *Equation 23*

$AR_{2011@76} = AR_{2015@76} - 0.001285 \times (V_{2015}-V_{2011})$ .... *Equation 24*

$Jnr_{2011@76} = Jnr_{2015@76} + 0.0001098 \times (V_{2015}-V_{2011})$ .... *Equation 25*

Where $AR_{2011/2015}$ = average recovery at the time of release/in 2015

$Jnr_{2011/2015}$ = creep compliance at the time of release/in 2015

$V_{2011/2015}$ = post-RTFO viscosity at the time of release and in 2015

The '@70' and '@76' indicate the applicable test temperature as 70°C or 76°C, respectively.

The estimated 2011 creep compliance (Jnr(3.2)) and recovery (AR(3.2)) values are presented in Table 54. Summary statistics and the p-value from the t-test for comparison of means for each feedstock are presented in Table 55. The negative estimated AR(3.2) values associated with Feedstock 2 were not logical and the associated CV values were high. These anomalies are addressed below.

Table 54 Estimated 2011 bitumen Jnr and AR values

Sample	Feedstock	Estimated AR(3.2) (%)		Estimated Jnr(3.2) (1/kPa)	
		70°C	76°C	70°C	76°C
28 Jan	1	5.1	0.4	0.76	1.83
02 Feb	1	8.4	2.2	0.68	1.63
10 Mar	1	1.3	-1.7	0.93	2.22
12 Mar	1	9.6	3.0	0.72	1.74
17 Mar	1	6.9	1.0	0.72	1.74
19 Mar	1	-0.2	-2.9	0.89	2.15
15 May	2	-5.5	-6.1	1.01	2.41
17 May	2	-1.4	-3.9	0.92	2.21
17 May	2	-2.7	-10.2	1.16	2.77
19 May	2	-3.6	-4.1	0.98	2.24
24 May	2	7.1	1.0	0.73	1.78
26 May	2	0.1	-2.8	0.89	2.13
21 Jun	2	5.3	0.8	0.81	1.93
23 Jun	2	-3.3	-4.8	0.92	2.21

Table 55 Estimated 2011 AR and Jnr summary statistics

Statistic	Estimated AR(3.2) (%)				Estimated Jnr(3.2) (1/kPa)			
	70°C		76°C		70°C		76°C	
	FS 1	FS 2	FS 1	FS 2	FS 1	FS 2	FS 1	FS 2
Average	5.18	-1.76	0.35	-3.75	0.78	0.93	1.89	2.21
SD	3.90	6.24	2.26	3.65	0.10	0.13	0.24	0.30
CV	75%	353%	643%	97%	13%	14%	13%	14%
p-value (feedstocks)	0.03		0.03		0.04		0.05	

The estimated Jnr(3.2) values at the time of release were higher for Feedstock 2 than for Feedstock 1. This resulted from the significantly greater in-storage hardening of Feedstock 2 samples. At the time of release, Feedstock 2 would have returned higher Jnr(3.2) results than Feedstock 1. This was the opposite of the 2015 results as illustrated by Figure 38, which shows the evolution of Jnr(3.2) at 70°C from 2011 (estimated) to 2015 (measured). The equivalent evolution at 76°C is in Figure 39. The Jnr(3.2) evolution gradients change at 2013 due the non-linear increase in retained bitumen sample viscosity with time (Table 49 and Figure 35). This further demonstrated the significant difference between the bitumen manufactured from the two different feedstocks. It was also consistent with stress sensitivity (%Jnr) results which indicated that samples manufactured from Feedstock 2 were more sensitive to higher stress levels than samples from Feedstock 1.

8.5.4.2 Validation of 2011 MSCR Prediction Models

The estimation of 2011 MSCR results from 2015 data relied on the assumption that the relationships between 2015 post-RTFO viscosity and MSCR results would have been valid at the time of release (2011). This could not be verified due to the inability to perform MSCR testing of 2011 bitumen samples that had not undergone significant in-storage ‘hardening’. However, three independent (manufactured in 2011, 2013 and 2014 by the same supplier) samples were available and were tested for both post-RTFO viscosity and MSCR. The measured results were compared to the estimated results as a means of validating the 2011 MSCR results from 2015 data.

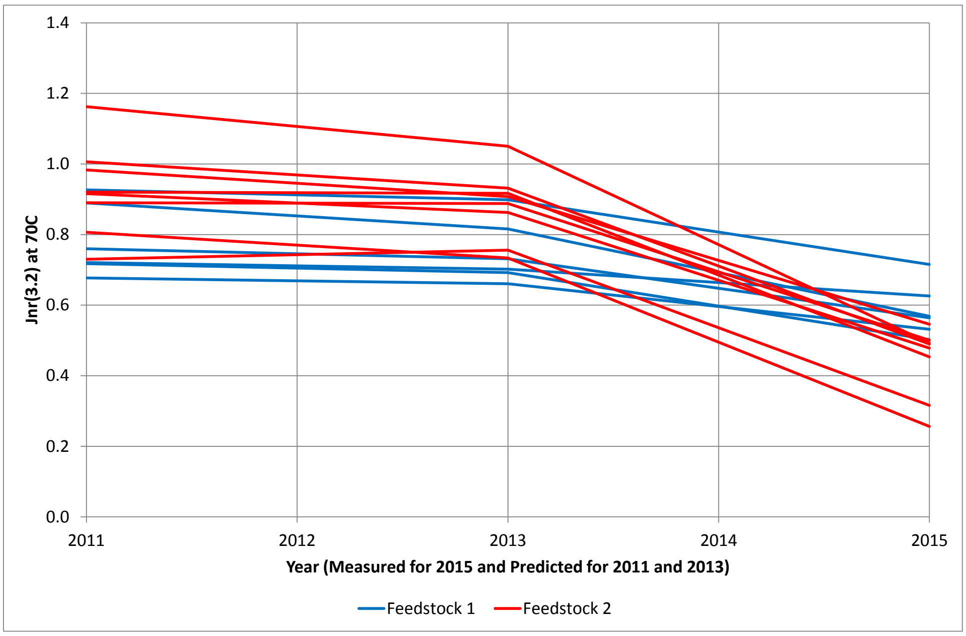

Figure 38 Evolution of Jnr(3.2) at 70°C

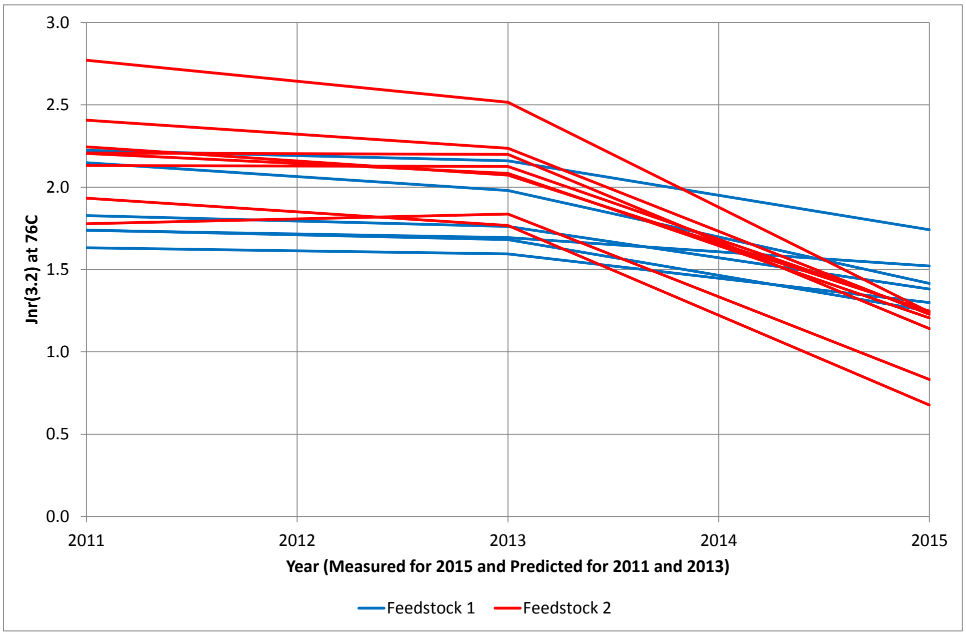

Figure 39 Evolution of Jnr(3.2) at 76°C

The estimated Jnr and AR values are compared to the measured values in Figure 40 (for 70°C) and Figure 41 (for 76°C). The agreement between estimated and measured Jnr(3.2) values was surprisingly high. It must be reinforced that the three additional samples were completely independent of the 2011 samples from which the estimation model was developed. The independent Jnr(3.2) results were consistent with the relationship developed from testing of 2015 samples. It followed that Equation 23 and Equation 25 were accepted as validated models for the estimation of Jnr(3.2) at 70°C and 76°C, respectively.

In contrast, the independent AR(3.2) values were less consistent with the estimated. The use of Equation 22 (70°C) and Equation 24 (76°C) to estimate time of release AR(3.2) values from viscosity measured after four years of storage was not reliable. This reinforced the concern regarding negative estimated AR(3.2) (Table 54) values and high associated CV (Table 55) noted above.

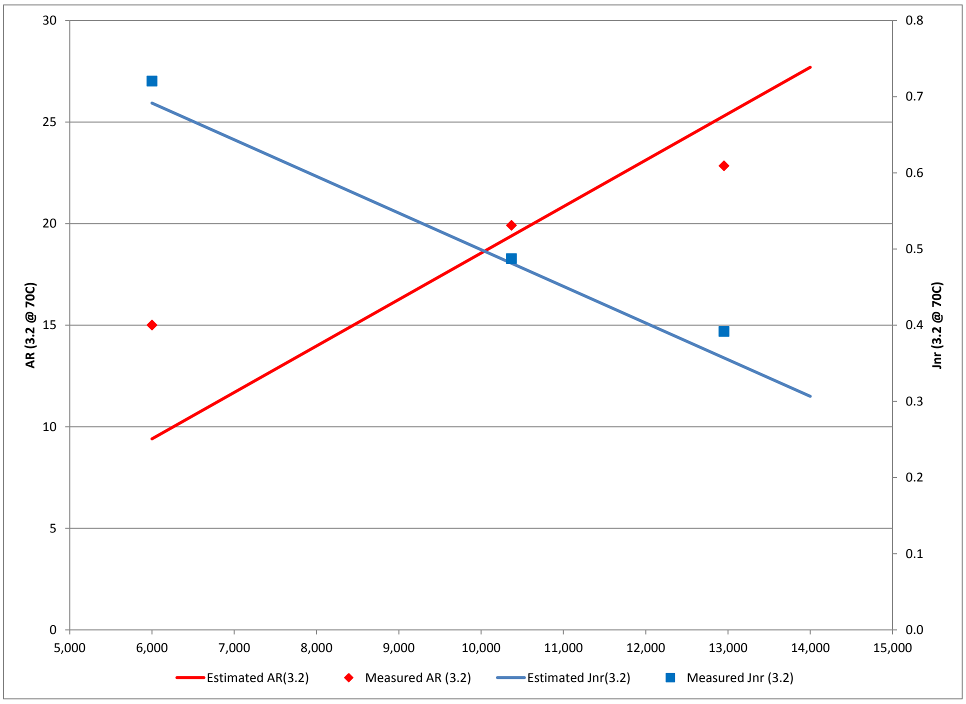

Figure 40 Comparison of estimated and measured independent Jnr/AR at 70°C

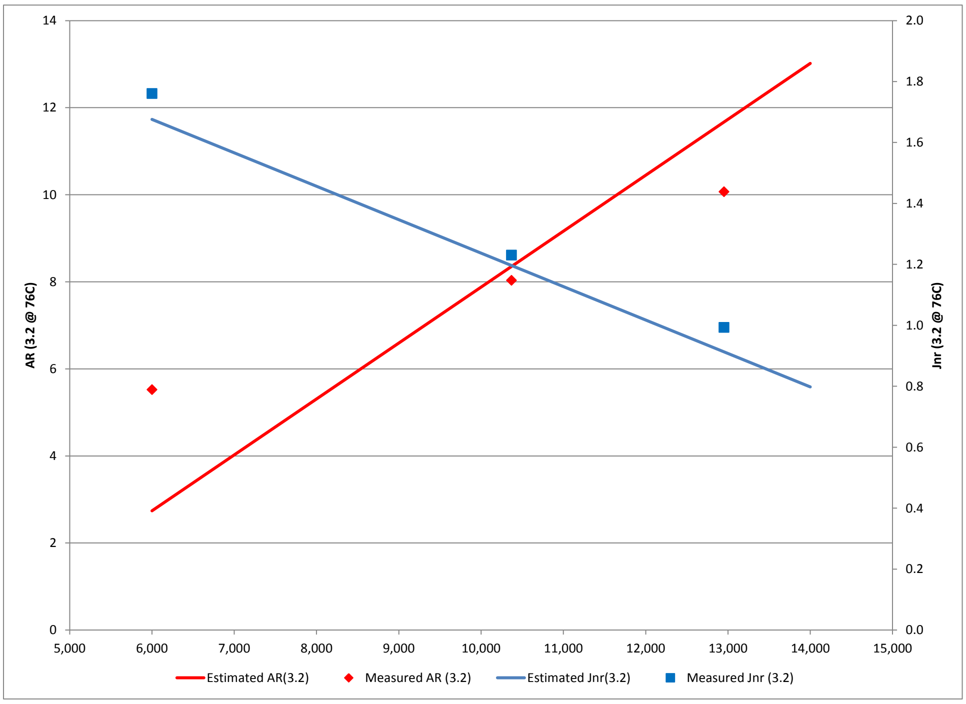

Figure 41 Comparison of estimated and measured independent Jnr/AR at 76°C

8.5.5 Evolution of Performance Grading

The average estimated PG grading was determined from AASHTO M332-14 (Table 56). The estimated average PG grading is based only on the estimated Jnr(3.2) values. Six out of eight Feedstock 2 samples would not have received a PG grading at 76°C due to high calculated stress sensitivity.

Table 56 PG evolution of retained bitumen samples

Average PG grading	At 70°C		At 76°C	
	Feedstock 1	**Feedstock 2**	**Feedstock 1**	**Feedstock 2**
2011 (estimated)	PG 70 V	PG 70 V	PG 76 H	PG 76 S
2015 (measured)	PG 70 V	PG 70 E	PG 76 H	PG 76 H

The PG grading for Feedstock 1 remained unchanged while the Feedstock 2 PG grading had increased from Very Heavy (2011) to Extreme (2015) traffic at 70°C, and from Standard (2011) to Heavy (2015) traffic at 76°C.

8.5.6 Summary of Retained Bitumen Testing

At the time of construction, M1000 manufactured from Feedstock 2 had lower resistance to shear deformation at 70°C and 76°C and increased sensitivity to stress level at all test temperatures. This reduced shear resistance and increased stress sensitivity correlated with the poor CSC resistance identified in the Runway 16/34 asphalt and the horizontal deformations observed in the heavy braking zone associated with Runway 16 landings.

8.6 OUTCOMES AND LIMITATIONS

The mastic testing indicated that the change in dust source, from Tylden Quarry to Matthews Quarry, had no adverse impact on the mastic (or asphalt) response to shear stress. In fact, the Matthews dust mastic samples were more resistant to shear stress. However, this reflected slight differences in the mastic volumetric properties resulting from the lower apparent density and higher absorption of the Matthews Dust.

The difference in response to shear stress between Feedstock 1 and Feedstock 2 bitumen was corrected by in-storage hardening, primarily between 2013 and 2015, as indicated by the measured increase in post-RTFO viscosity. The improvement in bitumen resistance to shear stress was consistent with the observed improvement in asphalt CSC resistance in the field.

The retained bitumen sample testing demonstrated that the bitumen properties had changed significantly since manufacture in 2011. Unchanged samples of bitumen manufactured from the project feedstocks could not be tested in 2015. The 2011 Jnr(3.2) values were estimated using a relationship developed for 2015 Jnr(3.2) and post-RTFO viscosity data. Although independent M1000 samples validated the developed relationship, it can not be categorically verified due to the inability to test 2011 retained bitumen samples that had not hardened significantly during storage.

8.7 SUMMARY

This Chapter presented the performance-based testing of mastic and bitumen samples. It also presented viscosity and penetration testing of retained bitumen samples. It was found that the bitumen feedstock (crude oil source blend) change adversely affected the Runway 16/34 asphalt surface performance. The confounded fine aggregate (dust source) change did not.

This is the final Phase of research presented in this Dissertation. The next Chapter will present the conclusions of this research as well as recommendations for future research efforts and industry practice. The overall limitations are acknowledged and a number of other (ancillary to the hypothesis) observations are summarised.

9. CONCLUSIONS AND RECOMMENDATIONS

The aim of this Dissertation (1.4.1 Aim) was to determine the root cause of the horizontal deformation failures observed in one runway at Melbourne Airport, shortly after the resurfacing of both runways in 2010 and 2011. This aim was to be addressed by testing the hypothesis (3.7 Hypothesis) that a single or combination of causes could be identified and that other potentially confounded factors could be excluded as explanatory causes.

The hypothesis was tested through the systematic examination of all potential confounding factors that could possibly lead to the shear (CSC) failures observed. The aim was achieved by answering four particular questions (1.3.3 Research Questions) and addressing the six gaps identified in the existing knowledge (Table 8). The research was progressed in four primary Phases. Each Phase incrementally and systematically narrowed and focused towards the identified root cause of the CSC failures (Figure 42).

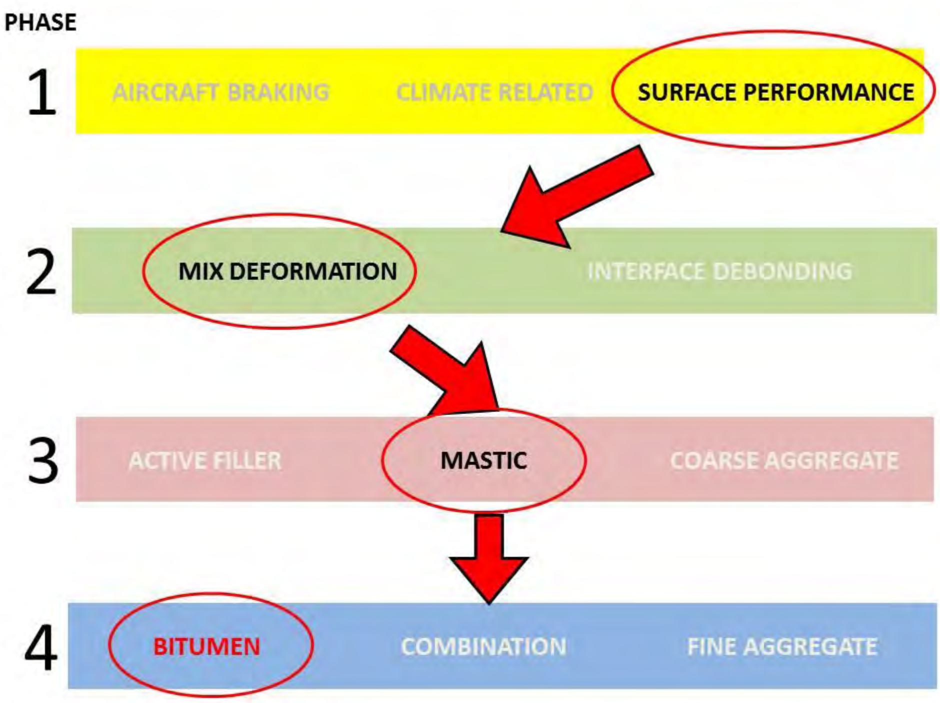

Figure 42 Completed sequential investigation framework

9.1 CONCLUSIONS

It was concluded that the horizontal surface deformation failures observed in the braking zone associated with Runway 16 landings at Melbourne Airport were the result of the change in M1000 feedstock (crude oil source) that occurred in April 2011. The April 2011 change in crude oil blend initially appeared moderate. However, the result was inadequate asphalt mixture resistance to shear creep, leading to permanent (horizontal) deformation under repeated shear stress cycles induced by braking aircraft. This conclusion was supported by the systematic exclusion of other potentially contributing factors, such as differential aircraft operations, interface de-bonding and the introduction of Hisingerite clay minerals into the fine aggregate (dust).

The inadequate CSC resistance self-corrected two to three years after construction. This indicated the observed failures were symptomatic of bitumen-related asphalt tenderness. At the time of writing (2015) no further CSC failures have been observed, regardless the hot weather experienced during the end of 2014 summer. The 'self-correction' conclusion was supported by the significant hardening of retained bitumen samples particularly after three years of controlled storage.

Concerningly, it was found that the change in M1000 performance occurred without any bitumen non-compliance being registered during the work. This was allowed by the empirical nature of the Australian viscosity-based specification for paving grade bitumens. Revision or supplementation of the specification is required to minimise the risk of recurrence in the future.

Based on the different modifying mechanisms and potential interactions between acid (PPA) and bitumen molecules in bitumens of different rheology and crude oil source, M1000 is concluded to be more susceptible to variable performance than other common binders, such as unmodified bitumen or PMB. The risk of PPA modified bitumen exhibiting variable performance will increase as sources of imported bitumen feedstock become more diverse. This has been occurring in Australia since the 1980s. When combined with the measured sensitivity of M1000 to shear stress at high temperatures, it is concluded that M1000 is at greater risk of leading to variable and unreliable asphalt surface performance for runways in the future.

These conclusions are based on answering the four questions raised by the observed failures at Melbourne Airport and addressing the six gaps identified in the existing knowledge. The four Phases of this (academic) investigation addressed these questions and gaps as follows.

9.1.1 Aircraft Induced Stresses

Phase 1 (Chapter 5) addressed the first research question (correlation between aircraft operational differences and runway surface performance) and existing knowledge gap 1 (stress induced in an asphalt surface and interface by an aircraft tyre) and gap 2 (the effect of aircraft braking on these stresses). Phase 1 also indirectly addressed the final research question (adequate performance of the Matthews Quarry fine aggregate asphalt on roads).

The similarity of calculated critical shear stress, and frequency of aircraft operations, led to the conclusion that there was a fundamental difference in the performance between the two runway surfaces. Differential aircraft operation was excluded as a potential factor contributing to the horizontal deformations in the braking zone associated with Runway 16 landings at Melbourne Airport.

When typical aircraft braking conditions were considered, it was concluded that the impact of the duration of increased shear stress was more significant to asphalt surface performance than the increase in maximum shear stress magnitude. This explained the concentration of horizontal deformation failures in the braking zone associated with Runway 16 landings, while the remainder of Runway 16/34 remained free of similar defects.

9.1.2 Interface Shear Resistance

Phase 2 (Chapter 6) addressed the second research question (interface shear resistance as a factor affecting surface performance) and existing knowledge gap 3 (typical interface shear resistance achieved by common airport asphalt resurfacing practice) and gap 4 (test methods for monotonic and repeated interface shear resistance).

From the monotonic (DS) testing it was concluded that a difference in interface shear resistance between the two runways was not a significant contributing factor for the horizontal deformation failures in the Runway 16/34 surface at Melbourne Airport. The level of bond achieved by following normal practice for airport surface construction in Australia resulted in a high level of interface shear resistance. Although not germane to this research, Australian airport overlay bond strength may be further improved by use of premium or modified tack coat products, such as those commonly used in the USA, as indicated by the literature review.

The cyclic (IRIS) testing of the layer-interface-layer systems failed to reliably measure the interface resistance to cyclic shearing. However, it did prove to be a reliable tool for the identification of the weakest element in the layer-interface-layer system. The weakest element deformed and failed under cyclic shear stress, while the other elements in each sample remained largely unaffected.

The combined DS and IRIS testing led to the conclusion that the asphalt containing Tylden Dust had a significantly higher resistance to cyclic shear deformation than the asphalt containing Matthews Dust. This resulted in a focus on identifying fundamental differences in the asphalt mixture constituents. The DS and IRIS test methods were also found to be reliable and effective.

9.1.3 Asphalt Constituents and Mastic

Phases 3 and 4 (Chapter 7 and 8 respectively) addressed the third research question (an unknown change in constituent materials) as well as the fourth question (identification of a single constituent change that explained the failures). Existing knowledge gap 5 (impact of Hisingerite on asphalt shear resistance) and gap 6 (impact of M1000 variability on asphalt shear resistance) were also addressed in these Phases.

It was concluded that both the fine aggregate (dust source) and the M1000 feedstock (crude oil source blend) changed at around the transition from Runway 09/27 to Runway 16/34 in April 2011. No other constituent materials were found to have changed in a significant way. The confounded change in dust and bitumen was concluded to have resulted in two significantly different asphalt mastics within an otherwise consistent matrix of nominally identical coarse aggregate.

Performance testing of mastics manufactured from both dust samples indicated the dust source was not an explanatory factor for the difference in CSC resistance between the two asphalt mixtures. It was concluded that the Matthews Dust (and associated introduction of Hisingerite clay minerals) had no adverse impact on the CSC resistance of the asphalt at Melbourne Airport.

In contrast, performance and other testing of the retained bitumen samples led to the conclusion that the change in feedstock introduced a less shear resistant and more stress sensitive bitumen. A tender asphalt surface resulted and then self-corrected after two to three years. The change in bitumen performance occurred despite all M1000 batches complying with the relevant standard.

9.2 RECOMMENDATIONS AND FUTURE WORK

This research identified a number of recommendations for consideration by the broader research and construction industries. It also identified a number of unresolved issues worthy of future research effort. It is recommended that these issues be considered in the future.

9.2.1 Recommendations to Industry

9.2.1.1 Verification of Trackless Tack Coat in Australia

The review of existing literature identified trackless or premium tack coat as a potential improvement in asphalt surface interface construction. These materials are already available in Australia and represent significant value at minimal additional cost. It is recommended that the benefits of trackless tack coat be verified and then introduced to Australian asphalt resurfacing practice, particularly for high stress pavements such as airport runways.

9.2.1.2 Development of new Airport Asphalt Binders for Australia

An unknown (at the time) change in crude oil source blend had a significant impact on the performance of otherwise similar asphalt surfaces exposed to shear stresses of similar magnitude and frequency. This occurred despite all batches complying with the Australian paving grade bitumen specification. The M1000 (acid modified) bitumen commonly used in Australian airport asphalt was found to be stress sensitive, significantly affected by the moderate change in feedstock composition and to age rapidly in controlled storage. It is recommended that alternate bituminous binders be investigated for airport asphalt in Australia.

9.2.1.3 Adaptation of MSCR to Australian Airport Binders

The MSCR protocol represents world-best practice for performance-based assessment of bitumen and mastic response to shear stress at elevated temperatures. In contrast, the Australian paving grade bitumen specification is empirical and based primarily on viscosity at 60°C. In an attempt to prevent future changes in crude oil source adversely impacting high stress and high temperature asphalt performance, the MSCR is recommended as an additional specification and quality control tool.

9.2.2 Recommendations for Future Work

9.2.2.1 Comparison of LE and FE models for near surface Shear Stress

This research adopted a LE tool for the calculation of stresses in the asphalt surface under various aircraft and braking conditions. It is recommended that LE tools (and the associated simple material characterisation allowed) be compared to FE tools (and the complex material characterisation possible) to assess the benefits of the more complex and demanding FE capabilities, with specific regard to surface layer stress calculations under braking aircraft.

9.2.2.2 Meta-analysis of Interface Shear Strength Results

The review of existing literature and knowledge identified inconsistent and even contradictory outcomes from various investigations of interface shear strength. It is recommended that a meta-analysis of available data be performed in an attempt to reconcile inconsistencies and to develop a consolidated theory of asphalt surface bond strength and the factors affecting it.

9.2.2.3 Development of a Framework for Shear Creep Diagnosis

This Dissertation represents the specific application of a framework for the diagnosis of sheer creep related distress in any asphalt surface. It is recommended that a general framework be developed to allow the same systematic approach to be applied to other shear creep distress diagnosis. The general framework would apply equally to all asphalt surfaced airport, road, highway and port pavements.

9.3 LIMITATIONS

The research presented in this Dissertation contains a number of unavoidable limitations. The application of the findings and conclusions are limited to airport asphalt surfaces of comparable mixture design, composition and construction. For example, the measured interface shear resistance would only be comparable to other asphalt surfaces constructed by similar methods and equipment. The DS test method would, however, apply broadly to the measurement of any airport, port or road asphalt surface interface. The limits of the scope of application extend to airport-quality runway surfaces constructed at airports in Australia and other countries that adopt similar design and construction practices, as described above (1.4.2 Scope).

There are two limitations associated with the investigation methods and procedures. First, the number and location of asphalt core samples recovered from the surface of the two runways was influenced by airport operational restrictions, convenience and the focus of the broader group directing the preliminary investigation. Similar limitations applied to the retained bitumen samples able to be recovered from storage for testing. While not significant, these limitations must be acknowledged.

Second, the retained bitumen sample testing demonstrated that the bitumen properties had changed significantly since manufacture in 2011. Unchanged samples of bitumen manufactured from the project feedstocks could not be tested in 2015. Some testing was performed on independent bitumen samples manufactured in 2011, 2013 and 2014 but the feedstock was unlikely to be identical to the 2011 feedstocks. Some ‘time-of-release’ MSCR properties were estimated from 2015 measurements for bitumen samples manufactured in 2011.

Similarly, reference samples of coarse aggregate and active filler (hydrated lime) were not able to be located. The actual materials incorporated into the two runway surfaces could not be directly assessed, even though materials produced in 2015 from the same suppliers/sources were available. The inability to test unchanged samples of the 2011 constituent materials is the greatest limitation associated with the findings presented in this Dissertation.

9.4 OTHER OBSERVATIONS

A number of other observations, not core to the hypothesis, were made during this research. A number of these observations represented novel and significant new knowledge in their own right. Some of these observations were ancillary to the research presented in this Dissertation but were inherently linked to it and/or the data generated.

9.4.1 Adequacy of interface construction practice

The stress analysis included the calculation of shear stresses at the surface layer interface under various aircraft braking conditions. These were noted to be similar in magnitude to the interface shear strength values measured from cores recovered from the two runways. An assessment of interface construction adequacy was made at various locations around the tyre-pavement contact zone. It was demonstrated that the factor of safety associated with interface shear strength is negligible during extreme aircraft braking (White 2015a). Appendix 1 includes the associated publication.

9.4.2 Effect of traffic on interface shear resistance

During the monotonic (DS) and cyclic (IRIS) testing a significant difference in interface shear resistance was noticed for samples from cores exposed to two years of significant aircraft traffic. Traffic exposure significantly improved the interface resistance to shear. Other surface properties, such as wheel tracking and modulus, also showed consistent improvement under traffic exposure. The aggregate skeleton and particle orientation were subsequently investigated.

The significant improvement in asphalt surface properties and a theoretical mechanism of asphalt mixture evolution were developed (White 2015b). The resulting publication is contained in Appendix 1.

9.4.3 Inter-batch variability of bitumen performance

The bitumen shear creep (MSCR) and compliance testing identified a significant change in M1000 properties part-way through the Melbourne Airport resurfacing project. This change was evidenced by measured differences in: hardening of retained bitumen samples, pre-RTFO properties at the time of production and the high temperature stress sensitivity under the MSCR protocol. These changes reflected a change in the M1000 feedstock (crude oil source blend). The inter-batch and inter-feedstock variability of M1000 properties were analysed. Concerningly, the significant differences in many properties were not identified by the Australian paving grade bitumen specification. Additional testing (such as the MSCR protocol) was recommended for M1000 and other bitumens used for high stress applications in high temperature environments (White 2015c). The associated paper is contained in Appendix 1.

9.4.4 Limitations of aircraft pavement strength rating systems

The stress analysis identified the limitations of the internationally adopted aircraft pavement strength rating system (ACN-PCN). The ACN-PCN system was developed to protect pavement subgrades from rutting. It does not reflect the impact of tyre pressure and wheel load on surface shear distress. Nor does it consider shear stresses associated with aircraft braking. This limitation has been investigated (White 2015d) and a modification to the ACN-PCN system developed and recommended (White 2015e). The associated papers are contained in Appendix 1.

APPENDIX 1. RELATED PUBLICATIONS

White, G 2015, 'State of the Art: Interface Shear Resistance of Asphalt Surface Layers', *International Journal of Pavement Engineering*, submitted but not yet published.

White, G 2015, 'The Multiple Stress Creep Recovery test for Airport Asphalt Binders', *Road and Transport Research*, Article in press.

White G 2014, 'Cyclic shear deformation of asphalt at an Australian Airport', *Proceedings 2014 Worldwide Airport Pavement Technology Transfer Conference*, Galloway, New Jersey, USA, 5-7 August, Federal Aviation Administration.

White, G 2015, 'Shear Stresses in an Asphalt Surface under Various Aircraft Braking Conditions', International *Journal of Pavement Research and Technology*, submitted but not yet published.

White, G 2015, 'Asphalt Tenderness in an Australian Runway Overlay', *Transportation Geotechnics*', Article in Press, doi 10.1016/j.trgeo.2015.08.001.

White, G 2015, 'Shear Creep Response of an Airport Asphalt Mastic', *International Journal of Pavement Engineering*, Article in Press, doi 10.1080/10298436.2015.1095914.

White, G 2015, 'Inter-batch and Inter-feedstock variability of an Acid Modified Bitumen', *Road Materials and Pavement Design*, Article in Press, doi 10.1080/14680629.2015.1108220.

White, G 2015, 'Limitations and Potential Improvement of the Aircraft Pavement Strength Rating System to protect Airport Asphalt Surfaces', *International Journal of Pavement Engineering*, submitted but not yet published.

White, G 2015, 'Modification of the Airport Pavement Strength Rating System for Improved Protection of Asphalt Surfaces', *International Journal of Pavement Engineering*, submitted but not yet published.

White, G 2015, 'Effect of aircraft on the structure and response of asphalt', *Transportation Geotechnics*, vol. 2, pp. 56-64, Elsevier.

White, G 2015, 'Adequacy of Runway Asphalt Overlay Interface Construction', *AAPA International Flexible Pavements Conference*, Gold Coast, Queensland, Australia, 13-16 September, Australian Asphalt Pavement Association.

APPENDIX 2. DS & IRIS TEST METHODS

NTL-TM001-13. Test Method for Repeated Load Creep of Inclined layer Interface in Triaxial Compression. Fulton Hogan Australia Pty Ltd.

NTL-TM002-13. Test Method for Determination of Bond Strength and Aggregate Interlock of Layer Interface-Direct Shear. Fulton Hogan Australia Pty Ltd.

Test Method for Repeated Load Creep of Inclined layer Interface in Triaxial Compression

1. Scope
   1.1. This test method covers the procedure for the preparation testing and measurement of permanent creep between two asphalt layers in a cylindrical asphalt specimen with an inclined layer interface under tri-axial compressive loading.
   1.2. The procedure uses a loading cycle of 1.0-seconds in duration, consisting of a 0.5-second haversine load, followed by a rest period of 0.5-seconds. Permanent axial strain is recorded throughout the test.
   1.3. The test is conducted at a single effective test temperature and design stress level
   1.4. The test method is applicable for field samples 75mm in diameter and 150mm in height for mixtures with a nominal aggregate size less than 20mm.
2. Referenced Documents
   2.1. FHWA-SA-95-003 Background of Superpave Asphalt Mixture Design and Analysis
3. Definitions
   3.1. Effective Temperature – is the effective temperature for deformation of asphalt mixture giving equivalent deformation as the sum of deformation occurring throughout the year.
   3.2. Flow Number-is defined as the number of cycles at which shear deformation of the interface occurs at an increasing rate of deformation.
4. Summary of Method
   4.1. A cylindrical specimen of two layers of an asphalt mixture(s), inclined at 45^o, are subjected to a haversine axial load of a 0.5-seconds followed by a rest period of 0.5-seconds. The interface is inclined at 45^o to subject the interface to maximum shear, as in a aircraft braking situation. The test is conducted with a confining load to better simulate field conditions. Cumulative permanent axial strains are recorded throughout the test
5. Significance of Use
   5.1. Several factors work together to resist slippage in a layered asphalt pavements, mechanical interlock, interfacial adhesion, and tensile, compressive, and shear strength of the uppermost layer. Nevertheless, slippage does occur at airfields due to a lack of one some or all of these parameters. In this test the resistance of a layer interface to undergo shear flow (Flow Number) is evaluated.
   5.2. This material property can be used as an indicator for compare shear resistance of different asphalt and tack coat types.
6. Apparatus
   6.1. Load Test System- A load test system consisting of a testing machine, environmental chamber, measuring system and specimen end fixtures. The AMPT (McGraths Hill and Auckland) shall be the preferred testing system for this testing.
      6.1.1. Testing Machine- The testing machine should be an electro-hydraulic machine capable of applying haversine loads up to 15kN.
      6.1.2. Confining Pressure- A system capable of applying a constant confining pressure of up to 200KPa, the system should be provided with a pressure relief value capable of pressurising and de-pressuring the cell with air.
      6.1.3. Environmental Chamber – A chamber for controlling the test specimen at the effective temperature. The chamber should be capable of controlling temperature within a range 25 to 60^oC to an accuracy of $\pm 1^oC$

6.1.4. Measurement System- The system shall include a data acquisition system capable of digitally storage and analysis on a computer. The system shall be capable of measuring and recording the time history of the applied load, axial deformations for the time duration of this test method. The system shall be capable of measuring the load and resulting deformation to within 0.5%.

6.1.4.1. Load- The load shall be measured by an electronic load cell having a capacity of up to 15kN

6.1.4.2. Axial Deformation- Axial deformation shall be measured by a displacement transducer mounted in the loading ram.

6.1.5. Loading Platens- Loading platens with a diameter equal to or greater than the specimen are required above and below the specimen to transfer the load from the testing machine to the sample. These platens shall be made of anodised high strength aluminium.

6.1.6. Flexible Membrane- The specimen shall be encased in an impermeable flexible membrane. The membrane should be sufficiently long enough to extend on to the platens and be of the same diameter as the sample.

6.1.7. End treatment- Friction reducing end treatments shall be placed between the specimen and the platens. End treatment shall be a two latex membranes separated with a water based lubricant.

6.2. Saw – a machine for sawing the test specimen ends to a length of 150mm, without excessive heating or shock.

6.3. Core Drill – a coring machine with a diamond bit for cutting nominal 75mm diameter test specimens.

7. Test Specimens

7.1. Size- Testing shall be performed on 75mm diameter by 150mm height test specimens, with the layer interface centrally located and aligned at a 45^{O} slope from the surface in the direction of milling. Test specimens shall be taken in the field or extracted from larger field cores or blocks.

7.2. Field cores- Extract minimum 200mm diameter cores or 200mm wide slabs from the pavement, marking the direction of the paving and profiling.

7.3. Coring- The test specimens are to be cored from the existing field cores or pavement using a 75mm coring bit, cores shall be aligned so the interface between 1st and 2nd layer is 45^{o} from the vertical aligned to the direction of the paving (see Fig 1). The core shall be adequately supported to ensure that the resulting test specimen is cylindrical with sides that are smooth, parallel and free from ridges and groves.

7.4. End Preparation- the ends of the test specimen shall be smooth and perpendicular to the axis of the specimen by sawing with a single or double bladed saw. Where layer the layer interface of the sawn specimen will be within 25mm of the surface, to avoid end effects the specimen shall be capped prior to sawing with a polyester resin based filler.

7.5. Sample storage- Wrap samples in polyethylene and store in environmentally controlled storage area at temperatures between 5-25^{o}C.

8. Procedure

8.1. Place the bottom platen in the loading frame and place the friction reducing membrane on the platen

8.2. Fit the flexible membrane over the sample , place the sample with the flexible membrane in the environmental chamber on the bottom platen/membrane

8.3. Place the upper friction reducing membrane an platen on top of the sample

8.4. Extend the membrane over both the top and bottom platen and attach the elastic bands/O-rings to seal the membrane. Centre the specimen visually with the loading actuator to avoid eccentric loading.

8.5. Ensure hose is connected to lower pattern so the sample voids is under atmospheric pressure during testing.

8.6. Lower Tri-axial cell and environmental chamber to ensure proper seal

8.7. After the time required for the sample to reach test temperature, see following, apply the confining pressure and seating load, which shall be 5% of the load applied to the sample.

8.7.1. 25^{o}C 0.5hrs

8.7.2. 30^{o}C 1.0hrs

8.7.3. 40^{o}C 1.5hrs

8.7.4. 50^{o}C 2.0hrs

8.8. Apply the haversine load which achieves the desired stress on the sample. Continue until 10,000 cycles or until the specimen fails and results in excessive tertiary deformation.

8.9. For each load application record the applied load, confining pressure, axial deflection.

9. Calculations

9.1. Convert the axial deformation to axial strain by dividing by the specimen length (typically 150mm)

9.2. Compute the cumulative permanent strain ε_p

9.3. Plot the cumulative axial permanent strain (ε_p) versus number of loading cycles (N) in log space.

9.4. The flow number is viewed as the lowest point in the curve of the rate of change in axial strain versus number of loading cycles $\frac{d\varepsilon_p}{dN}$. The rate of axial strain versus number of loading cycles should be plotted and the flow number taken as the minimum point or zero slope is observed.

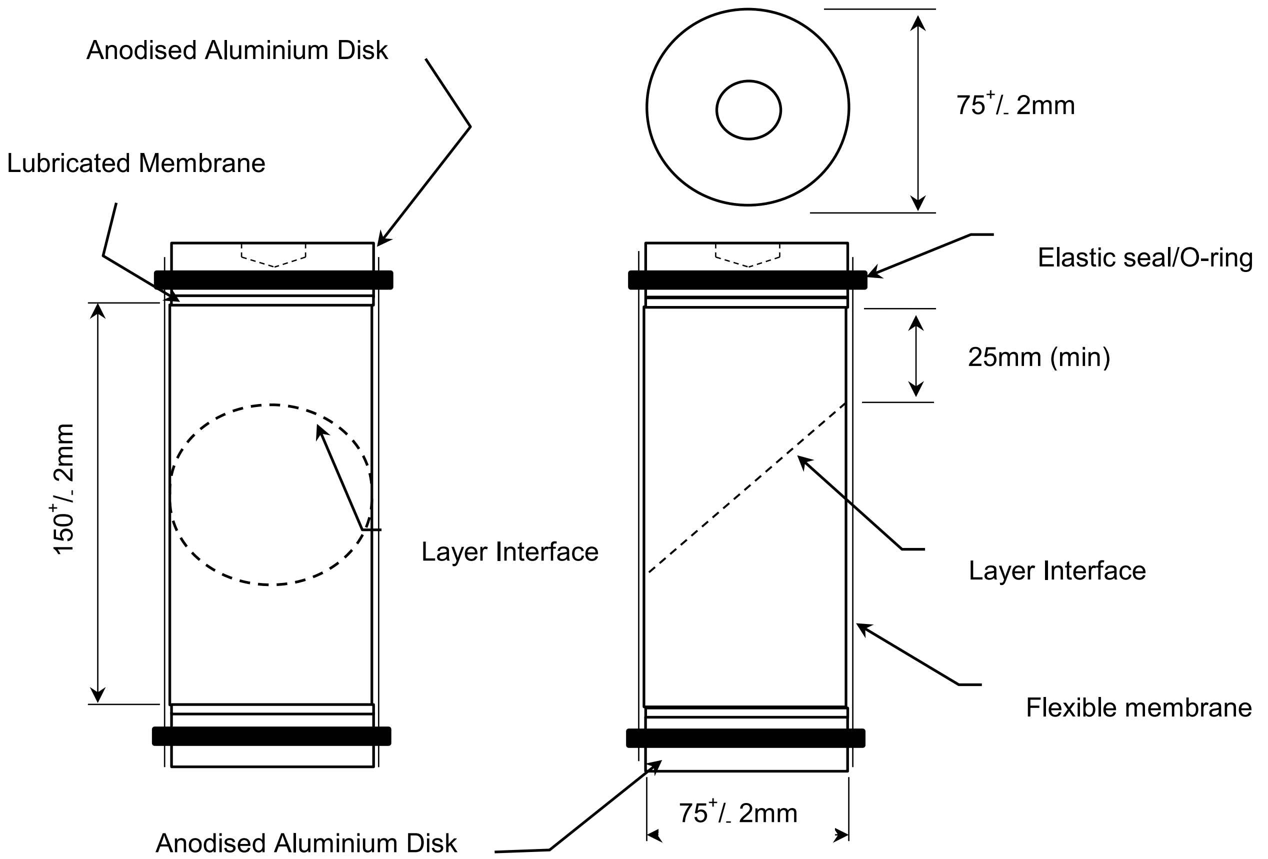

Figure 1 Test Specimen Setup

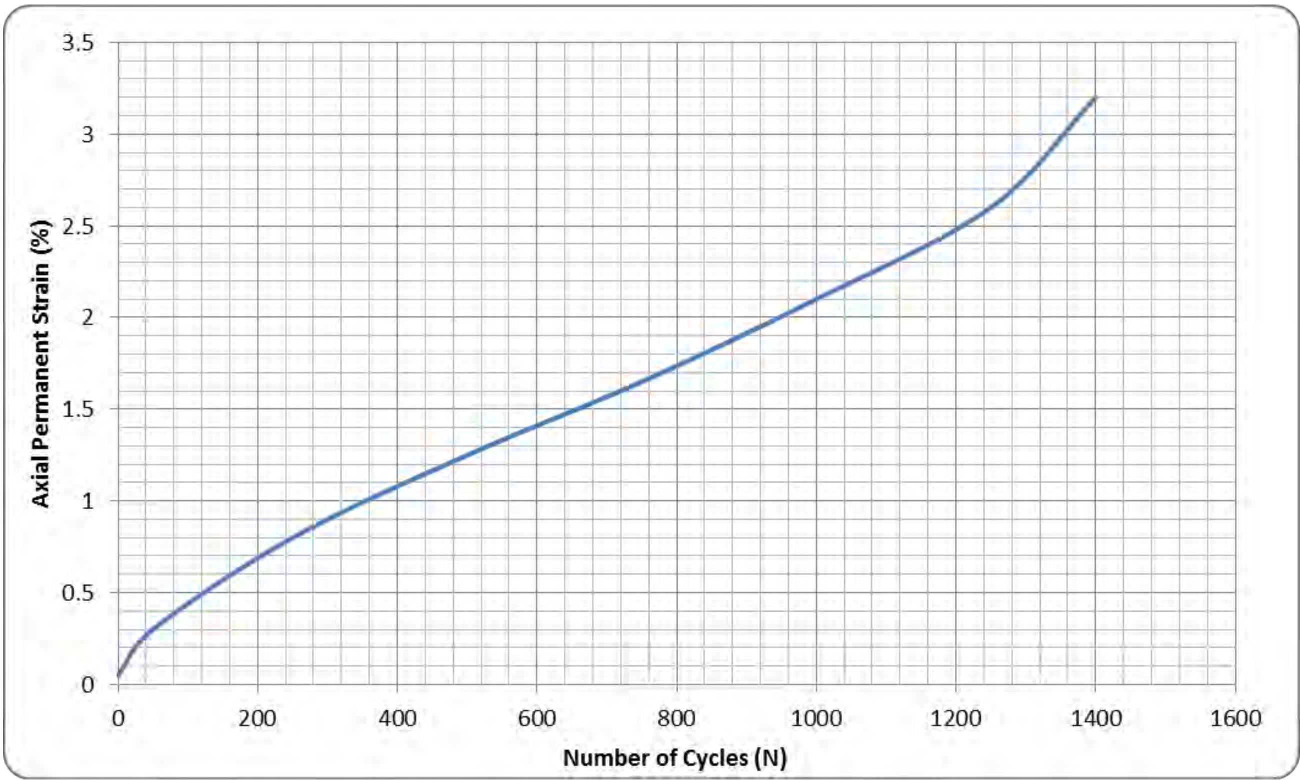

Figure 2 Cumulative permanent strain vs. loading cycles

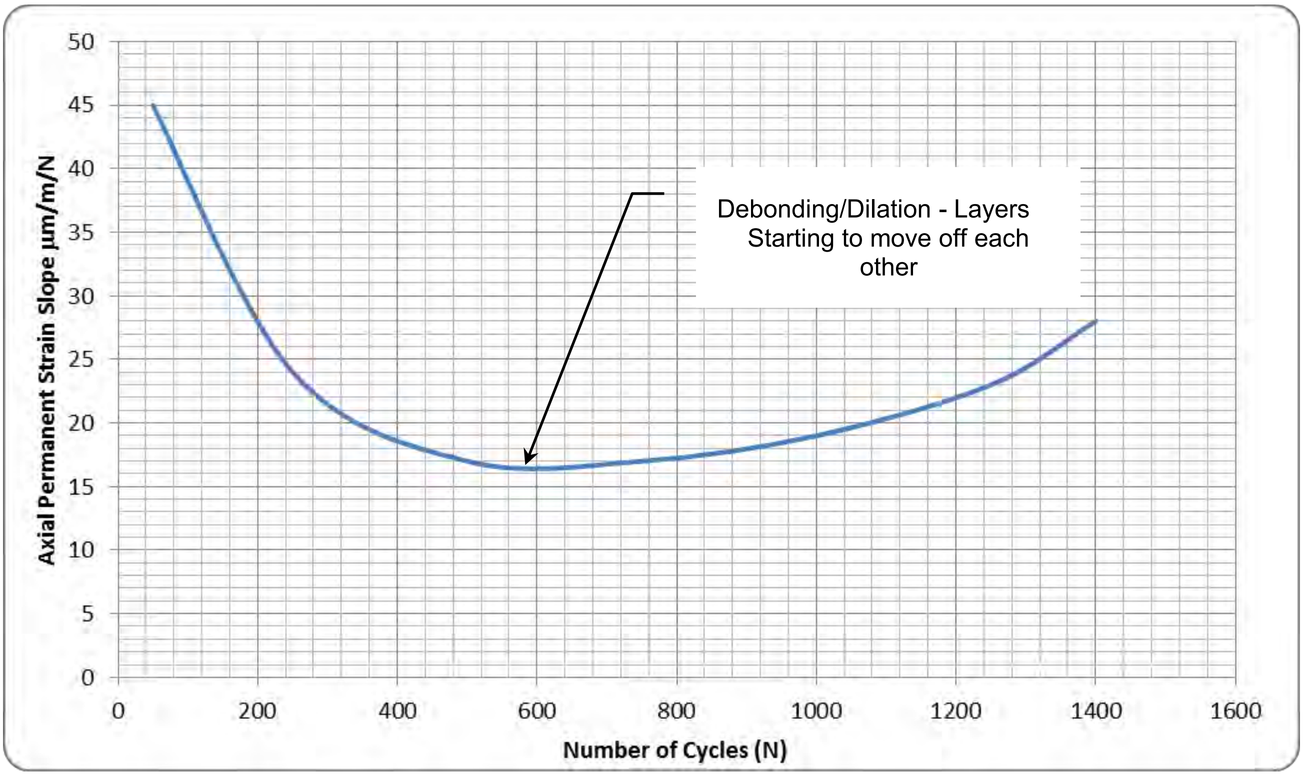

Figure 3 Typical Plot of Rate of Change of permanent strain vs. loading cycles

Test Method for Determination of Bond Strength and Aggregate Interlock of Layer Interface-Direct Shear

1. Scope
   1.1. This test method covers the procedure for the preparation testing and measurement of the peak shear strength between two asphalt layers using cubic briquettes by direct shearing.
   1.2. The procedure uses a constant deformation rate; axial deformation and load are recorded throughout the test.
   1.3. The test is conducted at a single effective test temperature and deformation rate.
   1.4. The test method is applicable for trimmed field samples 50mm square and typically 100mm in height for mixtures with a nominal aggregate size less than 20mm.
2. Referenced Documents
   2.1. FHWA-SA-95-003 Background of Superpave Asphalt Mixture Design and Analysis
3. Definitions
   3.1. Effective Temperature – is the effective temperature for deformation of asphalt mixture giving equivalent deformation as the sum of deformation occurring throughout the year.
4. Summary of Method
   4.1. A square specimen of two layers of an asphalt mixture(s) is subjected to a direct shear across the interface at a loading at a rate of 50mm/min. The test is conducted with a confining load (normal loads) to better simulate field conditions and separate aggregate and tack coat contribution to bonding. The peak force required to debond the layers and the deformation at debonding is recorded in the test.
5. Significance of Use
   5.1. Several factors work together to resist slippage in a layered asphalt pavements, mechanical interlock, interfacial adhesion, and tensile, compressive, and shear strength of the uppermost layer. Nevertheless, slippage does occur at airfields due to a lack of one some or all of these parameters. In this test the strength of the layer interface is evaluated.
   5.2. This material property can be used as an indicator to compare the shear resistance of different asphalt and tack coat types.
6. Apparatus
   6.1. Load Test System- A load test system consisting of a testing machine, environmental chamber, measuring system and specimen end fixtures.
      6.1.1. Testing Machine- The testing machine should be an electro-pneumatic machine capable of applying loads up to 5kN.
      6.1.2. Environmental Chamber – A chamber for controlling the test specimen at the effective temperature, throughout the test. The chamber should be capable of controlling temperature within a range 25 to 50^{o}C to an accuracy of ±1^{o}C
      6.1.3. Measurement System- The system shall include a data acquisition system capable of digitally storage and analysis on a computer. The system shall be capable of measuring and recording the time history of the applied load, axial deformation for the time duration of this test method. The system shall be capable of measuring the load and resulting deformation to within 0.5%.
         6.1.3.1. Load- The load shall be measured by an electronic load cell having a capacity of up to 5kN
         6.1.3.2. Axial Deformation- Axial deformation shall be measured by a displacement transducer mounted in the loading actuator.

6.2. Shear box – a box consisting of two separate halves which can be moved relative to each other, thus shearing the asphalt along the layer interface. The shear box shall be designed so that a normal load can be applied through a plate which rests on the surface of the 1st layer. The shear box shall be designed to accept 50mm square samples and made of anodised aluminium.

6.3. Loading Frame – A loading fame capable of pushing the layer interface in such a way that the 1st layer move relative to the 2nd layer. Force shall be measured in the plane of the layer interface.

6.4. Normal Force- This shall normally be applied by a pneumatically controlled actuator which can apply a constant normal pressure to the sample throughout the test. The actuator shall apply the force to the sample centrally through an anodised aluminium loading plate in a spherical seating.

6.5. Saw – a water cooled machine for sawing the test specimen to the required shape and size for the shear box, without excessive shock.

7. Test Specimens

7.1. Size- Testing shall be performed on 50mm square and nominally 100mm high test specimens, with the layer interface located within the central section of the height of the specimen. Test specimens shall be taken in the field or extracted from larger field cores or blocks.

7.2. Field cores- Extract minimum 150mm diameter cores or 150mm wide slabs from the pavement, marking the direction of the paving and profiling.

7.3. Cutting- The test specimens are to be trimmed from the existing field cores or cut directly from the pavement using saw. The faces of the specimen shall be aligned so one face is parallel to the direction of the paving and the other is perpendicular (see Fig 1). The specimen shall be adequately supported to ensure that the resulting test specimen is square with sides that are smooth, parallel and free from ridges and groves.

7.4. End Preparation- the ends of the test specimen shall be smooth and perpendicular to the axis of the specimen by sawing with a single or double bladed saw. Where the layer interface of the sawn specimen will be within 25mm of the surface, to avoid end effects the specimen shall be capped prior to sawing with polyester resin based filler.

7.5. Sample storage- Wrap samples in polyethylene and store in environmentally controlled storage area at temperatures between 5-25^{o}C.

8. Procedure

8.1. Using Vernier callipers measure the width of the sides and height of the specimen to the nearest 0.1mm.

8.2. Ensure the shear box is clean and apply a silicone or water based lubricant to inside faces of the shear box.

8.3. Locate the specimen in the shear box ensuring shearing will occur in the direction of traffic loading in the field.

8.4. Assemble the two halves of the shear box and locate the specimen in the shear box so the layer interface is centrally located between the two halves, separated by a 3mm spacing then locate the loading plate for the normal load.

8.5. After the time required for the sample to reach test temperature, see following, apply the normal load.

8.5.1. 25^{o}C 0.25hrs

8.5.2. 30^{o}C 0.5hrs

8.5.3. 40^{o}C 0.75hrs

8.5.4. 50°C 1.0hrs

8.6. Apply the shearing load at a rate of 50mm/min, continue to apply the load until the specimen fails and results in excessive deformation.

8.7. At regular intervals throughout the test record the applied load, normal pressure, and axial deflection. The recording shall be frequent enough to clearly define the peak force on the sample.

8.8. Repeat the shearing on 3 other replicate samples at different normal pressures.

9. Calculations

9.1. Convert the axial deformation to shear strain by dividing by the specimen length (50mm)

9.2. Calculate the Normal stress $\sigma_n = \frac{N \times 1000}{A}$ where, N is the normal force in Newtons, A is the cross sectional area of the sample in mm^2.

9.3. Calculate the Shear stress $= \frac{F \times 1000}{A'}$, F is the shear force in Newtons and A' is the corrected cross sectional area $A' = L(L - \delta)$, where L is the length of the inner side of the specimen, δ is the shear displacement (mm).

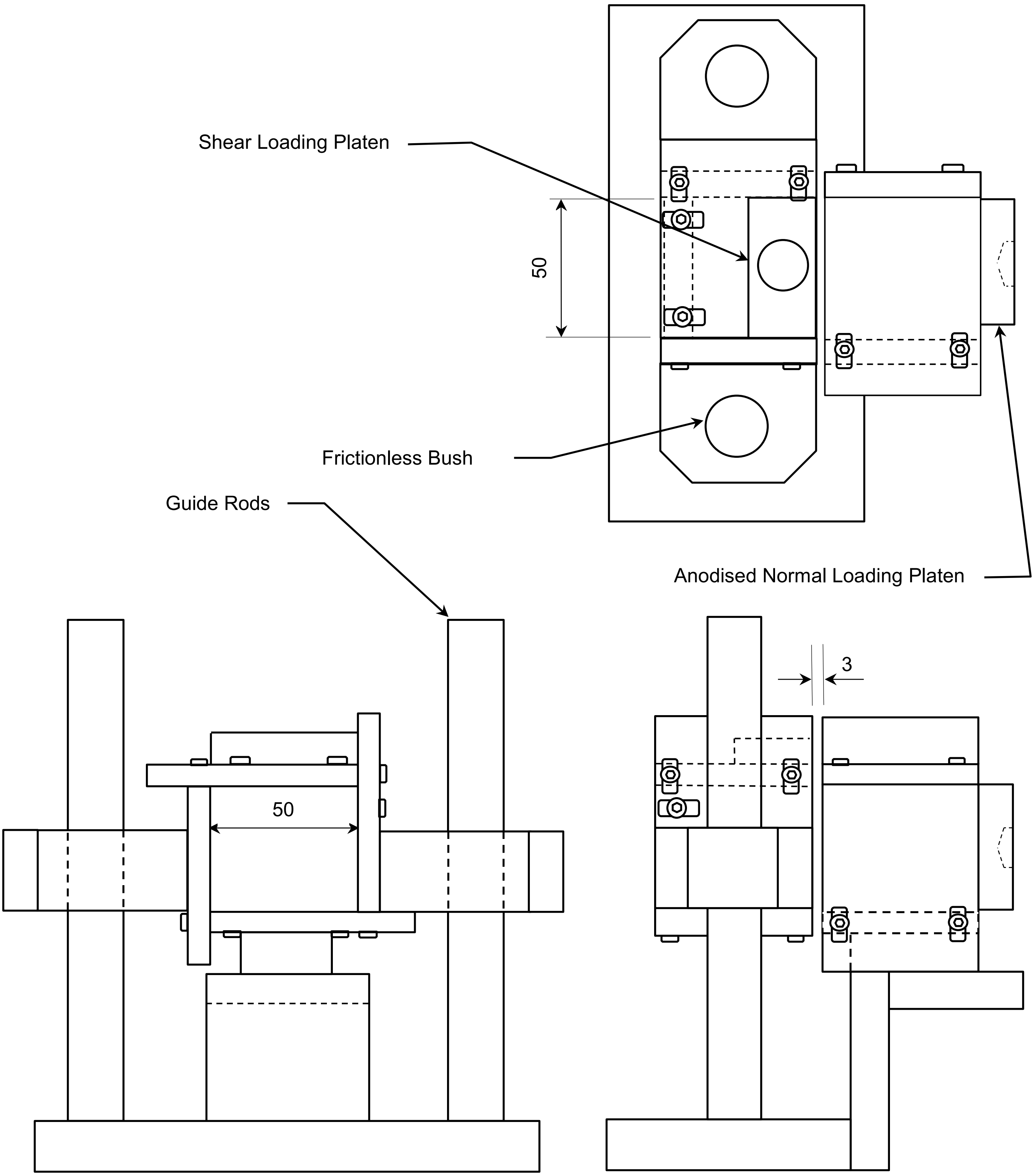

Figure 1 Test Specimen Setup

APPENDIX 3. SHEAR STRESS CALCULATIONS

Calculated Shear and Normal Stresses

Location	Depth (mm)	Shear Stress (kPa)	Normal Stress (kPa)
Extreme Braking Aircraft			
Centre of Tyre	5	408	1,348
	25	295	1,299
	45	195	1,197
Inside Leading Edge	5	522	712
	25	854	733
	45	883	674
In front of Leading Edge	5	205	-8
	25	721	312
	45	826	430
Landing on RWY 16			
Centre of Tyre	5	275	1,348
	25	199	1,299
	45	131	1,197
Inside Leading Edge	5	456	678
	25	797	692
	45	838	638
In front of Leading Edge	5	181	-9
	25	667	284
	45	780	400
Landing on RWY 34			
Centre of Tyre	5	110	275
	25	79	199
	45	52	131
Inside Leading Edge	5	374	456
	25	727	797
	45	782	838
In front of Leading Edge	5	151	181
	25	601	667
	45	723	780

Location	Depth (mm)	Shear Stress (kPa)	Normal Stress (kPa)
Non Braking Aircraft			
Centre of Tyre	5	<1	1,347
	25	<1	1,299
	45	<1	1,197
Inside Leading Edge	5	320	609
	25	680	605
	45	744	564
In front of Leading Edge	5	131	13
	25	557	226
	45	685	337
Heavy Braking Truck			
Centre of Tyre	5	361	848
	25	932	811
	45	442	723
Inside Leading Edge	5	394	810
	25	475	608
	45	421	483
In front of Leading Edge	5	355	248
	25	476	406
	45	423	378

Calculated Octahedral Shear and Octahedral Normal Stresses

Location	Depth (mm)	OSS (kPa)	ONS (kPa)
Extreme Braking Aircraft			
Centre of Tyre	5	1,233	3,026
	25	714	2,249
	45	265	1,498
Inside Leading Edge	5	1,187	2,261
	25	956	1,628
	45	813	1,122
In front of Leading Edge	5	1,114	1,537
	25	967	1,353
	45	826	1,006
Landing on RWY 16			
Centre of Tyre	5	1,208	3,026
	25	691	2,249
	45	238	1,498
Inside Leading Edge	5	1,047	2,059
	25	874	1,506
	45	755	1,038
In front of Leading Edge	5	998	1,385
	25	879	1,238
	45	760	925
Landing on RWY 34			
Centre of Tyre	5	1,190	3,026
	25	675	2,249
	45	217	1,498
Inside Leading Edge	5	888	1,811
	25	779	1,354
	45	687	935
In front of Leading Edge	5	868	1,198
	25	776	1,097
	45	684	824

Location	Depth (mm)	OSS (kPa)	ONS (kPa)
Non Braking Aircraft			
Centre of Tyre	5	1,187	3,026
	25	672	2,249
	45	212	1,498
Inside Leading Edge	5	795	1,645
	25	721	1,253
	45	645	866
In front of Leading Edge	5	793	1,074
	25	713	1,003
	45	636	757
Heavy Braking Truck			
Centre of Tyre	5	422	1,276
	25	194	892
	45	165	536
Inside Leading Edge	5	516	1,343
	25	427	792
	45	364	475
In front of Leading Edge	5	629	972
	25	465	689
	45	376	439

Calculated Asphalt Mixture Octahedral Shear Strength and Stress to Strength Ratios

Location	Depth (mm)	Asphalt Mixture Shear Strength (kPa)	Octahedral Shear Stress/Strength (%)
Extreme Braking Aircraft			
Centre of Tyre	5	2,702	46
	25	2,103	34
	45	1,523	17
Inside Leading Edge	5	2,111	56
	25	1,624	59
	45	1,233	66
In front of Leading Edge	5	1,553	72
	25	1,411	69
	45	1,144	72
Landing on RWY 16			
Centre of Tyre	5	2,702	45
	25	2,103	33
	45	1,523	16
Inside Leading Edge	5	1,956	54
	25	1,529	57
	45	1,168	65
In front of Leading Edge	5	1,436	70
	25	1,323	66
	45	1,081	70
Landing on RWY 34			
Centre of Tyre	5	2,702	44
	25	2,103	32
	45	1,523	14
Inside Leading Edge	5	1,764	50
	25	1,412	55
	45	1,089	63
In front of Leading Edge	5	1,292	67
	25	1,214	64
	45	1,003	68

Location	Depth (mm)	Asphalt Mixture Shear Strength (kPa)	Octahedral Shear Stress/Strength (%)
Non Braking Aircraft			
Centre of Tyre	5	2,702	44
	25	2,103	32
	45	1,523	14
Inside Leading Edge	5	1,636	49
	25	1,334	54
	45	1,036	62
In front of Leading Edge	5	1,196	66
	25	1,141	63
	45	952	67
Heavy Braking Truck			
Centre of Tyre	5	1,351	31
	25	1,056	18
	45	781	21
Inside Leading Edge	5	1,404	37
	25	978	44
	45	734	50
In front of Leading Edge	5	1,118	56
	25	899	52
	45	706	53

APPENDIX 4. INTERFACE SHEAR TEST RESULTS

Direct Shear Results

Code	Normal Stress (kPa)	ISS (kPa)	ISM (kPa/mm)	ISW (kN.m)
MPH_1	859	1,196	141	22.4
	544	860	203	16.4
	253	646	111	10.6
	119	363	81	6.9
	22	359	79	6
MPH_2	266	691	133	12.5
	562	864	140	17
	673	998	174	20.4
	121	359	110	5.3
	22	333	90	5.4
MPH_3	695	906	172	20.8
	22	422	144	5
	268	715	147	14
	553	613	145	9.7
	121	476	158	8.1
MPH_4	715	1,114	226	23.7
	564	721	164	14.1
	270	784	170	15.7
	123	681	164	12.1
	23	406	140	7.4
MUM_1	700	736	129	16.1
	544	780	103	14.1
	253	580	171	11.4
	117	469	175	5.8
	22	462	131	4.9
MUL_1	706	634	189	13.9
	571	490	126	9.3
	270	453	135	8.2
	119	368	131	4.9
	22	300	104	4.3

Code	Normal Stress (kPa)	ISS (kPa)	ISM (kPa/mm)	ISW (kN.m)
TUL_1	575	478	129	9.5
	721	531	90	12.1
	274	355	82	6.1
	120	461	171	8.1
	23	214	48	3.3
TUH_1	723	951	216	18.8
	560	643	166	14.2
	269	471	155	9.7
	124	495	114	8.7
	23	270	94	5.6
TPH_1	723	856	161	18.3
	562	826	177	16.7
	284	642	133	13.7
	114	588	96	9.6
	23	463	108	9.2
BUL_1	696	835	159	15.5
	574	734	204	14.8
	283	363	100	9.1
	119	288	98	6.2
	22	233	96	6.1

Inclined Repeated Interface Shear Results

MPH_1			MPH_2		
Cycles	Strain	Rate	Cycles	Strain	Rate
5	4,798	960	5	2,723	545
10	9,109	862	10	4,042	264
17	12,084	425	17	5,219	168
25	14,577	312	25	6,195	122
35	17,076	250	35	7,140	95
50	20,174	207	50	8,232	73
75	24,856	187	75	9,583	54
115	33,540	217	115	11,199	40
170	40,793	132	170	12,925	31
250	47,746	87	250	14,914	25
450	65,750	90	450	18,760	19
575	73,323	61	575	20,957	18
870	83,209	34	870	25,627	16
1,300	93,385	24	1,300	31,879	15
1,965	106,313	18	2,000	40,775	13
			3,000	51,048	10
			4,500	70,000	13
			6,500	88,172	9
			10,000	98,707	3
			11,178	101,526	2

MPH_3			MPH_4		
Cycles	**Strain**	**Rate**	**Cycles**	**Strain**	**Rate**
5	3,355	839	5	2,755	689
10	5,007	330	10	4,068	263
17	6,428	203	17	5,261	170
25	7,591	145	25	6,266	126
35	8,695	110	35	7,253	99
50	10,005	87	50	8,427	78
75	11,708	68	75	9,939	60
115	13,776	52	115	11,784	46
170	15,958	40	170	13,766	36
250	18,491	32	250	16,070	29
450	23,344	24	450	20,587	23
575	25,849	20	575	22,779	18
870	31,043	18	870	26,781	14
1,300	37,399	15	1,300	30,873	10
2,000	45,664	12	2,000	35,280	6
3,000	54,593	9	3,000	39,654	4
4,500	64,197	6	4,500	44,219	3
6,500	73,315	5	6,500	48,512	2
10,000	83,314	3	10,000	53,916	2
19,072	100,001	2	20,000	64,120	1

MPH_5			**MPH_6**		
Cycles	**Strain**	**Rate**	**Cycles**	**Strain**	**Rate**
5	3,015	754	5	5,239	1,310
10	4,228	243	10	9,158	784
17	5,343	159	17	13,099	563
25	6,296	119	25	16,643	443
35	7,215	92	35	20,282	364
50	8,288	72	50	24,722	296
75	9,670	55	75	30,777	242
115	11,334	42	115	38,568	195
170	13,323	36	170	47,079	155
250	15,789	31	250	56,559	119
450	20,387	23	450	72,579	80
575	22,678	18	575	79,727	57
870	26,899	14	870	91,377	39
1,300	31,336	10	1,143	100,019	32
2,000	38,641	10			
3,000	46,637	8			
4,500	55,590	6			
6,500	66,056	5			
10,000	78,697	4			
19,410	100,000	2			

MPH_7			MUL_1		
Cycles	**Strain**	**Rate**	**Cycles**	**Strain**	**Rate**
5	6,425	1,606	5	3,768	754
10	10,953	906	10	5,873	421
17	15,243	613	17	7,799	275
25	18,965	465	25	9,462	208
35	22,649	368	35	11,150	169
50	27,027	292	50	13,204	137
75	32,989	238	75	15,889	107
115	40,875	197	115	19,150	82
170	49,772	162	170	22,082	53
250	61,219	143	250	25,259	40
450	86,851	128	450	31,269	30
566	100,093	114	575	34,508	26
			870	41,231	23
			1,300	49,769	20
			2,000	60,536	15
			3,000	72,327	12
			4,500	85,226	9
			6,500	94,692	5
			9,193	100,000	2

MPL_1			MPL_2		
Cycles	**Strain**	**Rate**	**Cycles**	**Strain**	**Rate**
5	3,466	867	5	3,154	789
10	5,729	453	10	5,281	425
15	7,349	324	17	7,403	303
25	9,757	241	25	9,292	236
35	11,582	183	35	11,232	194
50	13,763	145	50	13,648	161
75	16,596	113	75	16,887	130
115	19,973	84	115	21,054	104
170	23,493	64	170	25,857	87
250	27,472	50	250	31,651	72
450	48,594	106	575	48,901	53
516	103,997	839	870	59,322	35
			1,300	70,432	26
			2,000	82,683	18
			3,000	94,261	12
			3,688	100,001	8

MUM_1			TPH_1		
Cycles	Strain	Rate	Cycles	Strain	Rate
5	4,355	871	5	7,644	1,911
10	6,713	472	10	12,243	920
17	8,823	301	17	16,513	610
25	10,577	219	25	20,262	469
35	12,232	166	35	24,079	382
50	14,223	133	50	28,692	308
75	16,853	105	75	34,915	249
115	20,074	81	115	43,040	203
170	23,481	62	170	52,071	164
250	27,375	49	250	62,834	135
450	34,436	35	450	81,782	95
575	37,720	26	575	89,107	59
870	44,056	21	822	100,029	44
1,300	51,138	16			
2,000	59,298	12			
3,000	66,300	7			
4,500	74,528	5			
5,302	100,016	32			

TPH_2			TPH_3		
Cycles	**Strain**	**Rate**	**Cycles**	**Strain**	**Rate**
5	7,239	1,810	5	7,352	1,838
10	11,630	878	10	10,612	652
17	15,551	560	17	13,136	361
25	18,843	412	25	15,088	244
35	22,110	327	35	16,868	178
50	25,969	257	50	18,912	136
75	30,964	200	75	21,594	107
115	37,125	154	115	25,314	93
170	43,971	124	170	29,972	85
250	52,766	110	250	37,153	90
450	71,501	94	450	62,714	128
575	82,158	85	541	101,089	422
835	100,022	69			

TPH_4			TPH_5		
Cycles	Strain	Rate	Cycles	Strain	Rate
5	8,138	2,035	5	5,426	1,357
10	12,146	802	10	8,266	568
17	15,397	464	17	10,755	356
25	17,995	325	25	12,774	252
35	20,499	250	35	14,706	193
50	23,503	200	50	16,946	149
75	27,505	160	75	19,748	112
115	32,759	131	115	23,043	82
170	39,429	121	170	26,425	61
250	50,424	137	250	30,100	46
382	10,1600	388	450	36,200	31
			575	38,808	21
			870	43,348	15
			1,300	47,907	11
			2,000	52,885	7
			3,000	57,656	5
			4,500	63,617	4
			6,500	68,595	2
			10,000	74,296	2
			20,000	82,582	1

TPL_1			TPL_2		
Cycles	**Strain**	**Rate**	**Cycles**	**Strain**	**Rate**
5	5,556	1,389	5	4,651	5
10	8,675	624	10	7,431	10
17	11,295	374	17	9,944	17
25	13,402	263	25	12,106	25
35	15,383	198	35	14,270	35
50	17,636	150	50	16,944	50
75	20,403	111	75	20,513	75
115	23,586	80	115	25,282	115
170	26,738	57	170	31,233	170
250	30,019	41	250	40,863	250
450	35,609	28	397	101,224	450
575	38,215	21			
870	43,041	16			
1,300	48,531	13			
2,000	55,387	10			
3,000	62,853	7			
4,500	72,145	6			
6,500	83,889	6			
10,000	99,431	4			
10,145	100,001	4			

TUL_1			TUH_1		
Cycles	**Strain**	**Rate**	**Cycles**	**Strain**	**Rate**
5	5,570	1,393	5	4,065	1,016
10	8,675	621	10	6,463	480
17	11,449	396	17	8,678	316
25	13,775	291	25	10,570	237
35	16,120	235	35	12,405	184
50	19,077	197	50	14,618	148
75	23,294	169	75	17,625	120
115	30,029	168	115	21,463	96
170	40,399	189	170	25,839	80
250	57,858	218	250	31,453	70
444	100,062	218	450	44,376	65
			575	51,643	58
			870	61,907	35
			1,300	70,896	21
			2,000	81,888	16
			3,000	93,069	11
			3,702	100,006	10

BUL_1			BUL_2		
Cycles	**Strain**	**Rate**	**Cycles**	**Strain**	**Rate**
5	6,249	1,562	5	6,631	1,658
10	9,313	613	10	9,876	649
17	12,823	390	17	12,742	409
25	14,481	345	25	15,167	303
35	17,011	253	35	17,642	248
50	20,347	222	50	20,874	215
75	25,523	207	75	25,640	191
115	34,614	227	115	33,075	186
170	52,496	325	170	46,572	245
225	95,884	789	225	86,913	733

APPENDIX 5. MASTIC & BINDER TEST RESULTS

Binder point of release specification testing in 2011

Release Date	Vis. Post-RTFO	Vis. Pre-RTFO	Pen. post-RTFO	Pen. pre-RTFO	Vis. 135°C
Feedstock 1					
13 Dec	4,740	1,085	31	46	1.138
31 Jan	5,860	1,057	32	48	1.106
09 Feb	4,077	987	31	45	1.036
11 Mar	4,673	1,082	35	41	1.046
16 Mar	4,076	1,054	28	44	1.084
07 Apr	5,228	1,128	32	44	1.191
11 Apr	5,673	1,202	38	45	1.158
Feedstock 2					
27 Apr	4,875	1,158	28	44	1.136
28 Apr	6,311	1,225	32	49	1.204
04 May	5,182	1,220	36	48	1.112
17 May	4,328	1,133	33	52	1.114
19 May	6,221	1,260	35	48	1.199
26 May	6,274	1,229	36	47	1.17
10 May	6,388	1,249	38	46	1.211

Pre- and Post-RTFO viscosity testing performed at 60°C. Pre- and Post-RTFO penetration testing performed at 25°C.

Mastic MSCR Results at 64°C

Sample	Binder	Dust	AR(0.1)	AR(3.2)	%AR	Jnr(0.1)	Jnr(3.2)	%Jnr
Feedstock 1								
1T	28 Jan	T	65	35	46	0.012	0.018	45
1M	28 Jan	M	69	34	44	0.012	0.015	28
2T	02 Feb	T	65	36	44	0.009	0.013	65
2M	02 Feb	M	66	37	44	0.012	0.017	66
3T	10 Mar	T	65	49	31	0.009	0.012	29
3M	10 Mar	M	61	49	30	0.006	0.007	9
Feedstock 2								
4T	26 May	T	70	41	37	0.009	0.013	49
4M	26 May	M	71	40	41	0.007	0.011	67
5T	21 Jun	T	72	35	46	0.012	0.018	45
5M	21 Jun	M	70	34	44	0.012	0.015	28
6T	23 Jun	T	66	47	33	0.007	0.008	14
6M	23 Jun	M	68	41	42	0.007	0.011	74

Mastic MSCR testing results at 70°C

Sample	Binder	Dust	AR(0.1)	AR(3.2)	%AR	Jnr(0.1)	Jnr(3.2)	%Jnr
Feedstock 1								
1T	28 Jan	T	61	27	55	0.027	0.031	18
1M	28 Jan	M	63	29	54	0.019	0.022	19
2T	02 Feb	T	60	27	54	0.027	0.031	16
2M	02 Feb	M	60	29	53	0.020	0.022	12
3T	10 Mar	T	57	27	52	0.030	0.033	10
3M	10 Mar	M	56	26	54	0.026	0.027	4
Feedstock 2								
4T	26 May	T	63	36	44	0.018	0.019	11
4M	26 May	M	58	32	44	0.020	0.019	2
5T	21 Jun	T	66	35	46	0.020	0.026	28
5M	21 Jun	M	68	38	44	0.011	0.014	19
6T	23 Jun	T	60	32	46	0.020	0.023	19
6M	23 Jun	M	59	31	49	0.017	0.019	15

Mastic MSCR testing results at 76°C

Sample	Binder	Dust	AR(0.1)	AR(3.2)	%AR	Jnr(0.1)	Jnr(3.2)	%Jnr
Feedstock 1								
1T	28 Jan	T	57	19	66	0.047	0.062	32
1M	28 Jan	M	58	21	63	0.035	0.041	17
2T	02 Feb	T	56	19	66	0.048	0.063	31
2M	02 Feb	M	59	21	64	0.030	0.039	29
3T	10 Mar	T	53	19	64	0.050	0.067	32
3M	10 Mar	M	51	19	63	0.047	0.052	10
Feedstock 2								
4T	26 May	T	59	25	58	0.033	0.043	29
4M	26 May	M	55	23	58	0.032	0.037	13
5T	21 Jun	T	61	27	56	0.039	0.050	28
5M	21 Jun	M	62	28	55	0.022	0.026	18
6T	23 Jun	T	56	23	58	0.037	0.047	26
6M	23 Jun	M	54	22	59	0.031	0.036	17

Binder re-heating assessment testing and statistics

Re-heating Cycles	Pre-RTFO Viscosity at 60°C		Post-RTFO Viscosity at 60°C	
	Mean	SD	Mean	SD
0	1,222	N/A	5,462	N/A
1	1,220	32	5,457	239
2	1,302	31	5,381	178
3	1,260	39	5,357	62
p-value (1 versus 2)	0.03		0.68	
p-value (2 versus 3)	0.22		0.84	
p-value (3 versus 1)	0.24		0.52	

Three tests were performed on the same sub-sample and the mean reported after each heating cycle.

Binder specification re-testing in 2014

Sample Date	Vis. post-RTFO	Vis. pre-RTFO	Pen. post-RTFO	Pen. pre-RTFO	Vis. 135°C
Feedstock 1					
28 Jan	7,033	898	26	50	1.03
02 Feb	8,300	1,394	26	41	1.33
10 Mar	7,385	1,464	24	37	1.26
Feedstock 2					
26 May	10,759	1,911	27	43	1.54
21 Jun	14,037	2,187	26	42	1.67
23 Jun	11,931	2,010	27	40	1.51

Pre- and Post-RTFO viscosity testing performed at 60°C. Pre- and Post-RTFO penetration testing performed at 25°C.

Binder post-RTFO viscosity at 60°C re-testing

Sample Date	Feedstock	2013	2015
28 Jan	1	5,338	8,807
02 Feb	1	6,199	8,884
10 Mar	1	4,664	8,470
12 Mar	1	4,472	6,046
17 Mar	1	5,204	9,153
19 Mar	1	5,608	10,751
15 May	2	6,428	15,606
17 May	2	6,284	14,279
17 May	2	6,653	18,256
19 May	2	7,786	15,305
24 May	2	5,738	14,885
26 May	2	6,327	14,382
21 Jun	1	7,903	17,828
23 Jun	1	6,465	16,104

Binder MSCR testing results at 64°C

Sample	FS	AR(0.1)	AR(3.2)	%AR	Jnr(0.1)	Jnr(3.2)	%Jnr
28 Jan	1	45.8	28.0	39	0.17	0.22	30
02 Feb	1	46.5	29.0	38	0.16	0.21	30
10 Mar	1	42.2	24.2	43	0.21	0.28	31
12 Mar	1	43.7	27.1	38	0.19	0.24	30
17 Mar	1	47.9	31.2	35	0.15	0.20	29
19 Mar	1	47.1	29.1	38	0.17	0.22	32
15 May	2	54.9	34.5	37	0.13	0.19	41
17 May	2	54.9	35.2	36	0.13	0.18	39
17 May	2	55.2	34.7	37	0.13	0.19	41
19 May	2	52.8	31.8	40	0.15	0.21	40
24 May	2	57.2	42.3	26	0.09	0.12	30
26 May	2	52.3	33.3	36	0.14	0.20	37
21 Jun	2	60.9	46.8	23	0.08	0.10	30
23 Jun	2	49.0	33.4	32	0.14	0.18	28

Binder MSCR testing results at 70°C

Sample	FS	AR(0.1)	AR(3.2)	%AR	Jnr(0.1)	Jnr(3.2)	%Jnr
28 Jan	1	39.6	14.4	64	0.38	0.56	47
02 Feb	1	40.4	15.3	62	0.36	0.53	47
10 Mar	1	35.3	11.4	68	0.49	0.72	45
12 Mar	1	37.3	14.1	62	0.43	0.63	45
17 Mar	1	42.3	17.1	59	0.34	0.50	48
19 Mar	1	40.7	15.1	63	0.38	0.57	49
15 May	2	49.5	19.0	62	0.30	0.49	65
17 May	2	49.5	19.4	61	0.29	0.48	65
17 May	2	49.8	19.1	62	0.29	0.49	67
19 May	2	47.5	17.2	64	0.33	0.55	64
24 May	2	52.0	26.8	48	0.20	0.32	54
26 May	2	46.6	18.6	60	0.32	0.50	58
21 Jun	2	56.1	31.5	44	0.17	0.26	55
23 Jun	2	42.7	18.9	56	0.31	0.45	46

Binder MSCR testing results at 76°C

Sample	FS	AR(0.1)	AR(3.2)	%AR	Jnr(0.1)	Jnr(3.2)	%Jnr
28 Jan	1	33.0	5.6	83	0.86	1.38	61
02 Feb	1	33.8	6.1	82	0.81	1.30	61
10 Mar	1	27.9	4.0	86	1.13	1.74	54
12 Mar	1	30.4	5.6	82	0.98	1.52	55
17 Mar	1	35.1	6.8	81	0.77	1.25	62
19 Mar	1	33.4	5.7	83	0.87	1.42	62
15 May	2	42.6	7.7	82	0.66	1.23	86
17 May	2	42.7	7.8	82	0.65	1.21	86
17 May	2	42.9	7.6	82	0.66	1.24	89
19 May	2	43.4	7.6	82	0.65	1.25	93
24 May	2	44.8	12.1	73	0.47	0.83	77
26 May	2	39.5	7.6	81	0.71	1.24	75
21 Jun	2	49.5	15.5	69	0.37	0.68	82
23 Jun	2	35.3	7.7	78	0.71	1.14	60

Independent (2015) Binder MSCR and Post-RTFO Viscosity

Sample	Vis. post-RTFO	AR(0.1)	AR(3.2)	Jnr(0.1)	Jnr(3.2)
MSCR at 70°C					
Independent_1	10,369	19.9	0.49	19.4	0.48
Independent_2	6,001	15.0	0.72	9.4	0.69
Independent_3	12,952	22.8	0.39	25.3	0.36
MSCR at 76°C					
Independent_1	10,369	8.0	1.23	8.4	1.20
Independent_2	6,001	5.5	1.76	2.7	1.68
Independent_3	12,952	10.1	0.99	11.7	0.91

Post-RTFO viscosity testing performed at 60°C.

REFERENCES

Abd El Halim, AO 2007, *Design, Development, and Validation of an Advanced In-Situ Shear Stiffness Test Facility for Asphalt Concrete Pavements*, Final Report for Highway IDEA Project 55, Transportation Research Board, December.

Abo-Qudais, S & Al-Shweily, H 2007a, 'Effect of aggregate properties on asphalt mixtures stripping and creep behaviour', *Construction and Building Materials*, no. 21, pp. 1887-1898.

Abo-Qudais, S & Al-Shweily, H 2007b, 'Effect of antistripping additives on environmental damage of bituminous mixtures', *Building and Environment*, no. 42, pp. 2929-2938.

Abraham, H 1962, *Asphalts and Allied Products: Their occurrence, Modes of Production, uses in the Arts and Methods of Testing: Volume Three: Manufactured Products*, 6th edn, D Van Nostrand Company, New York City, USA.

Airbus 2014, Toulouse, France, viewed 27 January 2014, <http://www.airbus.com/support/maintenance-engineering/technical-data/aircraft-characteristics/>.

Airey, GD 2003, 'State of the art report on ageing test methods for bituminous pavement materials', *International Journal of Pavement Engineering*, vol. 4, no. 3, pp. 165-176.

Ali Shafabakhsh, G & Akbari, A 2013, 'Numerical study of airplane wheel characteristics on the runway rigid pavement failure', *Journal of Scientific & Industrial Research*, vol. 72, pp. 348-357.

Al-Qadi, IL, Yoo, PJ, Elseifi, MA & Nelson, S 2009, 'Creep behaviour of hot-mix asphalt due to heavy vehicular tire loading', *Journal of Engineering Mechanics*, vol. 135, no. 11, pp. 1265-1273.

Al-Qadi, IL & Wang, H 2011, 'Prediction of tire pavement contact stress and analysis of asphalt pavement response: a decoupled approach', *Proceedings Asphalt Pavement Technology*, Tampa, Florida, USA, 27-30 March, Association of Asphalt Paving Technologists, pp. 289-315.

Al-Qadi, IL, Wang, H & Tutumluer, E 2010, 'Dynamic analysis of thin asphalt pavements by using cross-anisotropic stress-dependent properties for granular layers', *Journal of the Transportation Research Board*, no. 2154, pp. 153-163.

Amaral, PM, Cruz Fernandes, J & Guerra Rosa, L 2006, 'A comparison between x-ray diffraction and petrography techniques used to determine the mineralogical composition of granite and comparable hard rocks', *Materials Science Forum*, vols. 514-516, pp. 1628-1632.

Ameri-Gaznon, M & Little, DN 1990, 'Octahedral shear stress analysis of an ACP overlay on a rigid base', *Journal of Association of Asphalt Paving Technologists*, vol. 59, pp. 443-479.

Anochie-Boateng, J & Maina, J 2012, 'Permanent deformation testing for a new South African mechanistic pavement design method', *Construction and Building Materials*, vol. 26, pp. 541-546.

Austroads 2007, *Polyphosphoric Acid Modification of Binders*, Report AP-T87/07, Austroads, October.

Austroads 2010, *Laboratory study on Relationship between Binder Properties and Asphalt Rutting*, Report AP-T164/10, Austroads, August.

Austroads 2012, *Segregation and Degradation in Commercial SBS Binders*, Report AP-T204-12, Austroads, June.

Austroads 2013, *Effects of Polymer Segregation in Polymer Modified Binders on Field Performance*, Report AP-T254-13, Austroads, October.

Austroads 2014, *Effects of Hot Storage on Polymer Modified Binder Properties and Field Performance*, Report AP-T271-14, Austroads, September.

Bae, A, Mohammad, LN, Elseifi, MA, Button, J & Patel, N 2010, 'Effects of temperature on interface shear strength of emulsified tack coat and its relationship to rheological properties', *Transport Research Record: Journal of the Transportation Research Board*, no. 2180, pp. 102-109.

Bandyopadhyaya, R, Das, A & Basu, S 2008, 'Numerical simulation of mechanical behaviour of asphalt mix', *Construction and Building Materials*, vol. 22, pp. 1051-1058.

Baumgardner, G & D'Angelo, JA 2012, 'Evaluation of new dynamic shear rheometer testing geometry for performance testing of crumb rubber-modified binder', *Transport Research Record: Journal of the Transportation Research Board*, no. 2293, pp. 73-79.

Baumgardner, G, Masson, J-F, Hardee, JR, Menapace, AM & Williams, AG 2005, 'Polyphosphoric acid modified asphalt: proposed mechanisms', *Journal of Association of Asphalt Paving Technologists*, vol. 74, pp. 283-305.

Bayan, FP, Cornetto, AD, Dunn, A & Sauer, E 2010 'Brake timing measurements for a tractor-semitrailer under emergency braking', *SAE International Journal of Commercial Vehicles*, vol. 2, no. 2, pp. 245-255.

Bekheet, W, Adb El Halim, AO & Easa, S 2007, 'In-situ shear stiffness of asphalt concrete mixtures', *Proceedings Advanced Characterisation of Pavement and Soil Engineering Materials*, Athens, Greece, 20-22 June, Taylor and Francis, pp. 853-863.

Bessa, IS, Castelo Branco, VTF & Soares, JB 2012, 'Evaluation of different digital image processing software for aggregates and hot mix asphalt characterizations', *Construction and Building Materials*, vol. 37, pp. 370-378.

Bhasin, A & Little, DN 2007, 'Methods to quantify interfacial adhesion and debonding in bitumen-aggregate system in dry and wet conditions', *Proceedings Advanced Characterisation of Pavement and Soil Engineering Materials*, Athens, Greece, 20-22 June, Taylor and Francis, pp. 689-699.

Bianchetto, H, Miró, R, Pérez-Jiménez, F & Martínez, AH 2007, 'Effect of calcareous fillers on bituminous mix aging', *Transport Research Record: Journal of the Transportation Research Board*, no. 1998, pp. 140-148.

Boeing 2013, Seattle, Washington, USA, viewed 27 January 2014, <http://www.boeing.com/boeing/commercial/airports/plan_manuals.page>.

Bognacki, CJ, Frisvold, A & Bennert, T 2007, 'Investigation into asphalt pavement slippage failures on Runway 04R-22L Newark International Airport', *Proceedings 2007 FAA Worldwide Airport Technology Transfer Conference*, Galloway, New Jersey, USA, 16-18 April, Federal Aviation Administration.

BP Bitumen 2007, *Bitumen Basics*, viewed 11 December 2014, <http://www.bp.com/content/dam/bp-country/en_au/products-services/bp-bitumen/all-pages/Bitumen-basics.pdf>.

Brigatti, MF, Galan, E & Theng, BKG 2013, 'Structural mineralogy of clay minerals' in F Bergaya & G Lagaly (eds.), *Developments in Clay Science*, vol. 5.

Brindley, GW 1952, 'Structural mineralogy of clays', *Clays and Clay Materials*, vol. 1, pp. 33-43.

Bryant, P 2005, 'Filler: is it fixing your binder', *Proceedings AAPA Pavements Industry Conference*, Surfers Paradise, Queensland, Australia, 18-21 September, Australian Asphalt Pavements Association.

Buchanan, MS & Woods, ME 2004, *Field Tack Coat Evaluator (ATACKer)*, Final Report, Report No. FHWA/MS-DOT-RD-04-168, Mississippi Transportation Research Centre, December.

Buonsanti, M & Leonardi, G 2012, 'A finite element model to evaluate airport flexible pavement response under impact', *Journal of Applied Mechanics and Materials*, vols. 138-139, pp. 257-262.

Button, FW & Epps, JA 1985, 'Identifying tender asphalt mixtures in the laboratory', *Transport Research Record: Journal of the Transportation Research Board*, vol. 1034, pp. 20-26.

Canestrari, F, Cardone, F, Graziani, A, Santagata, FA & Bahia, HU 2010, 'Adhesive and cohesive properties of asphalt-aggregate systems subjected to moisture damage', *Road Materials and Pavement Design*, vol. 11, pp. 11-32.

Canestrari, F, Ferrotti, G, Partl, MN & Santagata, E 2005, 'Advanced testing and characterization of interlayer shear resistance', *Transport Research Record: Journal of the Transportation Research Board*, no. 1929, pp. 69-78.

Canestrari, F & Santagata, E 2005 'Temperature effect on the shear behaviour of tack coat emulsions used in flexible pavements', *International Journal of Pavement Engineering*, vol. 6, no. 1, pp. 39-46.

Celaya, M & Nazarian, S 2014, 'Field evaluation of NDT devices for delamination detection of HMA airport pavements', *Proceedings FAA Worldwide Airport Technology Transfer Conference*, Galloway, New Jersey, USA, 5-7 August, Federal Aviation Administration.

Chen, J-S, Wong, SY & Lin, KY 2005a, 'Quantification of movement of flat and elongated particles in hot mix asphalt subject to wheel load test', *Materials and Structures*, vol. 38, no. 277, pp. 395-402.

Chen, J-S, Chang, MK & Lin, KY 2005b, 'Influence of coarse aggregate shape on the strength of asphalt concrete mixtures', *Journal of the Eastern Asia Society for Transportation Studies*, vol. 6, pp. 1062-1075.

Chen, J-S & Huang, C-C 2010, 'Effect of surface characteristics on bonding properties of bituminous tack coats', *Transport Research Record: Journal of the Transportation Research Board*, no. 2180, pp. 142-149.

Clopotel, CS & Bahia, HU 2012, 'Importance of elastic recovery in the DSR for binders and mastics', *Engineering Journal*, vol. 16, no. 4, pp. 99-106.

Coenen, AR, Kutay, EM, Sefidmazgi, NM & Bahia, HU 2012, 'Aggregate structure characterisation of asphalt mixtures using two-dimensional image analysis, *Road Materials and Pavement Design*, vol. 13, no. 3, pp. 433-454.

Collop, AC, Sutanto, MH, Airey, GD & Elliott, RC 2009, 'Shear bond strength between asphalt layers for laboratory prepared samples and field cores', *Construction and Building Materials*, no. 23, pp. 2251-2258.

Collop, AC, Thom, NH & Sangiorgi, C 2003, 'Assessment of bond condition using the Leutner shear test', *Proceedings of the Institution of Civil Engineers: Transport 156*, no. TR4, pp. 211-217.

Crawford, C 1986, *Tender Mixes*, Report QIP 108, National Asphalt Pavement Association, Maryland, USA.

Curray, JR 1956, 'The analysis of two-dimensional orientation data', *The Journal of Geology*, vol. 64, no. 2, pp. 117-131.

D'Andrea, A, Russo, S & Tozzo, C 2013a, 'Interlayer shear testing under combined stress conditions', *Advanced Materials Research*, vol. 723, pp. 381-388.

D'Andrea, A, Tozzo, C, Boschetto A & Bottini, L 2013b, 'Interface roughness parameters and shear strength', *Modern Applied Science*, vol. 7, no. 10, pp. 1-10.

D'Angelo, JA 2009a, 'Current status of Superpave binder specification', *Roads Materials and Pavement Design*, vol. 10, suppl. 1, pp. 13-24.

D'Angelo, JA 2009b, 'The relationship of the MSCR test to rutting', *Road Materials and Pavement Design*, vol. 10, suppl. 1, pp. 61-80.

D'Angelo, J, Kluttz, R, Dongré, R, Stephens, K & Zanzotto, L 2007, 'Revision of the Superpave high temperature binder specification: the multiple stress creep recovery test', *Proceedings Asphalt Paving Technology*, San Antonio, Texas, USA, 11-14 March, Association of Asphalt Paving Technologists, vol. 76, pp. 123-162.

D'Angelo, J & Dongré, R 2009, 'Practical use of multiple stress creep and recovery test', *Transport Research Record: Journal of the Transportation Research Board*, no. 2126, pp. 73-82.

Dai, Q & You, Z 2007, 'Prediction of creep stiffness of asphalt mixture with micromechanical finite-element and discrete element models', *Journal of Engineering Mechanics*, vol. 133, no. 2, pp. 163-173.

De Beer, M, Fisher, C, Jooste, FJ 2002, 'Evaluation of non-uniform tyre contact stresses on thin asphalt pavements', *9th International Conference on Asphalt Pavements*, Copenhagen, Denmark, 17-22 August, International Society of Asphalt Pavements.

De Beer, M, Fisher, C & Jooste, FJ 1997, 'Determination of pneumatic tyre/pavement interface contract stresses under moving load and some effects on pavements with thin asphalt surfacing layers', *8th International Conference on Asphalt Pavements*, Seattle, Washington, USA, 10-14 August, vol. 1, pp. 179-227, International Society of Asphalt Pavements.

De Beer, M, Maina, JW, van Rensburg, Y & Greben, JM 2011, 'Towards using tire-road contact in pavement design and analysis', *September 2011 Meeting of the Tire Society*, Pretoria, South Africa.

Delaporte, B, Di Benedetto, H, Chaverot, P & Gauthier, G 2007, ‘Filler and binder influence on the linear viscoelastic behavior of mastics’, *Proceedings Advanced Characterisation of Pavement and Soil Engineering Materials*, Athens, Greece, 20-22 June, Taylor and Francis, pp. 3-13.

Delgadillo, R, Bahia, HU & Lakes, R 2012, ‘A nonlinear constitutive relationship for asphalt binder’, *Materials and Structures*, no. 45, pp. 457-473.

Denneman, E 2007, ‘The application of locally developed pavement temperature prediction algorithms in Performance Grade (PG) binder selection’, *Proceedings 26th Southern African Transport Conference*, Pretoria, South Africa, 9-13 July, pp. 257-266.

Diakhate, M, Millien, A, Petit, C, Phelipot-Mardele, A & Pouteau, B 2011, ‘Experimental investigation of tack coat fatigue performance: towards an improved lifetime assessment of pavement structure interfaces’, *Construction and Building Materials*, no. 25, pp. 3-13.

Diakhate, M, Petit, C, Millien, A, Phelipot-Mardele, A ,Pouteau, B & Goacolou, H 2007, ‘Comparison of direct shear and torque tests for determing viscoelastic shear behavior of tack coats’, *Proceedings Advanced Characterisation of Pavement and Soil Engineering Materials*, Athens, Greece, 20-22 June, Taylor and Francis, pp. 281-290.

Diakhate, M, Petit, C, Millien, A, Phelipot-Mardele, A ,Pouteau, B & Goacolou, H 2008, ‘Interface fatigue cracking in multilayerd pavements: experimental analysis’, *Proceedings Sixth RILEM International Conference on Cracking in Pavements*, Chicago, Illinois, USA, 16-19 June, Taylor and Francis, pp. 649-659.

Diakhate, M, Phelipot, A, Millien, A & Petit, C 2006, ‘Shear fatigue behaviour of tack coats’, *Road Materials and Pavement Design*, vol. 7, no. 2, pp. 201-222.

DoC 1978, *Repair and Maintenance of Slippage Cracking of Bituminous Aerodrome Pavements*, Department of Construction, Commonwealth of Australia, April.

Domingos, MDI & Faxina, AL 2015, ‘Rheological behaviour of bitumens modified with PE and PPA at different MSCR creep-recovery times’, *International Journal of Pavement Engineering*, vol. 16, no. 9, pp. 771-783.

Drescher, A, Kringos, N & Scarpas, T 2010, ‘On the behaviour of a parallel elasto-visco-plastic model for asphaltic materials’, *Mechanics of Materials*, vol. 42, pp. 109-117.

DuBois, E, Mehta, Y & Nolan, A 2014 ‘Correlation between MSCR results and polymer modification of binder’, *Construction and Building Materials*, vol. 65, pp. 184-190.

Eames, J 1998, *Reshaping Australia's Aviation Landscape: The Federal Airports Corporation 1986-1998*, Focus Publishing, Sydney, Australia.

EAPA 2003, *Airfield use of Asphalt*, European Asphalt Pavement Association, May, viewed 25 November 2013, <http://www.eapa.org/usr_img/position_paper/airfield.pdf>.

Eggleton, RA & Tilley DB 1998, 'Hisingerite: a ferric Kaolin mineral with curved morphology', *Clays and Clay Minerals*, vol. 46, no. 4, pp. 400-413.

Elnasri, M, Airey, G & Thom, N 2013, 'Experimental investigation of bitumen mastics under shear creep and creep-recovery testing', *Proceedings T&DI Airfield and Highway Pavement Speciality Conference*, Los Angeles, California, USA, 9-12 June, American Society of Civil Engineers, pp. 921-932.

Emery, S 2005a, 'Asphalt on Australian airports', *Proceedings AAPA Pavements Industry Conference*, Surfers Paradise, Queensland, Australia, 18-21 September, Australian Asphalt Pavements Association.

Emery, S 2005b, 'Bituminous surfacings for pavement on Australian airports', *Proceedings Australian Airports Association Convention*, Hobart, Tasmania, Australia, 14-17 November, Australian Airports Association.

Emery, S & Mihaljevic, I 2008, 'Accelerated load testing of asphalt mix design for heavy duty pavements in hot climates', *Proceedings 23rd ARRB Conference*, Adelaide, South Australia, Australia, 22-23 July, ARRB Transport Research.

Epps, AL, Ahmed, T, Little, DC & Hugo, F 2001, *Performance prediction with the MMLS3 at Westrack*, Report 2134-1, Texas Transportation Institute, Austin, USA, May.

EU 2000, *AMADEUS: Advanced Models for Analytical Design of European Pavement Structure*, Report RO-97-SC.2137, European Commission, 29 March.

FAA 1998, *Development of Advanced Computational Models for Airport Pavement Design*, Report DOT/FAAAR-97/47, Federal Aviation Administration, Washington, District of Columbia, USA, August.

Fabre, C 2011 'The Airbus high tyre pressure test', *Flight Airworthiness Support Technology*, no. 48, pp. 2-9, Airbus Industries.

Fabre, C, Balay, J, Lerat, P & Mazars, A 2009, 'Full-scale aircraft tire pressure test', *Proceedings Eight International Conference on the Bearing Capacity of Roads, Railways and Airfields*, Urbana-Champaign, Illinois, USA, 29 June – 2 July, pp. 1405-1413.

Faheem, AF & Bahia, HU 2010, 'Modelling of asphalt mastic in terms of filler-bitumen interaction', *Road Materials and Pavement Design*, vol. 11, pp. 281-303.

Faheem, AF, Bahia, HU, Yang, S-H & Al-Qadi, I 2010, 'Evaluation of Rigden fractional voids test method and the relation to mastic viscosity', *Proceedings Asphalt Paving Technology Conference*, Sacramento, California, USA, 7-10 March, Association of Asphalt Paving Technologists, vol. 79, pp. 1-25.

Farcas, FA 2012, *Evaluation of asphalt field cores with simple performance tester and x-ray computer tomography*, Licentiate Thesis submitted to the Royal Institute of Technology, Stockholm, Sweden.

Fee, D, Maldonado, R, Reinke, G & Romagosa, H 2010, 'Polyphosphoric acid modification of asphalt', *Transport Research Record: Journal of the Transportation Research Board*, no. 2179, pp. 49-57.

FHA 2011, *The Multiple Stress Creep Recovery (MSCR) Procedure*, Technical Brief FHWA-HIF-11-038, Federal Highways Administration, USA April, viewed 8 February 2015, <http://www.fhwa.dot.gov/pavement/materials/pubs/hif11038/hif11038.pdf>.

FHA 2013, *Asphalt Mixture Performance Tester (AMPT)*, Technical Brief FHWA-HIF-13-005, Federal Highway Administration, USA, February.

Gabrawy, T 2000, 'Towards laboratory replication of field compaction: asphalt shear box compactor', *Proceedings World of Asphalt Pavements International Conference*, Sydney, New South Wales, Australia, 22-25 February, Australian Asphalt Pavements Association.

Goodman, SN 2000, *Design Development and Validation of the In-situ Shear Stiffness Test (InSiSST) Facility for Asphalt Concrete*, A Thesis submitted to the Faculty of Graduate Studies and Research in partial fulfillment of the requirements for the degree of Master of Engineering, Carleton University, Ottawa, Canada, September.

Goodman, S, Bekheet, W, Hassan, Y & Adb El Halim, AO 2002, 'Rapid in-situ shear testing of asphalt pavements for runway construction quality control and assurance', *Proceedings 2002 FAA Airport Technology Transfer Conference*, Galloway, New Jersey, USA, May.

Hachiya, Y & Sato, K 1997, 'Effect of tack coat in bonding characteristics at interface between asphalt concrete layers', *Proceedings Eight International Conference on Asphalt Pavements*, Seattle, Washington, USA, 10-14 August, vol. 1, pp. 349-362, International Society of Asphalt Pavements.

Hafeez, I & Kamal, MA, 2014, 'Creep compliance: a parameter to predict rut performance of asphalt binders and mixtures', *Arabian Journal for Science and Engineering*, vol. 39, pp. 5971-5978.

Hafeez, I, Mian, I, Zaidi, B, Kamal, MA, Ahmed, N, Ullah, S, Hussain, J, Riaz, K & Hussain, S 2013, 'To study the viscoelastic behavior of asphalt binders using under multiple stress creep recovery test', *Life Sciences Journal*, vol. 10, no. 12s, pp. 921-925.

Hakimzadeh, S, Kebedem NA, Buttlar, WG, Ahmed, S & Exline, M 2012, 'Development of fracture energy based Interface bond test for asphalt concrete', *Road Materials and Pavement Design*, vol. 13, suppl. 1, 87th Association of Asphalt Pavement Technologists, 1-4 April, Taylor and Francis.

Hamzah, MO, Von, WC & Abdullah, NH 2013, 'Effects of compactor types on aggregate orientation in asphalt mixtures', *International Journal of Engineering Transactions A: Basics*, vol. 26, no. 7, pp. 677-684.

Harnsberger, PM, Farrar, MJ, Huang, S-C & Robertson, RE 2011, 'Comparative field performance using multiple crude oil sources', *Proceedings Transport Research Board Annual Meeting*, Washington, USA, 23-27 January.

Hassan, NA, Airey, GD, Khan, R & Collop, AC 2012, 'Nondestructive characterisation of the effect of asphalt mixture compaction on aggregate orientation and segregation using x-ray computed tomography', *International Journal of Pavement Research and Technology*, vol. 5, no. 2, pp. 84-92.

Hefer, AW, Little, DN & Labib, ME 2007, 'Advances using surface chemistry relations to quantify bitumen-aggregate stripping', *Proceedings Advanced Characterisation of Pavement and Soil Engineering Materials*, Athens, Greece, 20-22 June, Taylor and Francis, pp. 1607-1619.

Hernandez, JA & Al-Qadi, IL 2014, 'Airfield pavement response due to heavy aircraft takeoff: advanced modeling comparing single-tire and dual-tandem gear', *Proceedings FAA Worldwide Airport Technology Transfer Conference*, Galloway, New Jersey, USA, 5-7 August, Federal Aviation Administration.

Holleran, G & Holleran, I 2010, 'Bitumen chemistry using cheaper sources – an improved method of measurement by TLC-FID and the characterisation of bitumen by rheology and compositional means', *Proceedings 24th ARRB Conference*, Melbourne, Victoria, Australia, 12-15 October, ARRB Transport Research.

Holleran, G & Holleran, I 2012, 'Bitumen processing, rheology, composition and performance', *Proceedings 25th ARRB Conference*, Perth, Western Australia, Australia, 23-26 September, ARRB Transport Research.

Holleran, G, Holleran I, Vercoe, J, D'Angelo, A, Bearsley, S, Stevens, A & Towler, J 2014, 'Bitumen in New Zealand – performance based asphalt binder specification', *Proceedings NZTA/NZIHT 15th Annual Conference*, Queenstown, New Zealand, 2-4 November, New Zealand Transit Authority.

Holleran, G, McCaffrey, L & Wilson, D 2008, 'The effect of particle shape and angularity on SMA mix characterisation', *Proceedings 23rd ARRB Conference*, Adelaide, South Australia, Australia, 22-23 July, ARRB Transport Research.

Holtz, RD & Kovacs, WD 1981, *An introduction to Geotechnical Engineering*, Prentice-Hall, New Jersey, USA.

Horak, E, Emery, S, Maina, J & Walker, B 2009a, 'Mechanistic modelling of potential interlayer slip at base and sub-base level', *Proceedings Eighth International Conference on the Bearing Capacity of Roads, Railways and Airfields*, Urbana-Champaign, Illinois, USA, 29 June - 2 July, pp. 543-550.

Horak, E, Maina, J & Emery, S 2009b, 'A case study: quantification and modeling of asphalt overlay delamination on an airport pavement', *Proceedings Eight International Conference on the Bearing Capacity of Roads, Railways and Airfields*, Urbana-Champaign, Illinois, USA, 29 June - 2 July, pp. 1475-1483.

Horak, E, Emery, S & Mihaljevic, I 2011, 'Balancing asphalt rut resistance with durability and safety requirements on runway rehabilitations', *Proceedings Airfield Pavements Seminar, XXIVth World Road Congress*, Mexico City, Mexico, 28-29 September.

Howson, J, Masad, E, Little, D & Kassem, E 2012 'Relationship between bond energy and total work of fracture for asphalt binder-aggregate systems', *Road Materials and Pavement Design*, vol. 13, no. 1, pp. 281-303.

Hu, X & Walubita, M 2011, 'Effects of layer interfacial bonding conditions on the mechanistic responses in asphalt pavements', *Journal of Transportation Engineering*, vol. 137, no. 1, pp. 28-36.

Huang, YH 1993, *Pavement Analysis and Design*, Prentice-Hall, New Jersey, USA.

Hugo, F, Bowler, I, Liebenberg, J & Rossman, D 2011, 'Evaluation of performance of asphalt paving mixes under harsh conditions using the MMLS3', *Proceedings 10th Conference on Asphalt Pavements for Southern Africa*, Natal, South Africa, 11-14 September.

Hugo, F, de Witt, R & Helmich, A 2004, 'Application of MMLS3 as APT tool for evaluating asphalt performance on a highway in Namibia', *Proceedings 8th Conference on Asphalt Pavement for Southern Africa*, Sun City, South Africa, 12-16 September.

Hunter, AE, Airey, GD & Collop, AC 2004, 'Aggregate orientation and segregation in laboratory-compacted asphalt samples', *Transport Research Record: Journal of the Transportation Research Board*, no. 1891, pp. 8-15.

Ibrahim, A, Faisal, S & Jamil, N 2009, 'Use of Basalt in asphalt concrete mixes', *Construction and Building Materials*, no. 23, pp. 498-506.

Kaloush, KE 2001, *Simple Performance Test for Permanent Deformation of Asphalt Mixtures*, A Dissertation presented in Partial Fulfilment of the Requirements for the Degree of Doctor of Philosophy, Arizona State University, Tempe, Arizona, USA, May.

Kandhal, PS, Motter, JB & Khatri, MA 1991, *Evaluation of Particle Shape and Texture: Manufactured versus Natural Sands*, NCAT Report 91-03, National Centre for Asphalt Technology, Auburn, Alabama, USA, January.

Kandhl, PS, Khatri, MA & Motter, JB 1992, '*Evaluation of Particle Shape and Texture of Mineral Aggregates and their blends'*, NCAT Report 92-4, National Centre for Asphalt Technology, Auburn, Alabama, USA, May.

Kim, M, Tutumluer, E & Kwon, J 2009, 'Nonlinear pavement foundation modeling for three-dimensional finite-element analysis of flexible pavements', *International Journal of Geomechanics*, vol. 9, no. 5, pp. 195-208.

Kondo, T, Moriyoshi, A, Yoshida, T & Takahashi, S 2003, 'Movement characteristics of aggregate in asphalt mixtures during the wheel tracking test', *Journal of the Japan Petroleum Institute*, vol. 46, no. 3, pp. 172-180.

Kruger, J & Horak, E 2005, 'The appropriateness of accelerated pavement testing to assess the rut prediction capability of laboratory asphalt tests', *Proceedings 24th Southern African Transport Conference*, Pretoria, South Africa, 11-13 July.

Kruntcheva, MR, Collop, AC & Thom, NH 2006, 'Effect of bond condition on flexible pavement performance', *Journal of Materials in Civil Engineering*, vol. 18, no. 3, pp. 467-471.

Kruntcheva, MR, Collop, AC & Thom, NH 2005, 'Properties of asphalt concrete layer interfaces', *Journal of Transportation Engineering*, vol. 131, no. 11, pp. 880-888.

Kutay, ME, Arambula, E, Gibson, N & Youtcheff, J 2010, 'Three-dimensional image processing methods to identify and characterise aggregates in compacted asphalt mixtures', *International Journal of Pavement Engineering*, vol. 11, no. 6, pp. 511-528.

Labib, ME, Hefer, AW & Little, DN 2007, 'Surface-chemistry at the bitumen-aggregate interface', *Proceedings Advanced Characterisation of Pavement and Soil Engineering Materials*, Athens, Greece, 20-22 June, Taylor and Francis, pp. 1589-1599.

Lawson, J & Erjavec, J 2001, *Modern Statistics for Engineering and Quality Improvement*, Duxbury, California, USA.

Lesueur, D, Petit, J & Ritter, H-J 2013, 'The mechanics of hydrated lime modification of asphalt mixtures: a state of the art review', *Road Materials and Pavement Design*, vol. 14, no. 1, pp. 1-16.

Li, X, Nan, X & Wei, D 2012, 'High temperature rheology property of asphalt mastic with different mineral filler', *Advanced Materials Research*, vols. 450-451, pp. 527-531.

Li, X, Clyne, T, Reinke, G, Johnson, EN, Gibson, N & Kutay, ME 2011, 'Laboratory evaluation of asphalt binders and mixtures containing polyphosphoric acid', *Transport Research Record: Journal of the Transportation Research Board*, no. 2210, pp. 47-56.

Liao, M-C, Airey, G & Chen J-S 2013, 'Mechanical properties of filler-asphalt mastics', *International Journal of Pavement Research and Technology*, vol. 6, no. 5, pp. 576-581.

Little, DN & Epps, JA 2001, *The Benefits of Hydrated Lime in Hot Mix Asphalt*, National Lime Association.

Little, DN & Petersen, JC 2005, 'Unique effects of hydrated lime filler on the performance-related properties of asphalt cement: physical and chemical interactions revisited', *Journal of Materials in Civil Engineering*, vol. 17, no. 2, pp. 207-218.

Loizos, A & Charonitis, G 2004, 'Bearing capacity and structural classification of flexible airport pavements', *Journal of Transportation Engineering*, vol. 130, no. 1, pp. 34-42.

Lv, Y-J, Zhang, I & Zhou, X-L 2011, 'Microstructure index of hot mix asphalt', *Proceedings Road Materials and New Innovations in Pavement Engineering*, Hunan, China, 9-11 June, American Society of Civil Engineers, pp. 9-16.

Lysenko, J 1991, 'T230 plate stripping test and methylene blue value as a guide to asphalt stripping', *Proceedings AAPA Regional Lime in Asphalt Seminar*, Sydney, Australia, Australian Asphalt Pavements Association.

Lysenko, JE 2006, 'Development of shear testing of a bond coat emulsion', *Proceedings CME Congress,* Lyon, France.

Lysenko, JE 2009, 'An effective bond coat for longer pavement life', *Proceedings AAPA Pavements Industry Conference*, Gold Coast, Queensland, Australia, 16-18 September, Australian Asphalt Pavements Association.

Maina, JW, Denneman, E & De Beer, M 2008, 'Introduction of new road pavement response modelling software by means of benchmarking', *Proceedings 27th Annual South African Transportation Conference*, Pretoria, South Africa, 7-11 July.

Maina, JW & Matsui, K 2004, 'Development of software for elastic analysis of pavement structure due to vertical and horizontal surface loadings', *Proceedings 83rd Meeting of the Transport Research Board*, Washington, DC, USA, 11-15 January, Transport Research Board.

Maina, JW, Ozawa, Y & Matsui, K 2012, 'Linear elastic analysis of pavement structure under non-circular loading', *Road Materials and Pavement Design*, vol. 13, no. 3, pp 403-421.

Masad, E & Button, JW 2000, 'Unified imaging approach for measuring aggregate angularity and texture', *Computer-Aided Civil and Infrastructure Engineering*, vol. 15, pp. 273-280.

Masad, E, Huang, C-W, D'Angelo, J & Little, D 2009, 'Characterisation of asphalt binder resistance to permanent deformation based on nonlinear viscoelastic analysis of multiple stress creep recovery (MSCR) test', *Proceedings Asphalt Pavement Technology*, Minneapolis, Minnesota, USA, 15-18 March, Association of Asphalt Pavement Technologists, vol. 78, pp. 535-562.

Masad, E, Muhunthan, B, Shashidhar, N & Harman, T 1998, 'Aggregate orientation and segregation in asphalt concrete', *Proceedings Application of Geotechnical Principles in Pavement Engineering*, Geotechnical Special Publication Number 85, pp. 69-81.

Masad, E, Muhunthan, B, Shashidhar, N & Harman, T 1999a, 'Internal structure characterisation of asphalt concrete using image analysis', *Journal of Computing in Civil Engineering*, vol. 13, no. 2, pp. 88-95.

Masad, E, Mahunthan, B, Shashidhar, N & Harman, T 1999b, 'Quantifying laboratory compaction effects on the internal structure of asphalt concrete', *Transport Research Record: Journal of the Transportation Research Board*, no. 1691, pp. 179-185.

Medeiros, MS, Chehab, GR & Solaimanian, M 2012, 'Investigation of ultra-rapid setting emulsion for tack coat application', *Transport Research Record: Journal of the Transportation Research Board*, no. 2293, pp. 80-88.

Mehrara, A & Khodaii, A 2013, 'A review of the state of the art on the stripping phenomenon in asphalt concrete', *Construction and Building Materials*, vol. 38, pp. 423-442.

Mejia, D, Celaya, M, Iyer, S, Rao, C, Shokouhi, P & Nazarian, S 2008, *A Work Plan toward Evaluation of Technologies to Assess Presence and Extent of Delamination of HMA Airfield Pavements*, Research Project 06-04, Centre of Transportation Infrastructure Systems, El Paso, USA, June.

Miknis, FP & Schuster, WC 2009, 'NMR study of hydrated lime and limestone in polyphosphoric acid modified bitumen', *Road Materials and Pavement Design*, vol. 10, no. 4, pp. 815-831.

Minitab 2010, *Meet Minitab 16*, User Guide, Minitab, USA.

Mohammad, LN, Bae, A, Elseifi, MA, Button, J & Patel, N 2010, 'Effects of pavement surface type and sample preparation method on tack coat interface shear strength', *Transport Research Record: Journal of the Transportation Research Board*, no. 2180, pp. 93-101.

Mohammad, LN, Bae, A, Elseifi, MA, Button, J & Scherocman, JA 2009, 'Interface shear strength characterisation of emulsified tack coats', *Proceedings Asphalt Pavement Technology*, Minneapolis, Minnesota, USA, 15-18 March, Association of Asphalt Pavement Technologists, vol. 78, pp. 250-277.

Mohammad, LN, Hassan, M & Patel, N 2011, 'Effects of shear bond characteristics of tack coats on pavement performance at the interface', *Transport Research Record: Journal of the Transportation Research Board*, no. 2209, pp. 1-8.

Mohammad, LN, Rabiq, MA & Huang, B 2002a, 'Influence of asphalt tack coat materials on interface shear strength', *Transport Research Record: Journal of the Transportation Research Board*, no. 1789, pp. 56-65.

Mohammad, LN, Rabiq, MA, Wu, Z & Huang, B 2002b, 'Measurement of interlayer bond strength through direct shear tests', *Proceedings 3rd International Conference Bituminous Mixtures and Pavements*, Thessaloniki, Greece, 21-22 November.

Molenaar, P, Hugo, F, Buekes, J & Catin, G 2004, 'Rehabilitation of RWY 03L-21R at Johannesburg international airport: selection of asphalt mixes using MMLS3 testing', *Proceedings 8th Conference on Asphalt Pavement for Southern Africa*, Sun City, South Africa, 12-16 September.

Monismith, CL, Harvey, JT, Long F & Weismann, S 2000a, *Tests to Evaluate the Stiffness and Permanent Deformation characteristics of Asphalt/Binder-Aggregate systems*, Technical Memorandum TM-UCB PRC-2000-1, University of California, June.

Monismith, CL, Vallerga, BA, Harvey, JT, Long, F & Jew, A 2000b, 'Asphalt mix studies – San Francisco International Airport', *Proceedings of the 26th Air Transportation Conference*, San Francisco, California, USA, 19-21 June, American Society of Civil Engineers, pp. 113-124.

Mooren, F, Stet, M & Hopman, P 2014, 'Tire induced surface cracking due to extreme wheel loads', *Proceedings FAA Worldwide Airport Technology Transfer Conference*, Galloway, New Jersey, USA, 5-7 August, Federal Aviation Administration.

Moraes, R, Velaquez, R & Bahia, H 2011, 'Measuring effort of moisture of asphalt-aggregate bond with the bitumen bond strength test', *Proceedings Transport Research Board Annual Meeting*, Washington, DC, USA, 23-27 January.

Motamed, A & Bahia, HU 2011, 'Influence of test geometry, temperature, stress level and loading duration on binder properties measured using DSR', *Journal of Materials in Civil Engineering*, vol. 23, pp. 1422-1432.

Mrawira, D & Damude, DJ 1999, 'Revisiting the effectiveness of tack coats in HMA overlays: the shear strength of tack coats in young overlays', *Proceedings of the 44th Annual Conference of the Canadian Technical Asphalt Association*, Quebec, New Brunswick, Canada, 14-17 November, pp. 115-129, Polyscience Publications.

Muench, ST & Moomaw, T 2008, *De-Bonding of Hot Mix Asphalt Pavement in Washington State: An Initial Investigation*, Technical Report TNW 2008-10, Transportation Northwest, Seatle, Washington, USA, November.

Muraya, PM, Molenaar, AAA & van de Ven, MFC 2009, 'Contribution of asphalt mix components to permanent deformation resistance', *Proceedings Eight International Conference on the Bearing Capacity of Roads, Railways and Airfields*, Urbana-Champaign, Illinois, USA, 29 June - 2 July, pp. 259-268.

Neaylon, K 2013, 'Bitumen supply and testing', *Proceedings International Public Works Conference*, Darwin, Northern Territory, Australia, 11-15 August, Institute of Public Works Engineering Australasia.

Nosler, I & Beckedahl, H 2000, 'Adhesion between aggregate and bitumen – performance testing of compacted asphalt specimens by mean of the dynamic indirect tensile test', *Proceedings 2nd Eurasphalt and Eurobitume Congress*, Barcelona, Spain, 20-22 September, European Asphalt Pavement Association.

Oeser, M, Pellinen, T, Scarpas, T & Kasberger, C 2008, 'Studies on creep and recovery of rheological bodies based upon conventional and formulations and their application on asphalt mixture', *International Journal of Pavement Engineering*, vol. 9, no. 5, pp. 373-386.

Oliver, JWH 2009, 'Changes in chemical composition of Australian bitumens', *Road Materials and Pavement Design*, vol. 10, no. 3, pp. 569-586.

Pallant, J 2005, *SPSS Survival Manual: a step by step guide to data analysis using SPDD for Windows (Version 12)*, 2nd edn, Allen and Unwin, Sydney, Australia.

Park, S-W & Kim, YR 2001, 'Fitting Prony-series viscoelastic models with power-law presmoothing', *Journal of Materials in Civil Engineering*, vol. 13, no. 1, pp. 26-32.

Park, S-W & Lytton, RL 2004, 'Effects of stress-dependent modulus and Poisson's ratio on structural responses in thin asphalt pavements', *Journal of Transportation Engineering*, vol. 130, no. 3, pp. 387-394.

Partl, MN, Canestrari, F, Grilli, A & Gubler, R 2008, 'Characterization of water sensitivity of asphalt mixtures with coaxial shear test', *Road Materials and Pavement Design*, vol. 8, no. 2, pp. 247-270.

Pasindu, HR, Fwa, TF & Ong, GP 2011, 'Computation of aircraft braking distances', *Transport Research Record: Journal of the Transportation Research Board*, no. 2214, pp 126-135.

Pavement Interactives 2011, *Laboratory Wheel Tracking Devices*, 1 July, viewed 21 November 2014, <http://www.pavementinteractive.org/article /laboratory-wheel-tracking-devices/>.

Perdomo, D & Button, JW 1991, *Identifying and Correcting Rut-Susceptible Asphalt Mixtures*, Research Report FHWA/TX-91/1121-2F, Federal Highways Administration, February.

Pérez-Jiménez, FP, Miró Recasens, R & Martínez, A 2008, 'Effect of the nature and filler content on the behavior of the bituminous mastics', *Road Materials and Pavement Design*, vol. 9, pp. 417-431.

Petit, C, Millien, A, Canestrari, F, Pannunzio, V & Virgili, A 2012, 'Experimental study on shear fatigue behaviour and stiffness performance of warm mix asphalt by adding synthetic wax', *Construction and Building Materials*, no. 34, pp. 537-544.

Ping, L, Lieping, W, Wei, L & Baolin, X 2013, 'The research on the index of high temperature performance of asphalt mixture in airfield', *Advanced Materials Research*, vol. 723, pp. 1076-1083.

Qiu, H, Tan, X, Shu, S & Zhang, H 2013, 'Influence of filler-bitumen ratio on performance of modified asphalt mortar by additive', *Journal of Modern Transportation*, vol. 21, no. 1, pp. 40-46.

Raab, C & Partl, MN 2004, 'Interlayer shear performance: experience with different pavement structures, Proceedings 3rd Eurasphalt & Eurobitume Congress, Vienna, Austria, 12-14 May, vol. 1, pp. 535-545.

Raab, C, Partl, MN & Abd El Halim, AO 2010, 'Effect of gap width on interlayer shear bond results', *International Journal of Pavement Research and Technology*, vol. 3, no. 2, pp. 79-85.

Ramsey, FL & Schafer, DW 2002, *The Statistical Sleuth: A course in Methods of Data Analysis*, 2nd edn, Duxbury, California, USA.

Reyes, M & Zanzotto, L 2007, 'Analysis of superpave gyratory specimens internal structure', *Proceedings CSCE 2007 Annual General Meeting and Conference*, Yellowknife, Northwest Territories, Canada, 6-9 June, Canadian Society of Civil Engineers, pp. 641-647.

Riaz, K, Hafeez, I, Khitab, A, Hussain, M, Ali, F, Ashiq, SZ, Tariq, MK & Ahmed, I 2013, 'Comparison of neat and modified asphalt binders using rheological parameters under virgin, RTFO and PAV aged conditions', *Life Science Journal*, vol. 10. pp. 2041-2047.

Rickards, I & Gabrawry, T 2003, 'Fatigue testing of asphalt to improve the discrimination of moisture sensitivity in aggregate and bitumen systems', *Proceedings 21st ARRB Conference*, Cairns, Queensland, Australia, 19-22 May, Australian Road Research Board, pp. 243-255.

Rodway, B 2009, 'Asphalt deformation due to high tyre pressure', *FAA Airport Pavement Working Group Annual Meeting*, Atlantic City, New Jersey, USA, 21-23 July, Federal Aviation Administration.

Rodway, B, Wardle, LJ & Wickham G 1999, 'Interaction between wheels and wheel groups of new large aircraft', *Proceedings Airport Technology Transfer Conference*, Galloway, New Jersey, USA, April, Federal Aviation Administration.

Roginski, MJ 2007, 'Effects of aircraft tire pressures on flexible pavements', *Proceedings Advanced Characterisation of Pavement and Soil Engineering Materials*, Athens, Greece, 20-22 June, Taylor and Francis, pp. 1473-1481.

Roginski, MJ 2013, 'ICAO update – status of high tyre pressure revision to Annex 14', presented to the FAA Working Group Meeting, Atlantic City, New Jersey, USA 15-17 April, Federal Aviation Administration.

Romanoschi, SA & Metcalf, JB 2002, 'The characterization of pavement layer interfaces', *Proceedings 9th International Conference on Asphalt Pavements: Healing and Bonding session*, Copenhagen, Denmark, 17-22 August, International Society for Asphalt Pavements.

Sangiorgi, C, Collop, AC & Thom, NH 2002, 'Laboratory assessment of bond condition using the Leutner shear test', *Proceedings 3rd International conference Bituminous Mixtures and Pavements*, Thessaloniki, Greece, 21-22 November.

Santagata, E, Baglieri, O, Alam, M & Dalmazzo, D 2015, 'A novel procedure for the evaluation of anti-rutting potential of asphalt binders', *International Journal of Pavement Engineering*, vol. 16, no. 4, pp. 287-296.

Santagata, E, Baglieri, O, Dalmazzo, D & Tsantilis, L 2013, 'Evaluation of the anti-rutting potential of polymer-modified binders by means of creep-recovery shear tests', *Materials and Structures*, vol. 46, pp. 1673-1682.

Santagata, FA, Ferrotti, G, Partl, MN & Canestrari, F 2009, 'Statistical investigation of two different interlayer shear test methods', *Materials and Structures*, vol. 42, pp. 705-714.

Santagata, FA, Partl, MN, Ferrotti, G, Canestrari, F & Flisch, A 2008, 'Layer characteristics affecting Interlayer Shear Resistance in Flexible Pavements', *Proceedings Asphalt Pavement Technology*, Minneapolis, Minnesota, USA, 15-18 March, no. 77, Association of Asphalt Pavement Technologists, pp. 221-256.

Sangsefidi, E, Ziari, H & Mansourkhaki, A 2014, 'The effect of aggregate gradation on creep and moisture susceptibility performance of warm mix asphalt', *International Journal of Pavement Engineering*, vol. 15, no. 2, pp. 133-141.

Scarpas, A, Al-Khoury, R, van Gurp, CAPM & Erkens, SMJG 1997, 'Finite element simulation of damage development in asphalt concrete pavements', *Proceedings 8th International Conference on Asphalt Pavements*, Seattle, Washington, USA, 10-14 August, International Society of Asphalt Pavements, pp. 673-692.

Sefidmazgi, NR, Tashman, L & Bahia, H 2012, 'Internal structure characterization of asphalt, mixtures for rutting performance using imaging analysis', *Road Materials and Pavement Design*, vol. 13, suppl. 1, pp. 13-27.

Shayan, A 1984, 'Hisingerite material from a Basalt quarry near Geelong, Victoria, Australia', *Clays and Clay Minerals*, vol. 32, no. 4, pp. 272-278.

Shayan, A, Vickers, JV & Lancucki, CJ 1998, 'Hydrothermal alternations of Hisingerite material from a Basalt quarry near Geelong, Victoria, Australia, *Clays and Clay Minerals*, vol. 36, no. 4, pp. 327-336.

Shell 2013, *Multigrade Binders*, viewed 11 December 2013, <http://www.shell.com.au/products-services/solutions-for-businesses/bitumen/products/binders/multigrade.html>.

Shell Bitumen 2015, *The Shell Bitumen Handbook*, 6th edn, ICE Publishing, Italy.

Shen, S & Yu, H 2011, 'Characterize packing of aggregate particles for paving materials: particle size impact', *Construction and Building Materials*, vol. 25, pp. 1362-1368.

Shirodkar, P, Mehta, Y, Nolan, A, Dahm, K, Dusseau, R & McCarthy, L 2012, 'Characterization of creep and recovery curve of polymer modified binder', *Construction and Building Materials*, vol. 34, pp. 504-511.

Sholar, GA, Page, GC, Musselman, JA, Upshaw, PB & Moseley, HL 2002, *Preliminary Investigation of a Test Method to Evaluate Bond Strength of Bituminous Tack Coats*', Report FL/DOT/SMO/02-459, Florida Department of Transport, October.

Soenen, H, Blomberg, T, Pellinen, T & Laukkanen, O-V 2013, 'The multiple stress creep-recovery test: a detailed analysis of repeatability and reproducibility', *Road Materials and Pavement Design*, vol. 14, no. S1, pp. 2-11.

Sousa, JB, Solaimanian, M & Weissman, SL 1994, *Development and Use of the Repeated Shear Test (Constant Height): An optional Superpave Mix Design Tool*, Report SHRP-A-698, Strategic Highway Research Program, National Research Council, August.

Stastna, J, Zanzotto, L & Polacco, G 2011, 'Viscoelastic repetitive creep and recovery of bituminous materials', *Procedia Engineering*, vol. 10, pp. 2170-2177.

Stastna, J, Zanzotto, L, Wasage, TLJ, Polacco, G & Cantu, M 2007, 'Dynamic creep test in several asphalt binders: the role of temperature and stress', *Proceedings Advanced Characterisation of Pavement and Soil Engineering Materials*, Athens, Greece, 20-22 June, Taylor and Francis, pp. 303-315.

Su, K, Sun, L, Hachiya, A & Maekawa, R 2008, 'Analysis of shear stresses in asphalt pavements under actual measured tire – pavement contact pressure', *Proceedings 6th International Conference on Road and Airfield Pavement Technology*, Sapporo, Japan, 20-23 July, Pavement Engineering Society (Singapore), pp. 11-18.

Sutanto, MH, Collop, AC, Airey, GD & Elliot, RC 2007, 'Laboratory measurement of shear interface strength beneath a thin asphalt layer', *Proceedings Advanced Characterisation of Pavement and Soil Engineering Materials*, Athens, Greece, 20-22 June, Taylor and Francis, pp. 1327-1336.

Tabachnick, BG & Fidell, LS 2001, *Using Multivariate Statistics*, 4th edn, Allyn & Bacon, Massachusetts, USA.

Taherkhani, H 2011, 'Compressive creep behaviour of asphalt mixtures', *Procedia Engineering*, vol. 10, pp. 583-588.

Taherkani, HT, Grenfell, JRA, Collop, AC, Airey, GD & Scarpas, A 2007, 'Characterisation of repeated creep recovery behaviour of asphaltic mixtures', *Proceedings Advanced Characterisation of Pavement and Soil Engineering Materials*, Athens, Greece, 20-22 June, Taylor and Francis, pp. 271-279.

Taherkhani, H & Javanmard, M 2011, 'Steady-state deformation behaviour of asphalt mixtures', *Transaction of Civil and Environmental Engineering*, vol. 35, no. C1, pp. 81-94.

Tarrer, AR & Wagh, V 1994, *Factors Influencing mix setting Characteristics and Tests to Predict mix Setting Characteristics*, SHRP-A/UWP-91-508, Strategic Highway Research Program, Washington DC, USA.

Tashman, L, Nam, K, Papagiannakis, T, Willoughby, K, Pierce, L & Baker, T 2008, 'Evaluation of construction practices that influence the bond strength at the interface between pavement layers', *Journal of Performance of Constructed Facilities*, vol. 22, no. 3, pp. 154-161.

Tashman, L, Masad, E, Little, D & Zbib, H 2005, 'A microstructure-based viscoplastic model for asphalt concrete', *International Journal of Plasticity*, vol. 21, pp. 1659-1685.

Tashman, L, Wang, L & Thyagarajan, S 2007, 'Microstructure characterization for modeling HMA behaviour using imaging technology', *Road Materials and Pavement Design*, vol. 8, pp. 207-238.

Tayebali, AA, Rahman, MS, Kulkarni, MB & Xu, Q 2004, *A Mechanistic Approach to Evaluate contribution of Prime and Tack Coat in Composite Asphalt Pavements*, Research Report 2001-04, North Carolina State University, 25 June.

Tozzo, C, D'Andrea, A, Cozzani, D & Meo, A 2014a, 'Fatigue investigation of the interface shear performance in asphalt pavement', *Modern Applied Science*, vol. 8, no. 2, pp. 1-11.

Tozzo, C, Fiore, N & D'Andrea, A 2014b, 'Dynamic shear tests for the evaluation of the effect of the normal load on the interface fatigue resistance', *Construction and Building Materials*, vol. 61, pp. 200-205.

Tran, N, Willis, R & Julian, G 2011, *Refinement of the Bond Strength Procedure and Investigation of a Specification*, National Centre for Asphalt Technology, Report No. 12-04, October.

TRB 2001, *Characterization of Modified Asphalt Binders in Superpave Mix Design*, National Cooperative Highway Research Program, Report 459, Transportation Research Board, Washington, DC, USA.

TRB 2005, *Simple Performance Tests: Summary of Recommended Methods and Database*, National Cooperative Highway Research Program, Report 547, Transportation Research Board, Washington, DC, USA.

TRB 2009, *Polyphosphoric Acid Modification of Asphalt Binders*, Transportation Research Circular Number E-C160, proceedings from a workshop, Minneapolis, Minnesota, USA, 7-8 April 2009, Transportation Research Board, Washington, DC, USA.

TRB 2012, *Optimization of Tack Coat for HMA Placement*, National Cooperative Highway Research Program, Report 712, Transportation Research Board, Washington, DC, USA.

TRB 2013, *Nondestructive Testing to Identify Delaminations between HMA Layers*, vols. 1-5, Strategic Highway Research Board Program, Report S2-R06D-RR-1, Transportation Research Board, Washington, DC, USA.

Tredrea, PF 2007, 'Superpave binder properties and the role of viscosity', *Proceedings AAPA Pavements Industry Conference*, Sydney, New South Wales, Australia, 21-24 October, Australian Asphalt Pavements Association.

Tsubokawa, Y, Mizukami, J, Esaki, T & Hayano, K 2007, 'Study on infrared thermographic inspection of de-bonded layer of asphalt flexible pavement', *Proceedings FAA Worldwide Airport Technology Transfer Conference*, Galloway, New Jersey, USA,16-18 April, Federal Aviation Administration.

Uruquhart, R, Budjida, M & Wilson, G 2010, 'Investigations into the relationship between binder consistency/underlying viscosity and asphalt rutting', *Proceedings 24th ARRB Conference*, Melbourne, Victoria, Australia, 12-15 October, ARRB Transport Research.

Uzan, J 1999, 'Granular material characterization for mechanistic pavement design', *Journal of Transportation Engineering*, vol. 125, no. 2, pp. 108-113.

Uzan, J 2004, 'Permanent deformation in flexible pavements', *Journal of Transportation Engineering*, vol. 130, no. 1, pp. 6-13.

Uzan, J, Livneh, M & Eshed, Y 1978, 'Investigation of adhesion properties between asphaltic-concrete layers', *Journal of Association of Asphalt Paving Technologists*, vol. 47, pp. 495-521.

Vadnais, TH & Grimes, WD 2005, 'Heavy truck brake designer calibration test', *Proceedings Annual HVE forum 2005*, Miami, Florida, USA, 21-25 February.

Vallerga, BA, Jew, A & Nokes, WA 2000, 'Case study of an innovative high stability asphalt mix for heavy aircraft wheel loads', *Proceedings of the 26th Air Transportation Conference*, San Francisco, California, USA, 19-21 June, American Society of Civil Engineers, pp. 334-345.

Vismara, S, Molenaar, AAA, Crispino, M & Poot, MR 2012, 'Characterizing the effects of geosynthetics in asphalt pavements', *Proceedings 7th RILEM International Conference on Cracking in Pavements'*, Delft, Netherlands, 20-22 June, pp. 1199-1207.

Walubita, LF & van de Ven, MF 2000, 'Stresses and strains in asphalt-surfacing pavements', *Proceedings South African Transport Conference*, South Africa, 17-20 July.

Wang, H & Al-Qadi, IL 2010, 'Near-surface pavement failure under multiaxial stress state in thick asphalt pavement', *Transport Research Record: Journal of the Transportation Research Board*, no. 2154, pp. 91-99.

Wang, H, Al-Qadi, IL, Faheem, AF, Bahia, HU, Yang, S-H & Reinke, GH 2011, 'Effect of mineral filler characteristics on asphalt mastic and mixture rutting potential', *Transport Research Record: Journal of the Transportation Research Board*, no. 2208, pp. 33-39.

Wang, H, Al-Qadi, IL & Stanciulescu, I 2012, 'Simulation of tyre-pavement interaction for predicting contract stress at static and various rolling conditions', *International Journal of Pavement Engineering*, vol. 13, no. 4, pp. 310-321.

Wang, H, Li, M & Garg, N 2014, 'Simulation of NAPTF high tyre pressure tests with advanced finite element modeling', *Proceedings FAA Worldwide Airport Technology Transfer Conference*, Galloway, New Jersey, USA, 5-7 August, Federal Aviation Administration.

Wardle, LJ & Rodway, B 2010, 'Advanced design of flexible aircraft pavements', *Proceedings 24th ARRB Conference*, Melbourne, Victoria, Australia, 12-15 October, ARRB Transport Research.

Wasage, TLJ, Stastna, J & Zanzotto, L 2011, 'Rheological analysis of multi-stress creep recovery test', *International Journal of Pavement Engineering*, vol. 12, no. 6, pp. 561-568.

West, RC, Zhang, J & Moore, J 2005, *Evaluation of bond strength between pavement layers*, Report No. 05-08, National Centre for Asphalt Technology, December.

Wheeler, DJ 1988, *Understanding Industries Experimentation*, 2nd edn, Statistical Process Controls, Knoxville, Tennessee, USA.

White, GW 2007, *Thickness Design of Flexible Aircraft Pavements*, A Thesis submitted to the Faculty of Built Environment and Engineering, Queensland University of Technology, for the Award of Master of Engineering, July.

White, G 2013, 'Developing warm mix asphalt or airports', *Proceedings AAPA Pavements Industry Conference*, Brisbane, Queensland, Australia, 22-25 September, Australian Asphalt Pavements Association.

White, G 2015a, 'Adequacy of runway asphalt overlay interface construction', *AAPA International Flexible Pavements Conference*, Gold Coast, Queensland, Australia, 13-16 September, Australian Asphalt Pavement Association.

White, G 2015b, 'Effect of aircraft on the structure and response of asphalt', *Transportation Geotechnics*, vol. 2, pp. 56-64.

White, G 2015c, 'Inter-batch and Inter-feedstock variability of an Acid Modified Bitumen', *Road Materials and Pavement Design*, Article in Press, doi 10.1080/14680629.2015.1108220.

White, G 2015d, 'Limitations and potential improvement of the aircraft pavement strength rating system to protect airport asphalt surfaces', *International Journal of Pavement Engineering*, submitted but not yet published.

White, G 2015e, 'Modification of the airport pavement strength rating system for improved protection of asphalt surfaces', *International Journal of Pavement Engineering*, submitted but not yet published.

White, G & Rodway, B 2014, 'Distress and maintenance of grooved runway surfaces', *Proceedings Airfield Engineering and Maintenance Summit*, Furama Riverfront, Singapore, 25-28 March, Equip Global.

Williams, RC & Prowell, BD 1999, 'Comparison of laboratory wheel-tracking test results with WesTrack performance', *Transport Research Record: Journal of the Transportation Research Board*, no. 1681, pp. 121-130.

Witczak, MW & Uzan, J 1988, *The Universal Airport Pavement Design System, Report I of IV : Granular Material Characterization*, University of Maryland, College Park, Maryland, USA.

Wu, J, Lepercq, E & Airey, GD 2007, 'Aging bitumen in bulk versus the aging of bitumen in an asphalt mixture', *Proceedings Advanced Characterisation of Pavement and Soil Engineering Materials*, Athens, Greece, 20-22 June, Taylor and Francis, pp. 1631-1640.

Yang, X & You, Z 2015, 'High temperature performance evaluation of bio-oil modified asphalt binders using the DSR and MSCR tests', *Construction and Building Materials*, no. 76, pp. 380-387.

Yoo, PJ, Al-Qadi, IL, Elseifi, MA & Janajreh, I 2006, 'Flexible pavement responses to different loading amplitudes considering layer interface conditions and lateral shear forces', *International Journal of Pavement Engineering*, vol. 7, no. 1, pp. 73-86.

Zelelew, HM & Papagiannakis, AT 2012, 'Interpreting asphalt concrete creep behavior through non-Newtonian mastic rheology', *Road Materials and Pavement Design*, vol. 13, no. 2, pp. 266-278.

Ziari, H & Divandari, H 2013, 'Presenting asphalt mixtures flow number prediction model using gyratory compaction, *International Journal of Civil Engineering',* vol. 11, no. 2, pp. 125-133.

Zoorob, SE, Castro-Gomes, JP, Pereira Oliveira, LA & O'Connell, J 2012, 'Investigating the multiple stress creep recovery bitumen characterisation test', *Construction and Building Materials*, vol. 30, pp. 734-745.